A Rational Methodology for Determination of Service Life for a Delayed Coke Drum

by

John J Aumuller

A thesis submitted in partial fulfillment of the requirements for the degree of

Doctor of Philosophy

Department of Mechanical Engineering

University of Alberta

ABSTRACT

Delayed coking is an essential technology in the upgrading of heavy hydrocarbons in the Canadian oil sands for producing saleable liquid and gas products in order to sustain a viable national energy industry. Delayed coking units contain among the largest pressure vessels used in heavy industry and are operated under severe thermo-mechanical loading conditions.

Beginning in the late 1950's, it was recognized that drum shell cracking presented a major source of reduced unit reliability affecting safety and financial viability of the delayed coking process. There are very few focused studies in the open literature on coke drums investigating the root cause, the mitigation of the thermo-mechanical failure mechanism and remaining life prediction.

This work is a continuation of prior work to define, in detail, the thermo-mechanical loading of coke drums and evaluate its impact on service life. The available operating data in the open literature is limited and problematic; thus, the access given to proprietary data was invaluable in completing this effort.

In order to best serve the industry, this thesis has used as much data, techniques and methodologies currently available in the industry to perform the service life determination so that industry practitioners may implement this work without resorting to difficult and unnecessarily complicated methods and, better, to honour the vigor of industry practices and the contributions of the many mechanical engineers who developed them.

ACKNOWLEDGEMENTS

"Simplicity is the outcome of technical subtlety – it is the goal, not the starting point."
F.W. Maitland, 1850 – 1906, Domesday Book and Beyond
pg 50, "An Unfinished History of the World", Hugh Thomas, 1995

"Truth is ever to be found in simplicity, and not in the multiplicity and confusion of things." Quote attributed to Sir Isaac Newton, 1642 – 1727
www-history.mcs.st-andrews.ac.uk/Quotations/Newton.html; accessed 27 Oct 2016
John J O'Connor, Edmund F Robertson,
School of Mathematics and Statistics, University of St. Andrews, Scotland

Thanks are extended to Dr. Zengtao Chen and to Dr. Zihui Xia for his encouragement to pursue these studies. The meticulous work of Dr. Jie Chen and Mr. Bernie Faulkner in determining material properties are gratefully recognized in support of this effort and, as well, the contributions from past members of the Coke Drum research team.

A very deep heartfelt thank you to my wife, Diana whose infinite patience and support allowed me the luxury of time for study and research; and to my parents, who counselled perseverance as the foundation of achievement.

TABLE OF CONTENTS

LIST OF TABLES

LIST OF FIGURES

LIST OF NOMENCLATURE, ABBREVIATIONS, SYMBOLS

Code	- the ASME Boiler and Pressure Vessel Code [BPV] encompassing multiple volumes, and collectively, a document set governing the design, fabrication, construction and testing of pressure vessels and given the force of law in many legal jurisdictions, especially in Canada and the United States of America
	- individual volumes are referenced by section or section and divisions or parts, such as, ASME VIII Division 1
design life	- the anticipated life of a pressure vessel based on the design considerations of the Code of Construction; usually predicated on the anticipated material corrosion rate; a fatigue design life is also used
ductility	- ability of a material to deform plastically before fracturing and typically measured by elongation or reduction of cross-sectional area, among others
elastic limit	- the greatest stress which a material is capable of sustaining without any permanent strain remaining upon complete release of the stress
elastic true strain	- elastic component of the true strain
engineering strain	- a dimensionless value that is the change in length per unit length of original linear dimension along the loading axis of the specimen
engineering stress	- the normal stress, expressed in units of applied force per unit of original cross-section area
fatigue life	- the numbers of cycles of stress or strain of a specified character that a given specimen sustains before failure of a specified nature occurs, such as crack initiation or through section failure
fatigue ductility	- the ability of a material to deform plastically before fracturing, determined from a constant-strain amplitude, low cycle fatigue test; also referenced as fracture ductility
fatigue strength	- identifies the stress level at which fatigue failure will occur at a specified fatigue life
fatigue toughness	- materials with high fatigue (fracture) ductility and fatigue strength are designated as being fatigue tough; described as intermediate between strong and ductile materials

Nomenclature – cont'd

fracture strength	- one-reversal intercept of the elastic strain amplitude, from cyclic testing or approximated from monotonic true fracture strength
fracture stress	- the true normal stress on a minimum cross-sectional area at the beginning of fracture
mechanical properties	- those properties of a material that are associated with elastic and inelastic reaction when force is applied, or that involve the relationship between stress and strain, c.f. physical properties which refer to properties in a general sense
monotonic loading	- steadily rising portion of the stress-strain curve, with no reversal taking place during the continuously increasing loading path
modulus of elasticity	- the ratio of stress to corresponding strain below the proportional limit
nominal stress	- the stress at a point calculated on the net cross section by simple elastic theory without taking into account the effect on the stress produced by geometric discontinuities such as holes, grooves, fillets, etc.
normal stress	- the stress component perpendicular to a plane on which the forces act
plastic true strain	- the inelastic component of true strain
Poisson's ratio	- the negative of the ratio of transverse strain to the corresponding axial strain resulting from axial stress below the proportional limit of the material
proportional limit	- the greatest stress which a material is capable of sustaining without any deviation from proportionality of stress to strain
service life	- the anticipated operational life of a pressure vessel; for a coke drum in low cycle thermo-mechanical fatigue, the service life is a function of the severity of loading and the strain – fatigue life of the material of construction
spectrum loading	- in fatigue loading; a loading in which all of the peak loads are not equal or all of the valley loads are not equal, or both; also known as variable amplitude loading or irregular loading
strain	- the per unit change, due to force, in the size or shape of a body referred to its original size or shape. Strain is a non-dimensional quantity, but is frequently expressed in inches per inch, mm per mm or microstrain

Nomenclature – cont'd

strain hardening	- the increase in strength associated with plastic deformation
stress	- the intensity at a point in a body of the forces or components of force that act on a given plane through the point, expressed in force per unit area
stress – strain diagram	- a diagram in which corresponding values of stress and strain are plotted against each other; values of stress are usually ploted as ordinate and values of strain as abscissa
tensile strength	- the maximum tensile stress which a material is capable of sustaining; tensile strength is calculated from the maximum force during a tension test carried to rupture and the original cross-sectional area of the specimen
true stress	- the instantaneous normal stress calculated on the basis of the applied force divided by the instantaneous cross-sectional area.
true strain	- the natural logarithm of the ratio of instantaneous gage length to the original gage length
yield point	- term previously used to refer to upper yield strength
yield point elongation	- the strain separating the stress-strain curve's first point of zero slope from the point of transition from discontinuous yielding to uniform strain hardening. If there is no point at or near the onset of yielding at which the slope reaches zero, the material has zero percent yield point elongation
yield strength	- the engineering stress at which, by convention, it is considered that plastic elongation of the material has commenced. This stress may be specified in terms of (a) a specified deviation from a linear stress – strain relationship, (b) a specified total extension attained, or (c) maximum or minimum engineering stresses measured during discontinuous yielding. In summary, (a) 0.2% offset strain (b) 0.5% extension under load (c) upper or lower yield strength
Young's modulus	- the ratio of tensile or compressive stress to corresponding strain below the proportional limit of the material

Nomenclature – cont'd

References for Nomenclature

ASTM, "E 6 – 06 Standard Methodology Relating to Methods of Mechanical Testing" ASTM, West Conshohocken PA 2006

ASTM, "E 1049 – 05 Standard Practices for Cycle Counting in Fatigue Analysis" ASTM, West Conshohocken PA 2005

ASTM, "E 1823 – 05a Standard Terminology Relating to Fatigue and Fracture Testing" ASTM, West Conshohocken PA 2005

ASME, "VIII Division 1 Rules for Construction of Pressure Vessels", 2007 ASME, New York, NY

Collins, J.A., "Failure of Materials in Mechanical Design – Analysis, Prediction and Prevention", 2nd Ed., John Wiley & Sons, New York, NY 1993

Rees, D.W.A., "Basic Engineering Plasticity, An Introduction with Engineering and Manufacturing Applications", Butterworth Heinemann, Oxford, UK 2006

Dowling, N.E., "Mechanical Behavior of Materials", 3rd Ed, Pearson Prentice Hall, Upper Saddle River, NJ 2007

Abbreviations

A	a material designator for ASTM specified materials
API	American Petroleum Institute, an industry trade organization
ASME	American Society of Mechanical Engineers
ASTM	American Society for Testing and Materials
BIF™	bulge intensity factor, a contrived designation of coke drum shell damage
B&PV	boiler and pressure vessel, in reference to the ASME Codes of construction
BSF™	bulge severity factor, a contrived measure of coke drum shell stress
Btu	British thermal unit
CRD	collaborative research and development, an award designation from the Natural Sciences and Engineering Research Council of Canada; involves industrial client sponsorship
CS#	shell course designator
CTE	coefficient of thermal expansion
DCU	Delayed Cracking Unit
DNV	Det Norske Veritas, a standards writing body
EUL	extension under load; alternate measure of material yield strength
ETAN	Tangent modulus
EWI	Edison Welding Institute, a member organization providing services in applied research, services and manufacturing support; located in USA
FEA	finite element analysis or, alternatively, finite element method [FEM]
FSRF	fatigue strength reduction factor
FSRF’	fatigue strain reduction factor
gpm	gallons per minute
HAZ	heat affected zone
HPI	collective designation for the hydrocarbon processing industries
ID	inside diameter (of a pressure vessel, piping)

Abbreviations – cont'd

LCF	low cycle fatigue
MPC	Materials Property Council, a research organization associated with the ASME
MTR	material test report as required by the ASME Code providing the results of chemical analyses and mechanical tests made in accordance with Code requirements
OD	outside diameter (of a pressure vessel, piping)
PSI™	plastic strain index, a contrived measure of coke drum shell damage
psi	unit of pressure or force intensity in US customary units, pound-force per square inch of area; ksi ≡ thousands pound-force per square inch area
psig	unit of pressure in US customary units, pound-force per square inch of area – gauge reading; ksig ≡ thousands pound-force per square inch area – gauge reading
SA	a material designator for ASME specified materials
SA	a material designator for ASME specified materials
SCF	stress / strain concentration factor
sic	it is thus [from *Latin*], used within brackets to indicate that what precedes it is written intentionally or is copied verbatim from the original, even if it appears to be a mistake
SMTS	specified minimum tensile strength as given in the ASME Code
SMYS	specified minimum yield strength as given in the ASME Code
SS	stainless steel
TMF	thermo-mechanical fatigue
TP	abbreviation used by ASME for designating the type of stainless steel materials, e.g., TP 410S; stabilized grade of 410 stainless steel
TS	tensile strength as measured and listed on a material test report
YS	yield strength as measured or listed on a material test report
YP	yield point as defined by conventional definition; sometimes defined as departure from linear stress-strain behavior

Symbols [ROMAN]

A	area of cross section, a material designator for ASTM specified materials
°C	degrees Celsius, indicating magnitude of temperature on Celsius scale
C°	Celsius degrees, indicating difference in temperature on Celsius scale
C	carbon, co-fficient in Paris Law equation
Cr	chromium
D	diameter, Palmgren – Miner damage accumulation model
da	incremental increase in crack length described by the Paris Law equation
dN	incremental increase in fatigue exposure described by the Paris Law equation
ΔK	stress intensity value in Paris Law equation
E	Young's modulus, modulus of elasticity in tension or compression, weld joint efficiency; E_c ≡ modulus for clad material, E_b ≡ modulus for base material
F	force
°F	degrees Fahrenheit, indicating magnitude of temperature on Fahrenheit scale
F°	Fahrenheit degrees, indicating difference in temperature on Fahrenheit scale
f(x)	normalized fractional distribution
hr	hour
ke, Ke	penalty factor, used in ASME VIII Division 2 to account for plasticity in a simplified elastic – plastic analysis
kε	non-linear strain concentration factor
k_f, K_f	fatigue strength reduction factor, as used in ASME VIII Division 2

Symbols [ROMAN] – cont'd

k_t	stress / strain concentration factor
$k\sigma$	stress concentration factor
kPa	unit of pressure or force intensity in SI units, kilo-Pascals, 10^3 N/m^2
kPag	unit of pressure – gauge reading in SI units, kilo-Pascals, 10^3 N/m^2
ID	inside diameter
Δl	incremental increase in length
l, L	length
m	meter, exponent in Paris Law equation
mm	millimeter
Mo	molybdenum
Mn	manganese
MPa	mega Pascals, 10^6 N / m^2
n, N	cycles
Ni	nickel
N_f	cycles to failure
$2 \cdot N_f$	stress reversals to failure
OD	outside diameter
p, P	pressure, traction load
P	phosphorus

Symbols [ROMAN] – cont'd

P_m	primary membrane stress intensity per ASME VIII Div 2
r, R	radius, strain / stress ratio in fatigue loading = $\sigma_{min}/\sigma_{max}$
RA	reduction of area
S	sulphur, material allowable stress per ASME VIII Division 2
Sa	allowable stress per ASME VIII Division 1, allowable fatigue stress amplitude per ASME VIII Division 2
S_h, S_l	nominal hoop stress, nominal longitudinal stress
s_f	engineering fracture stress
Si	silicon
S_m	allowable stress intensity per ASME VIII Div 2
s_t	nominal tensile engineering stress
ΔT	temperature difference
TS	tensile strength (as stated in the material test report)
t, tk	thickness; $t_c \equiv$ thickness of clad material, $t_b \equiv$ thickness of base material
t	time
W	watt
YS	yield strength (as stated in the material test report)

Symbols [GREEK]

α	coefficient of thermal expansion, $\alpha_c \equiv$ clad material, $\alpha_b \equiv$ base material
α_{sl}	multi-axial material strain limit per API 579
Δ	increment, change or range
$\Delta\,\varepsilon$	true strain range
$\Delta\,\sigma$	true stress range
ε	engineering strain
ε^e, ε_e	elastic true strain
ε_{eff}	effective true strain
ε_f	true fracture strain
ε^p, ε_p	plastic true strain
ε_{mech}	mechanical true strain
ε_{YS}	strain corresponding to yield strength
ε_{SMYS}	strain corresponding to specified Code minimum yield strength
$\varepsilon_{thermal}$, ε^{th}	thermal true strain
ε^{total}, ε_t	total true strain
σ	nominal engineering stress
σ_f	true fracture stress
σ_t	tensile true stress
μ, ν	Poisson's ratio
σ_y	normal stress yield point
$\mu\varepsilon$	microstrain, $1{\cdot}10^{-6}$ strain or $1{\cdot}10^{-6}$ inch per inch, $1{\cdot}10^{-6}$ m per m

CHAPTER 1 INTRODUCTION

1.1 Background

Coke drums are a type of pressure vessel used in the hydrocarbon processing industry [HPI] to convert heavy molecule hydrocarbon factions (bottom of barrel) to lighter factions, such as naphtha, kerosene and gas oil for product sale and further upgrading. Refinery and oil sands processing facilities are the two primary users of this equipment.

Coke drums operate in a manufacturing process known as delayed coking; the facilities, in aggregate, are known as a delayed coking unit [DCU] and have been in routine service since the mid-1930's; the first modern plant being constructed in Whiting, Indiana, USA in 1929 [1, 2].

An early independent survey revealed that these drums were susceptible to a number of problems which were attributed to the severe service environment [3]. These problems included

- bulging of shell
- skirt cracking
- shell nozzle cracking

The first industry trade survey provided by the American Petroleum Institute [API] in 1968 highlighted shell through wall cracking as the major issue and this situation has remained so up to the current 4th industry survey completed in 2013 [4, 5]. The major reliability issues for coke drums remain

- shell cracking
- shell bulging
- skirt cracking

Since the first survey in 1958, it has been recognized that coke drums operate in a severe service environment caused by a combination of high bitumen temperatures of up to 900 °F [482 °C] with rapid water quenching leading to large thermo-mechanical strains in the shell. This heating and quenching operation occurs on a repetitive basis of nominally one (1x) times per twenty four [24] hour period (day).

The quantification of this thermo-mechanical loading and its impact in limiting the service life of coke drums has not been definitively established. Drum shells are routinely monitored for bulging and incipient cracking, shell cracking failures are repaired and, drums may be replaced from time to time when the apparent damage and the risk of unplanned shutdown are deemed excessive.

In contrast to industry practice with processing equipment operating under more moderate conditions, the service life of a delayed coker drum has not been established and replacement criteria and practices remain confidential among equipment owners.

Climate Warming / Climate Change

A stated goal of governments in addressing climate warming is to transition to a low carbon economy by the end of this century (and, some suggest by 2030) by increasing the proportion of energy supplied from alternative sources, so called green sources. For the hydrocarbon processing industry, the question of stranded assets becomes increasingly significant as these alternative energy sources become more prevalent. That investment in alternative energy sources has exceeded the investment in conventional carbon based sources is, already, being reported by public sources.

Existing energy industry equipment will need to operate to the end of its useful life and new equipment may need to be avoided. In particular, coker drums are very expensive investments due to their size, materials and number required in the delayed coker unit of an HPI facility.

Because of the severe service environment in which coke drums operate, accurate determination of the thermo-mechanical loads and service life of a drum have not been established.

Long term reliability of coker drums is impacted by thermo-mechanical damage mechanisms associated with self constraint of the drum shell and skirt during the formation of hot and cold temperature spots, patches and generally, elevated temperature exposure. By assessing the imposed thermo-mechanical strains, a more precise determination of drum fatigue may be made, allowing better estimation of service life. This service life may be estimated for newly fabricated drums and those drums with shell damage, such as bulging.

1.2 Thesis Objectives

The intent of this thesis is to estimate the service life of coke drums in the newly installed condition and for drums exposed to in-service conditions.

The newly installed drum is referred to as the “undamaged” or new drum; a drum exposed to service experiences shell distortions and is referred to as a “damaged” drum.

The estimate will be made on a “best estimate basis” for the available data, at hand. Each drum is unique with variation among material selection, design details, operation and maintenance practices, operational exposure and accumulated damage. However, the prescribed methodology in this work is

demonstrated for a posed drum, in the new and damaged conditions using a specific thermal loading exposure profile.

A particular difficulty in developing the best estimate service life for this thesis effort was the reticence of equipment owners in providing actual field data for their equipment. The reasons likely include the cost of data collection, competitive considerations, desire to limit publicity of equipment condition and concerns for public liability. Hence, a fully accurate and definitive service life determination was not possible for a specific candidate drum, as the necessary details were not available for this work.

User responsibility: The methodology delivered in this work will be sufficiently general to be applied for the specifics of a user's situation. The user will need to to be judicious in ensuring that any reliance on general data in lieu of specific user data is acknowledged in the results.

Service life is defined to be the anticipated actual useable operating life of the equipment compared to the Code designated design life [6]. As interpreted in this work, service life means the amount of time a coke drum can be expected to be crack free for the given operating exposures and capacities of the materials of construction of the coke drum.

Determination of service life for a new / undamaged drum provides a benchmark target for owner's asset integrity management and future integrity evaluations; owners currently monitor drum condition and will be able to determine the impact of incremental damage on service life using additional methods detailed in this work. The determination of service life for a representative in-service drum with measured bulging provides indication of damage progression and will affect the benchmark service life determined at original installation.

This is a long-time industry problem in an industry with a history of developing robust engineering design and assessment practices; this demands that fatigue life determinations be made using these industry practices wherever available. These long standing methodologies include rules for the construction of pressure vessels, such as ASME VIII Division 1 and ASME VIII Division 2 [7].

More recently, methodologies have been developed for damage assessment of pressure containing equipment such as API 579 – 1 / ASME FFS –1 [8]. These detailed damage assessment procedures have only been formally developed in the last fifteen years but have not been applied in detail nor with efficacy to the assessment of coke drums.

The reasons for this include

- thermo-mechanical loading for coke drums has not been characterized
- strain – life data for coke drum materials are not generally accessible

These industry practices, however, will be shown to be fundamental in determining the undamaged and damaged coke drum service life. Calculating service life using industry methods will be more readily accepted than alternative methods not in conformance with the paradigms currently offered by industry. The term “industry” is used to broadly describe equipment owners, code and standards producing organizations (such as ASME, API, ASTM), safety regulators and design and construction engineers involved in the construction and operation of coke drums.

Many aspects of service life determination were available shortly after the publication of the first drum survey i.e., the mid – 1960’s but use was inhibited by

- the lack of modern computational tools
- the inaccessibility of relevant industry data
- the lack of initiative and cooperation by industry

Some of these difficulties currently persist; access to construction and operating records, temperature and strain data continues to be guarded by equipment owners.

It should be noted that some data presented in this thesis is obtained by private communication and experiences gained by the author over a lengthy career in the HPI [9]. Personal knowledge of equipment design specifications, coke drum maintenance issues and operating practices are some examples of this experience.

Out of necessity, there is reliance on qualitative data to benchmark the quantitative results developed in this work. The 1996 and 2013 API surveys are core to identifying damage trends so that correlations and conclusions can be drawn for the analytical work presented in this thesis.

1.3 Operations Overview

Delayed coker drums are a specific type of coker drum in which a solid carbonaceous residual by-product or coke is created during the thermal cracking process in which reduced liquid bitumen feed at high temperature is injected into the drum. The vapour portion disengages, being withdrawn overhead and the residual solid by-product proportionately fills the drum plenum.

This by-product must be removed at the end of the oil injection / fill phase in order to restore the drum's empty fill volume prior to the next fill operation. Thus, the coke drum operation is a batch process.

Coke drums experience mild pressure loads but operational temperatures are relatively severe and large thermo-mechanical loads occur during the water quench phase. The water quench is necessary to cool the remnant coke mass to ambient temperature for evident reasons of safety and to minimize the turnaround time to the next fill sequence. This is essential for profitable operation of the unit.

These load exposures are repetitive and lead to apparent thermo-mechanical fatigue. It was reported that there were fifty three [53] DCU's in the United States of America in 2003 [10].

1.3.1 System of Units

Coke drum technology was developed and continues to be led by HPI users in the United States of America who continue to favor the US Customary system of units, these will be used in priority to SI units for this work. There is also advantage in using the Fahrenheit temperature scale which has finer resolution with 1.8 F° equal to 1 C° providing more detail in quantifying differences in temperature during transient conditions.

1.4 Coke Drum Operation

For reasons of economy, a minimum of two (2) drums are operated in a plant unit to effect a semi-batch / continuous product stream, but many DCU plants have up to eight (8) drums for production reasons as shown in **Figure 1.1** [1]. These drums operate consequently in pairs; while one (1) drum is filling, the second drum is being prepared for its fill cycle.

Figure 1.1 Photograph of Coke Drums in a Process Unit

A schematic of the delayed coke processing unit is given in **Figure 1.2** illustrating entry of reduced bitumen feed, through the coker heater and then to one of two coke drums for the delayed cracking (i.e., separation) into vapour and solid components. The overhead vapour stream is delivered to the fractionator for further separation into different hydrocarbon factions (“cuts”).

Figure 1.2 Delayed Coker Unit Process Flow Schematic [9]

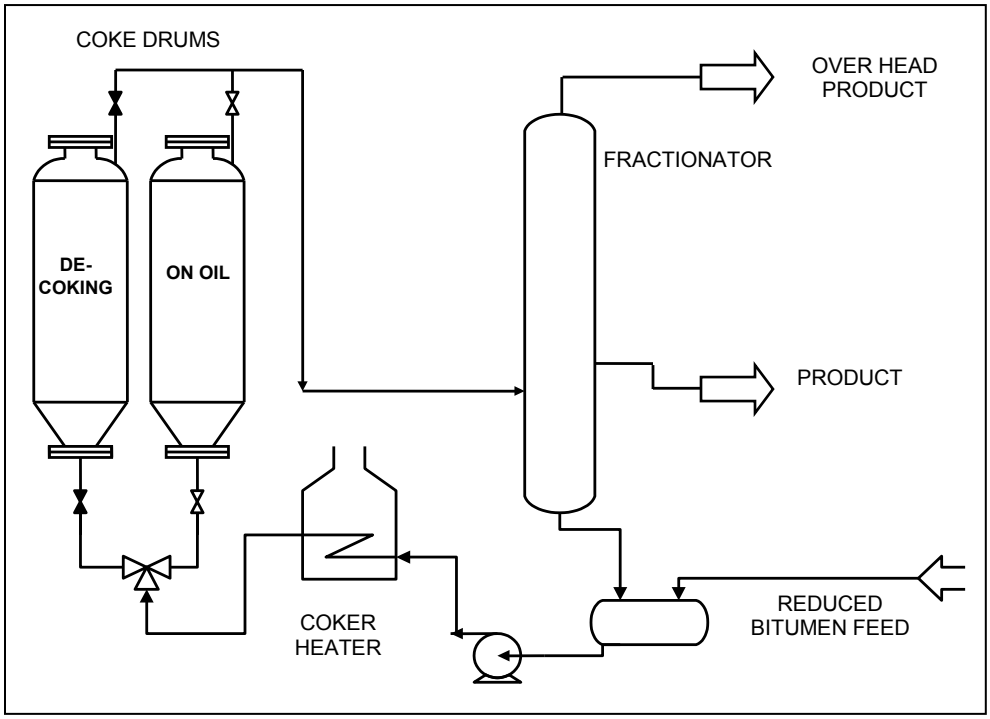

The operational cycle consists of several steps:

- drum tightness testing & initial (steam) heating
- vapour heating w/coke vapours
- bitumen / oil filling
- quenching by water
- coke removal

The entire operational cycle varies among plant operators but is usually consistent at any single facility location by reason of established practice. This complete operational cycle may vary from 20 to 30 hours. The vessels operate at a pressure of 35 to 55 psig [240 to 380 kPag]. A temperature cycle is illustrated in **Figure 1.3** using two (2) thermocouple measuring locations on the shell cylinder. In this instance, shell temperatures only approach a temperature of 700 °F [371 °C] and is indicative of less severe temperature exposure. Modern day operation reaches shell cylinder temperatures of 900 °F [482 °C].

The number of operational cycles incurred ranges from nominally 7,500 cycles to 20,000 cycles over the course of a twenty (20) to fifty (50) year conventional “life” of a delayed coke drum, dependent on operational specifics. Hence, the fatigue regime is low-cycle.

Figure 1.3 Vessel Shell Temperatures during Operational Cycle in ° F [9]

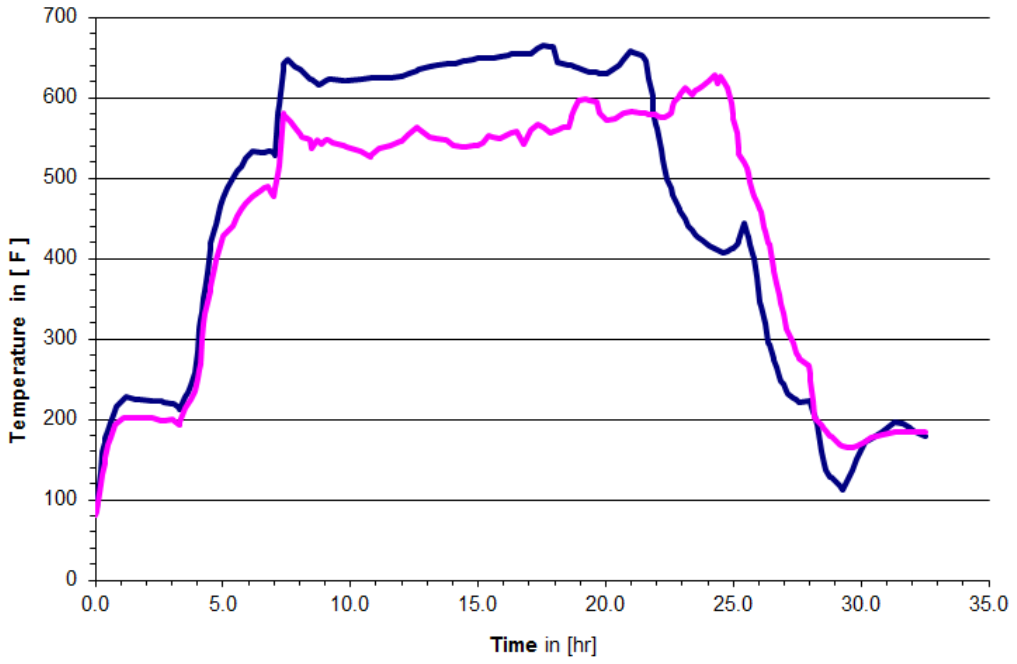

Notes
1 readings from the lower elevation thermocouple
2 readings from the upper elevation thermocouple

1.5 Drum Size

The physical size of the drums makes this equipment visually imposing in a refinery or oil sands plant; the drums are up to 30 feet [10 m] in diameter, 120 feet [38 m] tall and up to 220 feet [68 m] in elevation due to the need for access below the bottom of the drum. In contrast to its large physical size, the drum shell thickness is relatively thin, being approximately 1 inch [25.4 mm] to 1¾ inches [44.5 mm]. Early drums were only 16 feet [4,880 mm] in diameter and 35 feet [10,668 mm] in height [2]. Drums in excess of 30 feet [10 m] diameter are being planned.

The vessel thickness is governed by a Code of pressure vessel construction. For North American jurisdictions this is the American Society of Mechanical Engineers or ASME Boiler and Pressure Vessel Code Section VIII Division 1 Code Rules for Pressure Vessel Construction. This Code is enforced by the safety regulator for the specific jurisdiction where these drums are located.

1.6 Drum Construction

The ASME VIII Division 1 Code of construction addresses the design, material selection, fabrication, inspection and examination requirements, collectively referred to as the “construction” of the vessel.

Material selection for drums is usually low alloy clad carbon steel of various grades to reduce the relatively large cost of these vessels; the materials listed in **Table 1.1** are both historic and, currently used for coke drums. In addition, candidate materials, considered in current research, are also listed. A low alloy carbon steel base material is selected for reasons of strength at the elevated temperature of operation of the drum. The pressure retaining capability, in operation, is provided by the base material.

The clad material, of ferritic stainless steel [TP 405, TP410S], provides corrosion protection for the base material against sulfur and other corrosive compounds contained in the bitumen.

Table 1.1 Chemical Compositions for Materials of Construction in [%]

Material (1, 2)	**C**	**Mn**	**Cr**	**Mo**	**P**	**S**	**Si**	**Ni**
SA 240 TP 405	.08	1.0	13	-	.04	.03	1.00	.60
SA 240 TP 410S	.08	1.0	12½	-	.04	.03	1.00	.60
SA 516 70	.28	1.0	-	-	.035	.035	.45	-
SA 204 C	.26	.98	-	½	.035	.035	.29	-
SA 302 B (3)	.23	1½	-	½	.035	.035	.45	-
SA 302 C (3)	.23	1½	-	½	.035	.035	.45	½
SA 387 12	.1	.5	1	½	.035	.035	.3	-
SA 387 11	.1	.5	1¼	½	.035	.035	.6	-
SA 387 22	.1	.5	2¼	1	.035	.035	.50	-
SA 387 21	.1	.5	3	1	.035	.035	.50	-

Notes to Table 1.1

1. Nominal compositions are given; see reference [11] for composition limits
2. Other trace and alloying elements may be present as provided for by Code
3. SA 302 materials are possible materials of construction

The range of contaminants and content of bitumen feed contains [9], in percent [%]

- sulfur 6.0 – 6.9
- chlorides 0.0 – 0.04
- ash 0.2 – 7.0

Further, the ash contains a variety of metals and inorganics, such as [9]

SiO_2	Ge	As
Al_2O_3	Pb	Cd
TiO_2	Se	Cu
Fe_2O_3	Zn	Cr
CaO	Ni	Hg
V_2O_5	V	

Materials of construction are also referenced by their nominal composition as C – Mo or Cr – Mo steels for the base layer or by industry designator as TP 405 and TP 410S stainless steel for the clad layer.

Coker drums are designed on the basis of service conditions such as those listed in **Table 1.2** by assigning a design temperature and design pressure to capture the envelope of process conditions.

Table 1.2 Coke Drum Process Operating Cycle

Operating Step	Temp [°F]	Pressure [psig]	Temp [°C]	Pressure [kPag]	Duration [hrs]
Steam Test	220	35	104	241	< 3
Vapor Heat	600	35	316	241	3
Oil Fill – Coking	900	35	482	241	11 – 15
Steam Quench	350	35	177	241	< 1
Water Quench	200	35	93	241	3
Unhead	100	0	38	0	< 1
Decoke	100	0	38	0	1 – 3
Total Time					24 – 28

Notes to Table 1.2

1. Indicated temperatures are stream temperatures. Pressures are vessel internal pressures.
2. Possible design conditions for vessel; design pressure, 50 psig; design temperature, 900 °F
3. Reference: CRD information package; [9]

1.7 ASME VIII Construction Codes

The two Code divisions of interest, Division 1 and Division 2 provide two different levels of construction effort. The former uses a simplified design philosophy, requiring reduced engineering skill in its implementation while the Division 2 mandates a robust principles based engineering approach with certification and filing of a manufacturer's design report to be completed by a registered professional engineer.

The primary pressure design consideration of the Division 1 Code of construction is to provide a design resistant to collapse (i.e., general yielding) failure under pressure loading while in service.

The Code lists other pertinent loads to be considered by the designer including cyclic and dynamic reactions due to pressure or thermal variations, temperature gradients and differential thermal expansion. Specific methodologies are not presented in the Code. Unfortunately, definitive data is not provided to designers and these particular loads are ignored in practice, precluding a comprehensive design treatment of the vessel.

Safety regulators have not shown the same interest in these secondary loads. The regulators are focused on those loads causing "collapse" of a vessel, i.e., those sustained loads which would cause through-wall membrane yielding of the vessel. This collapse failure is modeled on use of an elastic – perfectly plastic material behavior model.

These sustained loads are specifically

- pressure
- live weight
- dead weight

The Code does not require calculation of stress but rather, only a design pressure thickness which must be able to contain the equivalent hydrostatic pressure from the combined internal pressure and weight loads. The Code is motivated by a "design by rules" approach to reduce engineering involvement; hence, vessel stresses are not explicitly calculated in design; rather, the designer calculates a pressure thickness using the temperature dependent allowable stress, the quantity "S" in **Table 1.3**, assigned for the material.

In contrast to the Division 1 Code, the alternative rules of the ASME VIII Division 2 Code practice methodology categorizes stresses as primary, secondary and peak and limits these based on consideration of their failure mode and loading source. Engineering skill and judgment are required to implement the process as the load – stress impact are not always evident. These limits are designated as "design by analysis" and their motivation is broadly divulged in the Code. Specific details, insights and background, however, are not discussed and the certifying engineer must take initiative to understand the underlying principles contained in these provisions. Some of these provisions can be readily recognized from strength – of – materials considerations; others, may be experientially based while others may be obscure. Ancilliary documents and practice studies are available, while original work may also need to be undertaken and is encouraged by the Code for specific designs.

The Division 2 Code design considerations are

- to limit loads to general and local primary stress limits
- to limit loads to secondary stress limits
- to limit loads to peak stress limits

For example, general membrane stresses, designated P_m stresses need to be limited to the allowable design stress, S_m which is derived as a function of the material specified minimum yield strength, SMYS or as a function of specified minimum tensile strength, SMTS. The internal pressure load develops P_m type stresses.

Cyclic thermo-mechanical loads give rise to fatigue failure which is limited to a peak stress limit. The two types of failures arising from exceeding the limit on general membrane stress and exceeding the limit on peak stress are very different. Consequently, regulators simply treat the failures caused by cyclic loads as reliability failures which have experientially not warranted the same consideration as failure associated with insufficient design pressure thickness. Cyclic loads are assumed to cause leak-type failures in coke drum vessels when they are not adequately designed to avoid fatigue failure. This stance not appropriate, in general, for industry applications since they may contain dangerous and lethal service fluids.

Industry practitioners have limited coke drum construction to the ASME VIII Division 1 Code on account of these considerations. Using the relevant Code such as ASME VIII Division 1, for a cylindrical shell section, the pressure thickness of interest, from the Code formula is derived from strength of materials considerations as: [6]

$$t = \frac{P \cdot R}{S \cdot E - 0.6 \cdot P} \qquad [1.1]$$

where, using consistent units:

t ≡ the required pressure thickness,
P ≡ the design pressure of the component,
R ≡ the radius of the cylindrical section,
S ≡ the allowable stress as set out in the Code for the design temperature,
E ≡ weld joint efficiency for the component, dimensionless

Temperature dependent allowable stress values are provided in Table 1.3 for the various materials of interest.

Therefore, a coke drum will be designed for pressure thickness, " *t* " using the internal design pressure and static head from dead and live weight loads at the appropriate temperature water,

P = pressure + static head = 55 psig + (120 ' elevation head / 2.3 ' / psi), head = 107.2 psig
R = 30'/2 * 12 = 180 inches
S = 15,800 psi at 900 °F based on using either of SA 387 11 or 22 Class 2
E = 1.0 since welds are fully radiographed

hence,

$$t = \frac{P \cdot R}{S \cdot E - 0.6 \cdot P} = \frac{107.2 \cdot 180}{15{,}800 \cdot 1 - 0.6 \cdot 107.2} = 1.226 \quad inches \quad [31 \quad mm] \text{ or} \qquad (1.1)$$

1¼" [32mm] for the base (i.e., pressure containing) layer,

This demonstrates the practice of constructing the coke drum with relatively thin shell wall thicknesses. Note that the density of bitumen feed to the coke drum [52 lb_f / ft^3] is slightly less than the density of water [60.0 lb_f / ft^3] at operating conditions. Coke density is usually stated as 58 lb_f / ft^3. Water fill is specified to the top of the vessel while a coke / water mix is specified to a normal fill height of approximately 80% of vessel height. By Code, shell thickness is calculated at drum design temperature.

Table 1.3 Allowable Stresses, SMYS for Materials of Construction in [ksi**]**

Material	S				SMYS			
	100 °F	900 °F	100 °F	900 °F	100 °F	900 °F	100 °F	900 °F
SA 240 405	16.7	11.3	-	-	25.0	16.9	-	-
SA 240 410S	17.1	12.3	-	-	30.0	20.3	-	-
SA 516 70	20.0	6.7	-	-	38.0	24.0	-	-
SA 204 C	21.4	13.7	-	-	43.0	30.0	-	-
SA 302 B	22.9	13.7	-	-	50.0	34.9		
SA 302 C	22.9	13.7	-	-	50.0	34.9	-	-
	Class I		Class II		Class I		Class II	
SA 387 12	15.7	14.7	18.6	17.4	33.0	30.0	40.0	27.2
SA 387 11	17.1	13.7	21.4	15.8	35.0	23.8	45.0	30.6
SA 387 22	17.1	13.6	21.4	15.8	30.0	25.6	45.0	32.4
SA 387 21	17.1	12.0	21.4	13.1	30.0	25.6	45.0	32.4

Notes to Table 1.3

1. Reference: ASME II Part D; [12]

A formal design will also take into account the other loads itemized above, such as wind and seismic loads using more detailed calculation protocols to determine a final Division 1 Code acceptable thickness. The pressure thickness is usually sufficiently robust to accommodate the additional loads. Historically, this pressure thickness was particularized for the elevation for the shell course under consideration resulting in varying shell course thicknesses over the height of the coke drum.

Figure 1.4 Typical Coke Drum Shell Plate Layout

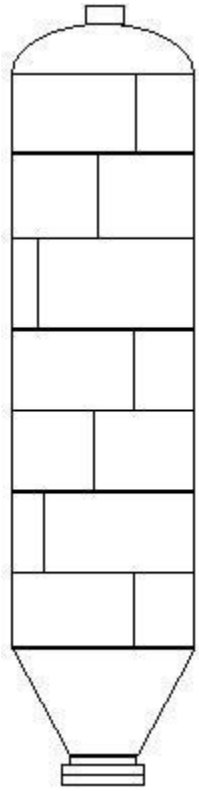

Shell courses are typically ten (10) feet [3.05 m] wide allowing the course design thickness to be conveniently varied over the height of the drum. Six (6) to ten (10) or more shell courses are assembled to form the overall height of the cylinder portion of a modern drum. **Figure 1.4** shows the typical shell layout with staggered vertical shell seams (a Code practice). The thickness of cladding (for corrosion protection) is arbitrarily chosen as 0.120 inches [3 mm] from industry experience but can vary for individual equipment per Owner preference.

To address thermo-mechanical loading, which has been recognized since the first survey in 1958, equipment owners have provided a general statement that a thermal load shall be considered in the design. However, no detailed definition of this load is provided in construction specifications and hence, design submissions do not contain any consideration of these loads other than listing the design temperature. Nonetheless, the industry has, by virtue of broader experience, incorporated fatigue compatible design features in recent modern coker drum construction.

Fatigue compatible fabrication, listed in Code practices, is implemented in modern coker drum construction, including

- use of flush weld profiles for all shell weld seams
- uniform shell plate thickness throughout the height of the drum
- fatigue compatible shell to skirt weldments such as integral transition
- top and bottom head located feed nozzles only, with no nozzles located on the main shell cylinder
- elimination of insulation support rings welded to the shell cylinder
- elimination of the derrick attachment to the top head of coker drum; modern practice is to support the derrick on an external structural frame

Figure 1.5 shows an independently supported derrick structure atop the drums

Figure 1.5 – Coke Drum Unit Derrick Structures

1.8 Thesis Summary

Delayed cracking unit coke drums are a vital technology for the HPI in the processing of heavy molecule hydrocarbons into marketable products. However, their use since the early 1930's has been problematic in realizing longer term integrity and reliability; industry engineering practitioners have been unable to definitively identify the damage mechanisms causing shell bulging and cracking and the impact on vessel service life.

Although a number of industry surveys, papers and practice documents have been published, there has been no satisfactory application of the body of knowledge to resolving coke drum service life deficiencies. Practitioners have listed the complexities of assessing service loads and damage mechanisms as the primary difficulty in determining service life and, thus, motivating the use of simplified, contrived and unsatisfactory damage criteria.

Our thesis demonstrates that the basic industry methodology has been available since the mid – 1960's but has been inadequately interpreted and incorrectly applied to the problem of coke drum service life determination. In addition, the basic methodology must be augmented in specific areas where the methodology is insufficiently detailed and inadequate for application to service-exposed equipment. These deficiencies in application have lead to the current inability to determine service life for either a new or a damaged coke drum.

Premature retirement of equipment from service has led to economic loss for equipment owners and the inability to assess quantitatively the safety risks from damaged equipment to which industry workers may be exposed.

CHAPTER 2 LITERATURE REVIEW

The HPI industry has provided a number of surveys since 1958 and more recently, technical reports specifying assessment methodologies to evaluate general pressure vessel damage and demonstrate suitability for continued operation. A limited number of papers have also been produced.

Industry surveys provide operational and maintenance information but have not elicited from equipment owners more quantified data which would assist more rigorous engineering analysis. However, these surveys do provide sufficiently reasonable data to qualitatively support the analytical efforts of the thesis work.

2.1 Industry Surveys

Weil & Rapasky, 1958 This survey of 16 coke drums was undertaken by an industry engineering contractor, MW Kellogg Company, Houston, Texas to address the number of reports of equipment distress. The paper indicates that coke drum temperatures operated to a temperature of 800 °F [427 °C] over a 24 to 48 hour cycle [3].

Drum dimensions were listed to be from 12 to 19 feet [3.6 m to 5.8 m] in diameter, 37.5 to 69.2 feet [11.4 m to 17.6 m] in straight side cylinder length, fabricated from carbon [SA 285 C] and low alloy carbon steel [SA 204 C i.e., C – ½ Mo] steel with TP 405 or TP 410 stainless cladding.

Severe shell diameter growth, bulging and skirt cracking were the major issues affecting drum integrity. The survey established that temperature gradients during quenching were severe with gradients of up to 27.1 F° per inch [15 C° / 25.4 mm] measured on the external drum shell surface. Channeling of quench water was identified to account for the gradients being noted in the lower shell courses but not in the bottom cone of the vessel.

The survey proposed an operating criteria to control the temperature gradients, the Unit Quench Factor [UQF] by throttling water flow to the coke drum to a threshold value. Slower water addition correlated with less bulging and cracking damage. This suggested water quench periods of 6 to 8 hours.

This survey established the notion that shell bulging resembled a ballooning of individual shell courses that migrated from the bottom course upwards. **Figure 2.1** illustrates this concept. Skirt cracking was identified as the most widespread maintenance difficulty occurring within 550 to 2,330 operational cycles, i.e., within 1½ to 7 years after startup.

Figure 2.1 Progressive Bulging Damage of Coke Drums

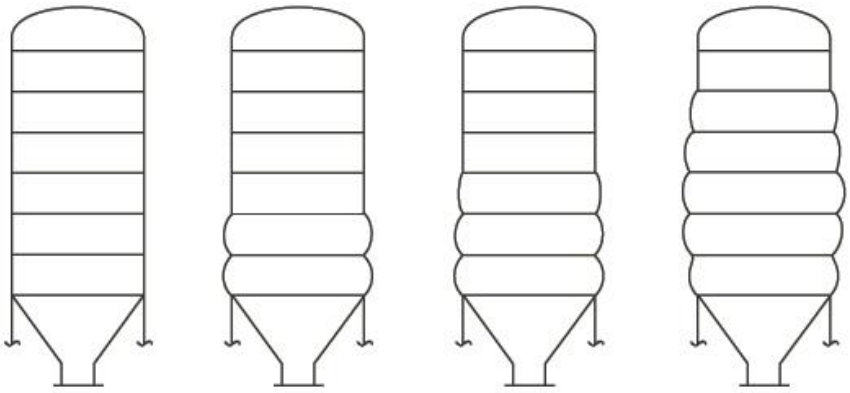

Thomas, 1968 & 1980 Two industry surveys were reviewed by Thomas. A summary of the 1968 API report revealed [4]

- the survey was motivated by drum shell cracking
- cracking in the shell followed minor to severe shell bulging
- cracking is circumferential at weld seams
- cracking may be in the apex or valley of shell bulge
- thin wall vessels experience cracking sooner
- C – ½ Mo drums appear to be more crack sensitive than carbon steel drums

The 1980 survey by Thomas reported on 62 drums

- a shift from carbon steels and C – ½ Mo to Cr – Mo steels had taken place from 1960 through the 1970's
- operating temperatures had increased to 900 °F [482 °C]
- drum diameter had increased to 22 feet [6.7 m]
- earliest cracking varied from 7 years (carbon steel) and 8 years (C – ½ Mo) to 12 years (Cr – Mo)
- drums with no cracking varied in service to 32 years (carbon steel), 22 years (C – ½ Mo) and 11 years (Cr – Mo)
- no correlation was found between drum thickness and first cracking for C – ½ Mo and Cr – Mo steels

API 1996 Survey The survey updated the prior surveys with the following information [13]

- *the survey reported on 145 drums*
- *new drum material selection showed a trend to increase Cr – Mo content*
- *clad material is either TP 410 or TP410S*
- *no correlation was found between drum cracking and fill cycle time*
- *drum operating parameters such as initial quench rate and proofing quench practice rather than metallurgy changes, appear to have a greater influence on drum cracking*
- *skirt cracking was reported by 73% of the surveyed companies; of the 23% that replaced skirts, re-cracking eventually occurred 43% of the time*
- *the first bulge appeared sooner than first through-wall cracks.*
- *shell bulging was reported by 57%. Shell cracking was reported by 57%*
- *of the drums that bulged, 87% also experienced cracks; cracking without bulging was reported only by 6%*
- *when cracking was reported, it occurred in the circumferential direction 97% of the time. Most of the cracks were located in courses 3, 4, and 5 (course 1 is at the bottom)*

Figure 2.2 shows a crack originating at the internal surface and initiating between the clad material and clad weld material.

Figure 2.2 Circumferential Weld Crack Initiating at ID Clad / Clad Weld [5]

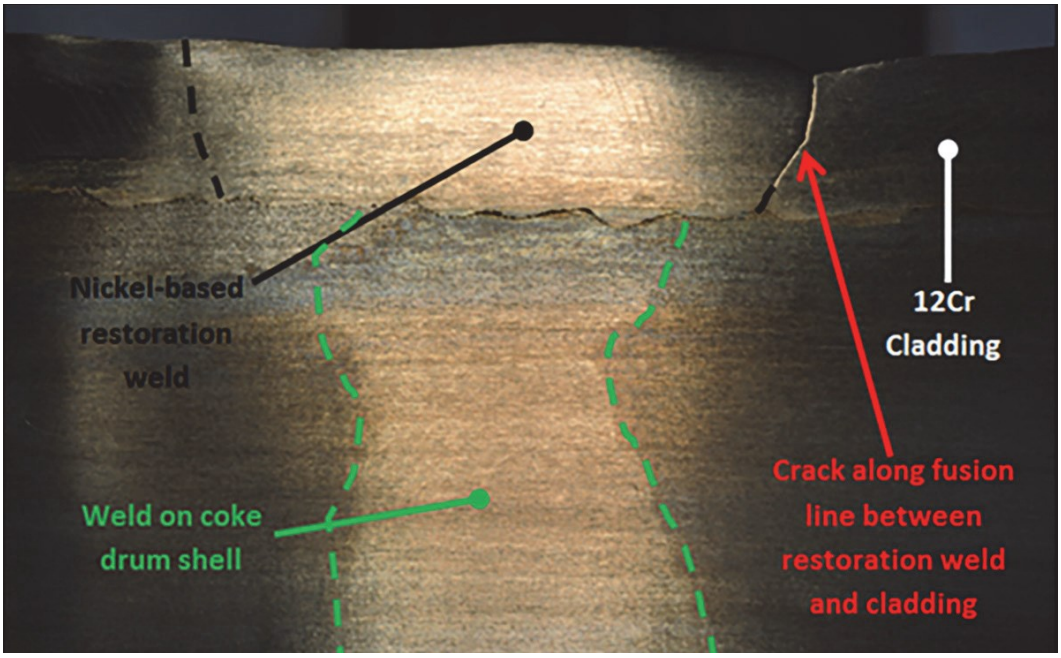

API 2013 Survey The 2013 survey wa published April, 2016 [5].

- *the survey reports on 164 drums*
- *75% of respondents reported that their drums' shell, cone and top of the skirt were fabricated from either 1 Cr – ½ Mo or 1¼ Cr – ½ Mo*
- *all materials showed a propensity to crack and bulge*
- *evaluation of responses related to the type of coke (shot, sponge and needle) and coke hardness showed no relation to the tendency for cracking and/or bulging*
- *furnace coil outlet temperature ranged from 896°F to 996°F with the average at 920°F.*
- *almost all respondents indicated a distinct difference between an initial quench rate and a final quench rate. Responses for an initial quench rate ranged from 42 to 350 gpm, while the final quench rate ranged from 400 to 6700 gpm, with a median final quench rate of 1013 gpm. 31% of the respondents reported that they also add quench water at the top of the drum*
- *44 of the 45 respondents reported their fill time for the operating cycle; the fill time ranged from 8 to 24 hours with an average time of 15.8 hours*
- *over 85% responded no to the question on whether an increase in the cycling frequency resulted in an increase in cracking rates*
- *20 of the 45 respondents reported the time in years and in a few cases the number of cycles before the first crack was observed in the skirt. The lowest number of years before cracks were observed was 5, while the average was 12 and the maximum number of years before cracks were observed was 29.*
- *71% of the respondents indicated that their coke drums were instrumented with either thermocouples and strain gauges or both. However, only 20% of those with instrumented drums reported using the information from the thermocouples and/or strain gauges to predict cracking and need for repairs, or to optimize operations during the cycle (such as during hot feed introduction and addition of quench water).*

Both the 1996 and 2013 surveys are very important in regard to benchmarking the analytical work presented in this thesis. The data contains extensive operational and inspection information and, although somewhat quantitative, lacks detailed data specific to the suspected primary damage mechanism to permit fully definitive engineering analysis and characterization of coke drum cracking.

2.2 Industry Practices

Industry may collaborate either through industry trade groups such as the ASME, API, DNV, EWI and others. In addition, joint industry programs [JIP] may be undertaken either publicly or exclusively among the JIP sponsors.

2.2.1 Industry Codes, Standards and Technical Reports

Industry has developed Codes and Standards since the first ASME Code committee was established in 1911 for the purpose of formulating standard rules for the construction of steam boilers and other pressure vessels [6].

The API and the ASME collaborated to produce a joint Code for Unfired Pressure Vessels first published in 1934. This effort has evolved into the ASME VIII Division 1 and ASME VIII Division 2 Codes for unfired pressure vessel construction. Reference to the term Code may mean either of these two Code sections, in this work. Collectively, the ASME Boiler and Pressure Vessel Code refers to twelve (12) sections covering heavy industry, nuclear facilities and commercial equipment.

Since pressure vessels are usually regulated by a jurisdiction through a competent regulator, other codes may be used in these jurisdictions.

ASME VIII Division 1

The basic construction Code for coke drums is ASME Section VIII Division 1 Rules for Construction of Pressure Vessels [6]. Engineering specifications provided by engineering contractors and equipment owners specify this Code and provides the “design by rules” determination of pressure thickness. Other Codes and standards are used to assess the coke drum when it has sustained damage such as bulging and cracking.

ASME VIII Division 2

ASME Section VIII Division 2 is a construction document which uses a "design by analysis" approach in the design of pressure vessels as an alternative to the "rules based" design of ASME VIII Division 1. As indicated, Division 2 provides an engineered approach to vessel design using detailed stress calculation, stress categorization and stress criteria to substantiate the design [7]. A methodology to address fatigue is provided which is motivated by fatigue initiation and uses the classic Wöhler S – N, stress – cycle life, design approach. However, pseudo – elastic stresses are used when yield strength is exceeded for simplification. More sophisticated analysis bases such as elastic – plastic methods are also allowed.

Fatigue curves are provided for smooth bar and welded joint specimens. Base material properties are designated as smooth bar design curves. The smooth bar fatigue curves may be used on components with or without welds.

A weld surface fatigue strength reduction factor [FSRF] is used to account for the effect of a local structural discontinuity or weld joint on the fatigue strength. It is the ratio of the fatigue strength of a component without a discontinuity or weld joint to the fatigure strength of a component with a discontinuity or weld joint. The concept is symbolized by K_f , in the Code, and values of the FSRF range from 1.0 to 4.0. The Code states that *fatigue cracks at pressure vessel welds are typically located at the toe of a weld. For as-welded and weld joints subject to post weld heat treatment, the expected orientation of a fatigue crack is along the weld toe in the through-thickness direction, and the structural stress normal to the expected crack is the stress measure used to correlate fatigue life data*.

Design fatigue curves for welded joints are presented on the basis of welded joint design with statistical confidence intervals varying from ± 68% to ± 99%, i.e. ± 1 σ to ± 2.33 σ.

This Code also provides for experimental stress and fatigue analysis. When invoked, temperature applicability is limited to not more than 700 °F [371 °C] and cyclic exposure to not exceed 50,000 cycles. The determination of fatigue strength uses a number of strength reduction factors to account for

- size
- surface finish
- cyclic rate
- test temperature
- thermal skin stress
- statistical variation

The strength reduction factors are prescribed by closed form expression. The establishment of a design curve is complex due to the number of factors and required manipulations.

The Code states a preference that the fatigue strength reduction factor be preferably determined by performing tests on notched and unnotched specimens, and calculated as the ratio of the notched stress to the unnotched stress for failure [7].

API 579 – 1 / ASME FFS-1 Fitness for Service

This is a dual marked industry practice document sponsored by API and ASME to determine the fitness of in-service equipment for continued operation in the event that damage is encountered in the equipment [8].

Stress analysis is required for many of the damage assessments and is detailed in Annex B1 of the standard. The methodology parallels ASME VIII Division 2 but does have peculiarities.

MPC Coke Drum Evaluation Report, 1999

An industry collaboration in 1999 resulted in confidential publication of the Materials Property Council [MPC] coke drum report. Sponsorship as a group project was provided by several DCU technology licensors, equipment owners and fabricators. The MPC is a not-for-profit scientific and technical corporation loosely aligned with the ASME. The report has restricted access [14].

The primary purpose of this effort was to establish evaluation procedures for coke drums in consideration of materials selection, evaluation software for bulging and cracking damage, repair guidelines, materials properties data and provision of a laser scan database for use with a software package called *CokerCola*™. Parametric finite element studies were completed to support the software.

The report provided focus on the operating conditions of coke drums and the role of water quenching in the development of thermo-mechanical strains. This provided definition to the vague descriptions of thermal fatigue stated in prior work.

Using experimental data from monitoring an operating coke drum, temperature and strain data were collected. The intent was to provide default histograms for use with the software; but, actual histograms can also be used to particularize results to the users' coke drums.

Fatigue failure is calculated in a two step process, crack initiation and crack propagation. Crack initiation is determined by the Manson – Coffin – Basquin expression (also known as "universal slopes") [15].

$$\frac{\Delta\varepsilon}{2} = \frac{\sigma_f}{E} \cdot \left(2N_f\right)^b + \varepsilon_f \cdot \left(2N_f\right)^c \qquad (2.1)$$

The exponent values b, c are calculated from the experimentally derived data for the other parameters contained in the expression.

Material properties are provided in an internal database and presented for interest. The material properties for welds are not differentiated. The source of the fatigue properties is not stated and inconsistent with properties listed in [12]. Also of interest is the uniformity in the listed values; the properties for TP 405 and TP410S stainless steels being identical to C – ½ Mo and Cr – Mo.

Crack propagation is modeled by use of the Paris equation available in the fracture mechanics literature [15].

For convenience, the Paris equation is provided herein;

$$da / dN = C \cdot \Delta K^m \qquad (2.2)$$

Strain histograms are included in the MPC document as an internal database and are categorized as light to severe. The strains are presented as strain ranges with an average strain range of

794 $\mu\varepsilon$ - 435 $\mu\varepsilon$ for -1σ log standard deviation

+ 966 $\mu\varepsilon$ for +1σ log standard deviation

The user may input temperatures, temperature gradients or strain gauge readings to generate a strain histogram for use by the program.

Figure 2.3 is a plot of the strain distribution with a negative skew in the data leading to modeling of the data as lognormal.

Figure 2.3 Strain Distribution as Provided by MPC [14]

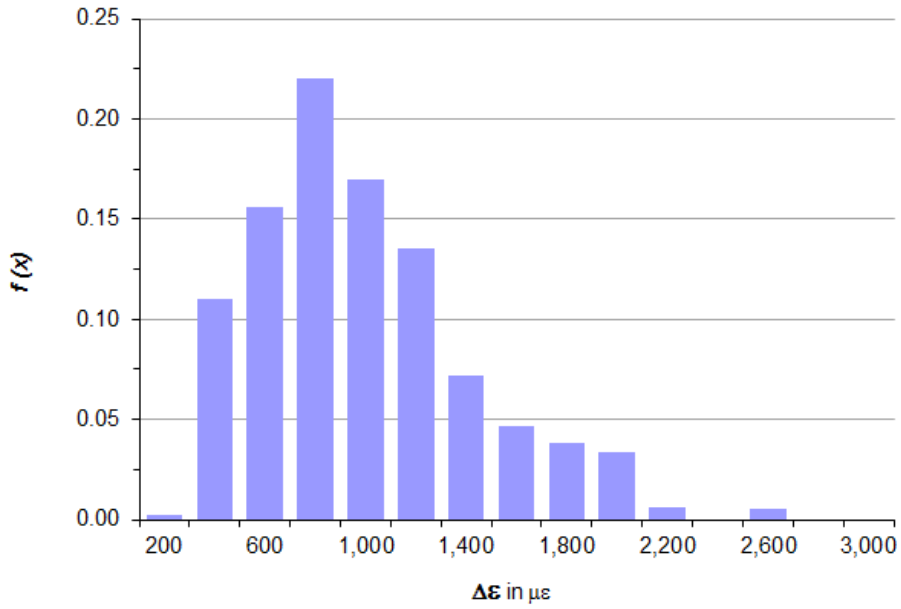

The strain range is asymmetric since the strains are lognormally distributed. The strains were also confirmed to be strain ranges and determined based on observation of strains during the quench wave ascribed to the rising water level during the quench phase.

Temperature gradients of approximately 1 F°/ inch to 14 F°/ inch are used in the software module. The actual temperature distributions were not used in the accompanying numerical analysis supporting the software.

A significant result of the MPC work is the assertion that strains could be adequately calculated through linear – elastic analysis.

Although bulges were evaluated, all bulge profiles use smooth transitions. The bulges were said to have little or no effect on thermal stresses due to axial temperature gradient but influence thermal stresses due to a circumferential gradient.

In general, feedback on the efficacy of the software is not widely available. Informal comment from a CRD partner indicates the software and methodologies are not sufficiently predictive or accurate to use results as a decision management tool.

API TR 934 – G

The API TR 934 – G is a comprehensive document covering

- a survey undertaken in 2013
- construction
- maintenance
- operations
- fitness for service evaluation

The release document contains some significant findings for consideration for this thesis;

- thermal fatigue is to be evaluated to the fatigue curves of ASME VIII Division 2; use limitations in temperature to 700 °F [371 °C] are not considered prohibitive
- alternatively, a fracture mechanics approach for identified cracks may be used; the use of industry practice documents API 579 / ASME FFS-1 may be utilized
- Cr – Mo materials are used in the Class 2 condition
- Cr – Mo materials in higher minimum yield strength to 60 ksi [415 MPa] are available for improved resistance to shell cylinder bulging
- reference to “ratcheting” mechanism leading to drum distortion
- bulging is attributed to differences in shell metal temperature
- circumferential cracking with and without noticeable bulging
- an alternative basis for material selection is fracture ductility such as exhibited by C – ½ Mo rather than Cr – Mo steels; bulging may be more prevalent but the tendency to crack will be reduced due to better ductility

The supply of the usual Cr – Mo materials of construction in minimum yield strengths to 60 ksi [415 MPa] would be considered special order since typical minimum yield strengths are much less than 60 ksi [415 MPa].

The document makes use of the terms “hot spot” and “cold spot” in regard to the design of the coke drum feed system; a single nozzle entry at the bottom of the vessel is seen to provide biased flow and promotes “hot / cold spots” on the vessel shell cylinder. A dual inlet nozzle is opined to better simulate a bottom center fluid up-flow to minimize “hot / cold spot” formation during the feed and quench phases [5].

BS PD 5500

British Standard PD 5500 Specification for Unfired Fusion Welded Pressure Vessels provides requirements for the assessment of pressure vessels subject to fatigue [16].

Although all North American jurisdictions use the ASME Code for pressure vessel construction and the dual marked standard, API 579 –1 / ASME FFS – 1 for fitness for service assessments, using PD 5500 for guidance in fatigue assessment is warranted based on its more transparent experimental data set including an explicit experimentally oriented treatment of welded construction and weld defects. The methodology is also much more streamlined to use thus making it more practical for industrial users compared to the “clean rewrite” edition of ASME VIII Division 2.

Major differences to the ASME Code approach are

- the nominal stress range is used in region of fatigue cracking to enter S – N curves
- the stress range is used to enter S – N curves, regardless of applied mean stress
- fatigue assessment is based on the primary plus secondary stress; i.e., direct stress is used [C.3.3.1]
- thermal stresses are treated as secondary stresses
- explicit attention is given to weld quality, both surface and through thickness condition; the limit on internal defects is more stringent
- justification for use of the design curve for unclassified details is based on testing; Table C.5 provides a factor to check against the published curves – this appears to be a design margin

Consistent with the ASME Code approach are;

- low cycle data uses a pseudo-elastic stress range (i.e., strain range multiplied by elastic modulus)
- S – N curves applicable to temperatures up to 350 °C [662 °F], creep is to be accounted for if the curves are used at higher temperatures
- Palmgren – Miner rule is used for limiting damage accumulation

2.2.2 Industry Trade Papers

Industry journals, conferences and symposia provide additional perspectives and insight into coke drum issues. Most are provided by the ASME Journal of Pressure Vessels and Piping and ASME PVP conference papers.

Local venues, especially in the US Gulf coast region provide opportunities for data sharing and networking, such as Stress Engineering Services Inc., a specialty engineering and design firm which hosts a coke drum reliability workshop on a regular basis in Houston, Texas [17].

Ramos, Rios Two papers by Ramos and Rios et al. explored low cycle fatigue tests for 1 Cr – ½ Mo and 1¼ Cr – ½ Mo low alloy carbon steel in base metal and welds in support of examining the fatigue life for the conventional shell to skirt connection and shell cylinder [18], [19].

Figure 2.4 presents a portion of the ε – N fatigue life testing observed by original testing in support of their work. Observations from the data indicate

- differing base metals exhibit similar ε – N life curves
- weld joints exhibit similar ε – N life curves, but lower than the base metal

Figure 2.4 Strain – Cycle Life for Cr – Mo Base and Weld Metal

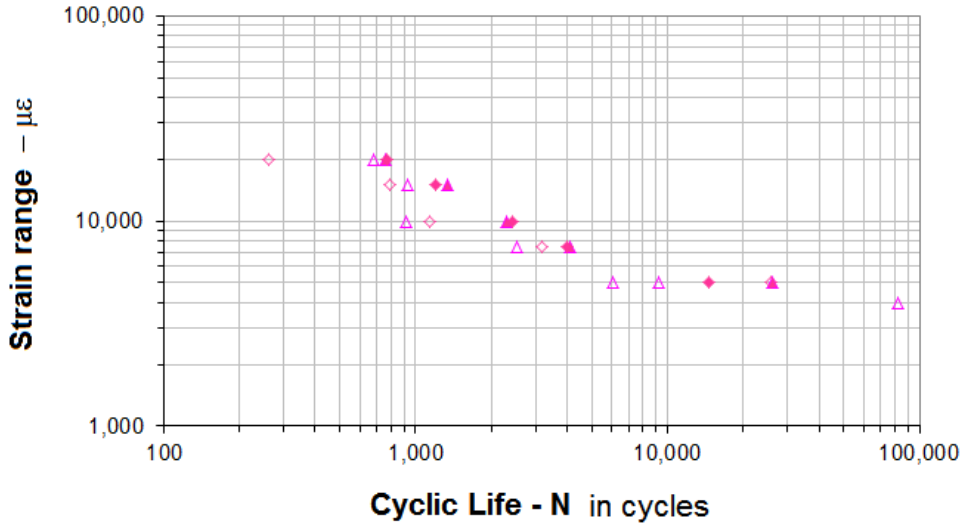

Notes
1 Open symbols present results from weld material
2 Closed symbols present results for wrought materials

The second paper describes a field study using temperature and strain gauge monitoring. A thermograph was presented which displayed a cold spot in the shell more than 400 F° cooler than the surrounding shell area and had formed within a 15 minute period. They noted that "*large strains will result from this temperature distribution due to differential thermal contraction*". The paper did not explore the extent to which these cold spots contributed to the observed strain ranges. Coke drum damage was ascribed to "*low cycle fatigue [LCF] is the main cause of damage in most coke drums. LCF is caused by cyclic strains.*" A cyclic strain range was defined as

$$\Delta\varepsilon = \max(\varepsilon_i) - \min(\varepsilon_i) \text{ at a point} \qquad (2.3)$$

where, max (ε_i) and min (ε_i) were defined to be the maximum and the minimum observed strain measured by strain gauge in one complete cycle. The cycle defined is an operational cycle.

The paper showed that lower shell strain ranges were related to reduced quench water rates.

Penso, Lattarulo et al. This paper from 1999 provides a thorough review of metallurgical analysis from coke drums and listed four different types and sites for cracking initiation and propagation [20]

- deep cracks in the clad HAZ
- shallow cracks in the clad
- interbead cracks in the high nickel weld
- inclusion cracks in the base metal HAZ

The parameters promoting crack initiation and propagation were listed as

- grain growth in the HAZ
- weld toe geometry
- strength mismatch among welds, clad metal and base metal
- thermal shock

Boswell, Farraro A 1997 paper on the experiences of a coke drum located at a refinery in Lake Charles, Louisiana suggests that the coke drum problems are accounted for by [21]

- repairs to the shell circumferential seams near large distortions,
- skirt junction cracking, and
- nozzle failure.

Presumably, failures of shell circumferential seams prompt repairs and these are more likely needed at large distortions. The paper also makes mention of local hot spots being identified and shows stress results for a quench cycle which attains a calculated strain of 3,090 $\mu\varepsilon$. This value matches the data of Ramos and Rios which showed a maximum strain of 3,400 $\mu\varepsilon$.

Boswell and Farraro introduce additional notions

- that the material elastic yield strength is related to low cycle fatigue and particularly the 2 · SY limit
- bulging is determined by the relative strength of the circumferential weld seam and the base metal
- a mechanical stress ratchet develops between weld seam and base metal
- when the weld seam has a higher yield strength than the base metal, the base metal distorts relative to the weld seam; the opposite occurs when base metal has higher yield strength than the weld metal
- wall thinning is suggestive of low cycle fatigue
- material properties are to be determined from samples removed from the drum
- the studied coke drum was built in 1968 and scheduled for replacement in 1996, a run of 28 years; accumulated cycles were approximately 5,497 cycles
- a fatigue life of 4,390 cycles was predicted using ASME VIII Division 2 Figure 5-110.1 which matches experience
- there are three stages to fatigue failure; from 50% to 95% of cyclic life cracks will grow to one-half (½) their final catastrophic size
- operating beyond 95% of cyclic life is dependent on finding, measuring and repairing the crack

Church, Lim, Brear et al. Church describes a damage mechanism for coke drums occurring during the quench phase involving "*contraction of a ring of the shell with a step change in diameter to the 'hot' coke drum above this quenched ring. This cold to hot shell transition (vase) rises up the drum wall with the steam and leads to the generation of thermal stresses* " [22].

Church considers a stress-based approach attributing stress development to through wall temperature gradients and the vasing effect from rising quench water. The stress amplitudes are derived, though, from measured strain amplitudes which are extracted from a distribution of measured strains.

At that point, Church describes a probabilistic methodology to predict the number of cycles to crack initiation, using the S – N fatigue life methodology and through-wall failure is determined by a linear – elastic fracture mechanics approach using the Paris expression (equation 2.2).

The strain or stress distribution is not provided but a cumulative probability distribution is shown that is benchmarked against an actual coke drum. The graph shows the following

- crack initiation begins at 1,000 cycles with 0.0001% probability, exponentially rising to 100% at 40,000 cycles
- cracking was actually observed at 2,000 and 3,000 cycles
- through – wall failure was predicted with 0.0001% probability at 4,000 cycles, rising exponentially to 100% at 50,000 cycles
- failure was actually experienced at 2,800 cycles

From the predicted values, the trouble free life of coke drums should be up to 30,000 cycles (P = 50%) or, nominally 82 years of operation, based on crack initiation.

Boswell, Wright This paper is an update of the prior paper by Boswell. A number of comments are made with regard to the operation and understanding of coke drum cracking failures [23].

- reduction of oil fill cycle times is down to 12 hours
- operating temperatures increased to 800 °F [427 °C]
- improved attention to fatigue compatible design details
- reference to US patent 5827403 which lists design improvements and material selection requirements to resist shell bulging and cracking
- coke crushing is attributed as the primary transient load causing high shell stresses leading to ratcheting
- formation of hot and cold spots is identified
- cracking due to creep and fatigue from hot oil contacting shell
- recommend coke drum materials of 2¼ Cr – Mo and 3Cr – Mo

The paper identified the formation of hot and cold spots from the non-uniform distribution of quench water but the significance of these hot and cold spots is not developed. The primary focus for the development of large stresses is the concept of coke crushing.

Ohata et al. The authors recognize the role of quenching in the cracking of girth (circumferential) welds and bulging of coke drums. Bulges are associated with this cracking through development of stress and strain concentrations. The issue of weld mismatch is raised in explaining the bulging profile of the drum shell and a figure is given that is consistent with the bulge characterization of Weil and Rapasky, already presented in **Figure 2.1**. The thermo-mechanical loads are developed through a heterogeneous axial temperature profile that was governed by the cooling of the shell by quench water attenuated by adherent coke on the shell. Stress amplitudes of 400 MPa [58 ksi] are calculated. An equivalent plastic strain of 2,000 με was reported. Mechanical properties were established by tensile testing; it is not clear whether cyclic or monotonic testing was used [24].

Yamamoto A second study by Yamamoto used direct data from a field study of more than 200 operational cycles of data and expanded on the sensitivity of the response of the coke drum shell temperature to coke film thickness. Simulation of heat transfer coefficients with variable adherent coke thickness varying from 0 mm [0 inch], 0.2 mm [0.008 inch] and 2.2 mm [0.087 inch] enabled close approximation of numerical results to actual strain measurements [25]. The effect on heat transfer was demonstrated to be uniform over a 30 minute cooling transient when comparing 3 separate locations during the same quench period.

The investigation demonstrated that the calculated mechanical strains at the inner surface of the drum could be as much as 30% higher than the measured strains on the outer surface, where the strain gauges were mounted, over the range of heat transfer rates. Bulging was characterized as being accumulative, eventually growing to a notable bulging deformation. The bulging is influenced by weld to base metal yield strength mismatch. The researchers tabled a number of opportunity areas to improve shell reliability.

Most of these are consistent with vessel construction practices and reflect modern improvements that have been undertaken by vessel designers since construction standards of earlier drum construction.

Other significant factors identified in this paper are

- the strength mismatch between weld and base metal,
- material yield strength,
- difference in the coefficient of thermal expansion between clad and base
- chemical makeup of the bitumen feed

Samman & Samman The paper explores in detail the effect of shell bulging on the reliability of coke drums. The authors opine that a Level 3 assessment to API 579 –1 / ASME FFS – 1 was not feasible due to the complex and random nature of the thermo-mechanical loads [26].

A linear – elastic analysis is presented which attempts to assess the severity of bulging and make prediction of the likelihood of bulging failures. Their experience suggests that neither the magnitude nor location of maximum stress at bulges correlate well with reported failures. The study conclusion is that linear elastic stress analysis may lead to erroneous conclusions since the dominant failure mode is strain – based and also, when a bulge is located in a vessel with global and / or local ovality. Stress concentrations were shown to reach 30:1 when ovality was present.

Samman, Tinoco and Marangone The authors explore stress and strain based approaches to benchmark performance for four operating coke drums of 1Cr – ½ Mo and TP 405 clad construction experiencing bulging and bulging induced cracks [27]. Earlier methodologies by Samman et al., known as the Bulge Intensity Factor [BIF™] and stress based approaches appear to be repudiated by the author since both false positives and false negatives were cited in using the methodology [28]. **Figure 2.5** illustrates the output from a BIF™ analysis.

Figure 2.5 Characterization by Bulge Intensity Factor [28]

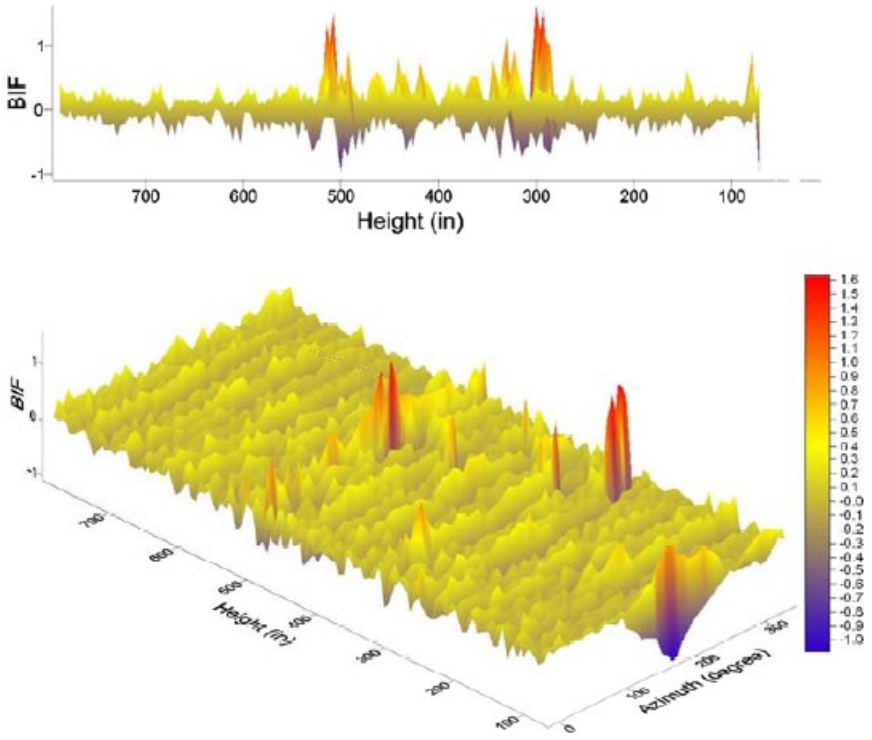

Two (2) of these drums had bulging related cracks within seven (7) years of commissioning. The drums suffered vertical bulging but cracking occurred in a single severe circumferential bulge about mid-height at or near a circumferential weld seam. The bulge was approximately 2⅜" [60 mm] over a height of 36" [910 mm], a relatively sharp peak.

Samman performed linear-elastic stress based studies with internal pressure loading, only and showed stress concentrations of up to 8. The areas of highest stress concentration did not correlate with bulge peaks and crack locations but rather at locations exhibiting local ovality. Thermal loading was not attempted by Samman "*given the randomness and complexity of thermo-mechanical loads …and the number and interconnectedness of bulges, it is virtually impossible to simulate the deformation process for entire drums . . .* ".

Strain based analysis was performed and a Plastic Strain Index [PSI] criteria concept was used to rank the calculated strains against the local strain limits given in API 579 – 1. The strain based approach was reported to correlate well with the damage locations.

Calculation of strains was based on a very simplified approach using the engineering definition of strain with change in length determined directly from the change in length between the original and deformed geometry as measured by laser scans; thus, strain was simply calculated using

$$\varepsilon = \frac{\Delta l}{l} \tag{2.4}$$

The actual application is not detailed. Although the correlation between PSI and failures appears reasonable, the strain limit criteria of ASME VIII Division 2 is used to protect against local failure. Its use as a fatigue limit criteria is arbitrary and serendipitous.

2.3 Summary

The relevant findings in the literature review can be summarized as follows.

Industry Surveys

While the surveys are helpful in forming an insight into coke drum issues and to help benchmark engineering analysis of coke drum integrity and reliability issues, they are largely qualitative and subjective and need to be used judiciously. The surveys have influenced the research to concentrate in areas that are not fully productive, some of which carries over to modern research efforts.

Some examples and comments are;

Weil & Rapasky [3]

- shell bulge profiles displaying large bulging at the bottom shell course and then diminishing is inconsistent with the bulging shown in laser scans where both vertical and circumferential bulging are evident
- the report also gave the impression that all bulging was constrained at the circumferential welds
- the Unit Quench Rate appeared to be a promising operational parameter but was not validated

Yamamoto and the Sumitomo researchers appear to have been influenced by the bulging characterization of the paper, as well as the Penso paper to concentrate on the concept of weld to base metal strength mismatch as a contributor to weld cracking.

API Survey 1968, 1980 [4]

- the actual surveys from 1968 and 1980 are no longer available
- survey methodology consisted of cataloging drum construction and failure counts
- analysis consists of simple correlation between drum thickness and incidence of through-wall cracking
- recorded a trend in material selection from C – ½ Mo to Cr – Mo steels

These surveys did not lead to more quantitative assessments.

API Survey 1996 [13]

- the survey continued with cataloging of trends, damage features and explored a number of correlations, such as
  - material selections to cycles for 1st through-wall crack
  - diameters to cycles for 1st through-wall crack
  - drum wall thickness to cycles for 1st through-wall crack
  - material selections to cycles for 1st shell bulge
  - diameters to cycles for 1st shell bulge
  - drum wall thickness to cycles for 1st shell bulge

- other similar correlations used furnace outlet temperature, fill time, steam strip time, proofing rate, quench rate, final quench rate

The survey did not review any analytical work on coke drum bulging and cracking.

The following descriptions from the survey are helpful in confirming research direction

- some 60% of vessels underwent shell bulging with cracking occurring in 90% of those; cracking only occurred in less than 10% of vessels without bulges
- cracking occurred in circumferential direction 97% of the time
- most cracks were in shell courses 3, 4 and 5

Material Properties Council [14]

The report is confidential and limited to the sponsoring group and not available to the public. It is not known with any certainty as to how effective the report and software module have proven. An MPC sponsor, who has also sponsored the CRD at the University of Alberta has commented that the software is not sufficiently predictive to be of practical use.

Our review of the report indicates the premise of the work is essentially sound and recognized some key concepts; however, the detailed effort relied on assumptions and expediencies and requires a high level of understanding of the drum thermo-mechanical loading and shell condition by users.

- thermo-mechanical loading was recognized as a key damage mechanism
- bulging was seen as an accelerator of crack damage
- bulging models were idealized using smooth transitions
- stainless steel, C – ½ Mo and Cr – Mo grades were assigned the same material properties
- crack damage was evaluated in two (2) parts; initiation and propagation
- crack initiation was based on a fatigue service life basis; it appears the data from Ramos was used [18]
- strains were determined from measurement and calculation
- temperature surveys were utilized to calculate vessel stresses and subsequent strains using temperature gradients
- vessel shell strains were best characterized as a log-normal distribution
- a service fatigue life was calculated using the log-normal distribution and bulge profile

A user would not be sufficiently informed to use the software effectively without

- a temperature profile
- an accurate dimensional scan
- a statistical thermo-mechanical strain profile

API TR 934 – G [5]

The document provides no additional insights into analytical evaluations of coke drum damage. A number of statements are made gratuitously and not demonstrated:

- that all thermal cycles are severe and contribute to ratcheting
- that circumferential weld cracking is due to the dissimilar weld fabrication
- Cr – Mo materials are more resistant to bulging on account of higher yield strength
- bulging is caused by coke crushing
- coke drums experience creep

The study makes note of an alternative material selection using C – ½ Mo for improved fracture ductility.

Industry Codes and Standards

While ASME VIII Division 1 is the code of construction for coke drums, ASME VIII Division 2 and API 579 – 1 / ASME FFS – 1 contain core design by analysis techniques to evaluate drum service life and damage. Portions of the calculation methodologies contained in API 579 – 1 / ASME FFS –1 duplicate the methodologies of ASME VIII Division 2.

The specific content of ASME VIII Division 2 and API 579 –1 / ASME FFS –1 which support an accurate drum assessment include detailed

- stress and strain based calculation approaches
- elastic and elastic – plastic material models
- stress and strain based criteria for local failure
- fatigue stress criteria based on stress fatigue curves
- fatigue strain criteria based on conversion to a structural stress range
- material creep data

The technical tools appear to be sufficient but with specific qualifications and limitations;

- the material fatigue curves
  - are design curves and not service life curves and, hence, do not calculate actual anticipated fatigue life
  - are based on material groups rather than being particularized for the specific material

- the material fatigue curves for welded joints are presented using statistical confidence intervals and,
  - are based on material groups rather than being particularized for the specific material

- strength reduction factor for welds
  - are provided on the basis of being weld surface fatigue strength reduction factors

- using a stress based focus, rather than strain based obscures the phenomenological relationship between low-cycle thermo-mechanical loading and service life

Industry Papers

The industry papers are relatively sparse, but understandable given the difficulty and expense in collecting temperature and strain data; much of the available work is confidential and closely held by industry sponsored groups such as the MPC and individual users.

The following observations and conclusions recur in the small body of open literature, although none of which are quantifiably demonstrated;

- temperature loading is most severe during the quench phase leading to thermo-mechanical strains
- cyclic thermo-mechanical strains are sufficiently severe to cause shell cracking
- thermo-mechanical loading is attributed to thermal gradients through the shell thickness
- thermo-mechanical loading is attributed to the circumferential and axial gradients as measured by OD mounted thermocouples
- thermo-mechanical loading is attributed to the temperature differences between regions as measured by OD mounted thermocouples
- crack failures are influenced by weld to base material strength mismatch
- crack failures are influenced by local shell distortions
- crack failures are influenced by weld quality defects
- shell bulging is attributed to use of low yield strength materials and coke crushing
- a strain limit criteria via a strain index criteria is of limited utility; it is acceptable for static criteria but gives no insight of fatigue life
- cracking can be reduced if higher alloy materials are used

2.4 Commentary

The following detailed commentary is provided in regard to the findings from research into the industry literature on coke drum cracking failures;

1. contrary to industry practice and regulatory requirements, the industry has not been able to provide definition of thermo-mechanical loadings for a coke drum, leading to an inability to determine an equipment benchmark service life

2. that fatigue assessments are made using material design fatigue curves rather than material service fatigue curves

3. that fatigue assessments are made with apparent incorrect determination of strain ranges and counting of cyclic exposures

4. while temperature mapping of the coke drum is technically easy, use of these profiles has been not been effectively utilized

5. the impact of the mismatch in the coefficient of thermal expansion between the clad liner (TP 410S stainless steel) and base material (C – ½ Mo, Cr – Mo) materials has not been generally recognized or used in fatigue assessments

6. the trend in using higher yield strength Cr – Mo materials since the mid-1960's has inadvertently resulted in drums being constructed from lower fatigue strength materials

7. weld fatigue strength and fatigue strength reduction has not been adequately recognized

8. that the dependence of fatigue strength reduction on the magnitude of strain / stress exposure is considered in industry practices. but is overly conservative

9. thermo-mechanical strain has not been explicitly addressed in coke drum design practice

10. the impact of shell bulging is thought to be a hindrance for determining a benchmark service fatigue life

11. thermal shock on surface strain development has been overlooked, the magnitude of this strain matches the large strains developed from through thickness temperature gradients

12. drum operation is not adequately considerate of the impact of quench water flow rates on the severity of thermomechanical loadings on the shell

2.5 Evaluation

Detailed comments are made for the first eight points as they will be addressed in the analytical section of this thesis.

1. contrary to industry practice and regulatory requirements, the industry has not been able to provide definition of thermo-mechanical loadings for a coke drum, leading to an inability to determine an equipment benchmark service life

   Coke drum construction specifications do not provide definition of thermo-mechanical loadings, only stating design temperatures, operating and design pressures, weight and environmental loadings. Temperature gradients and differences acting on the vessel shell are not available from equipment users due to the expense of temperature surveys of existing equipment and the lack of cooperation within the industry.

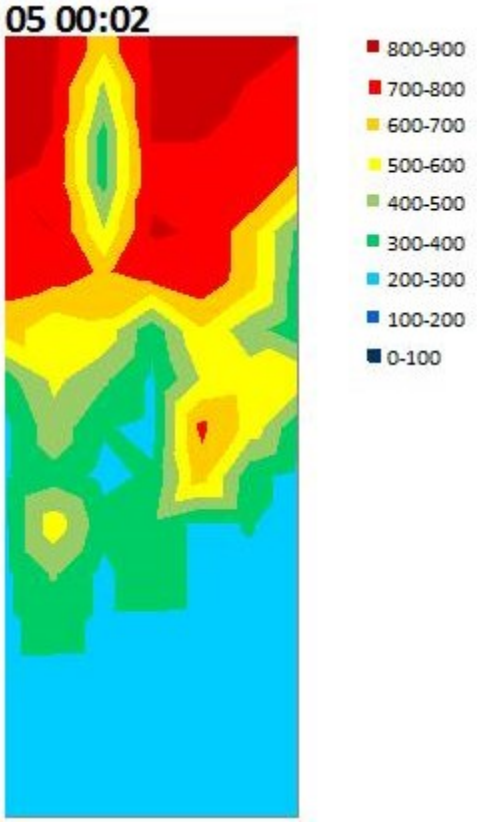

There is no published methodology in the industry literature on coke drum life assessments for using temperature profiles to determine thermo-mechanical loading.

A snapshot of shell temperatures is provided in **Figure 2.6** for a panel section of a coke drum during a quench sequence.

The panel is populated by one hundred nineteen (119) thermocouples arranged in seventeen (17) rows by seven (7) columns. Data was taken every minute for several months.

Figure 2.6 Coke Drum Shell Temperatures in [°F]

2. *that fatigue assessments are made using material design fatigue curves rather than material service fatigue curves*

   The conventional practice has been to use the ASME VIII Division 2 fatigue strength data. Earlier editions of ASME VIII Division 2 (prior to the 2007 edition) used a design margin of 2.0 on stress / strain or 20 on cycles, whichever was more conservative at each data point [29], [30].

   The margin on cycles was apportioned according to

   - 2.0 for scatter of data
   - 2.5 for size effect
   - 4.0 for surface finish, environment

   The most recent edition of the Code cites cyclic life values for smooth bar and weld joint specimens. The data for smooth bar specimens duplicates the life data provided in the earlier editions of the Code.

   The design curves are provided on a material group basis, e.g. carbon steel, low alloy ferritic steel, stainless steel, high alloy versus individual material grades which obscures actual fatigue performance for a specific material.

   Figure 2.7 shows the ASME fatigue design curve plotted against the data provided in **Figure 2.4.**

Figure 2.7 ASME Code Strain – Cycle Life Compared to Data

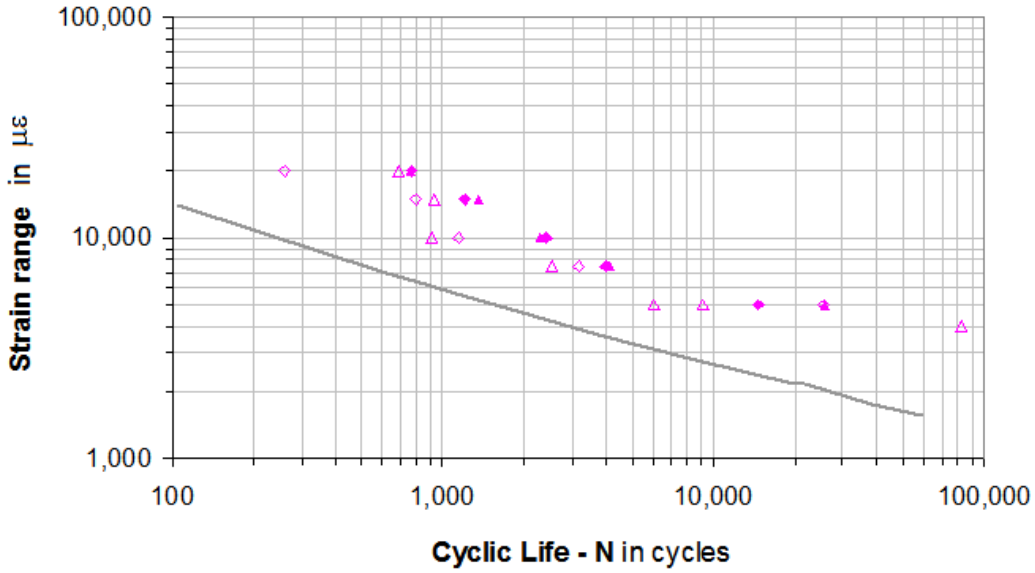

Notes

1 Data points from Ramos [19]

2 Smooth bar design curve from ASME VIII Division 2 [7]

Figure 2.8 compares the ASME strain – cyclic curve, ε - N against values calculated by the MPC method. The MPC method is intended to provide a service based estimate of drum life for measured conditions.

Figure 2.8 ASME Code Strain – Cycle Life Compared to MPC Data

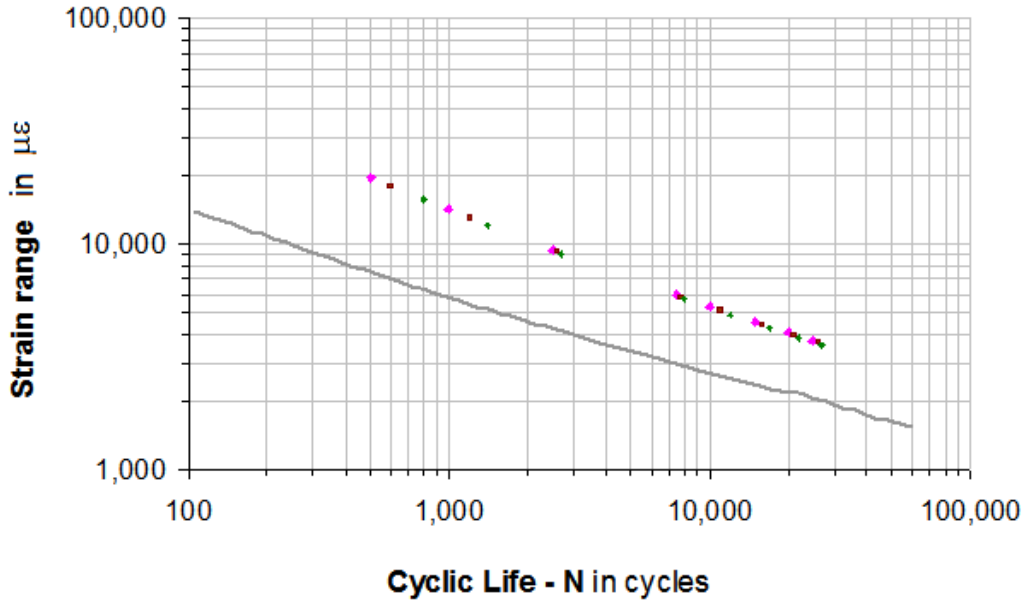

Notes

1 Data points from MPC Figure 3.1 [14]

2 Smooth bar design curve from ASME VIII Division 2 [7]

3. *that fatigue assessments are made with apparent incorrect determination of strain ranges and counting of cyclic exposures*

Strain ranges cited in all works are based on the measured strain range during an operational cycle. A strain gage can measure both compressive and tensile strains; for most of the strain exposures measured on the shell OD, the strain data shows the strain is either essentially tensile or compressive during the operational cycle.

Figure 2.9 shows strain profiles collected through five (5) operational cycles for three (3) strain gages mounted at the same elevation. Each operational cycle is about twenty four (24) hours in duration. The tracing spikes occur during the quench phase and display predominantly as either tensile or compressive strains and not as fully reversed strains.

The reported strain range is given as the range for each operational spike, only.

Consider the trace in **Figure 2.9**, a maximum tensile strain of 1,290 με is recorded in cycle 3, the minimum strain during the cycle is near 0 με. In cycle 4, a maximum tensile strain of 180 με and minimum compressive strain of 1,940 με is experienced. A strain range of 1,940 με is recorded for the operational cycle. However, the correct strain range for the two operational cycles is 1,290 – (– 1,940) or 3,230 με.

Figure 2.9 Strain Profile for Five Operational Cycles

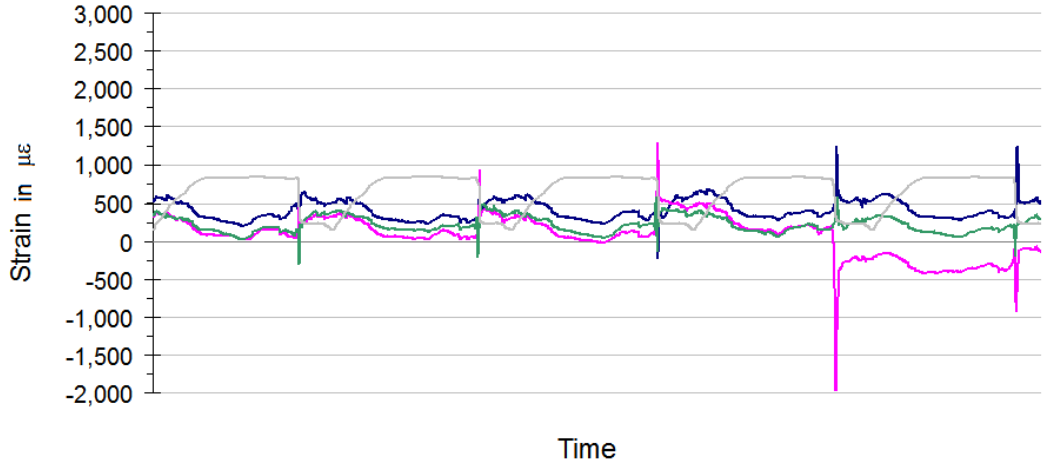

Notes
1 Time scale reflects data from five operational cycles

The conventional nomenclature used by industry practitioners conflicts with Code convention. The Code provides the following definitions [7]:

Cycle – A cycle is a relationship between stress and strain that is established by the specified loading at a location in a vessel or component. More than one stress-strain cycle may be produced at a location, either within an event or in transition between two events, and the accumulated fatigue damage of the stress-strain cycles determines the adequacy for the specified operation at that location. This determination shall be made with respect to the stabilized stress-strain cycle.

Stress Cycle – A stress cycle is a condition in which the alternating stress difference goes from an initial value through an algebraic maximum value and an algebraic minimum value and then returns to the initial value. A single operational cycle may result in one or more stress cycles.

Operational Cycle – An operational cycle is defined as the initiation and establishment of new conditions followed by a return to the conditions that prevailed at the beginning of the cycle. Three types of operational cycles are considered:

1. *the startup-shutdown cycle, defined as any cycle which has atmospheric temperature and/or pressure as one of its extremes and normal operating conditions as its other extreme;*

2. *the initiation of, and recovery from, any emergency or upset condition or pressure test condition that shall be considered in the design; and*

3. *the normal operating cycle, defined as any cycle between startup and shutdown which is required for the vessel to perform its intended purpose.*

The nomenclature practice among equipment users is to designate the process operation illustrated in **Figure 1.3** as an operational cycle.

Figure 2.10 illustrates the notion of the process operational cycle and Code practice operational cycle. Process operational cycle 3 displays an apparent strain range of 1,290 $\mu\varepsilon$ while process operational cycle 4 displays an apparent strain range of 1,940 $\mu\varepsilon$. However, terminology consistent with Code intent means that the strain range is 1,940 – (– 1,290) = 3,230 $\mu\varepsilon$.

Figure 2.10 Notional versus Code Operational Cycle

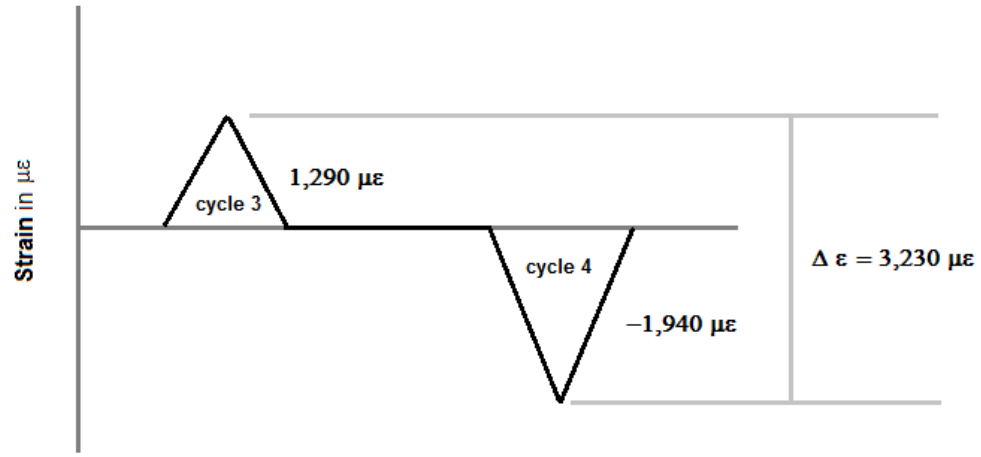

The Code compliant cycle counting technique is performed by pairing sequentially the maximum peak to minimum valley strain values over all the operational cycles over the entire loading block. The loading block is the representative count of process operational cycles that precisely reflect the repetitive cyclic loading. In regards to the rainflow cycle counting technique, Collins advises [15]

"*If cycles are to be counted over the duration of a duty cycle or mission profile block that is to be repeated block after block, the cycle counting should be started by initiating the first rain drop either at the most negative valley or the most positive peak, and continuing until all cycles in a complete block have been counted in sequence. This procedure assures that a complete strain cycle will be counted between the most positive peak and most negative valley in the block.*"

This parallels the methodology of [7, 8] which reference the rainflow counting technique, Annex 5B paragraph 5.B.4 [7] and Annex B3 paragraph B3.4 [8]. A more intuitive and uncomplicated approach is recognized by both these industry documents as the "max / min" technique and follows discussion of the rainflow technique in those documents.

4. *while temperature mapping of the coke drum is technically easy, use of these profiles has been not been effectively utilized*

   Samman states that "*shell bulges and cracks could not be readily assessed using this industry standard* [i.e., API 579 –1; author's note] *because of the randomness and complexity of defining the cyclic thermo-mechanical loads that the shell experiences during operations"* [26].

   The MPC document reports that it uses the equipment users temperature or strain histogram when available [14]. The temperature histogram appears to be based on a concept of "thermal demand" wherein temperature gradients are determined to calculate a thermo-mechanical strain. Strain gages are used sparingly due to their cost and short time reliability.

   Ramos noted the formation of cold spots but did not calculate thermo-mechanical strains using the temperature differences between shell locations and used strain gage readings [19]. Ramos used seventy five (75) thermocouples and six (6) strain gages over a grid of 2.7 m x 9.3 m.

   This thesis uses the temperature readings directly to determine the thermo-mechanical strains. Good agreement is achieved by comparison to strain measurements.

5. *the impact of the mismatch in the coefficient of thermal expansion between the clad liner (TP 410S stainless steel) and base material (C – ½ Mo, Cr – Mo) materials has not been generally recognized or used in fatigue assessments*

Although the MPC recognized thermal mismatch between cladding and base material, an over simplified strain relation was provided

$$\Delta\varepsilon_{\text{cladding}} = \gamma\,(T_{\text{operating}} - T_{\text{ambient}}) \qquad (2.5)$$

To account for the expansion mismatch of both clad and base material , the following was established by Aumuller [31];

for the clad layer

$$\sigma_c = \frac{(\alpha_b - \alpha_c)\cdot(T_h - T_0)\cdot E_c}{1 + \dfrac{t_c \cdot E_c}{t_b \cdot E_b}} \cdot \frac{1}{1-\mu} \qquad \text{and,} \qquad (2.6)$$

for the base layer

$$\sigma_b = \frac{(\alpha_c - \alpha_b)\cdot(T_h - T_0)\cdot E_b}{1 + \dfrac{t_b \cdot E_b}{t_c \cdot E_c}} \cdot \frac{1}{1-\mu} \qquad (2.7)$$

Substitution with actual material property values indicates that the clad layer will be in tensile stress and the base material layer will be in compressive stress when the vessel is exposed to a temperature above reference (T_0).

6. *the trend in using higher yield strength Cr – Mo materials since the mid-1960's has inadvertently resulted in drums being constructed from lower fatigue strength materials*

Strong materials, i.e., materials with high monotonic yield strength have been shown to not necessarily possess high fracture ductility or fatigue strength. The concept is illustrated in **Figure 2.11** showing that carbon and C – Mo have better low cycle fracture and fatigue strength in comparison to Cr – Mo low alloy steels currently favoured by equipment users [30], [32].

Figure 2.11 ε – N Fatigue Life for Pressure Vessel Steels

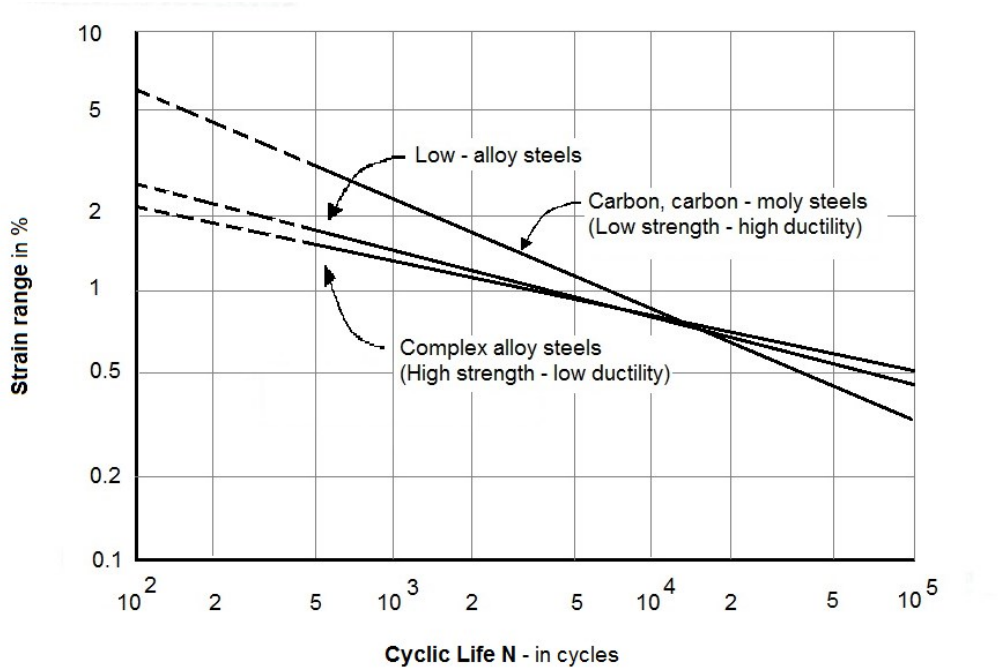

A combination of high plastic fatigue fracture ductility and fatigue strength over the cyclic life of interest, from start to 20,000 cycles, leads to the notion of relative fatigue toughness for C – Mo steels over Cr – Mo steels [33]. Original data, such as presented in Figures 2.12 – 2.17, indicates similar trending but that strain exposure below 3,500 με converges for the two materials with a slight advantage for C – Mo steels in TMF loading (Figure 2.13).

Table 2.1 quantifies the concept of ductility compared to material strength. C – ½ Mo is shown to have a higher proportional strain limit compared to Cr – Mo alloys except for 1 ¼ Cr – ½ Mo at 100 °F, only. In all other situations, C – ½ Mo is shown to have greater ductility.

Since the materials undergo cyclic loading, it is necessary to consider the cyclic properties for a more accurate estimation of a cyclic elastic strain limit. This is addressed in Chapter 3.

Table 2.1 Monotonic Code Properties for Materials of Construction

	SMYS [ksi]		SMTS [ksi]		E [10^3 ksi]		ε_{SMYS} [%]	
	100 °F	900 °F	100 °F	900 °F	100 °F	900 °F	100 °F	900 °F
SA 240 405	25.0	16.9	60.0	44.0	29.0	23.2	0.086	0.073
SA 240 410S	30.0	20.3	60.0	44.0	29.0	23.2	0.103	0.088
SA 516 70	38.0	24.0	70.0	52.3	29.2	22.5	0.130	0.107
SA 204 C	43.0	30.0	75.0	69.7	28.9	22.2	0.149	0.135
SA 302 B	50.0	34.9	80.0	73.1	28.9	22.2	0.173	0.157
SA 302 C	50.0	34.9	80.0	73.1	28.9	22.2	0.173	0.157
SA 387 12	40.0	27.2	55.0	51.4	27.7	23.2	0.144	0.117
SA 387 11	45.0	30.6	60.0	55.8	27.7	23.2	0.162	0.132
SA 387 22	45.0	32.4	60.0	58.2	30.5	25.6	0.148	0.127
SA 387 21	45.0	32.4	60.0	58.2	30.5	25.6	0.148	0.127

Notes

1 SMYS, SMTS, E derived from reference [12]

2 Values of ε_{SMYS} are calculated according to SMYS / E

Included in **Table 2.1** is SA 302 C, a steel used in the nuclear industry where transient temperature loadings occur in certain equipment [34]. The nominal composition is described as Mn – ½ Mo – ½ Ni. Although SA 204 C is referenced conventionally as C – ½ Mo, its nominal composition is C – Mn – ½ Mo. Since SA 302 C has comparable carbon content the steels should be compared by nominal composition, as

- SA 204 C C – 1 Mn – ½ Mo
- SA 302 C C – 1½ Mn – ½ Mo – ½ Ni

For high strain exposure, both of these low alloy steels have greater fatigue strength with SA 204 C showing improved ductility to SA 387 steels at ambient and high temperatures. SA 302 C shows markedly improved ductility to SA 204 C and SA 387 steels as an apparent result of increased Mn and Ni content.

Fatigue strength testing shows C – ½ Mo steels with greater fatigue life than Cr – Mo steels below 10,000 cycles per **Figure 2.12** [35]. These results occur under isothermal low cycle fatigue loading (ILCF).

Figure 2.12 Cycle Fatigue Life C – ½ Mo vs Cr – Mo at 900 °F [35]

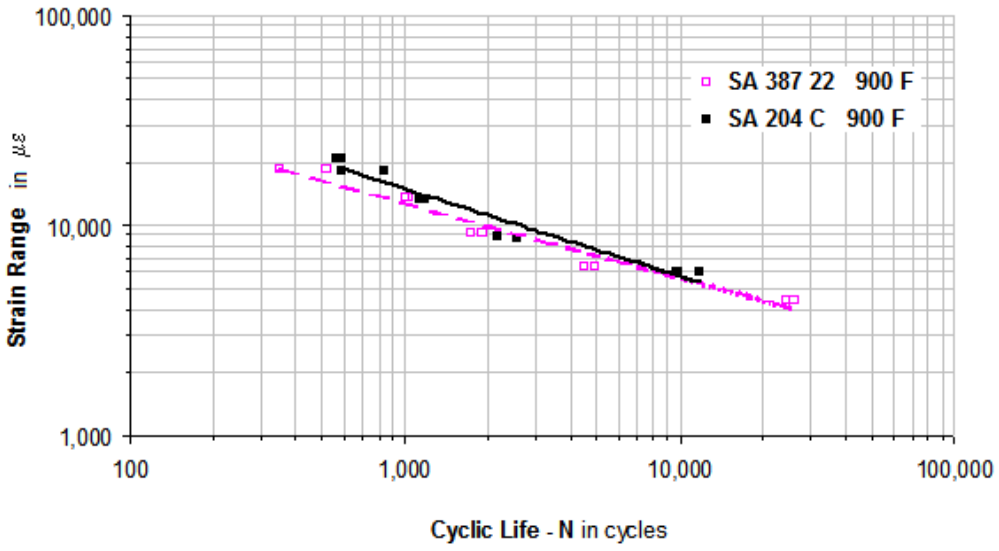

In **Figure 2.13**, C – ½ Mo steels indicate consistently better fatigue life than Cr – Mo steels under low cycle thermo-mechanical fatigue loading (TMF) over an extended cyclic range.

Figure 2.13 Cycle Fatigue Life C – ½ Mo vs Cr – Mo (TMF) [35]

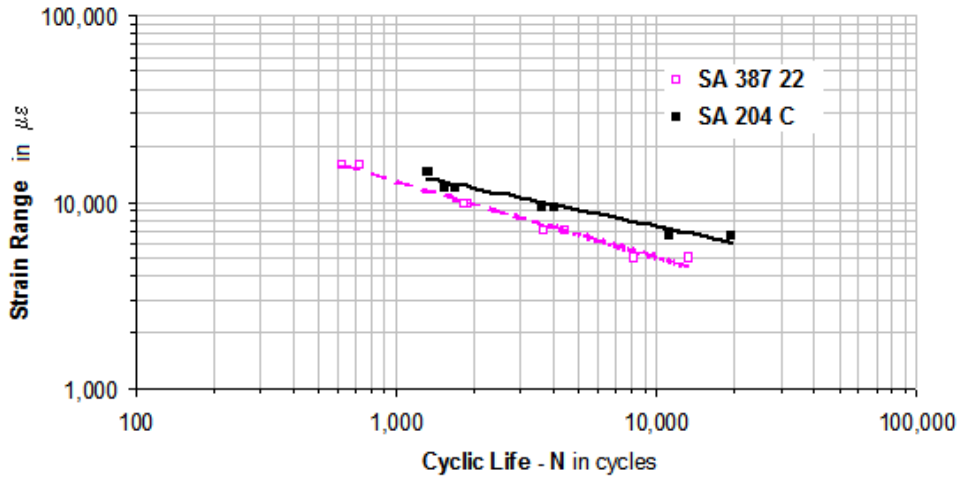

7. *weld fatigue strength and fatigue strength reduction has not been adequately recognized*

Weld fatigue strength is not accounted for in the MPC work.

Up to the 2007 edition of the ASME Division 2 Code, weld fatigue strength was accounted for on the basis of a fatigue strength reduction factor to be applied by the practitioner. Values were typically 2 for butt welds based on learnings from related piping construction codes [36]. This is still a current practice [37].

Current industry practice using ASME VIII Division 2 and API 579 –1 / ASME FFS – 1 account for weld material explicitly using fatigue strength curves for weld joints

Figure 2.14 compares the weld joint fatigue strength to the data of Ramos and Chen. It can be seen that the expected or average weld joint fatigue strength is well below the measured data. The + 3σ weld joint strength is just below the measured data which includes base and weld joint material.

Figure 2.14 Experimental Fatigue Strength vs ASME Code

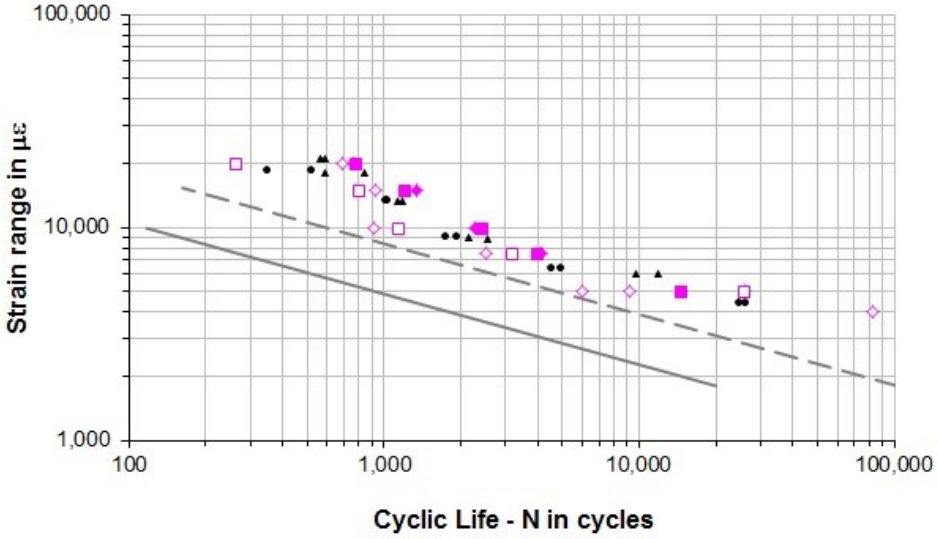

Notes

1 —— ASME average fatigue curve, welded joint, 900 °F
2 – – – ASME +3σ fatigue curve, welded joint, 900 °F
3 Individual symbols are data from Ramos [19] and Chen [35]

The data from Ramos, shown in **Figure 2.15** indicates lower fatigue strength for weld joints with very wide dispersion in the data.

Figure 2.15 Smooth Bar vs Welded Joint Fatigue Life, Ramos [19]

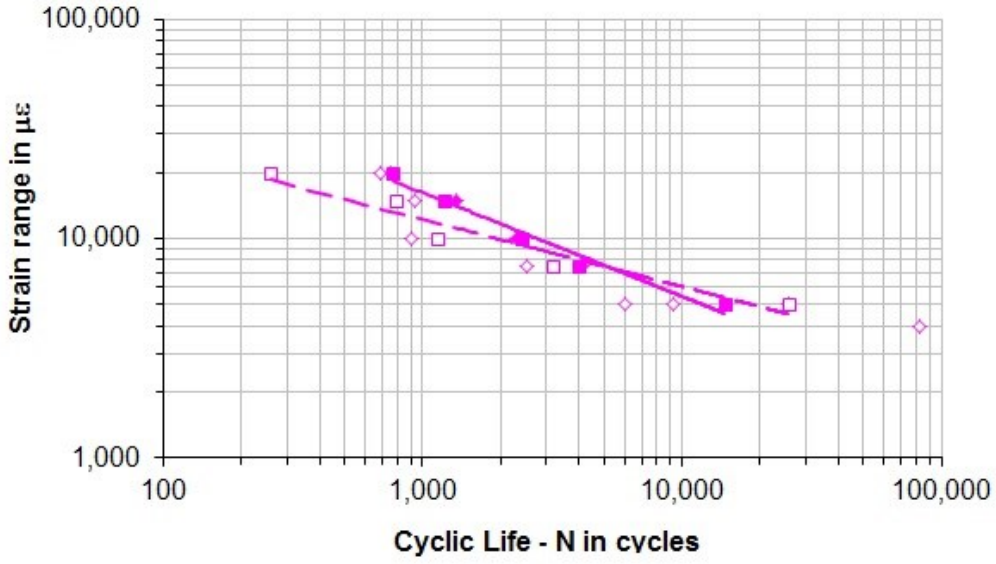

Notes
1 smooth bar data for SA 387 11, 850 °F
2 welded joint data for SA 387 11, 850 °F
3 Closed symbols for smooth bar data
4 Open symbols for welded joint data

The data from Chen shows better correlation, Figure 2.16 and suggests a fatigue strength reduction of 1.1 to 1.3.

Figure 2.16 Smooth Bar vs Welded Joint Fatigue Life, Chen [35]

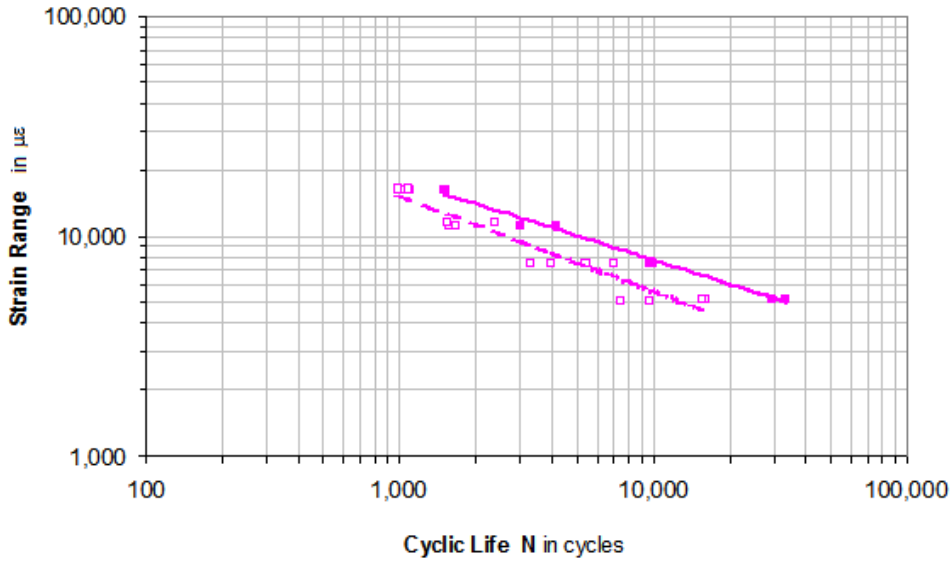

Notes

1 smooth bar data for SA 387 11 Class 2, 480 °F
2 welded joint data for SA 387 11 Class 2, 480 °F
3 Closed symbols for smooth bar data
4 Open symbols for welded joint data

8. *that the dependence of fatigue strength reduction on the magnitude of strain / stress exposure is considered in industry practices, but is overly conservative*

There are several items not well discussed in the literature

1. the dependence of fatigue strength reduction factor on strain
2. the fatigue strength reduction in the heat affected zone of the weld joint
3. the dependence on both geometry and material property factors

The FSRF concept is discussed by Jaske in WRC 422 and notes clearly that the FSRF increases as strain range decreases, or conversely, as cyclic life increases [36].

Chen's work is in agreement with Jaske but shows that the HAZ is more susceptible to fatigue strength reduction with the FSRF varying between 1.4 to 4.0 while the FSRF associated with weld failures varies between 1.6 and 2.1 [35].

The notion of fatigue strength reduction encompasses both a geometric component and a material property component and their interdependence.

Figure 2.17 presents the results of Chen's work.

Figure 2.17 Smooth Bar, Welded Joint and HAZ Fatigue Life, Chen [35]

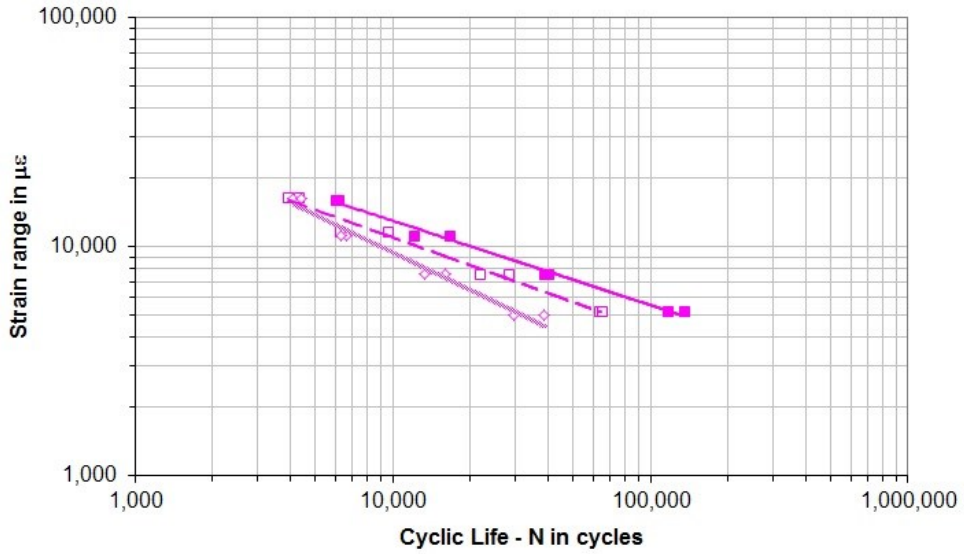

Notes

1 smooth bar data for SA 387 11 Class 2, 480 °F
2 welded joint data for SA 387 11 Class 2, 480 °F
3 HAZ data for SA 387 11 Class 2, 480 °F
4 Closed symbols for smooth bar data
5 Open symbols for welded joint, HAZ data

9. *thermo-mechanical strain has not been explicitly addressed in coke drum design practice*

   The data, describing the magnitude and occurrence of thermo-mechanical strain, is not widely available in the open literature. Ramos et al. have published the results from their work and provided strain exposures and material fatigue charts [19]. Their effort focused solely on the skirt to shell junction. There are no published reports on how thermo-mechanical strains have been used explicitly for the design of coke drums. However, the principles are long established and industry practice documents are appropriate for implementation.

10. *the impact of shell bulging is thought to be a hindrance for determining a benchmark service fatigue life*

    Shell bulging has not been combined with thermal loading to determine impact on drum service life; note, however, that indirect measures have been presented in the literature. Finite element analysis of coke drums is performed and can account for shell distortions. A number of indirect measures have been used, but, have limitations and have not been validated.

11. *thermal shock on surface strain development has been overlooked, the magnitude of this strain matches the large strains developed from through thickness temperature gradients*

    There is published work on through thickness thermo-mechanical strain development in coke drums and link to drum cracking. It will be reviewed in the next section

12. *drum operation is not adequately considerate of the impact of quench water flow rates on the severity of thermomechanical loadings on the shell*

    A Unit Quench Factor was introduced early in the survey of coke drum operations but has not been developed since then. The use of fast quench water addition during a so-called proof quench was seen to be damaging.

CHAPTER 3 THERMO-MECHANICAL LOADING

3.1 Industry Methodologies to Characterize Thermo-mechanical Loading

Three approaches are cited in the literature;

- shell temperature measurement by use of thermocouple grid
- determination of thermal gradients using a thermocouple triad
- use of high temperature strain gauges

Thermocouple Grid

Temperature measurements using a spaced grid are used for monitoring and correlation with other process variables, such as quench water injection rate. The literature does not indicate that temperature grid readings are directly used for determination of thermo-mechanical strains.

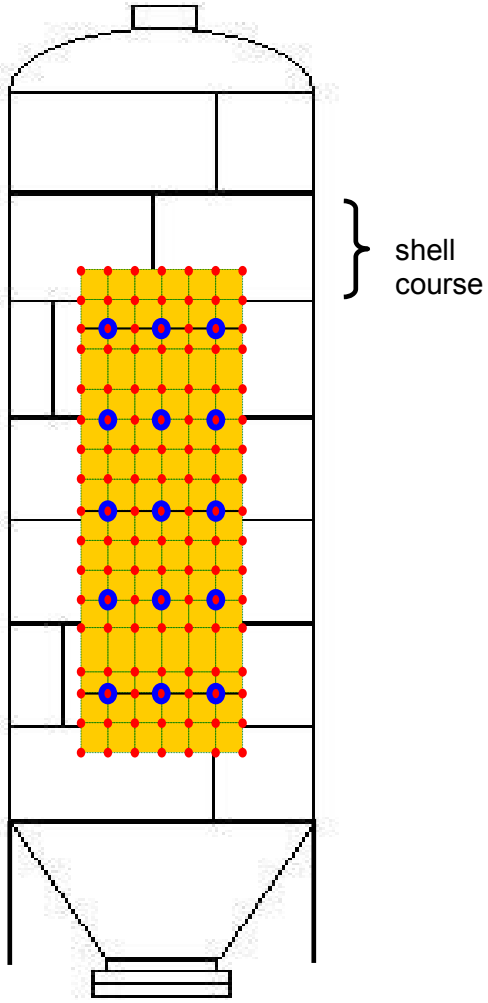

Figure 3.1 illustrates a typical thermocouple grid layout, with thermocouples identified by red-colored dots. The spacing is customized to the specific drum. The thermocouples can span some four (4) to six (6) shell courses vertically, as appropriate for the size of coke drum and some 60 degrees of drum circumference. More than 100 thermocouples are used to simultaneously monitor temperatures at one (1) minute intervals.

Figure 3.1 Coke Drum Thermocouple Grid

Thermocouple Triad

A thermocouple triad is intended to be used for determination of a thermal gradient from which a thermo-mechanical strain is deduced. The triad consists of three (3) thermocouples in axial and circumferential orientation at small spacing. **Figure 3.2** illustrates the thermocouple triad. The thermo-mechanical strain is inferred by calibrating against strain gauges placed adjacent the thermocouple triad.

The incentive to use this arrangement is the low cost of thermocouples and relative reliability in a corrosive environment. However, the thermo-mechanical strains determined by this arrangement are made by calibration of calculated gradients with collocated strain gauges. An apparent weakness of the approach is that the thermo-mechanical strain at a location does not depend uniquely on local thermal gradients, only. Thermo-mechanical strains are seen to occur in hot and cold spots where temperatures can be uniform and thermal gradients of minor magnitude. The usefulness of temperature gradient measurements and calculated thermo-mechanical strains is not discussed further in this thesis.

Figure 3.2 Thermocouple Triad for Measuring Temperature Gradient

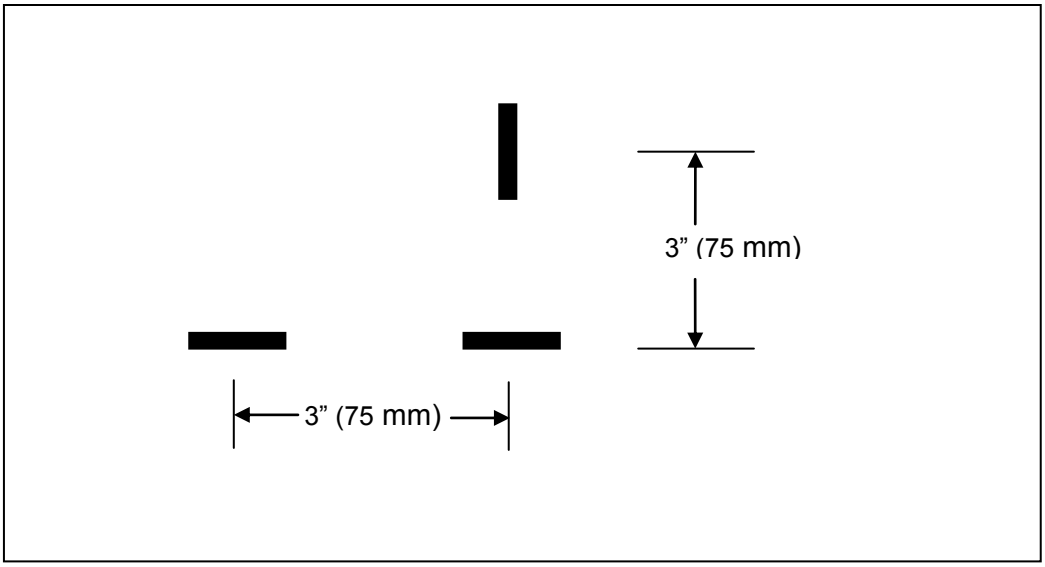

In **Figure 1.3**, a temperature profile illustrated how a coke drum shell cools nominally from bottom to top as

- oil fill progresses through the oil fill cycle of several hours duration
- quench water is rapidly added at completion of oil fill

Figure 3.3 shows the temperature response of another coke drum shell using three (3) thermocouples; two (2) of which are located at the same elevation and 665 mm [26.1 “] apart along the circumference, the third thermocouple is located 3,119 mm [122.8 inches] below the other two. The temperatures are seen to be nearly coincident during steam testing, vapor heating and the beginning of oil fill.

Figure 3.3 Coke Drum Temperature Profile during Operational Cycle

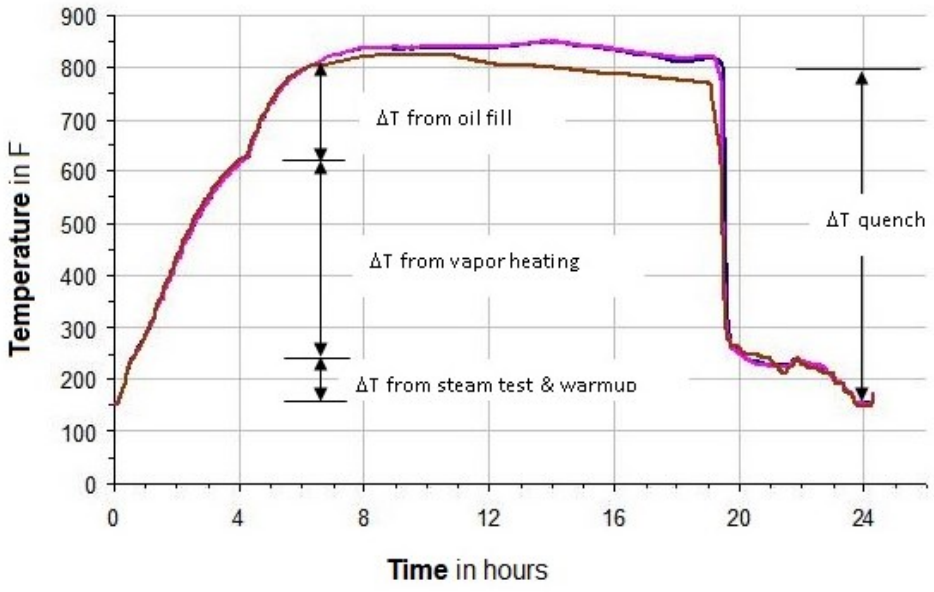

Similar to **Figure 1.3**, **Figure 3.3** clearly indicates shell cooling begins immediately as the oil fill level passes a thermocouple elevation but the large time scale in **Figure 3.3** erroneously suggests that the temperatures are uniform during the water quench phase.

Using a smaller time scale in **Figure 3.4** reveals the large differences in shell temperature between the thermocouples at two different elevations (marked as D3 – D8) and between two thermocouples at the same elevation (marked as C3 – D3). This more detailed view of thermocouple response reveals that the cooling down of the coke drum shell is not uniform but that circumferential gradients occur in addition to the expected axial gradients. This motivates the inclusion of the thermocouple triad arrangements to determine the circumferential, as well as the axial temperature gradients. This also shows the motivation to examine temperature differences.

Figure 3.4 Thermocouple Readings in Detail

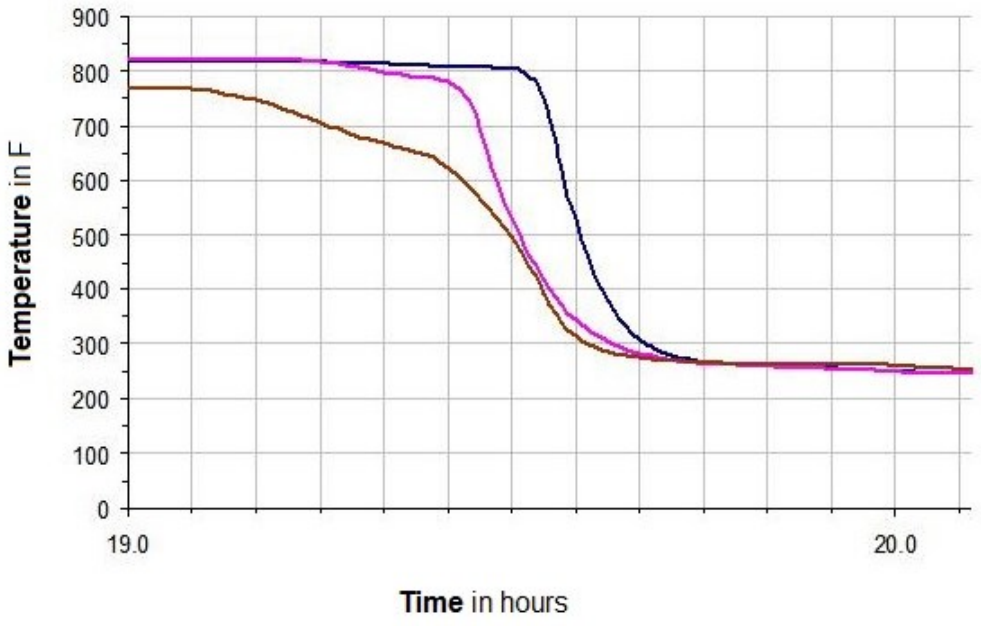

Notes

1 location D3, i.e., column D elevation 3
2 location C3, i.e., column C elevation 3
3 location D8, i.e., column D elevation 8 (a location 122.8 inches or 3,119 mm directly below elevation 3)

In a series of contour plots, the evolution of shell temperatures in four minute intervals is shown in **Figures 3.5a - l**. The following observations can be made from **Figure 3.4** and **Figures 3.5a – l**

- shell temperatures at a fixed location change rapidly, within about 15 to 25 minutes
- both cold and hot temperature regions form during the quench sequence
- cold spots can form spontaneously within an existing hot zone **(Figures 3.5d – 3.5f**; upper left quadrant)
- cold intrusions or "fingers" can form by non-uniform upflow **(Figures 3.5a – 3.5c)**
- the cold and hot regions may be extensive or localized

Figures 3.5 a – c Thermal Profile Snapshots – in [°F]

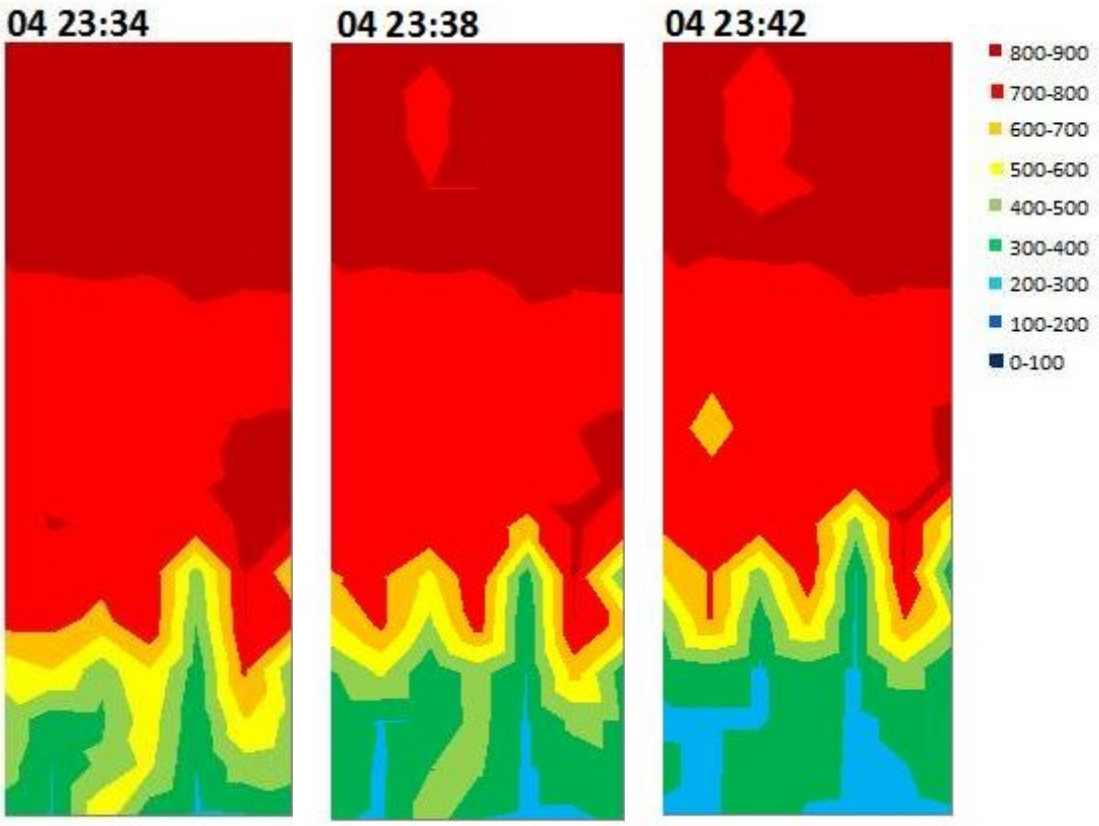

Figures 3.5 d – f (cont`d)

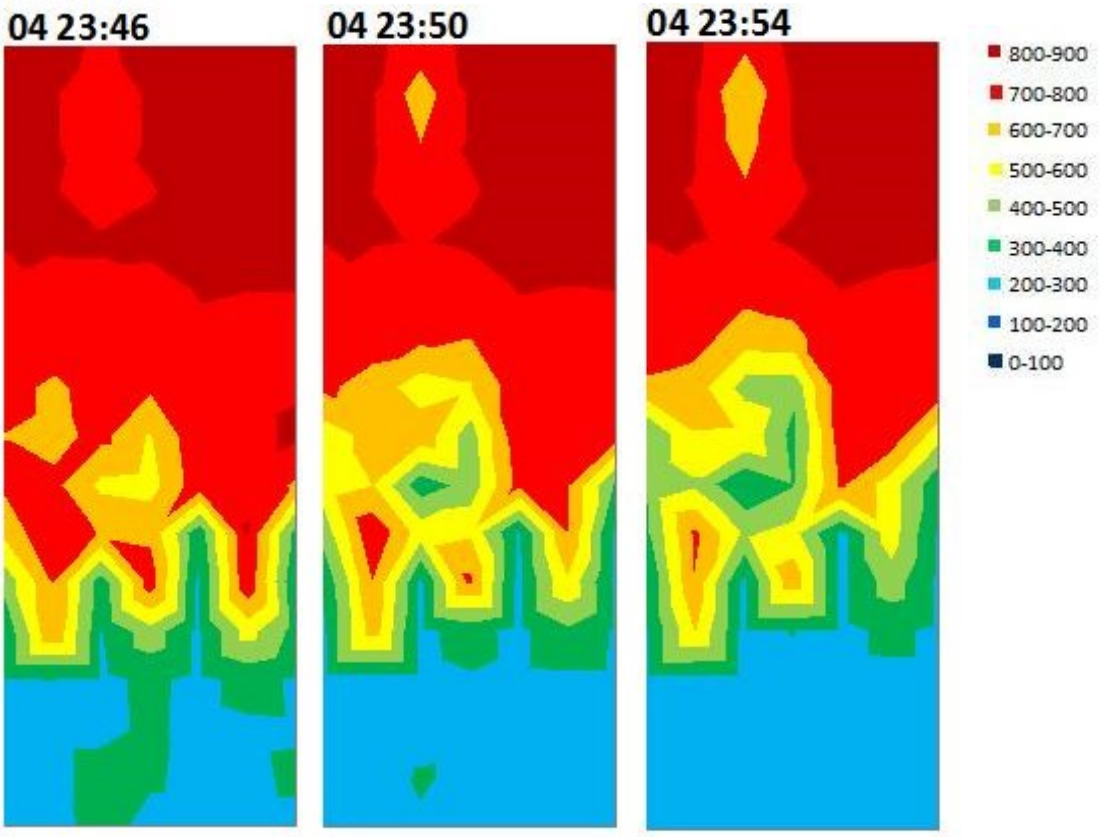

Figures 3.5 g – i (cont`d)

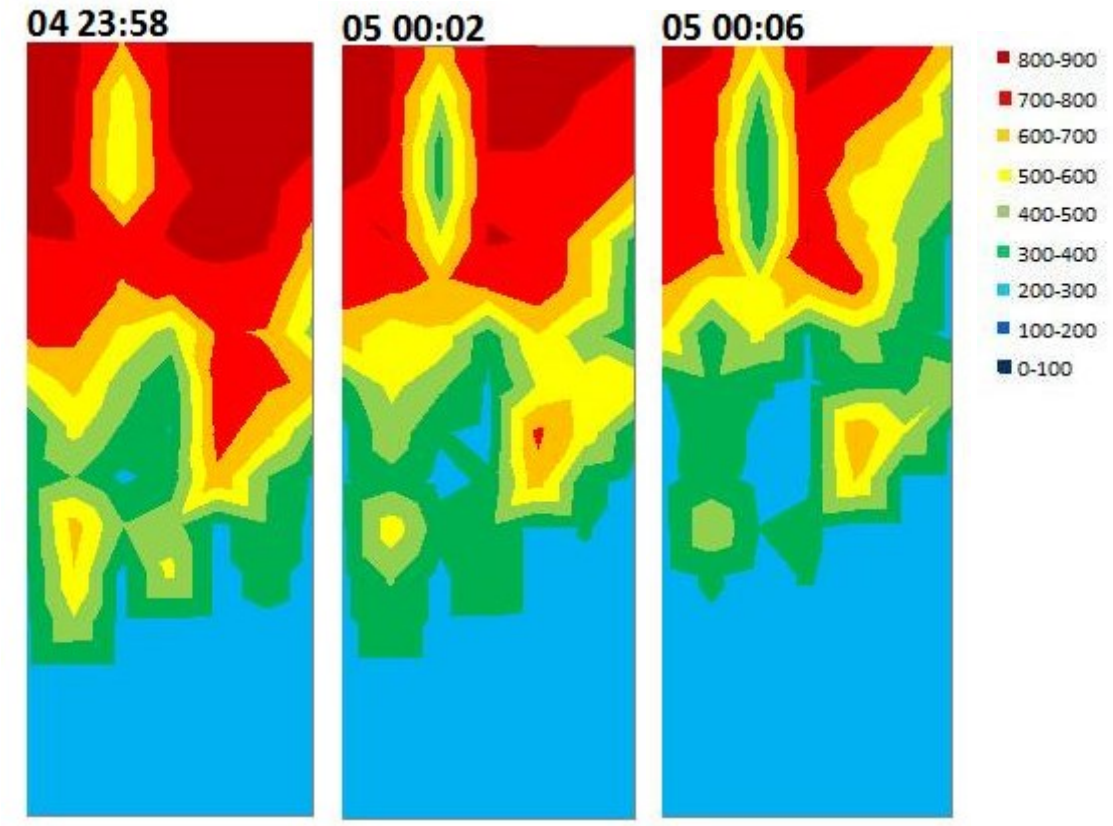

Figures 3.5 j – l (cont`d)

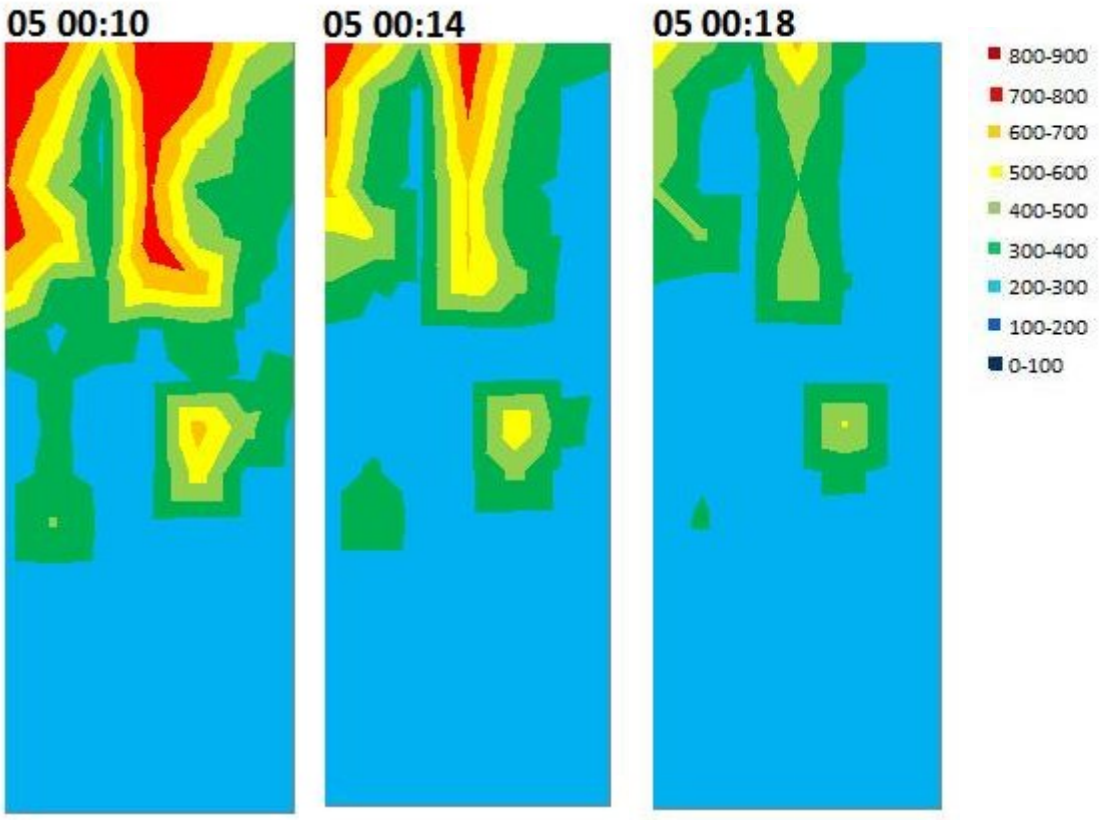

The extensive size of cold and hot spot regions jeopardizes a conventional approach using only thermal gradients as a method to determine thermo-mechanical strain.

While temperature gradients within the hot or cold spot may be relatively small, large thermo-mechanical strains can be present since the affected cold or hot spot is constrained by the surrounding structure. Zhang studied the impact on coke drum shell strains in conditions of regional temperature differences [38].

3.2 Strain Data Capture Results

Electrical resistance foil strain gauges provide measurement of strain, but the devices are expensive and short – lived due to the harsh operating environment. The devices are fragile, are exposed to high temperatures and large deflections in the shell from both thermal strain and bulging and, are in a corrosive environment caused by steam and coke dust forming sulfuric acid.

Figure 3.6 shows a typical resistance strain gauge installation for a coke drum. The gauges are spot electric resistance welded to the coke drum shell. Temperature compensation is required on account of two considerations [39]:

- the change in resistivity of the gauge material with temperature change
- the differential expansion existing between the gauge support and gauge proper resulting in a strain indistinguishable from load strain; hence an apparent strain

Temperature compensation for differential expansion is necessary because of the construction of the resistance strain gauge which consists of the gauge being mounted on a backing material which is supplied in Alloy 600 or TP 321 stainless steel. The strain gauge has an on-board thermocouple and compensation board.

Figure 3.6 Strain Gauges with Independent Thermocouple

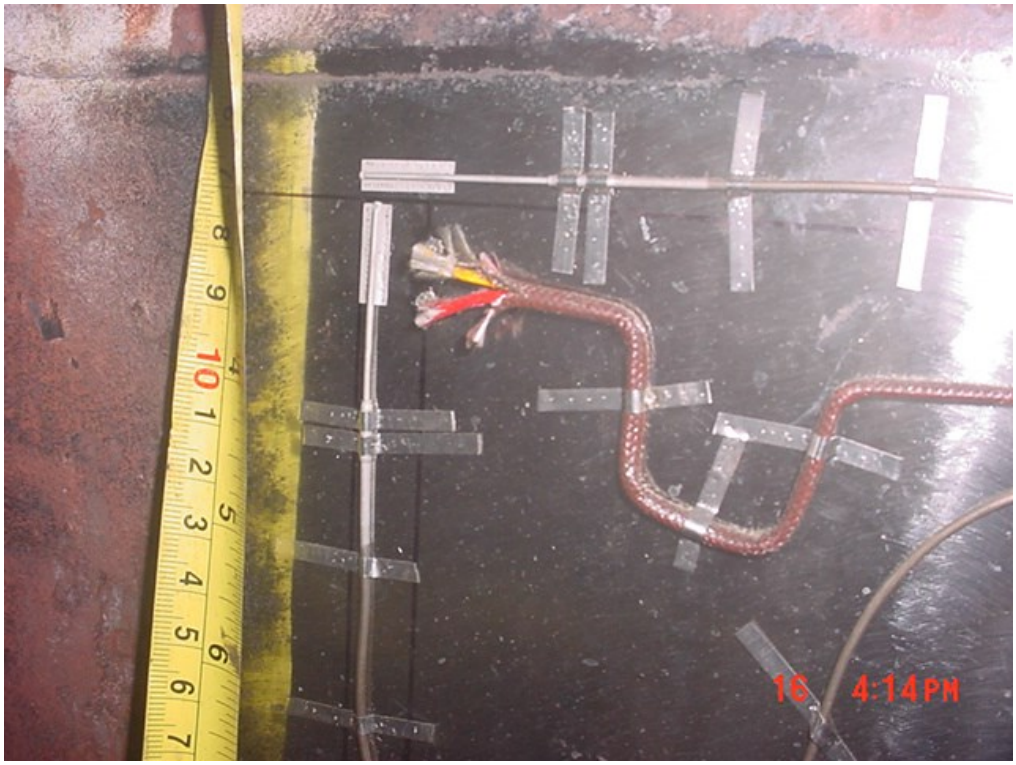

The temperature compensation circuit board is illustrated in **Figure 3.7**. The strain gauge favoured by industry is usually a high temperature weldable unit obtained from TML Tokyo Sokki Kenkyujo Type AWH [40].

An independent thermocouple arrangement is co-located and is identified by the yellow and red leads suggesting that it is a Type “K” thermocouple.

Figure 3.7 Schematic of Strain Gauge and Compensation Board

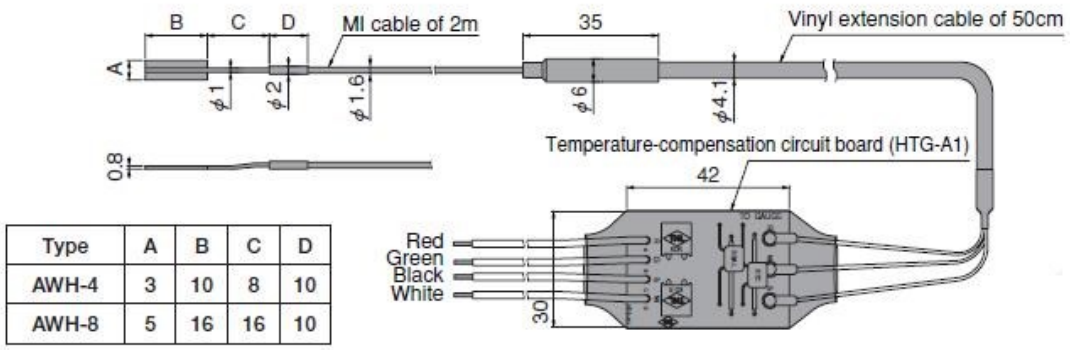

Type	A	B	C	D
AWH-4	3	10	8	10
AWH-8	5	16	16	10

A compensation scheme is provided and shown as **Figure 3.8.** The manufacturer advises that the corrected strain is obtained as

corrected strain = measured strain – apparent strain (3.1)

Figure 3.8 Manufacturer`s Strain Gauge Compensation Chart

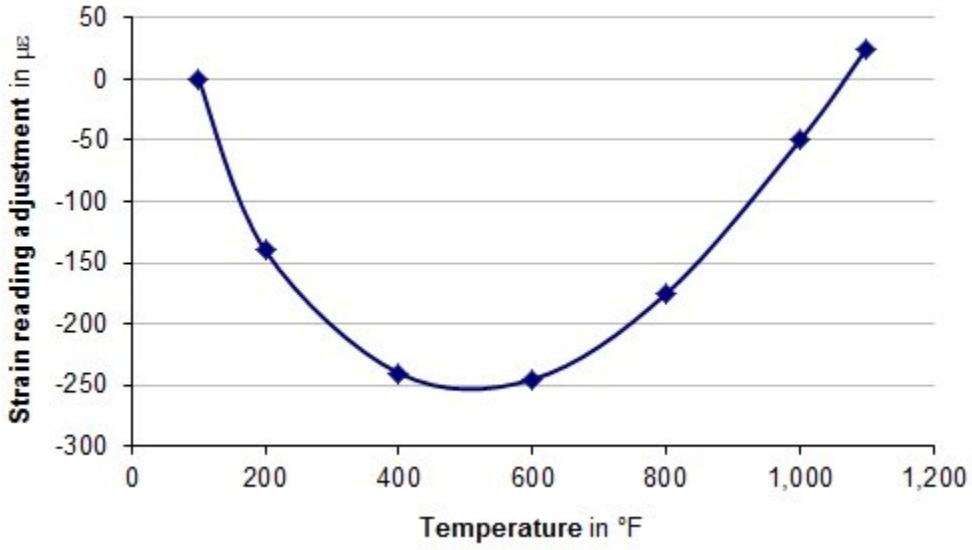

In **Figure 3.9**, the thermo-mechanical strain presented in equations (2.6) and (2.7) are plotted.

Figure 3.9 Thermo-mechanical Strain due to CTE Mismatch

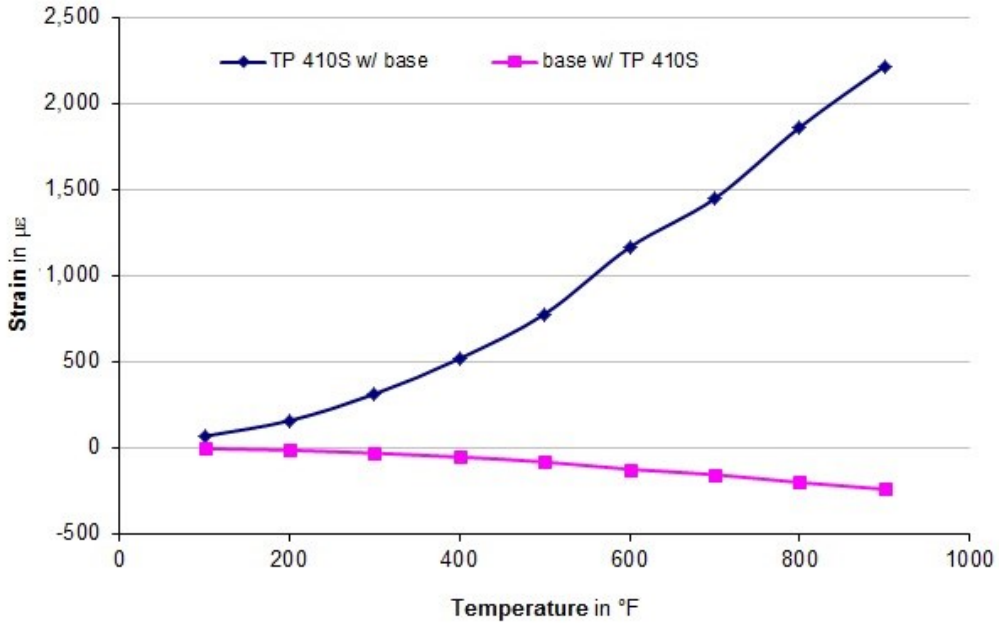

The expected strain at 900 °F [482 °C] plots as a value of 2,215 με for TP 410S SS and – 244 με for Cr – Mo steels. The strain plot is seen to continuously rise for TP 410S and continuously decrease for Cr – Mo steels. In **Figure 3.10**, the difference in thermo-mechanical strain reading between an Inconel backed thermocouple and coke drum base material is shown. The thermocouple will over-report the strain in the base by 1,240 με at 900 °F [482 °C], due to differences in the coefficient of thermal expansion between the base material and the thermocouple. The remaining error is attributable to the change in resistance of the strain gauge and lead wire with temperature.

Figure 3.10 Thermo-mechanical Strain in Inconel Thermocouple Pad

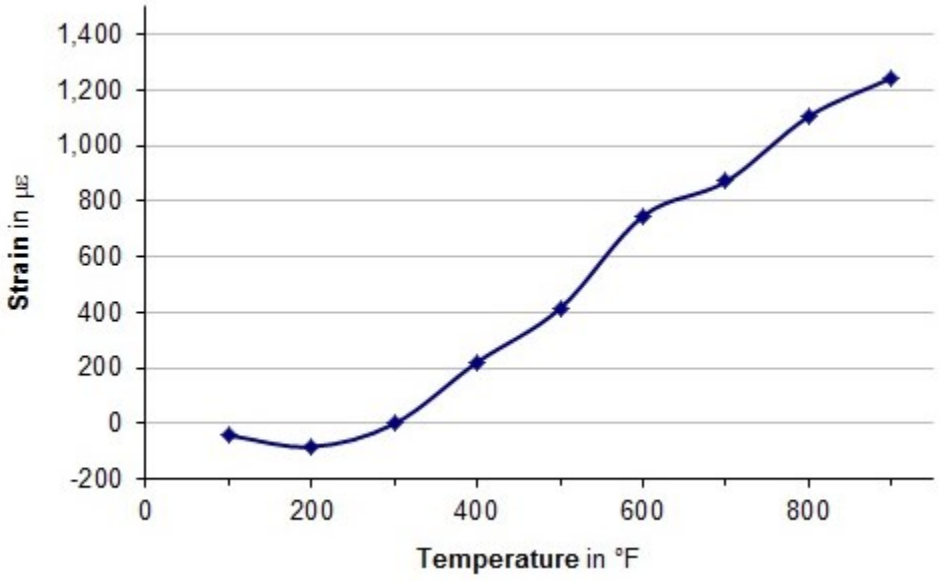

The gauge manufacturer states that a corrected stress is provided through this correction procedure and demonstrated by **Figure 3.11** showing that complete temperature compensation results in zero (0) strain indication due to temperature and thermal strain induced by the differences in coefficients of thermal expansion between the Type Alloy 600 gauge backing material and the low alloy steel coke drum.

Figure 3.11 Strain Gauge Compensation [40]

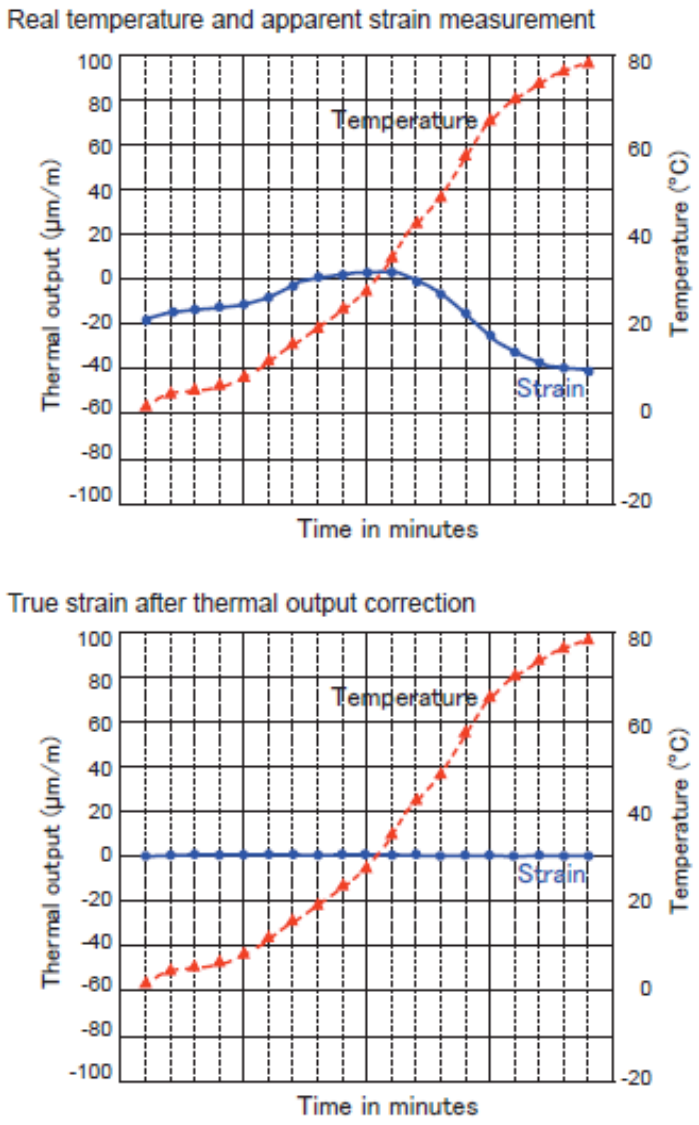

Strain History – Unit # 1

A strain tracing for an undisclosed coke drum shown in **Figure 3.12** where D = 312 inches, t = 1 inch. Since the unit is pressurized during steam testing to 35 psig [241 kPag] and 250 °F [120°C], the calculated strains are:

$$\Delta\varepsilon_1 = (\sigma_1 - \mu\sigma_2) / E \quad (3.2)$$
$$= (5{,}460 - 0.3 * 2{,}730) / 28.5$$
$$= 163\ \mu\varepsilon \text{ – circumferential}$$

$$\Delta\varepsilon_2 = (\sigma_2 - \mu\sigma_1) / E \quad (3.3)$$
$$= (2{,}730 - 0.3 * 5{,}460) / 28.0$$
$$= 38\ \mu\varepsilon \text{ – axial}$$

Accounting for the differential thermal expansion of clad to base materials, using (2.6)

$$\sigma_b = \frac{(\alpha_c - \alpha_b)\cdot(T_h - T_0)\cdot E_b}{1 + \frac{t_b \cdot E_b}{t_c \cdot E_c}} \cdot \frac{1}{1-\mu} \quad (3.4)$$

$but,$

$$\varepsilon_b = \frac{(6.3 - 6.9)\cdot(150)}{1 + \frac{1 \cdot 28.5}{0.110 \cdot 27.9}} \cdot \frac{28.5}{28.5} = -8.6\mu\varepsilon$$

A difficulty with the strain history is correct interpretation of the operational sequencing; the times for the transition in sequencing was not provided, hence the analysis of strain gauge behavior is impaired.

Figure 3.12 Strain Profile #1

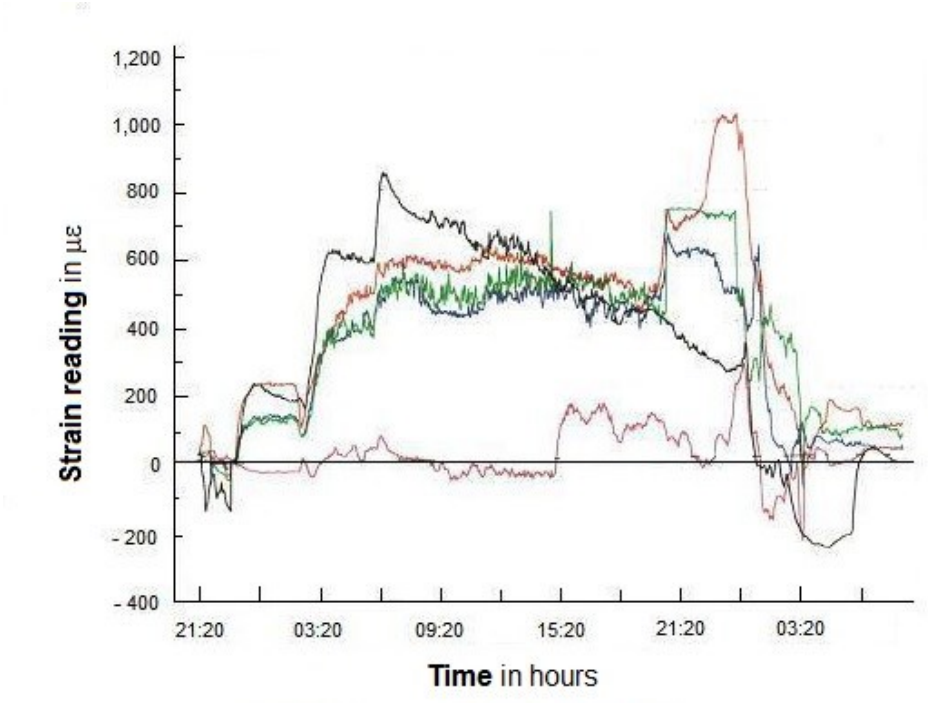

A decrease in thermo-mechanical strain is expected at the start of sequencing since only pressure and temperature load are applied; i.e., 38 + (– 8.8) = 29 με. This would persist until a hydrostatic head load occurs due to oil filling. If the apparent strain gauge factor of – 175 με is subtracted, then a corrected strain of - 145 με results and should be reported up to the start of water quenching.

Two (2), of four (4) strain gauges installed on the coke drum shell show some fidelity to the expected trend for pressure and steam heating. Given that a compressive strain develops in the base layer due to the effect of internal cladding, the strain should decrease slightly during vapor heating, from time 03:20 to 04:20 until the oil fill phase begins. A short time decrease is noted and then oil filling begins at an unspecified time which could be also reported as vapor heating.

The phasing of operations is dependent on operator intervention and oil filling could take place immediately after a short vapor heating phase.

Using the data from equation (1.1), the expected axial strain for combined pressure and hydrostatic head (70 psig, 650 °F in this instance) is

$$\Delta\varepsilon_1 = (\sigma_1 - \mu\sigma_2) / E \quad (3.5)$$
$$= (10{,}920 - 0.3 * 5{,}460) / 25.9$$
$$= 360\ \mu\varepsilon \ -\ \text{circumferential}$$

$$\Delta\varepsilon_2 = (\sigma_2 - \mu\sigma_1) / E \quad (3.6)$$
$$= (5{,}460 - 0.3 * 10{,}920) / 25.9$$
$$= 84\ \mu\varepsilon \ -\ \text{axial}$$

A thermal strain of approximately – 88 $\mu\varepsilon$ is expected using (2.6).

$$\sigma_b = \frac{(\alpha_c - \alpha_b)\cdot(T_h - T_0)\cdot E_b}{1 + \frac{t_b \cdot E_b}{t_c \cdot E_c}} \cdot \frac{1}{1-\mu} \quad (3.7)$$

$but,$

$$\varepsilon_b = \frac{(6.9 - 8.5)\cdot(550)}{1 + \frac{1\cdot 25.9}{0.110\cdot 25.9}} \cdot \frac{25.9}{25.9} = -88\mu\varepsilon$$

The corrected axial strain is determined by (3.1) as

corrected strain = measured strain – apparent strain
= [84 + (– 88)] – (– 225)
= [– 44] + 225 = 180 $\mu\varepsilon$

The reported strain (i.e., strain gauge plot) should be then calculated as a corrected strain of 180 $\mu\varepsilon$. The plotted strains in **Figure 3.12** vary between approximately 500 $\mu\varepsilon$ and 600 $\mu\varepsilon$ with average coker drum shell temperature at 650 °F [343 °C].

Note that the black colored tracing is for a strain gauge located at the skirt which is subject to shell wall cooling which initiates early in the oil filling sequence.

Thus, the strain gauges mounted on the shell read higher than expected and are not consistent with the pressure and final live weight loading in the coke drum. A maximum reading of 1,250 με - axial is reported in this operational cycle which occurred during the quench phase of operations; during the quench phase, coker drum shell temperature decreases as quench water is added to the coke drum. This strain development is representative of additional observations over a block of eighteen (18) days.

Strain History - Unit # 2

The strain history for a second coke drum unit was examined for comparison. **Figure 3.13** shows the circumferential strains for several strain gauges and temperature (the temperature is shown in gray and uses the left hand scale) collocated at one of the gauges.

Figure 3.13 Circumferential Strain Profile # 2 for Five Operational Cycles

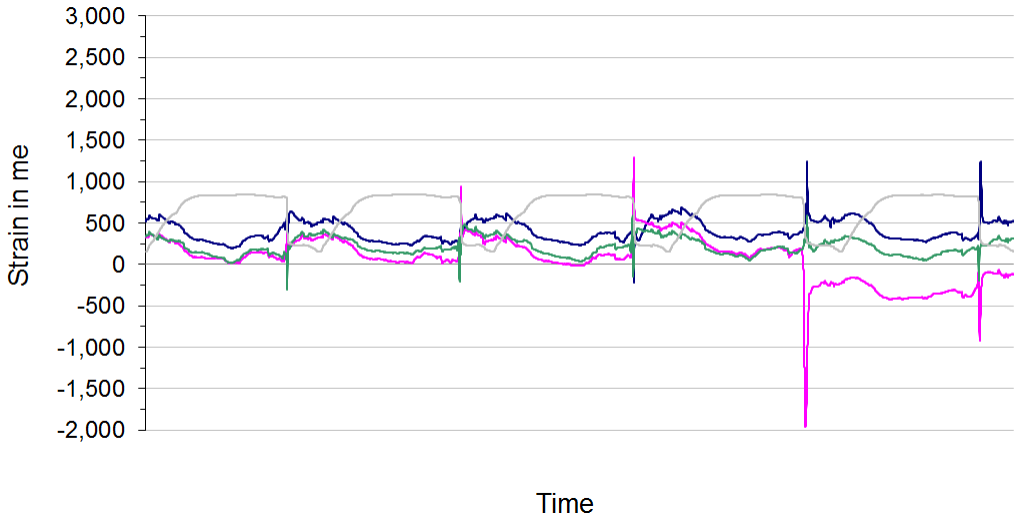

Figure 3.14 displays the axial strain for the same strain gauges and temperature (shown in gray) for the same time span.

Figure 3.14 Axial Strain readings for Same Five Operational Cycles

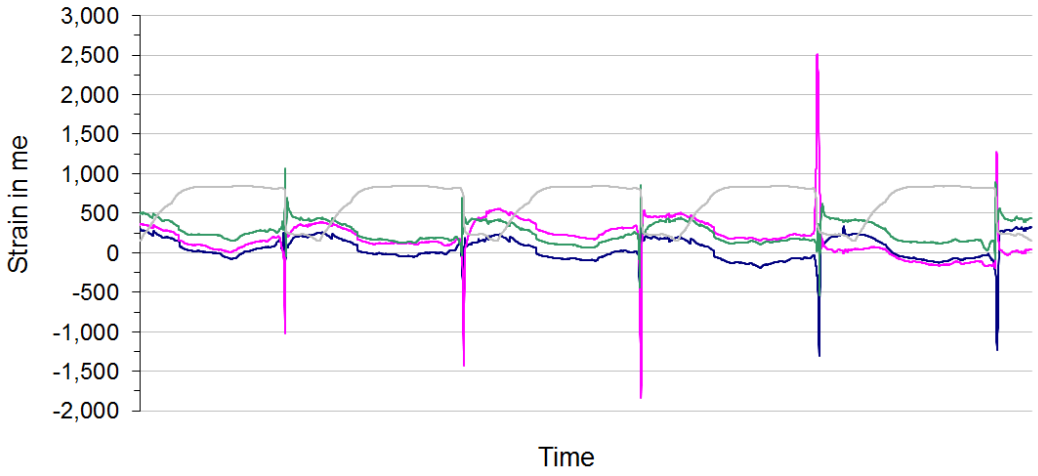

The tracings are partly inconsistent with expectation for the three operating phases of steam test, vapor heating and oil filling; low strain values are initially expected, as determined previously, with rising strain values as oil fill occurs. **Figure 3.13** and **Figure 3.14** show high strain readings at start of the operational cycle, then decreasing strain values as oil fill progresses up to water quench.

This decreasing trend appears to be inconsistent with the expectation that the strain gauge should only reflect the strains from

- pressure + hydrostatic load from oil filling
- thermo-mechanical strain in the base due to the effects of differential expansion between clad and base materials

The strain response between circumferential strains and axial strains is not reasonable; circumferential strains should be higher due to the higher hoop stresses under pressure and hydrostatic loading; as depicted, the hoop and compressive strains trend similar.

However, all tracings are consistent in showing that the highest strains

- occur during the water quench phase, only
- are of short duration
- are an order of magnitude larger during the quench phase than strains measured during the other phases of operation
- are within the elastic strain limit of the materials and within the shakedown limit of 2· YS provided in the Codes

Overall, the strain tracings for Unit # 2 are not fully consistent with expected response of the temperature compensated strain gauges.

3.3 Discussion of Measured Strains

These tracings indicate that the correct observation of strain using high temperature strain gauges under high temperature conditions is problematic.

1. In the available reports, the validation of the reported strain gauges reading is not provided.

2. The accuracy of strain gauge reading is not established; there is no discussion to verify the readings

   The elastic strain limits given in **Table 2.1** were presented on the basis of Code specified minimum yield strength properties [SMYS].

   However, the elastic limit values provided in Table 3.1 are determined on the basis of actual supplied yield strength [YS] properties. The SMYS is a Code requirement while YS values are the actual monotonic yield strength properties for the supplied material.

   Figure 3.15 shows the results from a monotonic tensile test of a 2¼ Cr - 1 Mo used for construction of a coke drum.

Figure 3.15 Monotonic Stress – Strain Curve for 2¼ Cr – 1 Mo Material

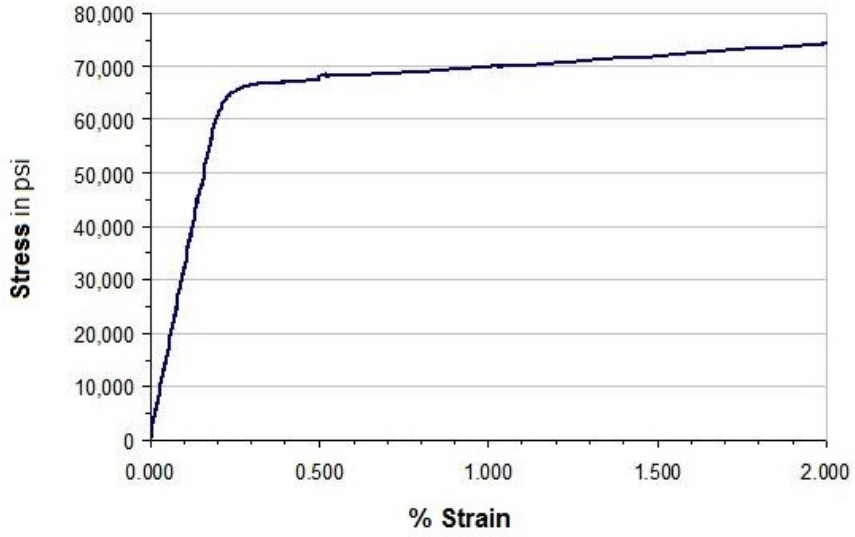

The Code SMYS, defined as the 0.2% offset strength is shown to be 67,116 psi [462.7 MPa]. The actual extension under load [EUL] of the test piece is 0.423%. The proportional limit is determined with strain at 0.2% EUL and tensile stress at 60,810 psi [419.3 MPa] resulting in a Young's modulus of 30.6 E6 psi [210.7 GPa]. The supporting MTR for this specimen cited the material as SA 387 22 Class I. The elastic limit in **Table 3.1** is 2,190 με at 100 °F [38 °C]. It should be noted that yield strength may be stated on the basis of 0.2% offset or 0.5% EUL [41].

Table 3.1 Actual Material Properties for Coke Drum Construction

Material	YS		TS		E		ε_{YS}	
	100 °F	900 °F	100 °F	900 °F	100 °F	900 °F	100 °F	900 °F
SA 240 405					29.0	23.2		
SA 240 410S					29.0	23.2		
SA 516 70					29.2	22.5		
SA 204 C	56.0	35.9*	81.0	75.3	28.9	22.2	1,940	1,620*
SA 302 B	56.3	39.3*	83.7	-	28.9	22.2	1,950	1,770*
SA 387 12 – II	63.1	42.9*	83.5	-	27.7	23.2	2,280	1,850
	61.5	41.8*	80.5	-			2,220	1,800
	65.9	44.8*	84.1	-			2,380	1,930
	65.7	44.7*	82.7	-			2,370	1,925
	60.8	41.3*	79.6	-			2,195	1,780
SA 387 11 – I	59.0	40.1*	76.3	-	27.7	23.2	2,130	1,725*
	56.0	38.0*	76.5	-			2,020	1,640*
	60.2	40.9*	78.7	-			2,170	1,765*
	57.2	38.9*	77.2	-			2,065	1,675*
	60.0	40.8*	80.4	-			2,165	1,760*
SA 387 22 – I	38.1	27.4*	69.3	-	30.5	25.6	1,250	1,070*
	40.9	29.4*	70.2	-			1,340	1,150*
SA 387 22 – II test	67.1	48.3*	83.1	-	30.6	25.6*	2,190	1,885
SA 387 21					30.5	25.6		

Notes

1. * indicates value is estimated from MTR and Code data
2. elastic strain limit ε_{YS} calculated according to YS / E
3. stress values in ksi; strain values in $\mu\varepsilon$

SA 387 / Cr – Mo materials are routinely specified in the Class II condition resulting in higher monotonic strength properties. The grade 11 and 12 Cr – Mo materials, i.e., 1¼ Cr – ½ Mo and 1Cr – ½ Mo were supplied in both Class I and Class II condition. However, the actual measured monotonic elastic strain limits are well above the measured coke drum shell strains for Unit # 1 and for four of five strain excursions shown for Unit # 2. The maximum excursion for Unit # 2 is within the 2 · YS / E limit.

The monotonic elastic strain limits are summarized in Table 3.2 for SA 387 [Cr – Mo] materials.

Table 3.2 Monotonic Elastic Strain Limits for SA 387 Materials – in με

	YS / E				2 · YS / E			
	100 °F		900 °F		100 °F		900 °F	
SA 387 12 – II	2,195	2,380	1,780	1,930	4,390	4,760	3,560	3,860
SA 387 11 – I	2,020	2,170	1,640	1,760	4,040	4,340	3,280	3,520
SA 387 22 - test	-	2,190	-	1,885	-	4,380	-	3,770

3. A difficulty in assessing measured strain readings is the accuracy and precision of the reported strain.

   Strain gauges by necessity are mounted external to the coke drum. Hence, the gauges measure the thermo-mechanical strain imposed by the aggregate of both the through thickness temperature gradients and the temperature differences with surrounding locations.

Figure 3.16 conceptually illustrates the impact from quench water contacting the coke drum shell ID and the transient temperature evolution as the shell cools.

Figure 3.16 Effect of Quench Water on Coke Drum Wall

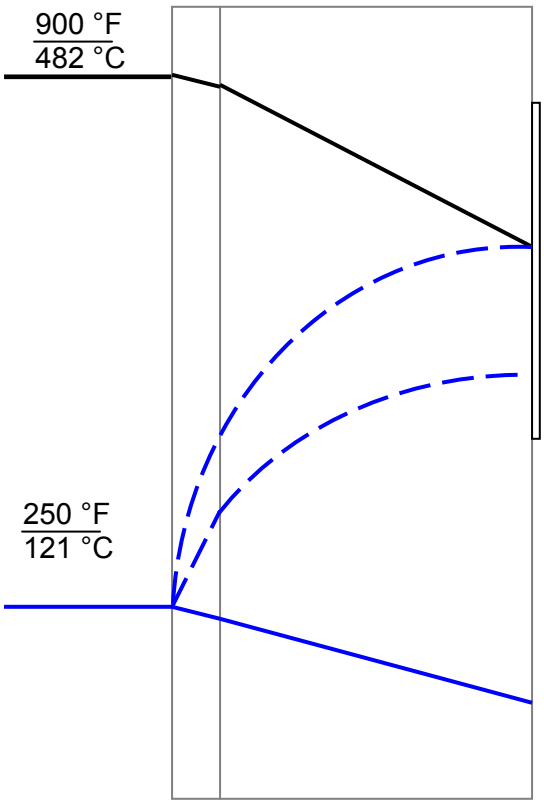

Notes

1 initial steady state temperature profile
2 transient temperature response during quench in shell wall
3 steady state temperature at cessation of quench

Some industry researchers have investigated the effects on heat transfer rate from quench water to coke drum shell ID and quench water rise rate on shell distortion (bulging) and plastic strain development [24][25]. Ohata concludes from transient thermal and strain analysis that the maximum strains approach 0.2% plastic strain, **Figure 3.17**.

Figure 3.17 Equivalent Plastic Strain in Coke Drum Wall

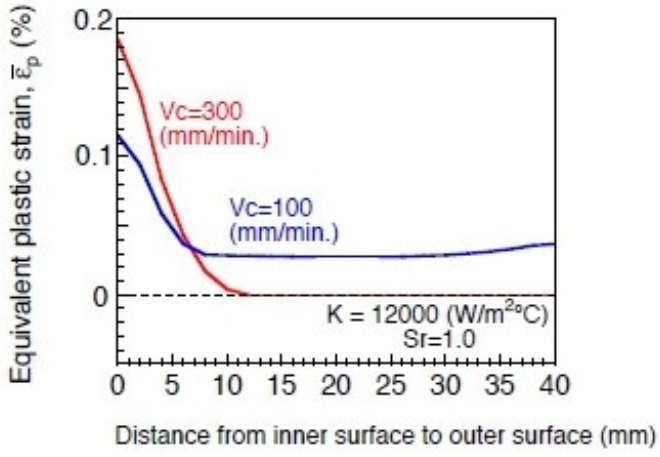

A bounding approach based on the model of **Figure 3.16** suggests that the total bounding strain could be calculated as [33]

$$\varepsilon = \alpha \cdot \Delta T = 7.1 \cdot 10^{-6} \cdot (900 - 250) = 4{,}615 \ \ \mu\varepsilon \tag{4.8}$$

The bounding model is overly-conservative since it presumes that the coolest possible water temperature contacts the hottest coke drum shell region instantaneously and is completely encircled by the hot zone. This strain value, consisting of elastic and plastic components aligns with Ohata's assumptions.

The actual heat transfer rate is limited by the surface boiling conductance. Aumuller determined surface conductance during water quench and suggested a limit value of 1,280 W / m^2 - °C [225.6 Btu / hr – ft^2 - °F] [31].

Ohata et al. indicate that when using a surface boiling conductance of 1,200 W / m^2 - °K and a fast water rise rate, the equivalent plastic strain developed in their model was zero (0); **Figure 3.18** is provided from the reference [24].

Figure 3.18 Plastic Strain Development during Likely Water Quench

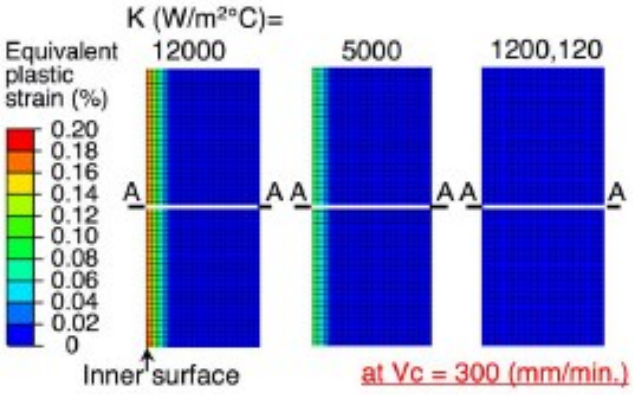

Ohata et al. used the 0.2% yield strength criterion to determine the elastic strain limit for their model. Their model used an isotropic hardening model, cycling loading was not used. Ohata does not report the actual proportional limit strain; however, using experimental data by the author, this could coincide with a proportional strain limit of 0.213%. **Figure 3.19** presents results from room temperature monotonic testing of 1¼ Cr – ½ Mo pressure vessel construction material similarly specified by Ohata.

Figure 3.19 Monotonic Stress Strain Curve for 1¼ Cr – ½ Mo

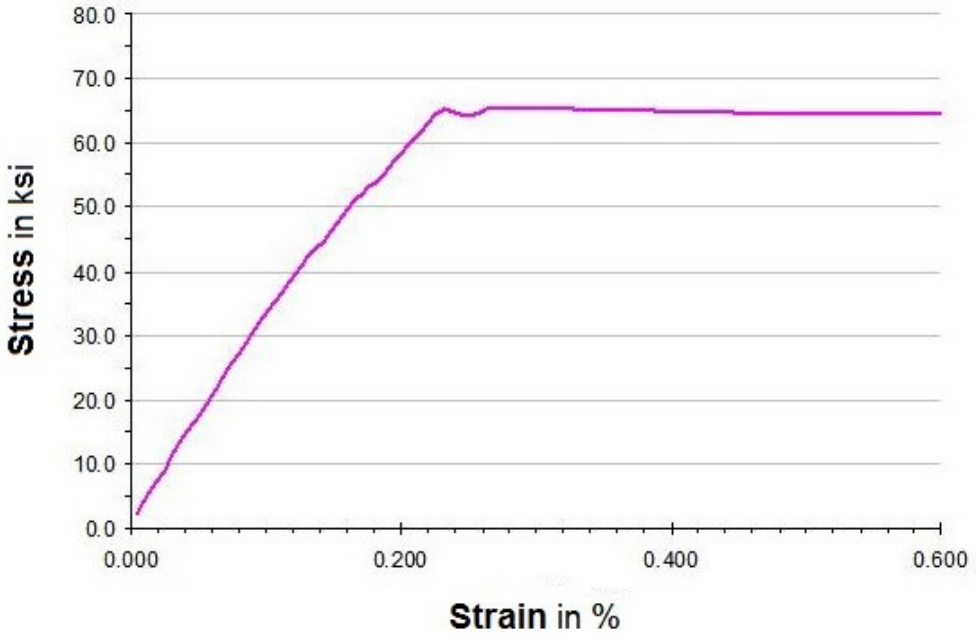

Figure 3.20 presents another strain histogram from a coker drum which is consistent with the expected strain history behaviors described above for Unit # 1 and Unit # 2:

- mechanical strain readings are near zero (0) during oil fill since only thermal strains are present; thermal strains cause zero thermo-mechanical strains
- a small negative strain reading occurs due to differential thermal expansion between clad and base material; this is about – 200 με and somewhat consistent with calculation (3.7)
- strain readings rise linearly when the oil fill elevation exceeds the strain gauge elevation, somewhat consistent with calculation (3.6)
- a negative strain spike occurs of approximately – 2,000 με consistent with quench water contacting the shell ID; a rapid shell temperature decline from 720 °F [382 °C] to 250 °F [121 °C] occurring in 15 minutes.

Figure 3.20 Operational Data from Coke Drum

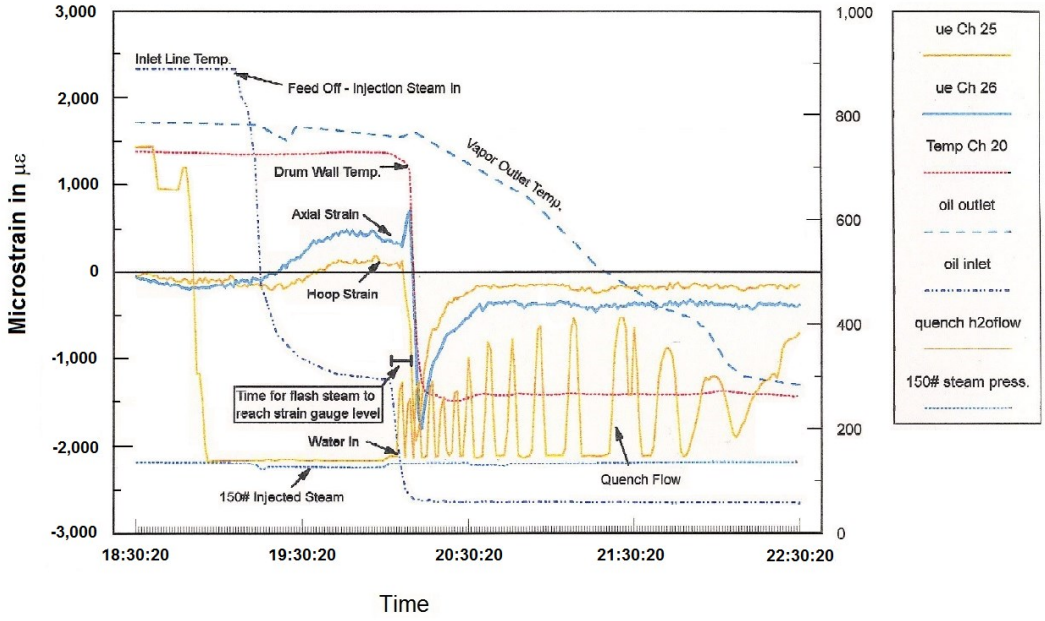

Summarizing from the Ohata study

- a room termperature monotonic elastic strain limit using the 0.2% offset strength was used
- strains do not exceed elastic strain limits for realistic heat transfer rates during water quenching, i.e.,
  1,280 W / m^2 – °C [225.6 Btu / hr – ft^2 - °F]

Strain readings for surface mounted strain gauges, as applied to coke drums, can occur from several sources

- through thickness temperature differences
- temperature gradients between shell locations
- temperature differences between shell locations

3.4 Interpretation of Strain Data

Strain data are necessary to determine the cyclic life of coke drums exposed to thermomechanical loadings using the ε – N approach.

The strain measurements captured by strain measurement gauges from the available literature and industry partner were examined. These are given in **Figures 3.21a through 3.21d.**

Figure 3.21a Strain Gauge Data Distributions from the Literature – # 1

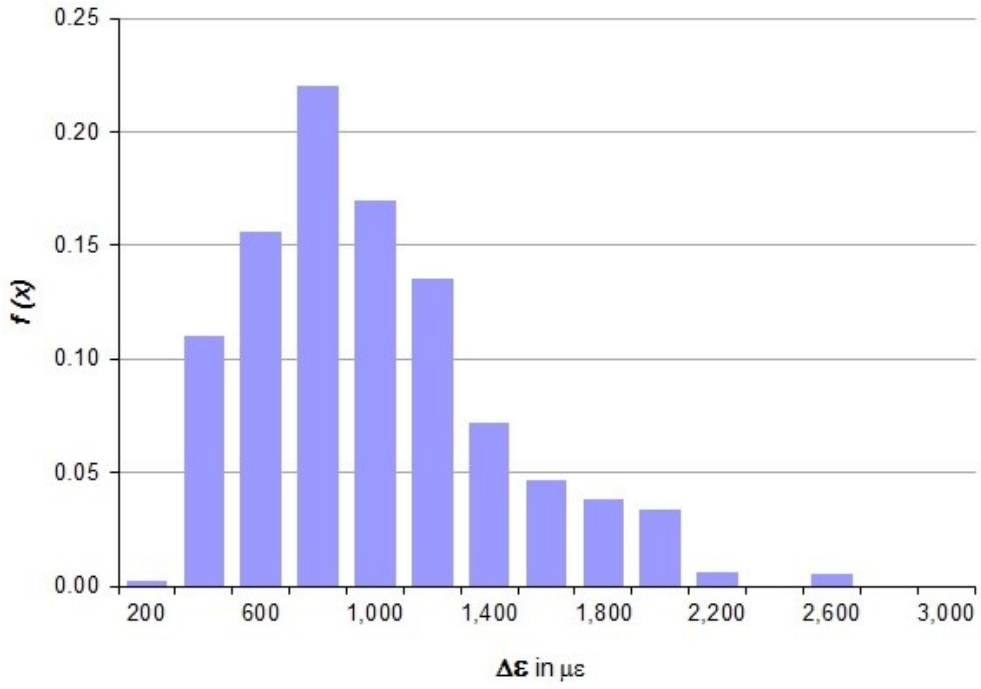

Figure 3.21b Strain Gauge Data Distributions from the Literature – # 2

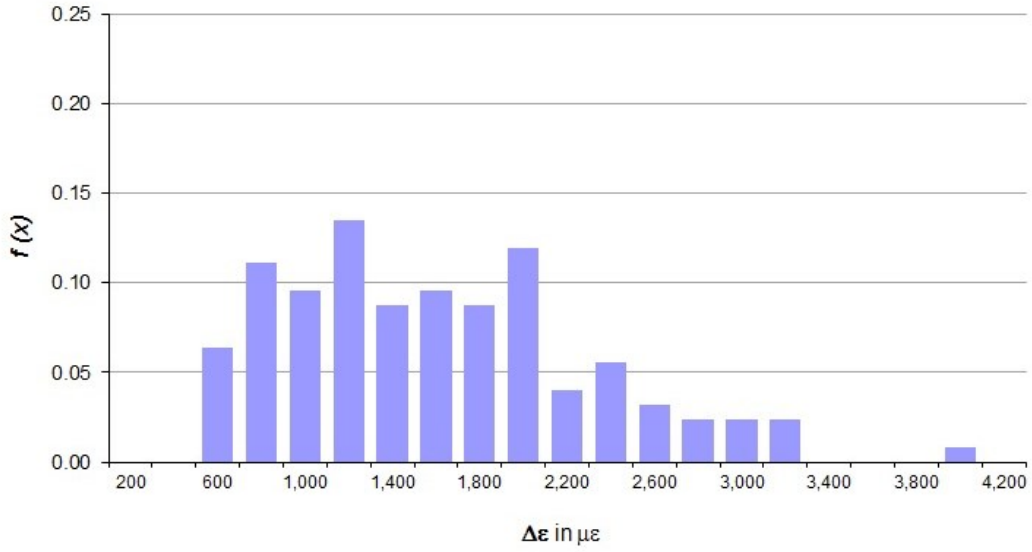

Figure 3.21c Strain Gauge Data Distributions from the Literature – # 3

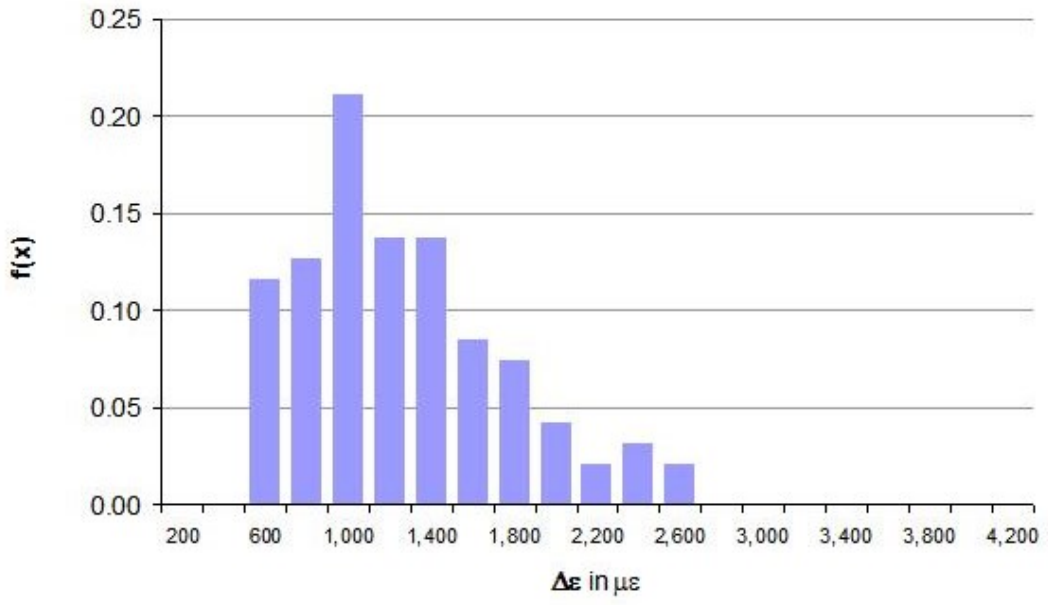

Figure 3.21d Strain Gauge Data Distributions from the Literature – # 4

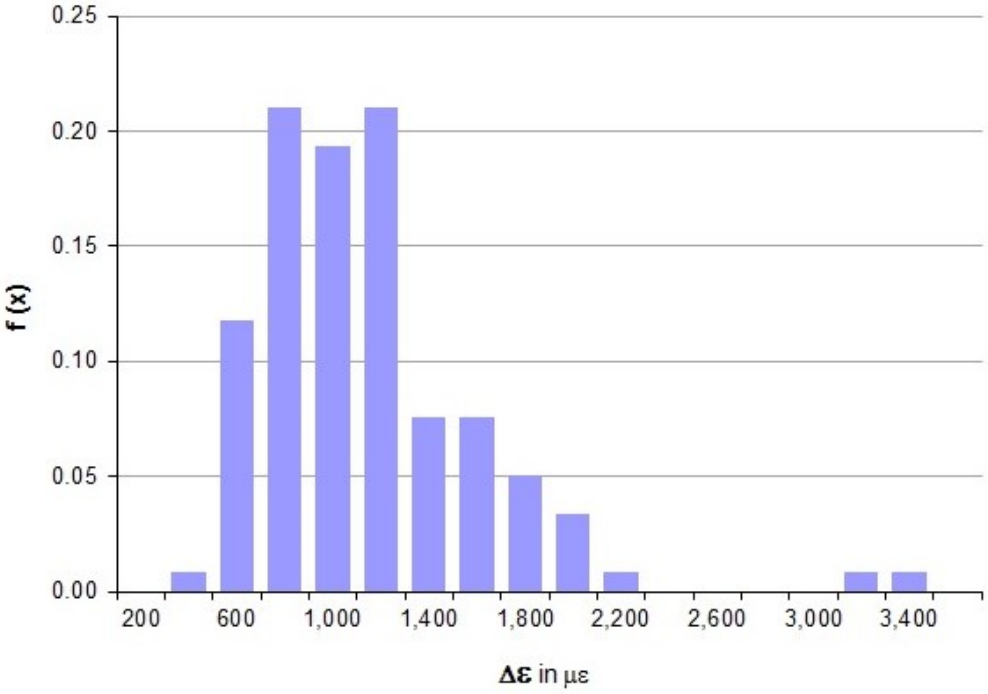

For convenience, the four (4) strain signatures are collated and displayed in **Figure 3.22** and labeled # 1 to # 4. Data set # 4 is taken from the open literature.

Figure 3.22 Collated Strain Distributions

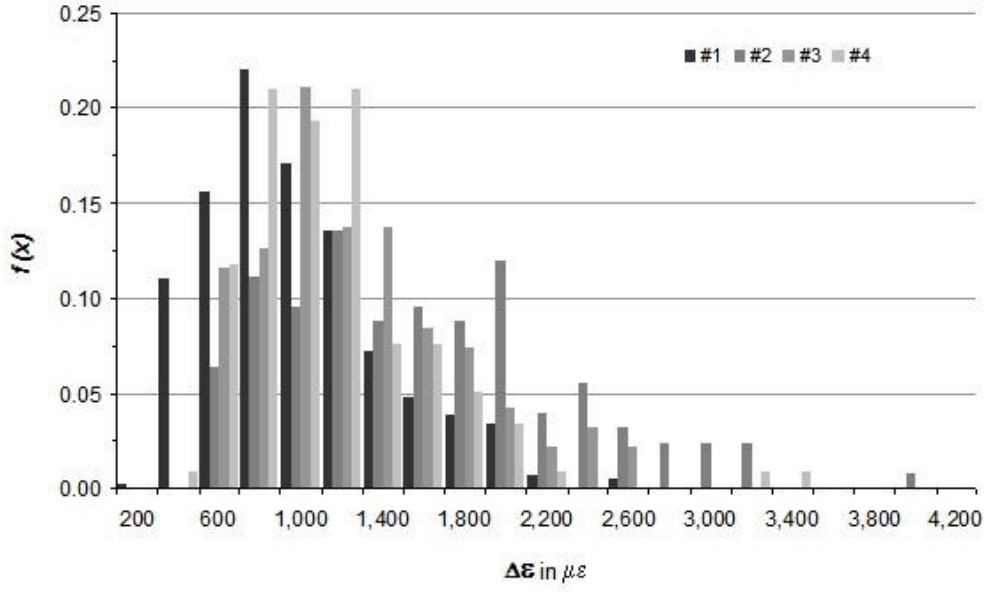

The individual strain results for each location are combined to form a single distribution and shown in **Figure 3.23** for purposes of statistical characterization. An average strain range of 1,190 με, and variation of +1σ = 590 με was calculated. This indicates that nearly 90% of the strains as reported by the industry occur within the monotonic 1 · YS / E strain limit.

Figure 3.23 Aggregated Strain Distributions

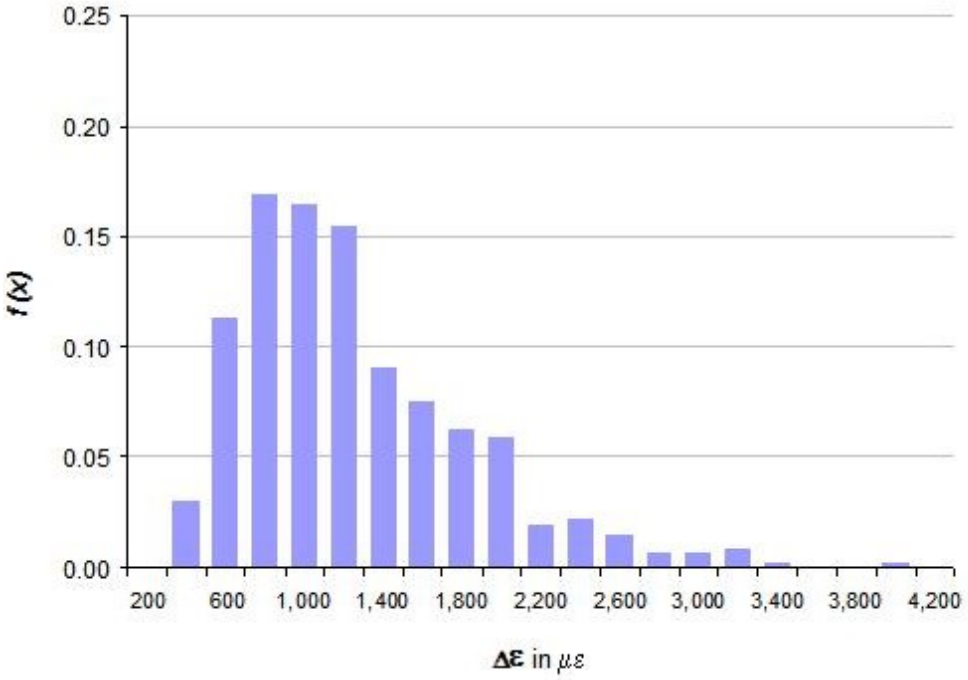

Using **Table 3.3**; only 1 of 458 readings, i.e., 0.2% of the data is outside of the

2 · YS / E strain equivalent shakedown limit stipulated by Code criteria. An upper temperature limit of 650 °F is used to correspond to the upper temperature limit experienced under quench conditions.

Table 3.3 Monotonic Elastic Strain Limits SA 387 Materials, 650 °F in με

	YS / E				2 · YS / E			
	100 °F		650 °F		100 °F		650 °F	
SA 387 12 – II	2,195	2,380	1,910	2,071	4,390	4,760	3,819	4,141
SA 387 11 – I	2,020	2,170	1,759	1,888	4,040	4,340	3,518	3,776
SA 387 22 - test	-	2,190	-	1,980	-	4,380	-	3,961

The cyclic stress – strain curve for 1¼ Cr – ½ Mo coke drum shell material shown in **Figure 3.24** shows that the elastic strain range in cyclic loading is approximately 4,600 με which exceeds the strain distributions summarized in **Figure 3.23**. Hence, the strain exposures in coke drums under thermomechanical loading are likely all in the cyclic elastic strain range.

Figure 3.24 Cyclic Stress – Strain Curve for SA 387 Grade 11 Material

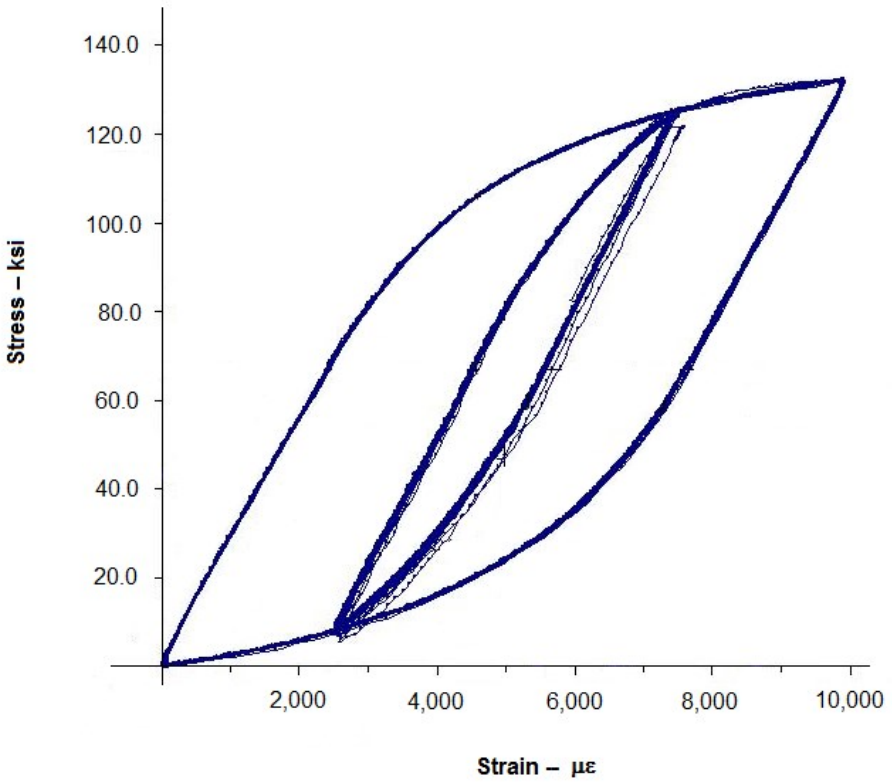

CHAPTER 4 FATIGUE LIFE CRITERIA

The ASME Code limits design fatigue life by stipulating an allowable number of cycles for the stress or strain experienced by a component. The basis of the ASME fatigue curves is based on a phenomenological treatment of fatigue which spans both the high cycle and low cycle regimes comprising mechanical fatigue.

The current industry Code, ASME VIII Division 2 provides a combined stress based criteria and using a pseudo-elastic stress criteria for the low cycle portion of the normally referenced S – N curve. The curves are particularized for material groups and operating temperature to a maximum component temperature of 700 °F [371 °C]. This temperature limit is based on creep considerations; but, in practice the curves are used above this temperature and are extrapolated using the methodology available within the Code rules.

4.1 Criteria of the ASME Code

The origin of low cycle fatigue curves derived with the separate works of Coffin and Manson [42] and, Manson [43]] in the 1950's who proposed a low cycle fatigue curve using two monotonic properties; ultimate tensile strength and reduction of area. The ASME Code simplified this, as explained by Langer building on the work of Coffin [see [ref 7] in Langer paper [44]] to present the following development [44, 45]:

Referencing Coffin (LF Coffin, A Study of the Effects of Cyclic Thermal Stresses on a Ductile Metal", Trans. ASME Vol 67, 1945) [45, 46]

$$\sqrt{N} \cdot \varepsilon_p = c \tag{4.1}$$

where

$c = \frac{1}{2} e_f$; $e_f \equiv$ the fracture ductility or true strain at fracture, i.e.

$$\varepsilon_f = \ln \frac{100}{100 - RA} \tag{4.2}$$

hence

$$\varepsilon_p = \frac{1}{\sqrt{N}} \cdot \frac{1}{2} \ln \frac{100}{100 - RA} \tag{4.3}$$

Since $\varepsilon_t = \varepsilon_p + \varepsilon_e$ then,

$$\varepsilon_t = \frac{1}{\sqrt{N}} \cdot \frac{1}{2} \ln \frac{100}{100 - RA} + \varepsilon_e \tag{4.4}$$

Since the Code was intended to be applicable to high cycle fatigue, as well, strain was converted to a linearized stress expression, as

$$\begin{aligned} 2 \cdot S = E \cdot \varepsilon_t &= E \frac{1}{\sqrt{N}} \cdot \frac{1}{2} \ln \frac{100}{100 - RA} + E \cdot \varepsilon_e \\ &= E \cdot \frac{1}{\sqrt{N}} \cdot \frac{1}{2} \ln \frac{100}{100 - RA} + 2 \cdot \Delta S_e \end{aligned} \tag{4.5}$$

The expression, ΔS_e was set at the endurance limit and an error of 16% was estimated at N = 1,000 cycles. This provided for a continuous curve spanning both the low cycle ($< 10^5$) and higher cycle portions ($> 10^5$) to use in pressure vessel construction.

Langer shows the development to the more recognizable form using Manson's approach by partitioning the phenomenological expression into a plastic range and an elastic range by letting

$$\varepsilon_p = MN^z \quad and \quad 2\Delta S_e = GN^k \tag{4.6}$$

then

$$\varepsilon_t = MN^z + GN^k \tag{4.7}$$

and

$$\varepsilon_t = \frac{1}{2} \cdot \ln \frac{100}{100 - RA} \frac{1}{\sqrt{N}} + 2.5 \frac{\sigma_f}{E} N^k, or, as \tag{4.8}$$

$$= \frac{1}{2} \cdot e_f \cdot \frac{1}{\sqrt{N}} + 2.5 \frac{\sigma_f}{E} N^k \tag{4.9}$$

Hence, the coefficient "z" in (4.7) is – 0.5 using Coffins approach.

Manson showed that the coefficients "k" and "z" can be determined from a minimum of two (2) strain – fatigue tests at well-separated values of strain to observe ΔS and N. Manson tested a number of materials, **Figure 4.1** and presented universal slope values to be used for estimates for cyclic life when the complication of an assumption of the exponents as a material property was not warranted [43].

Figure 4.1 Strain versus Cyclic Life [43]

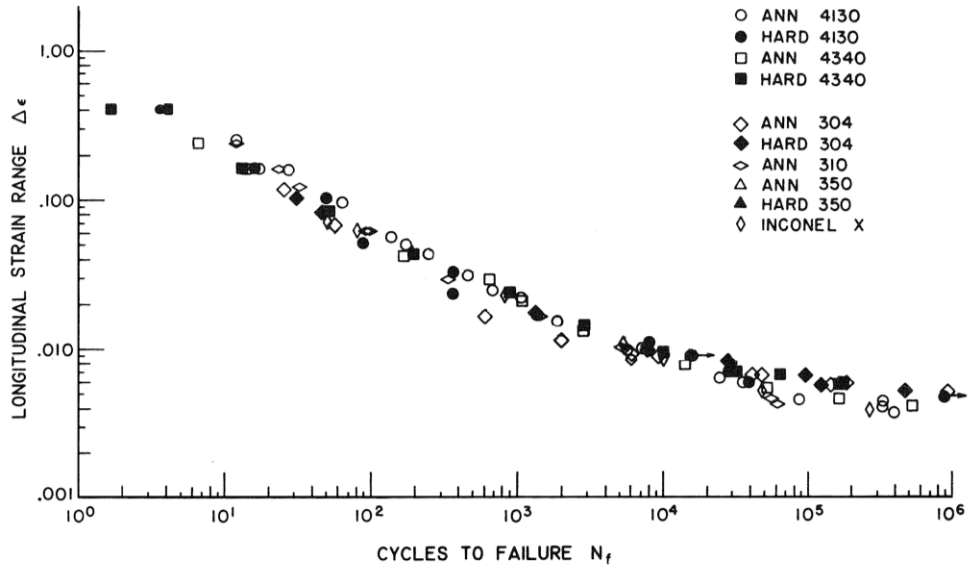

The values of – 0.12 for the elastic component and – 0.6 for the plastic component were recommended as indicated in **Figure 4.2.**

Figure 4.2 Coffin – Manson Universal Slopes Approach [42]

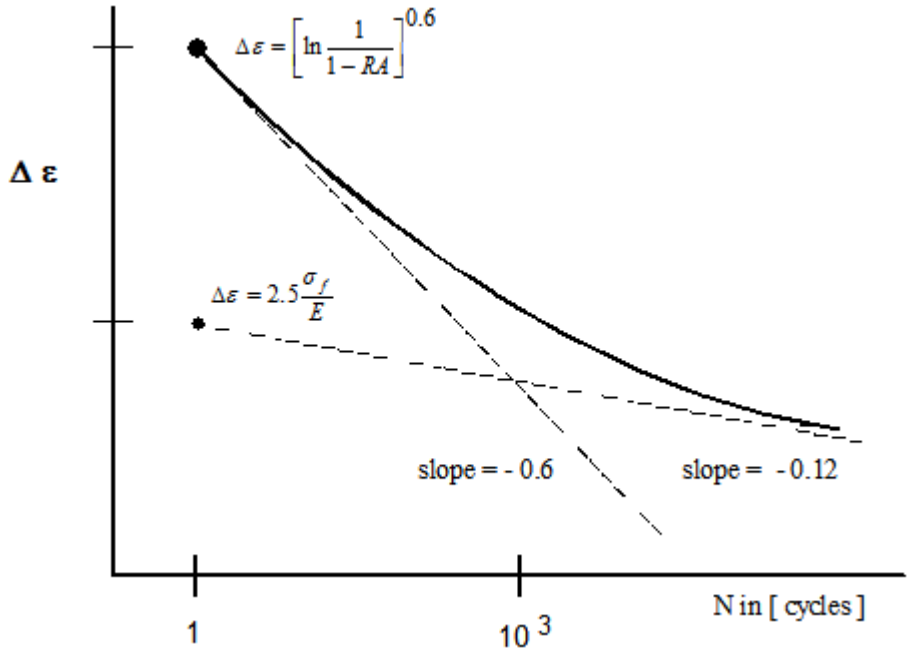

Hence,

$$\varepsilon_t = \frac{1}{2} \cdot \varepsilon_f \cdot N^{-0.6} + 2.5 \frac{\sigma_f}{E} N^{-0.012} \tag{4.10}$$

Later, Manson and Hirschberg presented a modification [47]

$$\varepsilon_t = \left[\ln \frac{100}{100 - RA} \right]^{0.6} \cdot N^{-0.6} + 3.5 \frac{\sigma_u}{E} N^{-0.012} \tag{4.11}$$

Manson stipulated that the Universal Slopes Equation was not intended for use with specific materials; rather, if specific materials were tested the appropriate material properties would need to be established and substituted into equation (4.7).

Manson later explained the difference between his formulation, which used an exponent of - 0.6 for low cycle fatigue, to the value of the exponent of - 0.5 in Coffin's formulation.

ASME VIII Division 2 adopted the Manson expression using an exponent of – 0.5 and explicitly provides the development of the Code basis in reference [48]**.** This is a key document in understanding and using the Code.

The ASME Code prescribes the design fatigue curve provided in **Figure 4.3**. Carbon, low alloy steels and TP 4xx, low chrome stainless steels are grouped in the design fatigue curve which may be particularized using the specific Young's modulus value at temperature. The ASME design curve is developed from smooth bar test specimens and presented as a pseudo-elastic stress amplitude.

Figure 4.3 Fatigue Design Curve Prescribed by ASME VIII Division 2

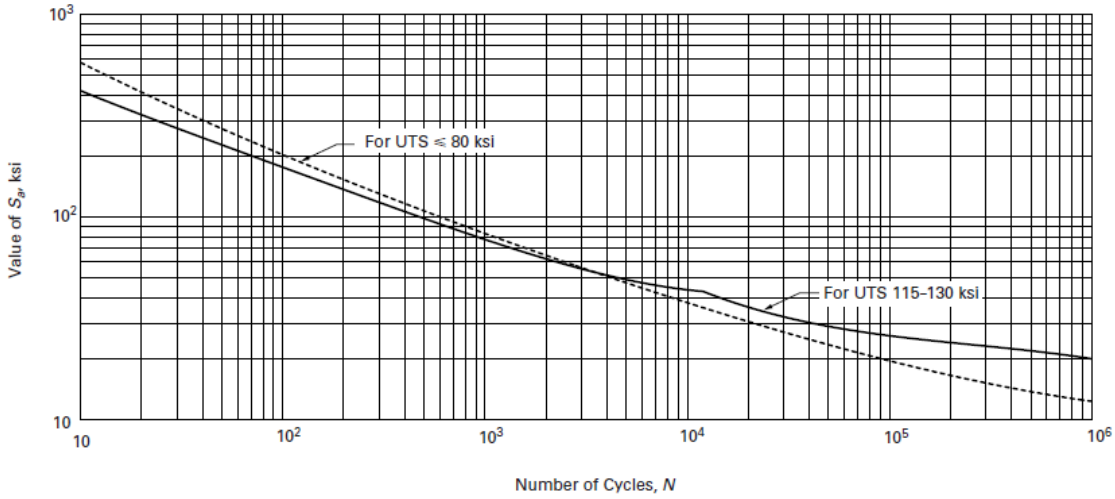

Notes:

1. Stress amplitude – N curve from ASME VIII Division 2, as published prior to the 2007 edition

Both elastic – structural stress analysis and elastic – plastic analysis approaches are allowed. A structural stress range is employed for the former and an equivalent structural stress is employed for the latter. The structural stress is a function of the membrane and bending stresses normal to the hypothetical crack plane and modified for low cycle fatigue using Neuber's rule [48].

The smooth bar fatigue design curve is consistent with Code practice from introduction of the 1st edition of ASME VIII Division 2 in 1963 and up to the edition released in 2004. The approach to determination of the fatigue life of welds was to use a fatigue strength reduction factor applied to the elastically calculated stress. For full penetration butt welds, as used to join pressure vessel shell sections, this was taken as two (2) to 2.5. The factor was applied by multiplying the calculated stress amplitude by 2 to 2.5 prior to entering the fatigue design curve.

Jaske presented data showing that non-isothermal thermo-mechanical fatigue are much more damaging to fatigue strength than isothermal strain cycling [49, 50]. **Figure 4.4** – is reprinted from Figure 3 from STP 770, with clean up of data at 800 °F for AISI 1010 carbon steel. The results from in – phase and out – of – phase thermo-mechanical loading was shown to be both more deleterious than isothermal fatigue.

Figure 4.4 Comparison of Thermo-mechanical to Isothermal Fatigue [49]

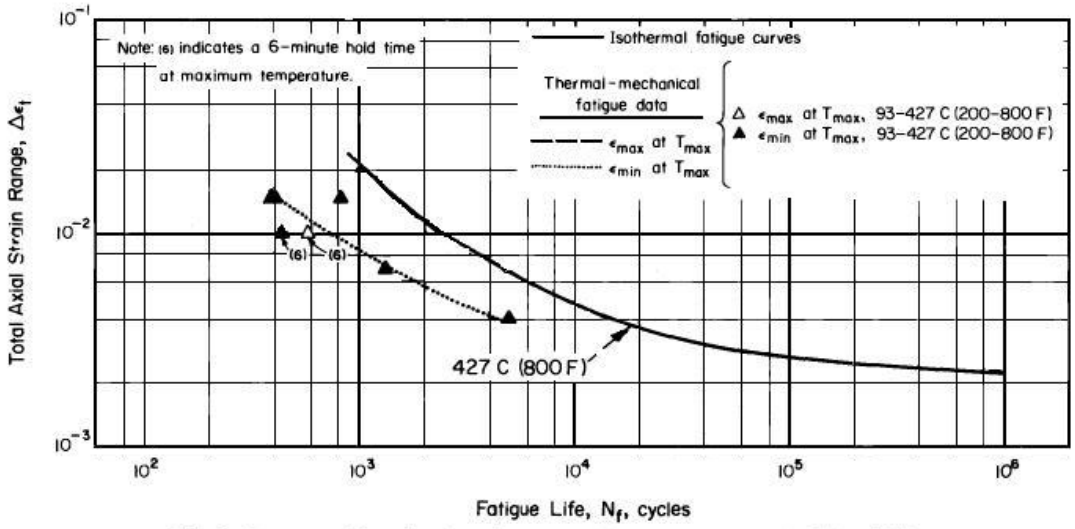

A clean sheet rewrite of the Code was released in 2007 which introduced a separate curve for the design fatigue assessment of welded joints based on use of elastic – structural stress analysis. The release has not addressed Jaske's concerns about non-isothermal strain cycling.

There are several important considerations in using the Code fatigue design curves for the purpose of determining a service fatigue life for coke drums.

Three considerations are listed

1. the curves are design curves intended for the design life estimation of pressure vessel components in fatigue service. By using a design margin, use of the Code curve ensures safe operation of the pressure vessel throughout the design life by providing an alert point

2. the extent of failure is not specified within the Code; the Code does not state the failure criterion in establishing fatigue failure, namely, whether complete through thickness separation or incipient cracking

3. the applicability to non-isothermal strain cycling

4.2 ASME Design Fatigue Life Margins

The ASME design fatigue curves are intended to determine a design life. In comparison, the notion of service life for a pressure vessel is defined to be the reasonably expected life in service under actual service conditions rather than design operating conditions. The Code design life definition includes margins to account for uncertainty in determination of service loads as well as crack initiation or fracture.

The design approach is a combined approach using the following:

1. Equipment owners add a small margin to the maximum temperature and pressure loads expected in service

2. The Code mandates a design margin on the use of the allowable stress to be used for the determination of the pressure thickness by equation (1.1). The allowable stress, S is based on the lower of

   - $^{2}/_{3} \cdot$ SMYS, or
   - $^{1}/_{3.5} \cdot$ SMTS

   at the design temperature.

Since most pressure vessel construction materials are supplied to a higher quality than stipulated by the Code, additional margins are provided implicitly. **Tables 2.1 and 3.1** demonstrate the difference between Code minimum strength requirements and material measured strengths.

For a coke drum, the design margins on pressure and temperature are verified by review of the design specification sheet provided by the equipment owner. For example, the CRD partner coke drums have a declared design temperature of 925 °F [496 °C], but operated well below this temperature at 700 °F [371 °C](Fig 4.23) for a long period prior to temperatures rising to more modern targets of 850 °F [454 °C] to 900°F [482 °C]

Figure 4.5 plots the ASME smooth bar design curve for the material group including carbon, low alloy and TP 4xx stainless steels adjusted to 900 °F [482 °C] against the experimental data of Ramos and Chen.

Figure 4.5 Comparison of ASME Smooth Bar Design to Measured Data

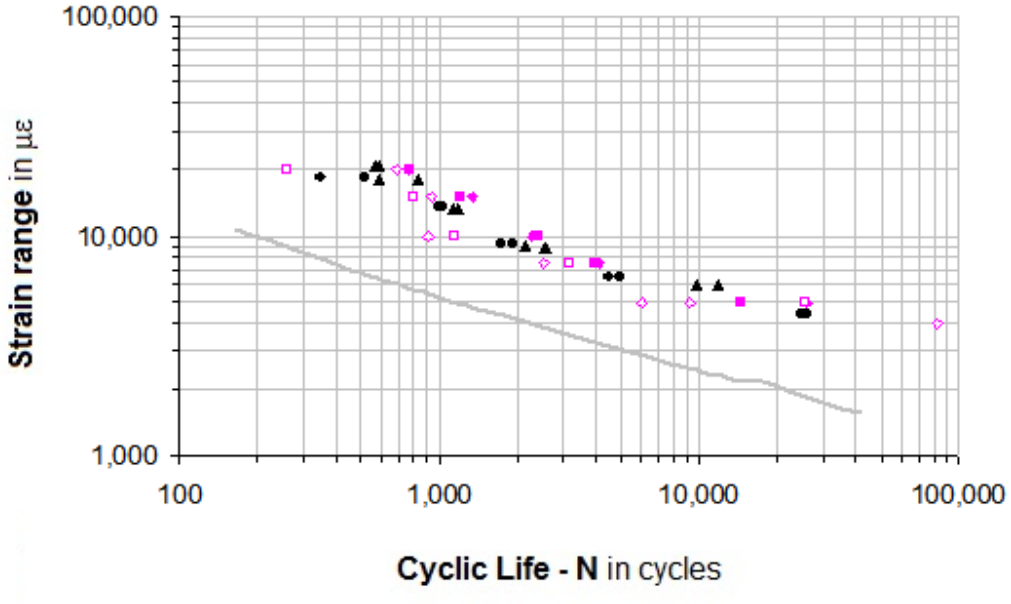

Notes

1 smooth bar design curve for ferritic steel material category – [900 °F]
2 Closed symbols for smooth bar experimental data
3 Open symbols for welded joint, HAZ experimental data

The design margin for the ASME smooth bar design curves is 20:1 on cycles and 2:1 on stress / strain [30, 36].

Figure 4.6 plots the (1) ASME design curve, (2) the curve based on use of the 20:1 factor applied to cycles and, (3) the curve based on the 2:1 factor applied to strain, with all three curves corrected to 900 °F [482 °C]. The curves are plotted against the data from Ramos for 1Cr – ½ Mo and 1¼ Cr – ½ Mo steels tested at 850 °F [454 °C] and the data from Chen at 900 °F [482 °C]. The plot indicates that the design margin of 20:1 on cycles is appropriate at low cycles to approximately 50,000 cycles and confirms the disclosure in references [30, 36]. Here, Barsom and Vecchio advise that the fatigue design curves were obtained from mean curves by applying a factor of 20 on cycles and 2 on stress and using the more conservative resulting value. The factor of 20 prevailed in the low-cycle regime (i.e., below about 10,000 cycles). The presented plot, **Figure 4.6** indicates differences consistent with the ASME methodology.

Figure 4.6 ASME Fatigue Curve Design Margins

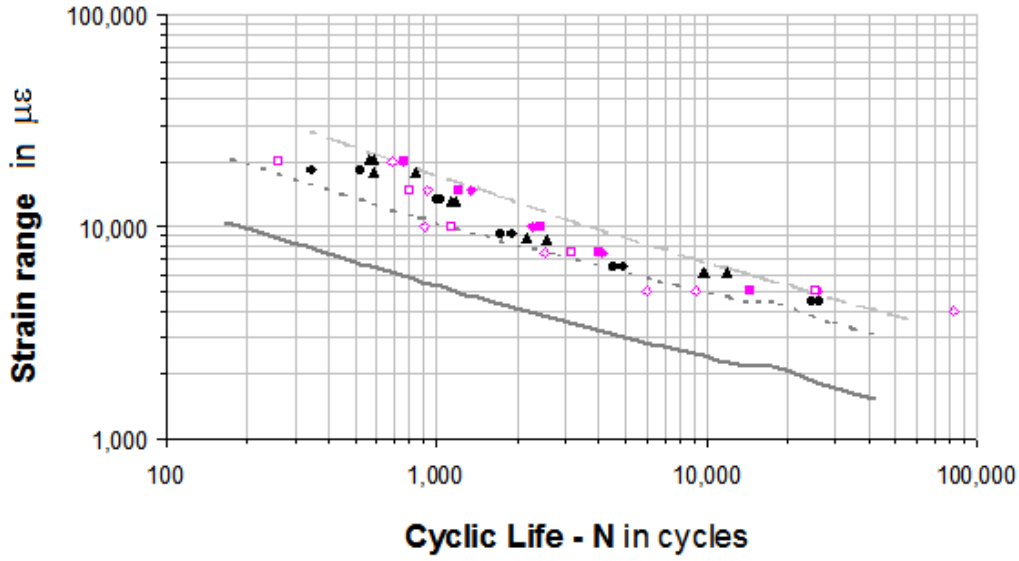

Notes

1 welded joint design curve for ferritic steel material category – [900 °F]
2 design curve multiplied by 20 on cycles
3 design curve multiplied by 2 on stress
4 Closed symbols for smooth bar data
5 Open symbols for welded joint, HAZ data

For the clean sheet rewrite of the Code, ASME included a welded joint design curve with confidence intervals for ±1σ, ± 2σ, and ± 3σ standard deviations. The welded joint design curve and the +3σ curve at 900 °F [482 °F] are plotted against the Ramos and Chen data in **Figure 4.7**. The +3σ welded joint curve plots at the lower bound of the experimental data and suggests a bounding limit for C – ½ Mo and Cr – Mo alloys that are used for coke drum fabrication.

Figure 4.7 ASME Design Curve with + 3σ Confidence Interval

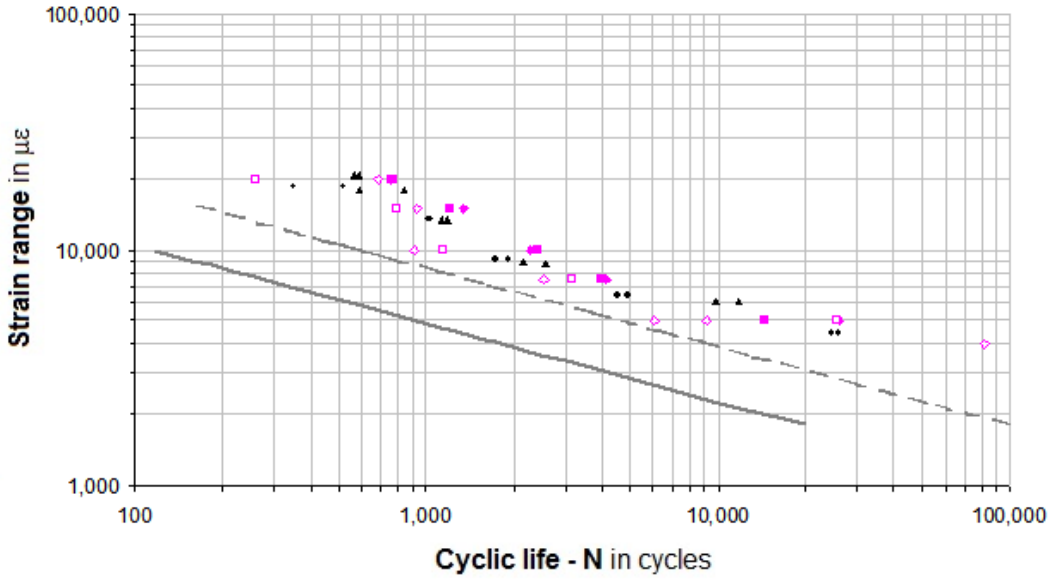

Notes

1 ——— welded joint design curve for ferritic steel material category
2 – – – + 3σ confidence interval
3 Closed symbols for smooth bar data
4 Open symbols for welded joint, HAZ data

Note that for the design of welded joints, the ASME Code prescribes the use of a lower bound welded joint design curve of – 3σ limited to 700 °F (ref: ASME D2 par #.F.2.2(a)). The work of Ramos and Chen show that the fatigue strength fatigue curves can be extended to 900 °F [19, 35]. It is not known whether the welded joint fatigue curves are overly conservative since the experimental data is not available to the public.

4.3 Code Fatigue Failure Defined

The Code does not describe the anticipated failure mode being protected against; i.e., crack initiation or specimen separation.

Manson studied both crack initiation and crack fracture and noted the ambiguity in the literature. However, he did show that an exponent of – 0.5 for the plastic strain range aligned with crack initiation. Crack initiation was defined to be the number of cycles to initiate a 0.003 inch [0.080 mm] deep crack in a ¼" [6.35 mm] diameter fatigue specimen. Failure life, N_f was defined to be the number of cycles to separate the specimen [48, 51, 52].

Kalnins established independently that Code failure corresponds to observation of a small crack of 0.5 mm [0.020 inch] in fatigue specimens and not crack propagation through the thickness [53]. Another key observation is that geometries which possess a uniform strain through their thickness will behave consistent with Code rules. Hence, the fatigue models were indicative of membrane strains (i.e., low cycle fatigue) and membrane stresses (i.e., high cycle fatigue).

The Code assesses crack propagation using fracture mechanics approaches in order to predict final failure i.e., separation of components. However, for the determination of service fatigue life for coke drum service, this effort uses the definition of fatigue failure as implicitly practiced by the Code because

- coke drum thicknesses vary according to pressure thickness criteria
- the specific environmental factors present in a coke drum and their impact on crack propagation are not established
- use of the initiation criterion provides a level of conservatism

4.4 Non- Isothermal Loading

Jaske showed that non-isothermal loading was more damaging than isothermal loading for AISI 1010 carbon steel [49]. Chen shows that the fatigue life of C – ½ Mo and Cr – Mo steels is comparable under either loading condition at high strain but a significant benefit is observed with C – ½ Mo at the lower portion of the strain levels used in the study [35].

Chen felt that thermo-mechanical fatigue testing simulated the thermal and mechanical loading conditions experienced by coke drums [35].

The operational sequencing of a coke drum is illustrated in more detail in **Figure 4.8.** The temperature and pressure scales are intentionally not plotted.

1. pressure loading occurs at the start of the production cycle and remains nominally constant throughout the oil filling cycle
2. steam heating occurs simultaneously as pressure loading
3. a vapor heat up occurs in follow up to the steam heat / pressure loading
4. oil filling commences after steam heating and vapor heating
5. hydrostatic loading from live weight loading occurs under isothermal conditions
6. on completion of oil filling, water quenching is initiated; thermo-mechanical strains occur under isothermal and non-isothermal conditions depending on whether “hot spots” or “cold spots” develop

   Large compressive strains occur during nominally isothermal conditions when “hot spots” form. For “cold spots”, large tensile strains form under in-phase non-isothermal conditions since they are related to non-uniform contact of quench water with the shell.

Figure 4.8 Sequencing of Coke Drum Operational Cycle

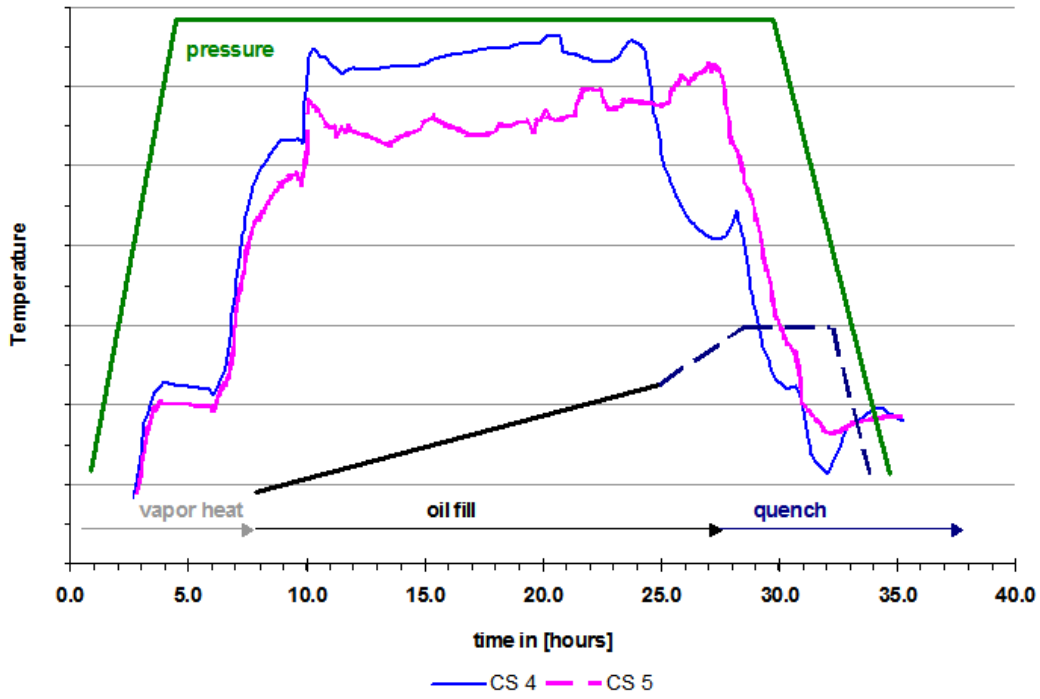

Notes

1 CS 4 refers to temperature evolution at shell course 4
2 CS 5 refers to temperature evolution at shell course 5
3 pressure evolution in coke drum
4 vapour heat, oil fill and quench time spans as indicated

For determination of a service fatigue life, a reasonably conservative approach is needed but with less conservatism than used by the Code design fatigue life methodology.

This is complicated by the behavior of so-called “strong” materials, exemplified by Cr – Mo steels (SA 387 22), and ductile materials, such as the C – ½ Mo and C – Mn – Mo or Ni steels (SA 204 / SA 302). **Figure 4.9** shows the iso-thermal, low cycle fatigue (ILCF) behavior and non-isothermal, thermo-mechanical (TMF) behavior of the two steels over the low cycle range of the strain – fatigue life curve. For the C – ½ Mo steels, the ILCF curve is more conservative in the range of interest [35].

The operating temperature is specific to the equipment and may be in a temperature range extending from 650 °F to 900 °F [343 °C to 482 °C]. For this work, a temperature of 900 °F [482 °C] will be used for convenience. Particularization to specific units is necessary for application to actual coke drums.

Figure 4.9 Fatigue Life Comparison of Strong versus Ductile Materials

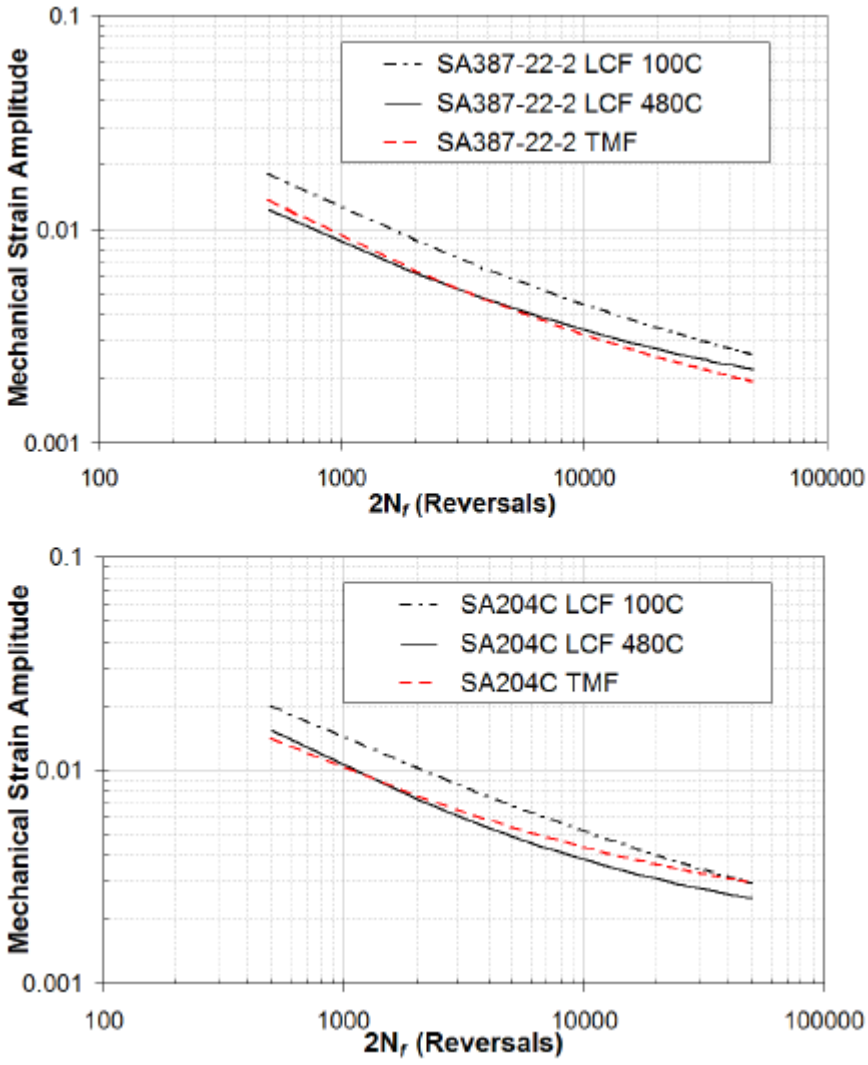

Notes

1 LCF means isothermal low cycle strain fatigue testing
2 TMF means in-phase thermal and strain fatigue testing

4.4 Creep & Creep – Fatigue Considerations

The operating temperature of coke drums extends to 900 °F [482 °C] which is well beyond the conventional applicability limits of the ASME VIII Division 2 fatigue analysis methods, i.e. 700 °F [3781 °C]. This limit was chosen by the ASME to avoid creep interaction effects and reflects the original purpose of the Code; i.e. nuclear applications. Therefore, some discussion of this constraint is needed.

Equipment owner's design specifications do not reference that coke drums operate in the creep regime.

API 579 – 1 / ASME FFS provides a methodology to examine creep effects in coke drums [8].

Referring to **Figure 4.8**, it is apparent that the coke drum experiences stress at high temperature. The primary load carrying structure is the base material. The membrane stress in service is the allowable stress value assigned by the Code for the design temperature. Table 1.3 lists these values which can be used to enter the creep damage curves of the API 579 – 1 publication. As a benchmark, a service life of forty (40) years will be arbitrarily used. From **Figure 4.8,** the time at temperature is about eighteen (18) hours. Modern day operation will incur an oil fill period of twelve (12) hours and this will be used for arithmetic convenience. The data does not indicate whether shortened oil filling period coincides with higher coke drum operating temperatures [13].

Accordingly, 40 years of service results in a high temperature exposure duration of 175,200 hours. In **Figure 4.10,** a screening level methodology is provided and indicates for a coke drum fabricated from C – ½ Mo steels, the service temperature limit would need to be held to 850 °F [454 °C]. At 900 °F [482 °C], the interpolated life expectancy is 40,000 exposure hours or 9 service years.

Figure 4.10 ASME Level 1 Creep Screening Criteria for C – ½ Mo

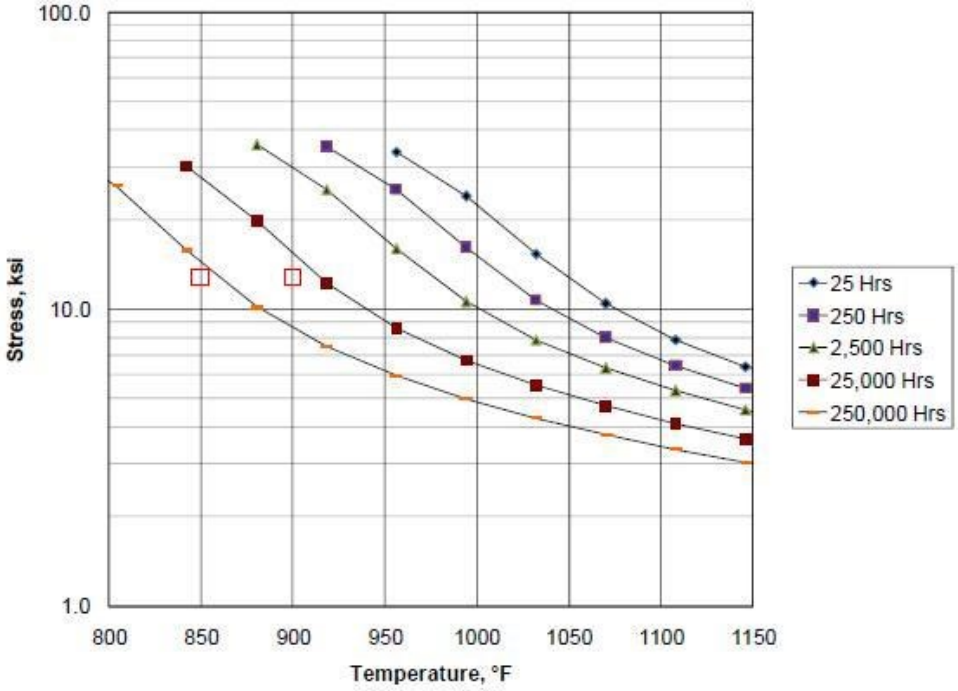

Notes

1 Open symbol plots operation of interest in Figures 5.10 – 5.12

For 1¼ Cr – ½ Mo steels, using **Figure 4.11**, the anticipated life 140,600 hours.

Figure 4.11 ASME Level 1 Creep Screening Criteria for 1¼ Cr – ½ Mo

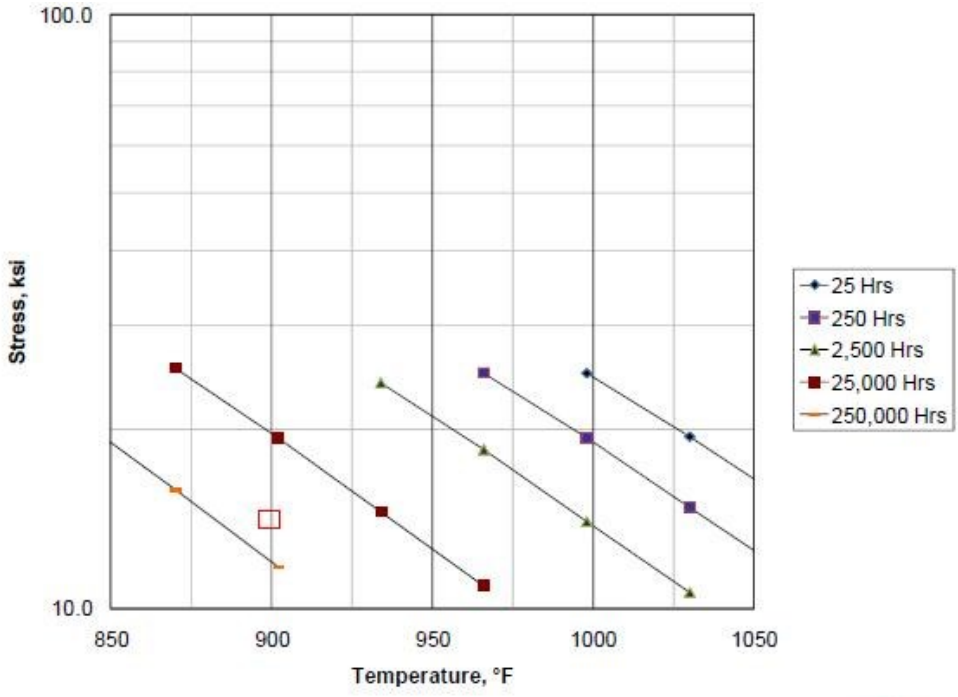

For 2¼ Cr – 1 Mo steels, the anticipated life is in excess of 250,000 hours as shown in Figure **4.12.**

Figure 4.12 ASME Level 1 Creep Screening Criteria for 2¼ Cr – 1 Mo

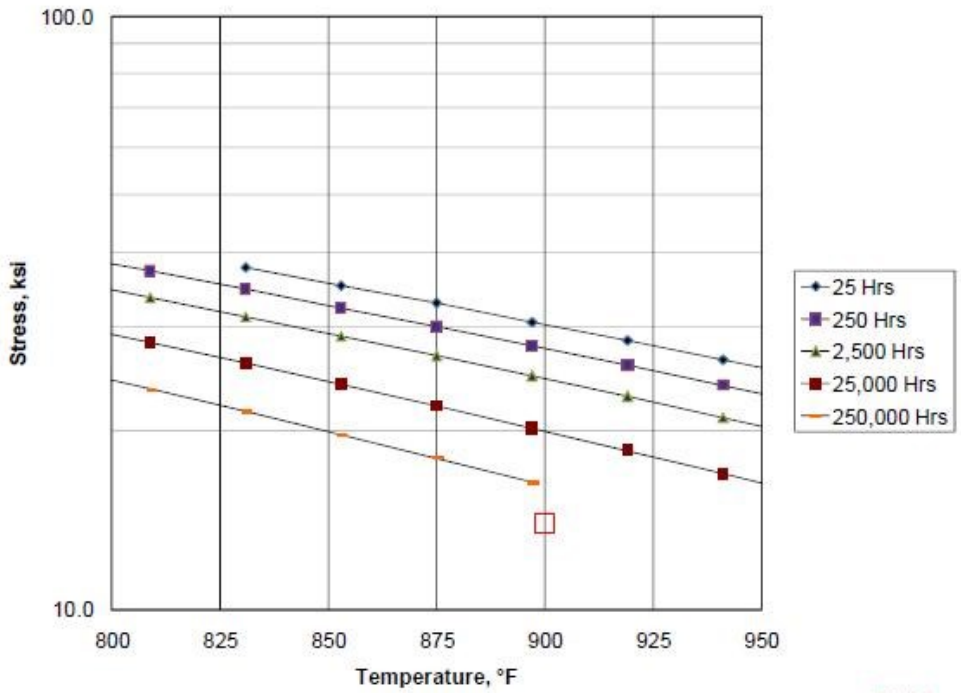

For the TP410S clad layer, differential thermal expansion at service temperature results in a pseudo – elastic stress of

$$\sigma_c = \frac{(\alpha_b - \alpha_c)\cdot(T_h - T_0)\cdot E_c}{1 + \dfrac{t_c \cdot E_c}{t_b \cdot E_b}} \cdot \frac{1}{1-\mu} \tag{4.11}$$

$$\sigma_c = \frac{(9.1 - 7.2)\cdot(900)}{1 + \dfrac{0.110 \cdot 23.2}{1 \cdot 24.8}} \cdot \frac{23.2}{1} \cdot \frac{1}{1-0.3} = 67{,}615\ \text{psi}$$

Entering **Figure 4.13** from API 579 – 1, the stress load exceeds the screening level criterion and creep cracking is to be expected. A detailed study by Penso et al. of the metallurgical condition of a coke drum found extensive cracking in the clad material. The most prevalent cracking was shallow, *"spread on the entire internal surface in all samples analyzed"* with average depth of 1 mm. Cracks of greater depth occurred in the fusion boundaries of clad and clad weld [20]. The 1996 API survey reported that 64% of survey respondents reported ID initiated cracking while 71% reported OD initiated cracking [*sic*] [13]. The survey did not clarify how ID to OD crack initiation was established.

Figure 4.13 ASME Level 1 Creep Screening Criteria for 12 Cr / TP410S

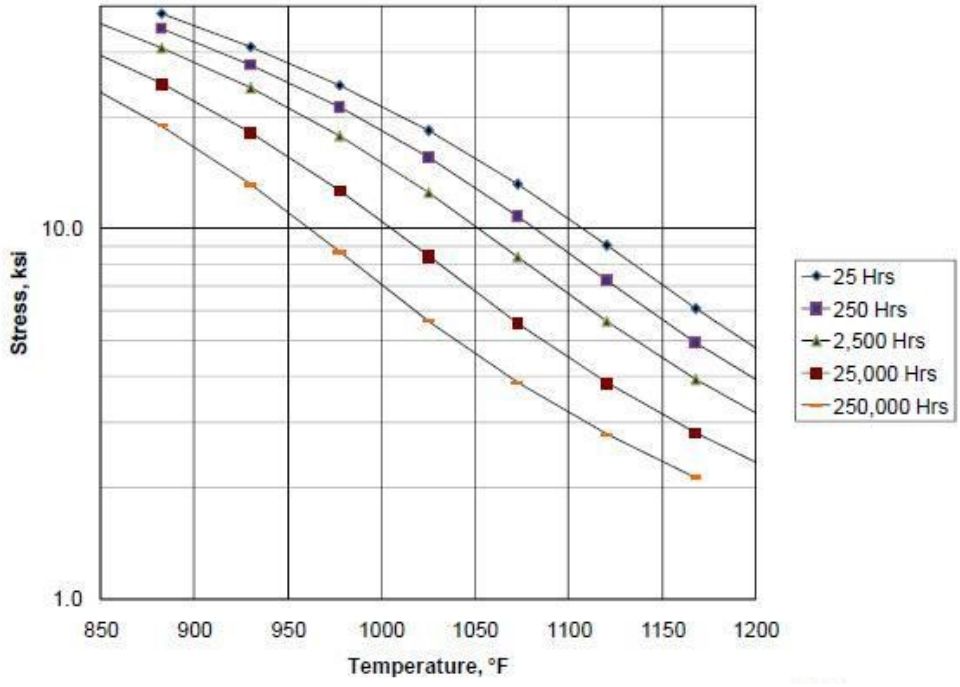

4.5 Fatigue Curves

The numerous fatigue studies available in the open literature allow determination of a specific fatigue curve for the materials of construction of coke drums. The design fatigue curves in the industry standard literature, however, are not sufficiently detailed.

4.6 Mean Strain Effects

Mean strain effects are acknowledged by the ASME criteria but are stated to be inconsequential for low and medium-strength materials and no adjustment for mean stress is necessary where stress reaches yield strength. Hence, for low cycle fatigue, mean stress effects are not required [48].

In contrast, O' Donnell states, in the ASME Companion Guide, that mean stress effects necessitate determination of an equivalent alternating stress component prior to entering the fatigue life curve [54]. He refers to use of the modified Goodman diagram or use of the closed form expression

$$S_{eq} = \frac{S_{alt}}{1 - \frac{S_{mean}}{S_u}} \tag{4.12}$$

where

S_{eq} ≡ equivalent alternating stress amplitude to enter the S – N graph
S_{alt} ≡ apparent alternating stress amplitude
S_{mean} ≡ mean stress
S_u ≡ ultimate tensile strength

Collins provides data showing that mean strain effects are negligible from N_f = 100 to chart end at N_f = 10,000 cycles i.e., the low-cycle range according to **Figure 14.4** [15].

Figure 4.14 Impact of Mean Strain on Fatigue Life, Collins [15]

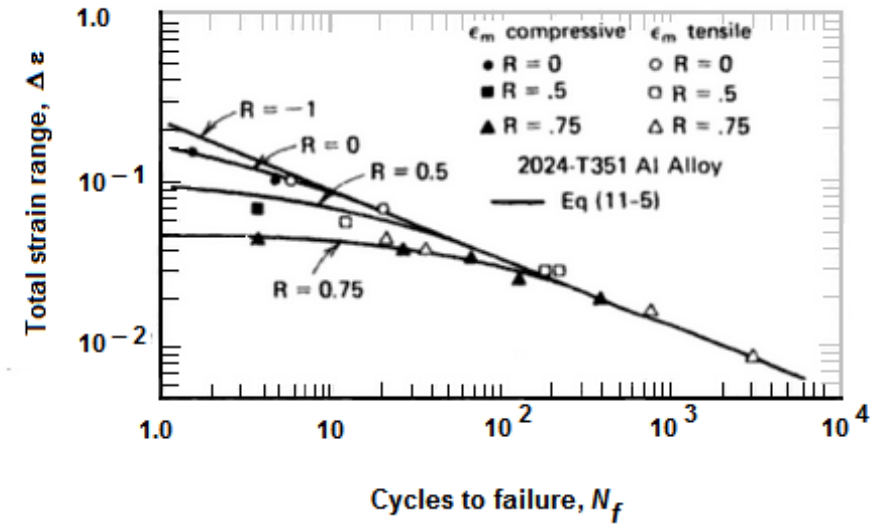

Alternatively, Stephens, Fatemi et. al present data which suggests mean strain (stress) does have influence in the low cycle fatigue life range, **Figure 4.15** [55].

Figure 4.15 Impact of Mean Strain on Fatigue Life; Stephens, Fatemi [55]

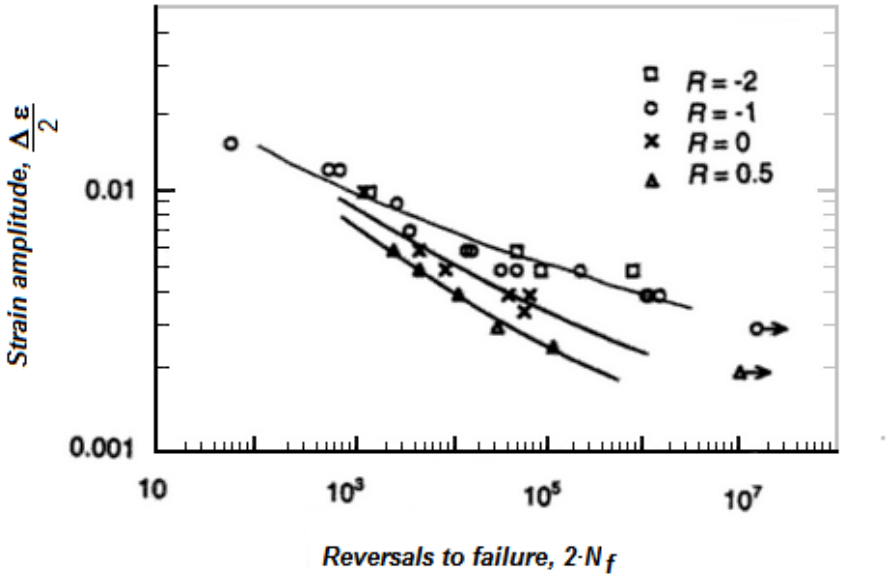

Notes

1. For SAE 1045 low carbon steel, hardened

Stephens, Fatemi et al. argue that because of stress relaxation at large strain amplitudes due to the presence of plastic deformation, mean stress effects on fatigue life is small in the low-cycle fatigue region.

Reference is made to “Morrow’s mean stress method” in which the strain amplitude,

$$\varepsilon_a = \frac{\Delta \varepsilon}{2} = \frac{\sigma_f^{'} - \sigma_m}{E}\left(2 \cdot N_f\right)^b + \varepsilon_f^{'}\left(2 \cdot N_f\right)^c \qquad (4.13)$$

is adjusted by inclusion of the σ_m term in the elastic portion of the Basquin equation, refer to equation (2.1). This follows the trend displayed in **Figure 4.15** which applies to a high carbon content plain carbon steel, while it is inconsistent with the data of **Figure 4.14** which is for an aluminum alloy.

CHAPTER 5 ANALYSIS OF COKE DRUM THERMO-MECHANICAL STRAINS

Strains may be obtained directly from an operational drum using high temperature strain gauges, as discussed in § 3.2. Strain gauges are used sparingly, though, in practice due to

- their high unit cost
- limited operating life
- inaccuracies and improper use

The operating life for strain gauges is limited due to

- the large, imposed thermal strains
- their mechanical fragility in comparison to the imposed strains
- high operating temperatures
- corrosive environment

The accuracy and precision of strain gauges has not been investigated for this work and has not been demonstrated in the available literature as previously discussed in § 3.2. A more robust approach is provided by the use of thermocouples.

In **Figure 3.1**, 15 strain gauges and 119 thermocouples are used in the test panel. Strain gauge locations are represented by blue circles enclosing the red-colored dots representing thermocouple locations. As seen in **Figures 3.6** and **3.7**, the thermocouple is much simpler, consisting of thermocouple wire requiring only spot welding to the pressure vessel shell. When damaged in service, the thermocouple can be quickly repaired and reattached with small effort. The existing wire can be reused and reattached by trimming the corroded portion attaching to the shell. A recent design practice by equipment users is to use replaceable insulation panels on the shell that allow quick access to the shell surface.

The accuracy of strain gauge readings in the high temperature and corrosive environment of coke drum application has not been discussed in the literature although it is well known that coke drums experience large thermal strains in addition to large localized deformation. **Figure 5.1** illustrates the complicated deformation that can be experienced by a coke drum with both vertical and circumferential bulging occurring.

Figure 5.1 Coke Drum Shell Projected Deformation Profile

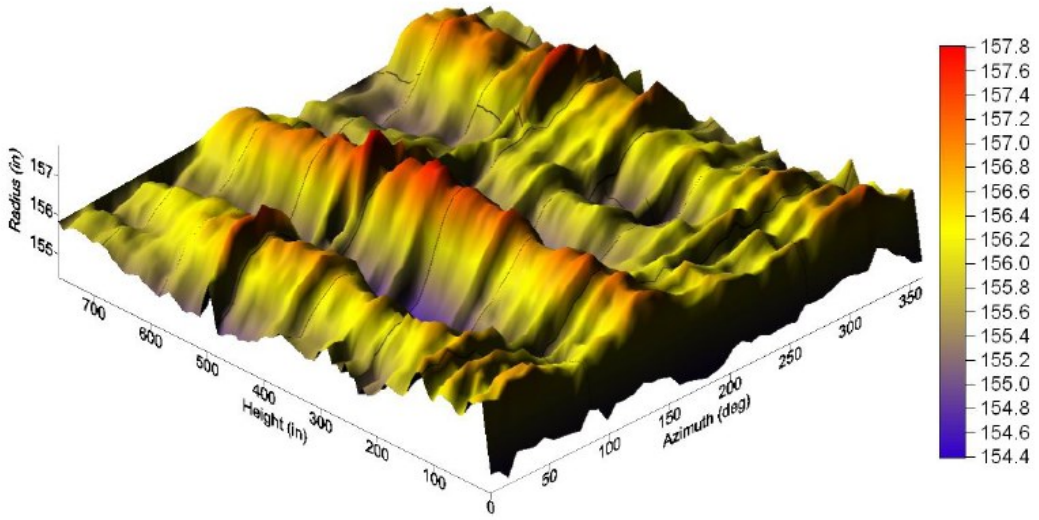

The literature indicates that thermocouples have been used to determine a temperature gradient from which a thermo-mechanical strain has been inferred by correlation with adjacent strain gauge readings. The method can be ineffective in that the length over which the gradient is measured is limited as was shown in **Figure 3.2**. Similarly, a line of close-spaced thermocouples may be used to capture a gradient in horizontal or axial directions. The difficulty is that it is physically impractical and cost prohibitive to apply the technique to an entire test panel.

The temperature gradients inferred from the tightly spaced grid do not necessarily correlate with strain gauges which will also include thermo-mechanical strains from more extensive effects, not only local temperature gradients. The practice has been to space the grids on approximately 1 inch centers over a single 2 foot length arc and vertical cross. Additionally, the data from this arrangement has not been made available in the industry literature.

Temperature data can be inexpensively obtained during coke drum operation over an extensive area and extended time period by use of simple thermocouple devices as pictured in **Figure 3.6**.

5.1 Temperature Based Life Estimate Methodology

The objective of this thesis is to estimate a service life based on temperature data since this data can be more simply and reliably retrieved. The essential steps in considering and accomplishing this are

- to retrieve temperature data for a suitable grid over a statistically relevant period
- that actual drum temperature data is used; this has been provided by a confidential source which logged temperature data at one-minute intervals for a one-year period
- that data from 51 or more consecutive cycles is taken; a block of 52 operating cycles was used
- that the temperature readings be interpolated in order to provide suitable input for determination of corresponding thermo-mechanical strains; an appropriate interpolation scheme must be established
- to assign the interpolated temperatures to a corresponding finite element grid to calculate the associated thermo-mechanical strains
- to repeat the process for an appropriate interval during the significant portion of the water quench cycle; this is the portion of the operating cycle which contains the maximum strain response
- to assemble the maximum and minimum strain exposures established for an individual water quench cycle
- to assemble the exposures from successive operational cycles as a block strain exposure profile and make a numerical count of maximum / minimum counts consistent with industry methodology
- to make a life estimate consistent with the precision stated in § 1.2

Temperature Evolution During Water Quench

In **Figures 3.5a – l**, a sequence of snapshots demonstrate the evolution of temperatures for a thermocouple grid presented in **Figure 3.1** during the water quench phase for an operational cycle. The grid spacing is approximately 665 mm [26.181”] horizontal and varying in the vertical direction between 570 mm [22.4”] and 683 mm [26.890”]. Spacing variations are due to field obstructions.

Figure 3.5g is reproduced as **Figure 5.2** with grid lines whose intersections represent the thermocouples.

Figure 5.2 Detailed Thermal Snapshot Profile, Part Grid 04 23:58

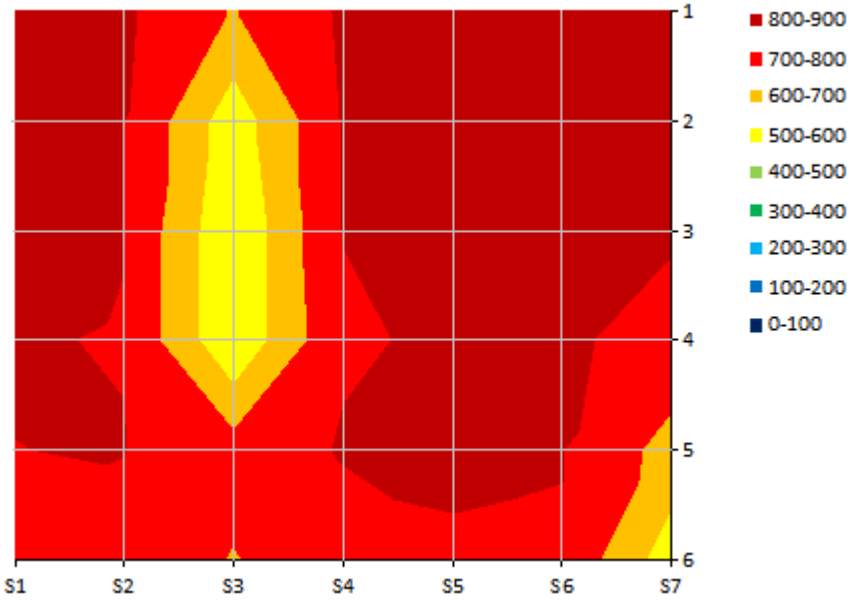

Table 5.1 lists the associated temperature readings for each of the grid points for comparison to **Figure 5.1.**

Table 5.1 Local Grid Temperature Readings for Figure 5.1

							Row
822	817	694	813	826	821	817	1
814	806	544	803	821	816	802	2
818	802	511	802	821	819	809	3
804	797	509	790	812	812	771	4
800	803	739	807	812	806	665	5
784	762	695	758	791	787	546	6
S1	S2	S3	S4	S5	S6	S7	
			Column				

Figure 5.3 details the local temperature distribution as presented by data display software at grid point 4 – S3 where a low temperature of 509 °F is measured. Temperature gradations are easily seen to be linear along the horizontal and vertical grid lines.

Figure 5.3 Local Thermal Snapshot Profile, Part Grid 04 23:58

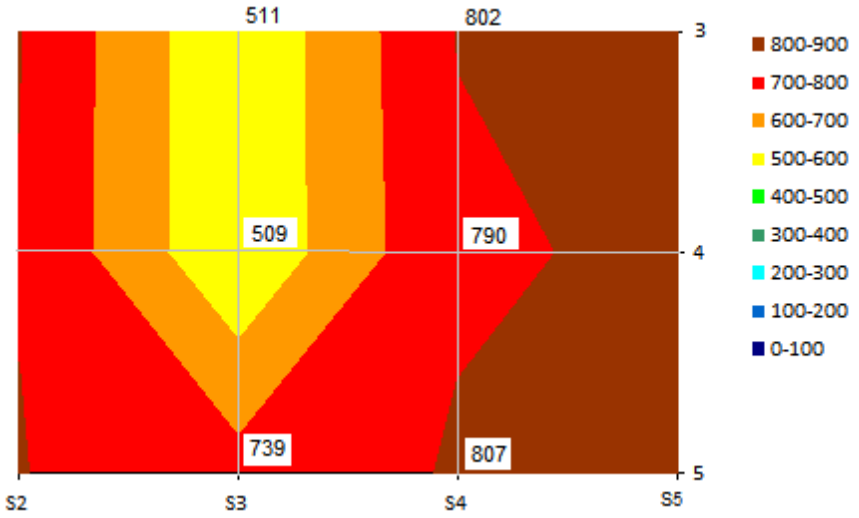

The physical distance between data points is large, nominally on the order of 665 mm [26”] and is too coarse to provide a valid FEA input mesh for calculation of thermo-mechanical strains.

There is no data available in the industry literature on coke drum temperature surveys to provide insight to the temperature distribution between discrete data points. The same situation applies to strain data recovered at discrete data points; only fifteen (15) strain gauged data points were provided among one hundred nineteen (119) thermocouple data points presented in **Figure 3.1**.

Heuristic Temperature Interpolation

Review of multiple temperature histograms such as depicted in **Figures 3.5a – l** show similar behaviors during water quenching;

- coke drum temperatures decrease in a nominally axisymmetric pattern in the bottom shell courses; this is consistent with the expected uniform rise in the level of water and consequent uniform decrease in shell temperature from bottom to top
- as water fill progresses into the cylindrical section, channeling occurs between the coke bed and coke drum shell and present as periodic intrusions (“fingers”) as exemplified in **Figure 3.5b**
- as internal channeling allows water to migrate into the higher temperature parts of the coke bed and, consequently, horizontal water flow makes contact with the coke drum shell, cold spots form above the nominal water level as revealed in **Figure 3.5c - f**
- the cold spots span a shorter distance circumferentially (3 consecutive t/c locations), but span a longer distance vertically (6 consecutive t/c locations), Figure **3.5h** is presented as **Figure 5.3** with grid markings, the intersections of the grid markings are t/c
- hot spots can span both small and large distances; the larger hot spots occur in the upper portions of the coke drum shell, while smaller hot spots occur in lower and upper portions; **Figure 5.4**. Note that this thermal profile is the interpolated linear profile from the captured (i.e., as measured) field data.

Hot spots occur where portions of the coke drum shell are protected from contact with water by, ostensibly, tightly adhering coke; eventually this effect dissipates as water eventually fills and soaks the interior of the coke drum.

Figure 5.4 Thermal Snapshot Profile, Measured Full Grid 05 00:06 in [° F]

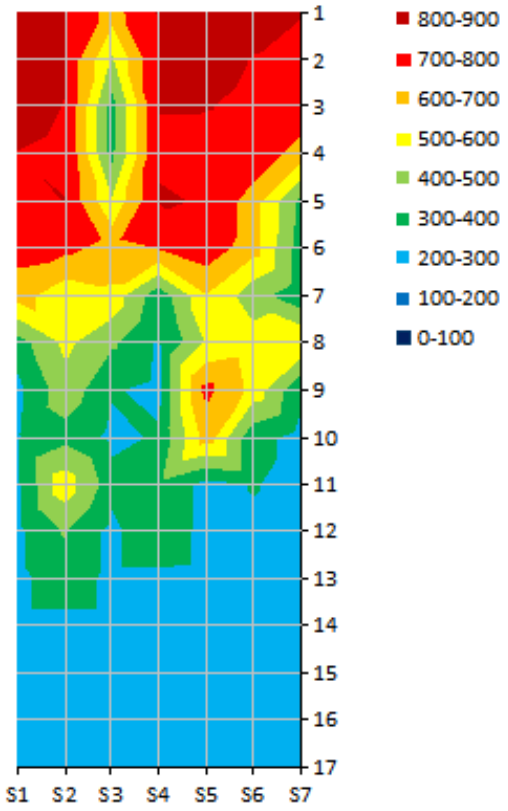

A number of interpolation schemes may be considered to model the temperature gradient between thermocouple locations; Kreith presents solutions to analogous situations such as [56]

- the temperature profile of the billet undergoing rapid heat transfer; the billet is initially at a uniform temperature and subjected to rapid cooling during the quenching bath. The temperature distribution, subject to Newtonian cooling, is expressed as a negative exponential relationship

- for an extended surface under forced convection, the temperature distribution along its length is given by:

$$\frac{d^2T}{dx^2} = m^2\left(T - T_\infty\right) \; where \tag{5.1}$$

T ≡ temperatature along the extended surface
T_s ≡ temperature at base of extended surface
T_∞ ≡ temperature at end of extended surface
x ≡ distance along the extended surface
m ≡ characteristic geometry and heat transfer properties of the extended surface

The solution is given in the form:

$$T - T_\infty = C_1 e^{mx} + C_2 e^{-mx} \tag{5.2}$$

for which the solution in simplified dimensionless form becomes

$$T_i - T_\infty = \left(T_s - T_\infty\right) \cdot \frac{\cosh m\left(L - x_i\right)}{\cosh\left(mL\right)} \tag{5.3}$$

The parameter "m" effectively constrains the quantity ($T_i - T_\infty$) between T_s and T_∞ by setting "m" to 1; the quantities T_s and T_∞ are the bounding temperatures. The usual application of this expression in heat transfer problems uses a calculated value of "m" in order to establish a predicted value of T_i along L up to the end of the extended surface T_∞, which for infinitely long surfaces may be the ambient temperature.

In this case, T_∞ bounds the end temperature limit for a finite length surface. Simple plotting for values of "m" in equation (5.3), to compare the numerator to denominator of the hyperbolic cosine terms, readily reveals this bounding behaviour.

Thus, Kreith's approach suggests an interpolation function in final form such as

$$T_i - T_f = (T_0 - T_f) \cdot \frac{\cosh(L - x_i)}{\cosh(L)} \tag{5.4}$$

where, T_0, T_f are the measured temperatures at the boundary points, T_i the interpolated temperature at distance x_i, L being the distance between the boundary points. The use of an interpolation scheme is heuristic since the transient temperatures at intervening locations are not measured and are likely as random as the measurements at the thermocouple locations; accordingly, other interpolation schemes could be explored that may be more convenient or simpler.

Data for the coker drum is provided at one-minute intervals, hence the coke drum surface temperature distributions are posed as successive realizations and result in recovery of a spectrum exposure profile.

Figure 5.5 displays the exponential interpolation of temperature locally in the vicinity of the cool spot for the full grid profile presented in **Figure 5.4.** The profile extends across the full width of the panel and for the top six (6) rows. At intersection points, temperatures match exactly the measured data points.

Figure 5.5 **Local Interpolation of Thermal Snapshot Profile** in [° F]

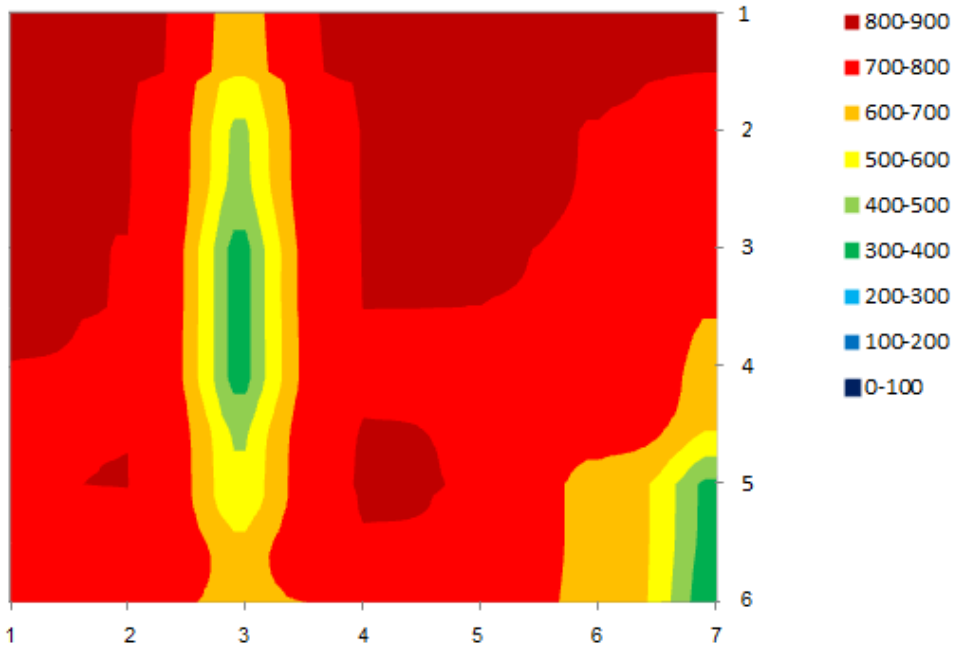

In **Figure 5.6**, a simple comparison is made between the measured data and the linearly interpolated and exponentially interpolated local temperatures. The exponentially interpolated data can be seen to impose a more severe gradient with the expected increased severity in thermo-mechanical strain.

Figure 5.6 Local Interpolation of Thermal Snapshot Profile

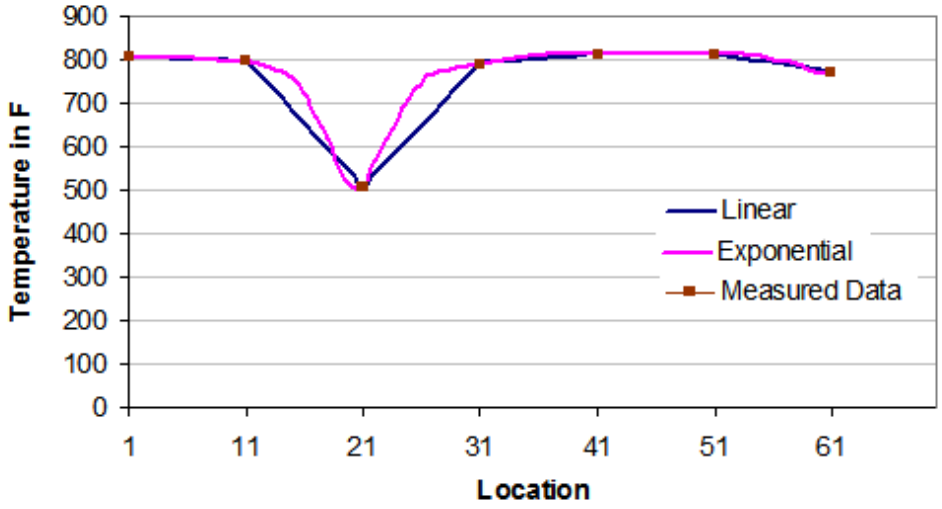

5.2 Schema for Strain Determination

To determine the mechanical strain generated by the temperature differences indicated by the data, a finite element analysis is made. The considerations in developing the models are

- the most simplified model that accurately estimates the thermo-mechanical strains should be used; testing models of varying sophistication and complexity may be required
- repetitive modeling will be required in order to establish the thermo-mechanical strain evolution throughout the water quench period for each operational cycle
- the FEA model will not require consideration of time dependent effects, coke drum materials are selected to avoid creep, by specification and demonstrated in §5.4; but, should address temperature dependent material properties, as warranted
- the finite element model should be simple and efficacious to alleviate computational effort and minimize error potential in recognition of practices by industrial end users; the simplifying practices of the nuclear industry should be considered in execution of FEA approaches
- the coke drum shell is composed of a clad and base layer; a composite shell element is desirable but will be limited to linear analysis due to the underlying application of composite shell FEA modeling and software limitations
- analysis is made using a hierarchy of effort; the simplest approach is made initially, more sophisticated approaches are made consequently as demonstrated by need; this is consistent with industrial practices and practices in the nuclear industry [54]
- data is available at one-minute intervals; for 119 t/c grid points and 271 operational cycles results in 2 to 3 million data points to be processed to isolate the thermo-mechanical strains; to manage this large data base a sampling approach is used which truncates the number of data points to 42 t/c grid points over 52 cycles at four-minute intervals resulting in a sample data load of 34,000 to 51,000 data points
- the temperature interpolation of these data points results in a data load of 3 to 5 million data points for execution of the FEA modeling for 42 t/c grid points and 52 operational cycles

- a sufficient number of temperature snapshots (these are at one minute intervals) need to be processed to identify the maximum thermo-mechanical strain and strain range during the operational cycle

- the maximum and minimum mechanical strain values for an operational cycle are then isolated

- the consecutive maximum and minimum pairing of strain values for an operational block are isolated to establish the mechanical strain exposure for the loading block

- the loading block is the representative loading exposure for the grid and is representative of the repeated thermo-mechanical loading for the coke drum over its service life

- accounting for the loading effects of pressure, live weight and deadweight loads (§ 1.6) is specifically disregarded due to their marginal contribution as demonstrated by both Aumuller and Chen [32, 34]; this brings focus onto the impact of the thermo-mechanical loading

5.3 Service Life Estimate Schema

The maximum / minimum pairing of strain values defines the thermo-mechanical strain signature for the loading block and provides the data for establishing the damage accumulation. The calculation process is outlined;

- for a fixed location, list the maximum, ε_{max} and minimum, ε_{min} thermo-mechanical strain determined in an operational cycle
- list the maximum, $\varepsilon_{max,i}$ and minimum, $\varepsilon_{min,i}$ thermo-mechanical strains determined for the 52 operational cycles / loading block
- rearrange in order to pair each maximum strain with each minimum thermo-mechanical strain, in succession, for the loading block to define the thermo-mechanical strain range signature, $\Delta\varepsilon_k = [\varepsilon_{max,i} - \varepsilon_{min,i}]_k$
- for each strain range pairing, enter the service strain – life graph and determine the damage fraction for the strain range pair, $u_k = n_k / N_k$
- sum the damage fractions, $U = \Sigma\, u_k$ for the loading block
- determine the service life

5.4 Defining a 1st Pass Finite Element Model

The 1st pass model presents a reasonably simplified model consistent with industrial and nuclear industry practices; this includes

- use of a composite shell element to distinguish clad and base layer construction
- partially dependent temperature; use respective material properties at 650 °F; for coke drums, final operating metal temperatures vary according to specific installation and operational requirements; this temperature is a sufficiently conservative and practical 1st pass choice
- truncated shell section
- 4 minute snap shot intervals
- cylindrical coordinate system; Z (vertical), R (radial), T (circumferential); (NB: occasionally, T is assigned the label Y)
- material of construction is taken as SA 204C for the base layer, TP 410S stainless for clad layer; these are typical materials used in the industry
- thickness is 1 inch [25.4 mm] thick for the base layer, ⅛ " [3.2 mm] for the clad layer; the thickness for the base layer is consistent with conventional construction Code rules which take into account specific mechanical loads, temperature and material selection;
- the radius for the shell model is taken from incidental information taken from the temperature data base; coke drums have radius dimensions determined by specific production requirements and hence, will vary from installation to installation
- pressure loading is not applied for two reasons
  - to isolate the thermo-mechanical loading
  - it does not materially affect calculation of the strain range in the loading block and entry in the strain – life (ε – N) curve on account of its small value

  for information,

  - the mechanical strain occasioned by pressure loading is only approximately 0.000186 or 186 $\mu\varepsilon$ and thermo-mechanical loadings exceed a range of 5,000 $\mu\varepsilon$ (demonstrated later); hence, any impact is not distinguishable given the accuracy in service life fatigue life data

The model is presented in **Figure 5.7**.

Figure 5.7 1st Pass FEA Model

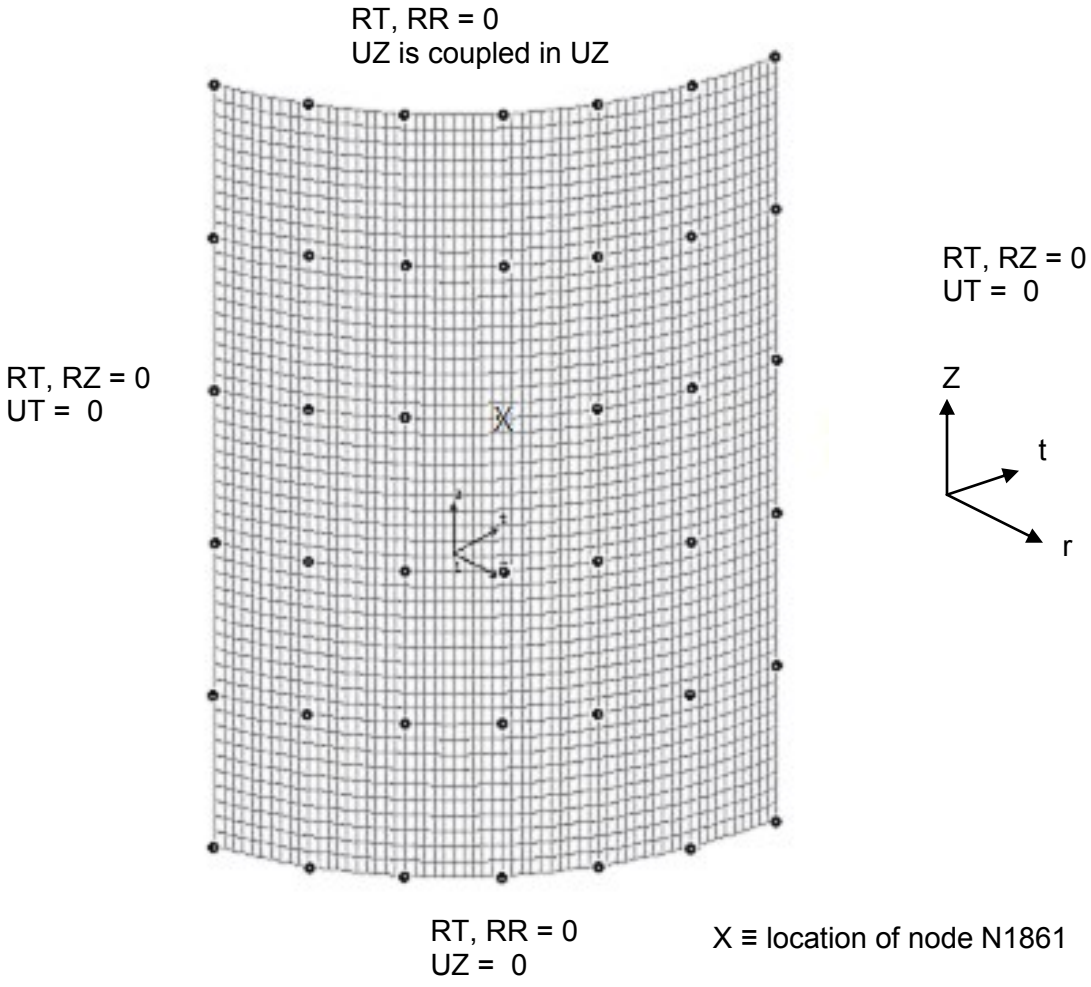

Notes to Figure 5.7

1. The element used for the model is the SHELL4L 4-node multi-layer quadrilateral shell element with
   - membrane and bending capabilities for the analysis of three-dimensional structural and thermal models
   - up to 50 layers can be used; 2 layers are used for this analysis
   - six degrees of freedom (3 translations and 3 rotations) are considered per node
   - one degree of freedom per node representing the temperature is used in the thermal analysis
   - each layer can be associated with different isotropic or orthotropic material properties; isotropic material behaviour is used for the model
2. UZ, UR, UT ≡ translational displacement;
   RZ, RR, RT ≡ rotational displacement; in the cylindrical coordinate system
3. The top edge of the model is coupled / constrained to preserve plane-remains-plane boundary condition; this ensures no node can displace axially relative to other nodes
4. No displacement occurs acriss tge circumferential boundaries
5. Radial displacement is unconstrained
6. Dimensional information for the panel, the panel comprises a 60° arc of a cylinder with the following attributes;

mean radius	150 inches	[3,810 mm]
thickness of base layer	1 inch	[25.4 mm]
thickness of clad layer	0.118 inch	[3 mm]
height	290 inches	[7,366 mm]

7. Uniform mesh size is used without localized mesh refinement since the undamaged surface is uniform
8. Software used:
   - COSMOSM™ Version 2.8, Structural Research & Analysis Corporation, Los Angeles, CA
   - COSMOSM™ Version 2010, SolidWorks 2011 Simulation, Dassault Systèmes SolidWorks Corporation, Waltham, MA

   Structural Research and Analysis Corporation [SRAC] was founded in 1982 by Dr. Victor I. Weingarten, Department of Civil Engineering at the University of Southern California, Los Angeles. It was acquired in 2001 by Dassault Systems S.A.

Temperature Interpolation; In reference to the finite element model proposed in **Figure 5.7** above, the explicitly marked node points (small circle, symbolized by ○) are the forty two (42) node points at which measured temperature is provided in a data set that was recorded for 52 operational cycles at one minute intervals. This results in a data set of 60,480 (42 x 60 x 24) data points for each cycle, (3,145,400 data points for 52 cycles). In order to determine the thermo-mechanical strains, a structural analysis, using temperatures from intermediate data points are needed. These temperatures are interpolated using a specific scheme based on heat transfer considerations as suggested by expression (5.4).

Accordingly, from forty – two (42) measured temperature points, a total of 3,069 (i.e., 3,111 – 42) interpolated temperature data points are established to form the input to the thermo-mechanical analysis; these input data points form the thermal snapshot (i.e., the temperature status is available for each minute of the operational cycles but, four (4) minute intervals are used to reduce the data management effort.

5.5 Evolution of the Thermo-mechanical Strain Profile

Temperature loading of the coke drum shell results in thermal expansion of the shell; the shell expanding in height and diameter by virtue of the increase in temperature during the various temperature increases caused by operation. These are

- steam test phase; ΔT is from ambient to steam test temperature, 100 °F to 250 °F [38 °C to 121 °C]
- vapor heating phase; ΔT is from 250 °F to 600 °F [121 °C to 316 °C]
- oil fill phase; ΔT is from 600 °F to 900 °F [316 °C to 482 °C]

Thermo-mechanical strains arise due to the differential heating of the shell and, also, from differences in the coefficient of thermal expansion (CTE) of clad and base layers. The effect of CTE has been addressed by the presented equations.

During steam testing and vapor heating phases, the coke drum is empty and all parts of the coke drum are exposed to temperature increases uniformly, as evidenced by the data.

To isolate the effects of differential temperature exposure over a coke drum shell, consider a drum shell with only one type of material, thereby, no CTE effect occurs and the following expressions apply:

The total strain developed in the shell is expressed by

$$\boldsymbol{\varepsilon}^{\boldsymbol{total}} = \boldsymbol{\varepsilon}^{\boldsymbol{mech}} + \boldsymbol{\varepsilon}^{\boldsymbol{thermal}} \tag{5.5}$$

for which,

$\varepsilon^{thermal} = \alpha \cdot \Delta T$ i.e., coefficient of expansion x the temperature difference

thus,

$\varepsilon^{mech} = 0$ when only thermal loading is present, and

$\therefore \quad \varepsilon^{total} = \varepsilon^{thermal}$ for steam test and vapor heat phases (5.6)

and, as already indicated, the mechanical strain, ε^{mech}, developed from pressure and hydrostatic loads is included during the operational cycle.

During the water quench phase, uneven cooling results and the posed single layer coke drum shell is no longer unconstrained resulting in development of a mechanical strain from self constraint from by differential temperatures; in the following, there are no external mechanical loads and hence,

$$\varepsilon^{total} = \varepsilon^{mech} + \varepsilon^{thermal}$$

$$0 = \varepsilon^{mech} + \varepsilon^{thermal} \quad and, thus$$

$$\varepsilon^{mech} = \varepsilon^{thermal} = \alpha \cdot \Delta T \tag{5.7}$$

The temperature distribution for a specific snapshot is shown in **Figure 5.8.**

Figure 5.8 Interpolated Temperature Snapshot Profile in [°F]

In **Figure 5.9**, the longitudinal and circumferential strains are displayed for the base layer. These are consistent with industry feedback indicating that circumferential cracking is most prevalent (due to higher longitudinal strain). Industry practices vary in which strain quantity is to be used with some indicating the equivalent strain quantity, ε_{eq} is the required quantity while the fracture mechanics practice of using the nominal strain quantity, ε_i to evaluate fracture propagation is used by some industry Code practices. Using the nominal strain value is slightly more conservative, as shown later.

Figure 5.9 Circumferential, Longitudinal Strain Snapshot Profiles in [με]

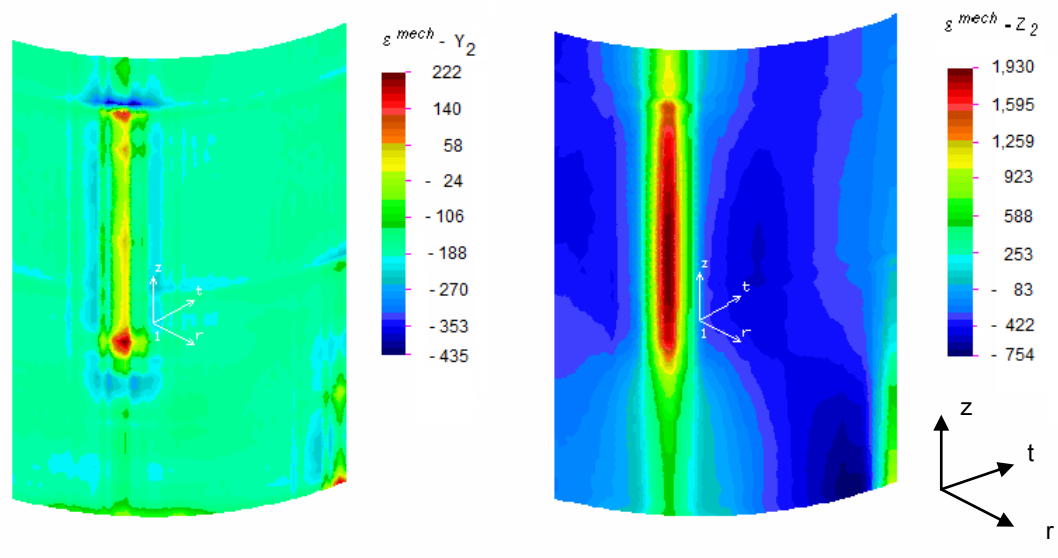

Notes to Figure 5.9

1. cylindrical coordinate system is used
2. Y ≡ circumferential / tangential direction; also "t"
3. Z ≡ longitudinal / axial direction
4. r ≡ radial direction
5. subscript "2" refers to base layer
6. CTE for the base and clad layers differ
7. strain profile for base layer, only shown for clarity

In this figure, the compressive longitudinal strains are located in the "hot" regions immediately adjacent to the tensile longitudinal strain of 1,930 μstrain in the "cold spot" evident in **Figure 5.8**. The circumferential strains (labelled as $\varepsilon^{mech} - Y_2$) are much less and attributable to the reduced stiffness of the shell in the circumferential direction.

Flexural Rigidity From bending theory of circular cylindrical shells, it is known that the flexural rigidity of a cylinder is given by [57]

$$D = \frac{E \cdot t^3}{12(1-\upsilon^2)} \tag{5.8}$$

The internal bending moments when radial deflections are imposed are

$$\begin{aligned} M_x &= D \cdot \kappa_x \\ M_\theta &= \upsilon \cdot D \cdot \kappa_x \end{aligned} \tag{5.9}$$

where,

M_x ≡ the internal moment in axial direction associated with κ_x
M_θ ≡ internal moment in circumferential direction associated with κ_x
κ_x ≡ is the change of curvature in axial direction
υ ≡ Poisson's ratio

The indicates that the internal bending moment in the circumferential direction will always be less than the internal bending moment in the axial direction for the shell of a cylinder when subjected to radial displacement.

In **Figure 5.10,** consecutive strain snapshots, for another sequence, are plotted for a specific location to reveal that the strain response is positive (tensile). The data in **Figure 5.10** is presented for the portion of the total operational cycle focused on the quench stage; prior to the quench stage, the thermo-mechanical strain profile initiates at a value of zero (i.e., there is no mechanical strain at ambient / reference temperature) and rises proportionally with the increase in temperature, as operation proceeds, as profiled in **Figure 3.3**.

Figure 5.10 Strain Evolution in Clad and Base during Water Quench

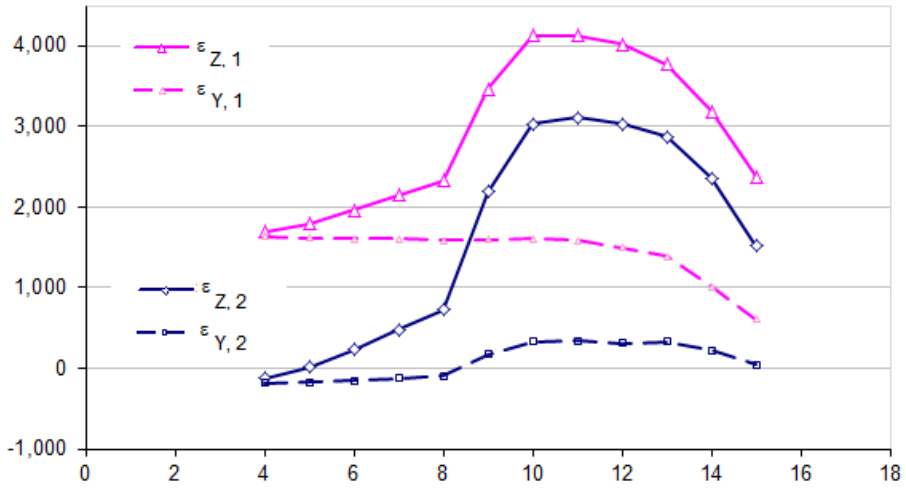

Notes to Figure 5.10

1. $\varepsilon_{Z,1}$ ≡ nominal strain in axial direction, material 1 (clad)
   $\varepsilon_{Z,2}$ ≡ nominal strain in axial direction, material 2 (base)
   $\varepsilon_{Y,1}$ ≡ nominal strain in circumferential direction 1 (clad)
   $\varepsilon_{Y,2}$ ≡ nominal strain in circumferential direction 2 (base)
2. Abscissa represents snapshot points during course of quench phase

The strain values, starting at the left edge of the plot, shown in Figure 5.10 correspond to the thermo-mechanical strain induced by the mismatch in coefficient of expansion [CTE] between clad and base material layers and calculable by closed form solution, as demonstrated.

Using equation (2.6), for the clad layer

$$\varepsilon_c = \frac{(\alpha_b - \alpha_c)\cdot(T_h - T_0)\cdot E_c}{1 + \frac{t_c \cdot E_c}{t_b \cdot E_b}} \cdot \frac{1}{E_c} \tag{5.10}$$

and, on substitution (using data from Figures 7.1, 7.2);

$$\varepsilon_c = -\frac{(9.2 - 7.2)\cdot(900 - 100)}{1 + \frac{0.118 \cdot 21.8}{1 \cdot 20.0}} \cdot = 1{,}418\ \mu\varepsilon \tag{5.11}$$

For the base layer;

$$\varepsilon_b = -\frac{(\alpha_b - \alpha_c)\cdot(T_h - T_0)\cdot E_b}{1 + \frac{t_b \cdot E_c}{t_c \cdot E_b}} \cdot \frac{1}{E_b} \tag{5.12}$$

and, on substitution;

$$\varepsilon_b = -\frac{(9.2 - 7.2)\cdot(900 - 100)}{1 + \frac{1 \cdot 21.8}{0.118 \cdot 20.0}} = -156\ \mu\varepsilon \tag{5.13}$$

This demonstrates that the thermo-mechanical strain evolution prior to the start of quench is governed by the CTE mismatch.

Repeating this for other operational cycles reveals that the individual operational cycles are predominantly either positive (tensile) or negative (compressive) during the thermal transient event occassioned by water quenching.

Also to note, is that the strain response in the circumferential direction is much less in both clad and base material layers; this aligns with the industry observation that weld crack development is much less in the circumferential direction for coke drums. This effort is completed for each data point for fifty two (52) operational cycles to produce the strain exposure block histograms.

In **Figure 5.11a-c**, the maximum and minimum longitudinal strains occurring at a single location in clad and base material layers, are plotted for the fifty two (52) operational cycles that were reviewed.

Figure 5.11a Longitudinal Max / Min Strain, Clad in 52 Operational Cycles

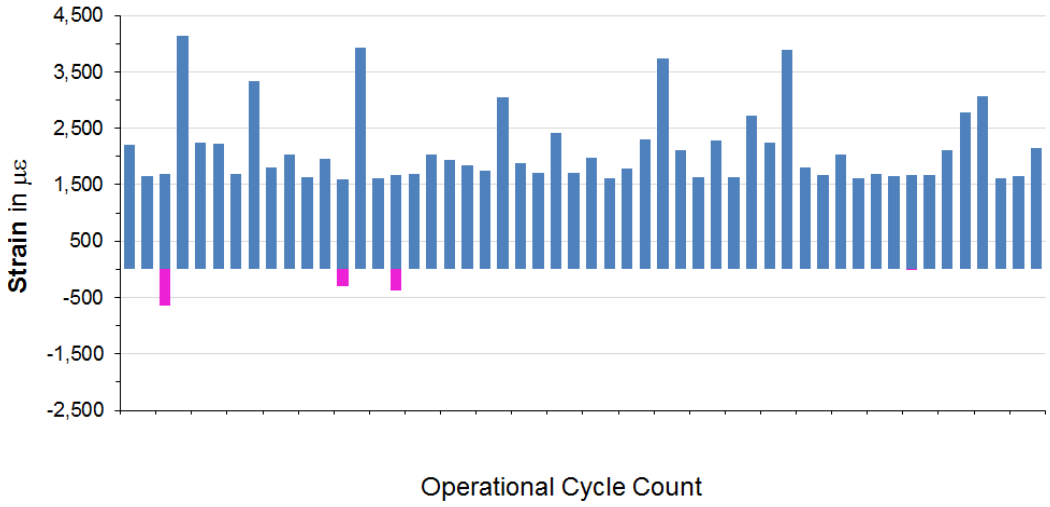

Figure 5.11b Longitudinal Max / Min Strain, Base in 52 Operational Cycles

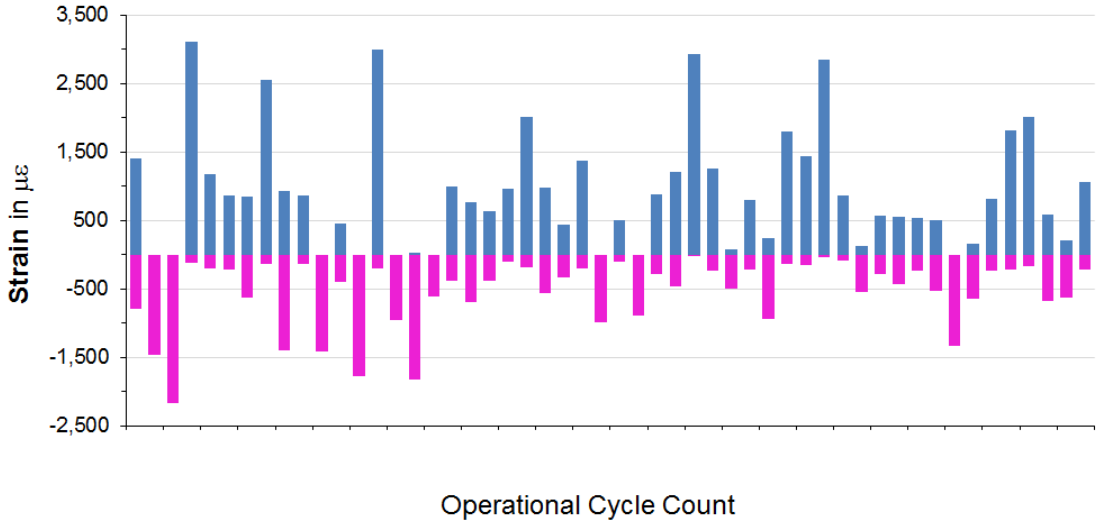

Figure 5.11b shows that that the evolution of a large tensile strain (cold spot) during an operational cycle does not necessarily pair with a large compressive strain (hot spot) during the same operational cycle; as well, the opposite condition where a compressive strain (hot spot) precedes evolution of a tensile strain (cold spot) is not evident. Hot and cold spots occur in random manner / spectrum loading at any given location from operational cycle to cycle

Figure 5.11c Circumferential Max Min Strain, Clad in 52 Operational Cycles

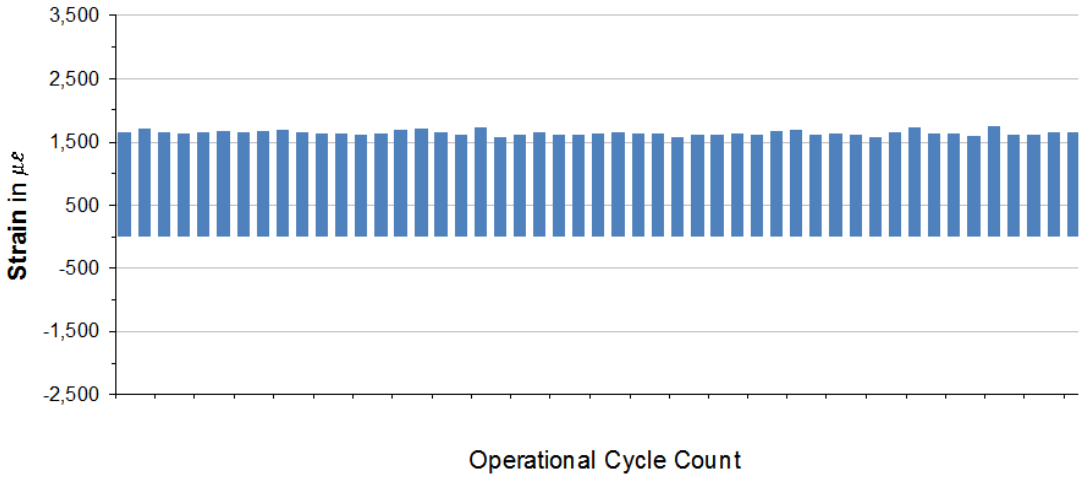

Figure 5.11d Circumferential Max Min Strain, Base in 52 Operational Cycles

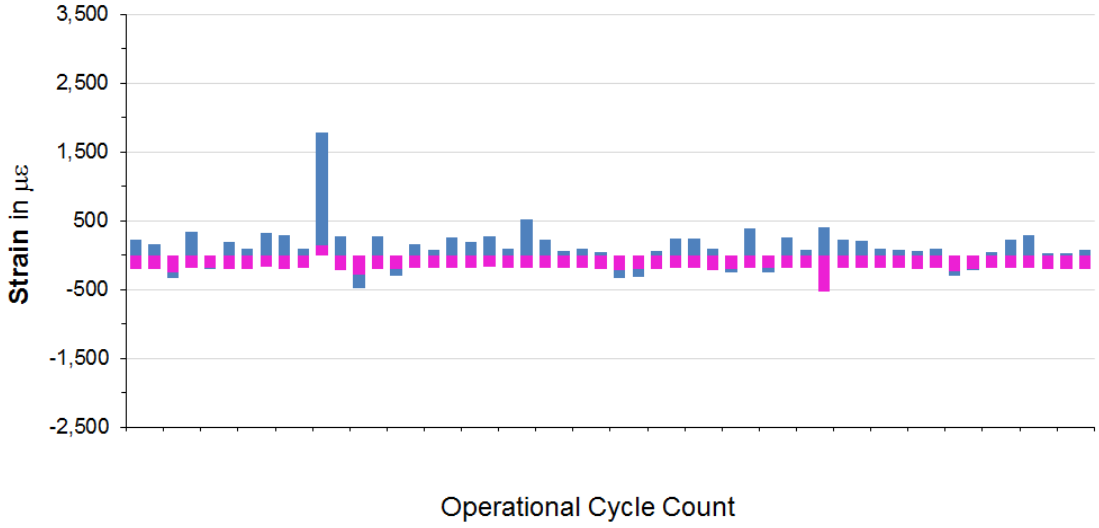

It is readily observed that the circumferential strains for clad and base material layers, **Figures 5.11c, d** are much lower than the respective axial / longitudinal strains given in **Figures 5.11a, b** falling well below the threshold fatigue strain exposure of 3,000 με (the conservative lower bound for fatigue damage as established in **Figure 2.13**).

However, for the axial direction, it can be seen that the tensile profiles for the clad and base track consistently; wherever large tensile strain excursions occur for the base layer, the clad layer also exhibits a comparable excursion. For compressive strains, the clad layer does not apparently track the strain profile of the base layer; instead, only three small, compressive strain excursions are noted which match the very large compressive strain loadings imposed on the base layer. Thus, while the base layer experiences large tensile and compressive strain exposures, the clad layer experiences essentially, only, a tensile strain exposure. This is indicative of the "pre-load" effect of the large tensile strain developed in the clad material layer which is due to the mismatch in the coefficients of expansion between clad and base materials.

Industry practice, to date, has been to declare the difference between the measured maximum / minimum strains, as measured on the base material layers, during an operational cycle as the strain range. As shown by **Figure 5.11b**, these "strain range" values correspond to the strain exposure distributions cited in the literature as previously presented in **Figures 3.21 to 3.23.** Mistakenly, these values have been used to enter industry design fatigue life limits.

The results of **Figures 5.11a-b** are re-ordered to assemble the correct strain ranges to illustrate the impact and are presented as **Figure 5.12a** and **Figure 5.12b** for clad and base material layers, respectively.

Figure 5.12a Strain Range Assembly for Clad Layer, Axial Direction

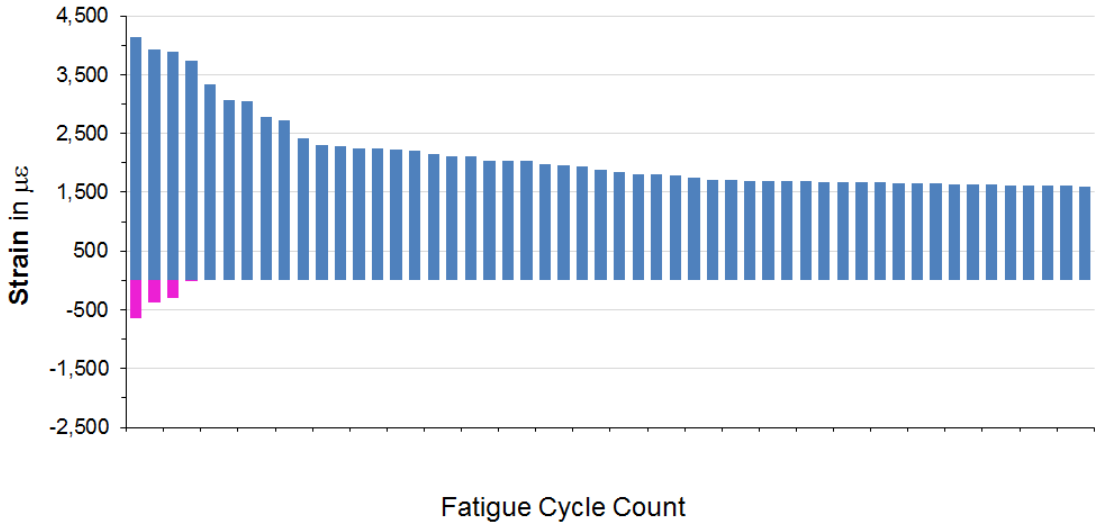

Figure 5.12b Strain Range Assembly for Base Layer, Axial Direction

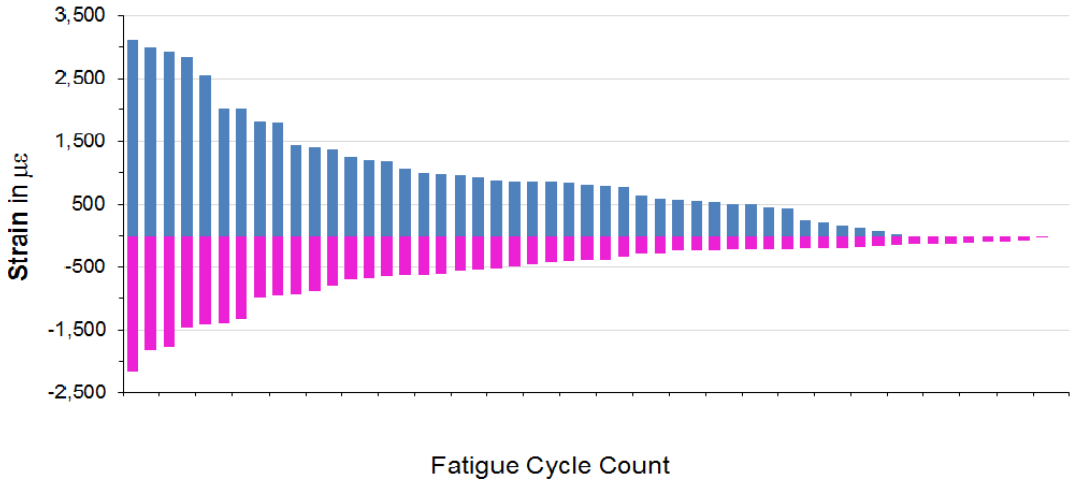

The appropriate strain ranges for clad and base materials are then appropriately recast and presented in **Figures 5.13a, b** respectively.

Figure 5.13a Strain Range for Clad Layer, Axial Direction

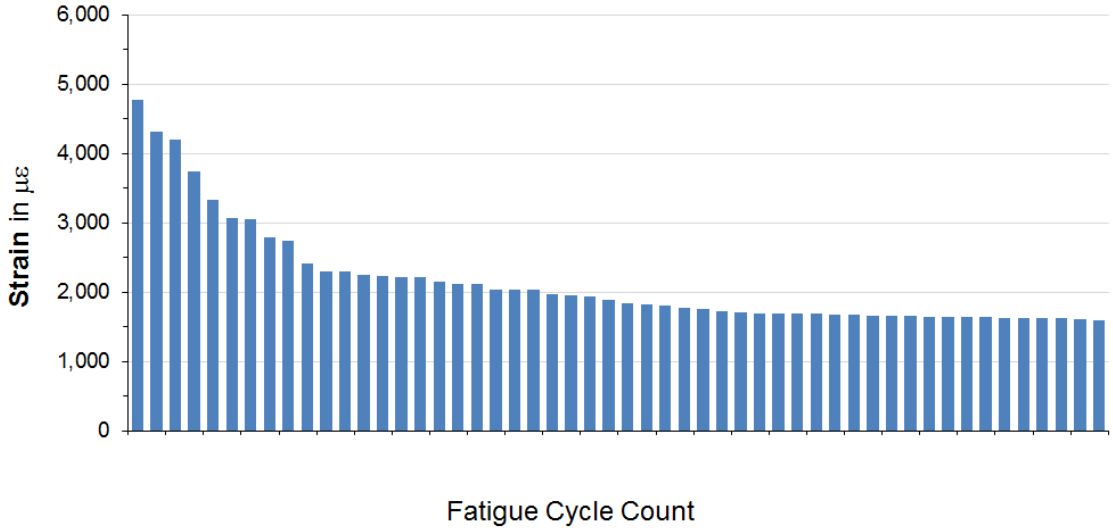

Figure 5.13b Strain Range for Base Layer, Axial Direction

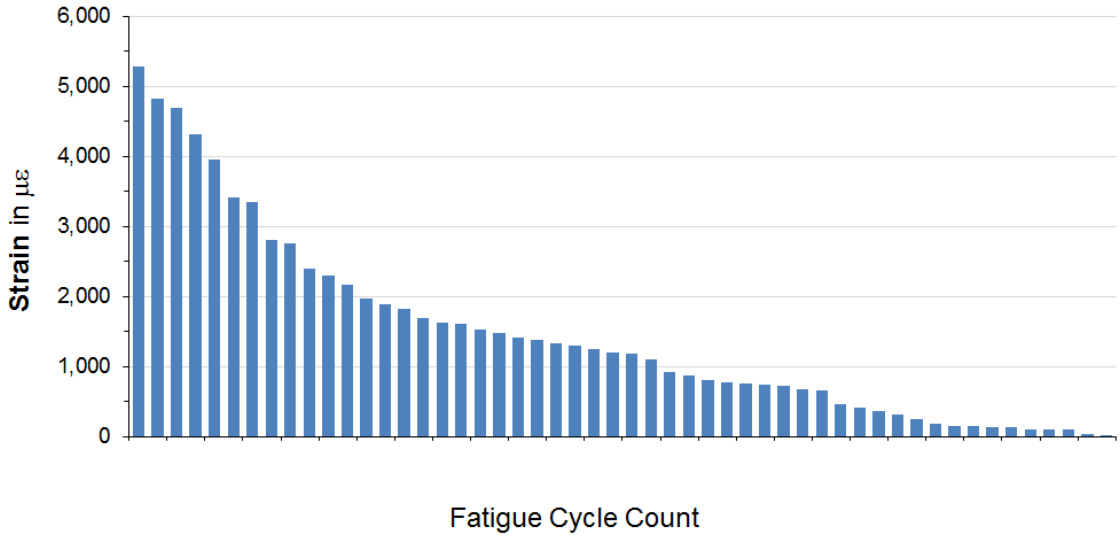

From these recast figures, it is readily observed that the base layer experiences, in comparison to the clad layer, a larger apparent strain range (5,375 με to 4,750 με) and with similar number of exposures (7 to 7) over a threshold value of 3,000 με.

5.7 Mean Strain Effects

The clad layer experiences a reduced apparent strain range; but, the strain exposure is mostly tensile resulting in a possible mean strain effect. The impact of mean strain for clad and base can be estimated using equations (2.1) for no mean strain and equation (4.13) to account for mean strain. For convenience, these equations are repeated;

$$\varepsilon_a = \frac{\sigma'_f}{E} \cdot \left(2 \cdot N_f\right)^b + \varepsilon'_f \cdot \left(2 \cdot N_f\right)^c \tag{5.14}$$

and, to account for mean strain / stress;

$$\varepsilon_a = \frac{\sigma'_f - \sigma_m}{E} \cdot \left(2 \cdot N_f\right)^b + \varepsilon'_f \cdot \left(2 \cdot N_f\right)^c \tag{5.15}$$

Hence, the effect of mean strain / stress can be computed and summarized in Table 5.2.

Table 5.2 Cyclic Service Life with Specific Mean Strain Effects

Cycle Count	Clad				Base			
	$\Delta\varepsilon$	N_f		ratio, %	$\Delta\varepsilon$	N_f		ratio, %
		R = -1	R ≠ -1			R = -1	R ≠ -1	
1	4,776	18,700	9,350	50	5,279	7,850	7,320	93
2	4,320	27,850	13,350	48	4,822	10,400	9,450	91
3	4,200	31,050	14,800	48	4,692	11,350	10,300	91
4	3,740	51,500	23,250	45	4,315	14,950	13,150	88
5	3,336	87,200	37,800	43	3,962	20,000	17,850	89
6					3,405	34,700	32,200	92
7					3,343	37,200	34,400	93

Notes
1. R = -1 defines fully reversed cycling; R ≠ -1 defines cycling with mean strain
2. Mean strain effects are determined by the modified Morrow equation (5.15)
3. ratio ≡ (N_f accounting for mean strain) / (N_f for fully reversed conditions)

From Table 5.2, the service fatigue life counts for clad and base are comparable for equivalent strain exposures; however, actual failure could be expected to initiate slightly sooner and more often in the base layer since it experiences a slightly larger strain range exposure profile, but that cracking would present in either material.

This is evidenced by industry survey which indicated that *"64% of surveys indicated that cracks initiated from the ID while 71% indicated that cracks initiated from the OD"* [13]. The survey summarized that the occurrence of ID / OD cracking was comparable. The survey also reported that 97% of survey responses indicated cracks were primarily circumferential which agrees conclusively with the thermo-mechanical strain data in **Figures 5.11a-d.**

The further evaluation of the clad material layer strain exposure would proceed identically to the evaluation for the base layer and provides no further insights into estimation of fatigue service life for the coke drum. The service life fatigue assessment methodology, being general, can be explicitly applied to the clad layer as specific details for a specific application would demand. In development of this work, this effort is not warranted and redundant.

The data and calculations above indicate that there is an initial biaxial strain induced in the clad of approximately 1,500 με during the initial portion of the coke drum operational cycle which starts at steam test / vapor heat to completion of oil fill (**Figure 3.3, 4.8**). The data (**Figure 5.11a**) shows that the induced strain in the clad increases during formation of a "cold spot" but during formation of a "hot spot", the clad layer seldom reaches a negative strain state. Hence, the effect of the CTE mismatch is to cause the clad layer to "pre-load" and limit the majority of strain range exposures in the clad material layer to less than the low cycle threshold damage level (3,000 με). This suggests the clad layer also serves a useful mechanical role, in addition to serving as a corrosion protection liner.

The strain ranges assembled in Figures 5.12a, b and Figures 5.13a, b conform to the cycle counting methods recognized in industry practices and the Code, specifically.

While many schemes are available for spectrum loading [15, 29], ASME VIII Division 2 [7] explicitly references two methods taken from [58]

- rainflow method
- max – min method (peak or level crossing counting)

Using the later due to its computational convenience, clarity and conservatism, range cycles were determined from pairing the maximum strain reversal with the minimum strain reversal, then continuing to the next peak – valley pair and so on to completion for the representative duty block. The duty block is the collection of strain reversals occurring during subsequent operational cycles which fairly represents the strain exposure for a location.

Commentary on Thermo-mechanical Strain Range The strain quantities displayed in the forgoing are those due to thermo-mechanical loading, only. Other mechanical loadings have been disregarded and based on their impact upon the net strain range exposure.

In **Figure 2.9**, it was demonstrated that the correct strain range to consider for cyclic loading was the Code compliant strain range and cycle count. The effect of considering the operating pressure load of 35 psig is to impart a biaxial stress field resulting in a triaxial strain field. The nominal strains, calculated from strength of materials consideration vary and are a maximum for the hoop (circumferential) direction of

$$\sigma_h = \frac{pr}{t} = \frac{35 \cdot 150}{1} = 5{,}250 \ psi \tag{5.16}$$

and

$$\varepsilon_h = \frac{1}{E}\left[\sigma_h - v\left(\sigma_l + \sigma_r\right)\right]$$
$$= \frac{1}{25.9}\left[5{,}250 - 0.3\left(2{,}625 + 0\right)\right] = 172.3 \ \mu\varepsilon$$

The mechanical strain contribution from pressure and other mechanical loadings, in this instance, have been disregarded for two primary reasons;

1. the pressure strain of 172.3 $\mu\varepsilon$ is small
2. the sustained loads are constant over the operational cycle and do not substantively impact the fatigue range

In **Figure 5.14,** the mechanical strain, due to pressure loading, is added to the mechanical strain determination from thermal loading, i.e., the thermo-mechanical strain. It is seen, by comparison to **Figure 2.9** that the net effect on the strain range is zero (0). An inconsequential impact from mean strain effects may be noted., but is small in this instance.

Figure 5.14 Pressure Strain & Thermo – mechanical Strain Range

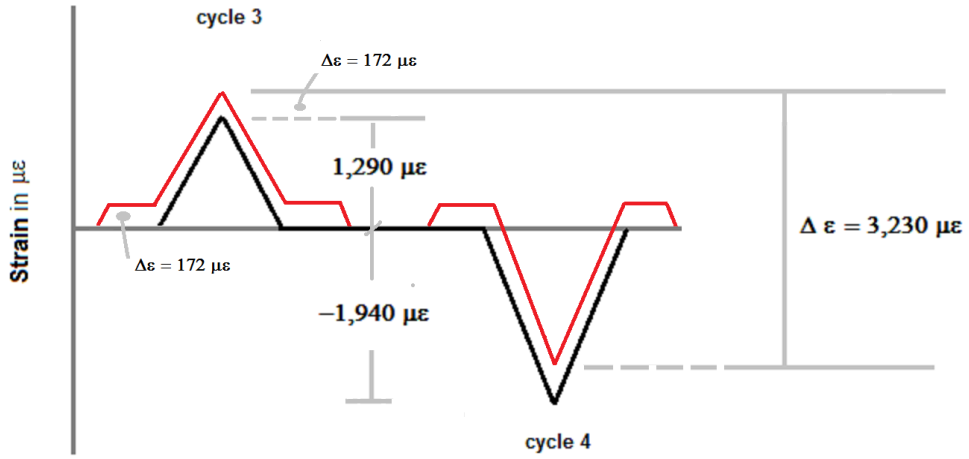

Simplified Strain Range Component Determination Industry practices consider use of either the equivalent or structural stress methodology to calculate the strain range [7, 8]. In **Table 5.3,** a simplified structural stress component approach is applied. The mechanical strain components are retrieved for the maximum and minimum strain values presented for the base material layer in **Figure 5.12b** corresponding to operational cycle # 4 and cycle # 3, respectively in **Figure 5.11a**. The strain range is calculated on a strain component-by-component basis to determine the von Mises / equivalent mechanical strain.

The top and bottom surfaces were not treated explicitly since both values are nearly identical to the membrane component, typically < 5% difference. It is also apparent that the equivalent strain value differs from the structural stress value by about 15%, the equivalent strain being smaller and, hence, less conservative. Industry practices specify using the equivalent strain / stress (von Mises strain / stress) in design for strength [7, 8]. However, designers are not prevented from using more conservative criteria.

The computational burden of calculating the equivalent strain is much greater and is not justified given the purpose of estimating a service life where other uncertainties are greater (i.e., variability in fatigue life, refer to **Figures 2.6, 2.13**). The more conservative approach of using the difference in strain components is reasonable in this instance.

Table 5.3 Strain Range Determination, Mechanical Strain Components in με

Layer	Cycle	Surface	strain component ε, X	ε, Y	ε, Z	von Mises ε, vM
Clad	# 4	Top	- 1,692	293	3,654	
		Bot	- 1,743	383	3,683	
		Mem	-1,717	338	3,669	
	# 3	Top	- 163	1,381	- 1,000	
		Bot	- 149	1,338	- 989	
		Mem	- 156	1,359	- 995	
				$\Delta\varepsilon$		
	$\Delta\varepsilon$		$\Delta\varepsilon_X$	$\Delta\varepsilon_Y$	$\Delta\varepsilon_Z$	
		Top	- 1,528	- 1,088	4,654	3,983
		Bot	- 1,593	- 955	4,673	3,982
		Mem	- 1,561	- 1,021	4,663	3,982
Base	# 4	Top	- 816	- 974	2,879	
		Bot	- 1,252	- 219	3,141	
		Mem	- 1,034	- 597	3,010	
	# 3	Top	637	679	- 2,164	
		Bot	757	307	- 2,074	
		Mem	697	493	- 2,119	
				$\Delta\varepsilon$		
			$\Delta\varepsilon_X$	$\Delta\varepsilon_Y$	$\Delta\varepsilon_Z$	
		Top	-1,453	- 1,653	5,043	4,399
		Bot	- 2,009	- 526	5,215	4,406
		Mem	- 1,731	- 1,090	5,129	4,375

Damage Exposure The data shows that a small portion of events, 7 of 52 instances (< 15%) exceeds a strain range of 3,000 μstrain; in **Figure 2.3** it was shown that strain ranges below 3,000 μstrain have a very long cyclic life, exceeding 100,000 cycles or nominally, 270 years of coke drum operation. Therefore, only those strain range exposures exceeding 3,000 μstrain are considered to be damaging.

This exposure distribution is exhibited in **Figure 5.15**. This presents the thermo-mechanical strain distribution for a single, base material data point for 52 cycles.

Figure 5.15 Strain Distribution, Single Location for 52 Operational Cycles

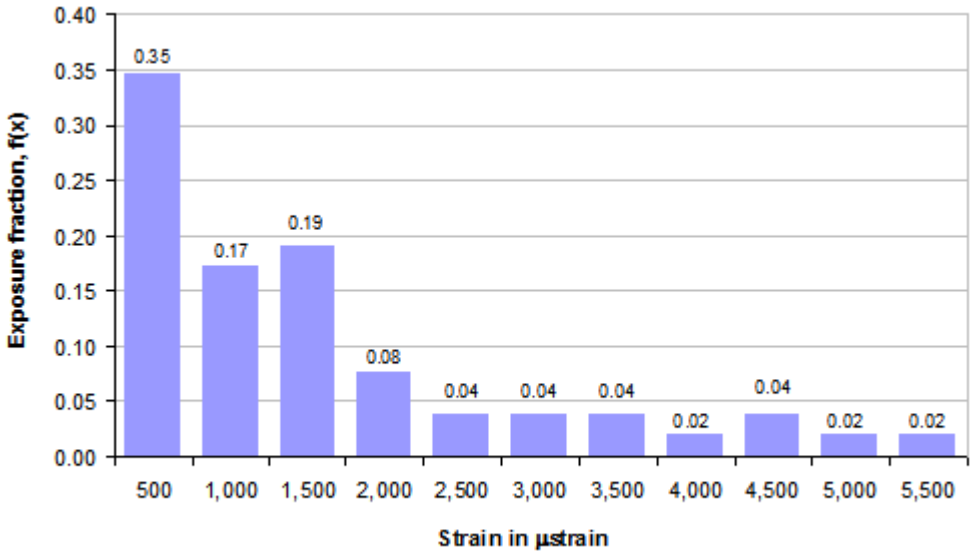

The strain exposure distriubution for the 20 interior data points, in the base material, for the 52 operational exposures is presented in **Figure 5.16**. The data is consistent with the strain distribution for the single data point in that the damaging strain exposures are less than 15% of the total strain exposures caused by thermo-mechanical fatigue.

Figure 5.16 Strain Distribution, 20 Locations for 52 Operational Cycles

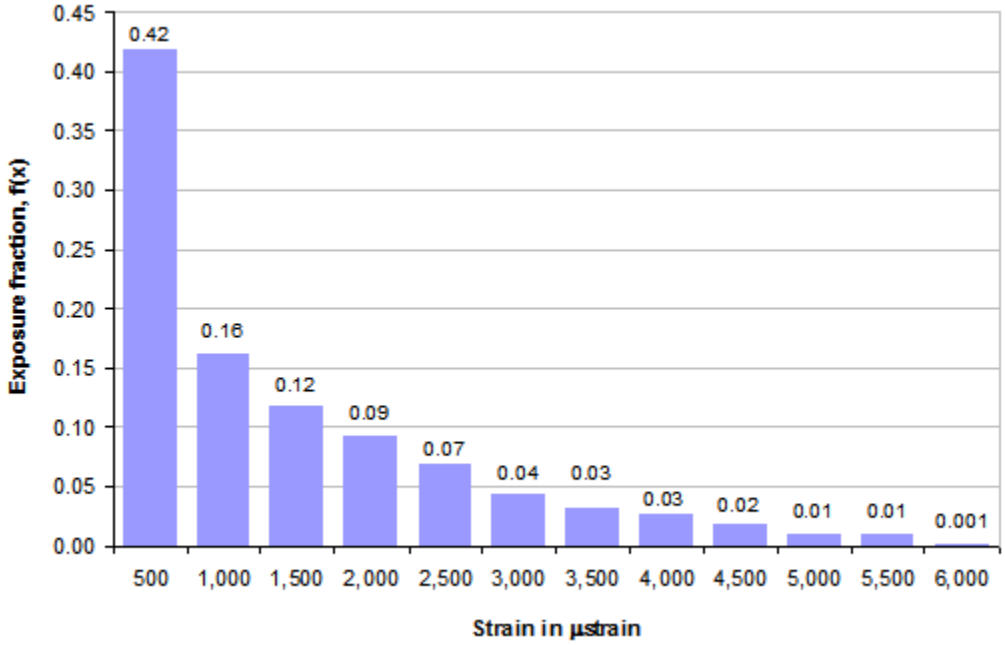

5.7 Strain Exposure Profile and Cyclic Life Criteria

To determine the cyclic life of an as – constructed coke drum, the representative thermo-mechanical strain loading profile is applied to the strain fatigue life curve for the material of construction.

The categorical thermo-mechanical loading profile for the data points of **Figure 5.16** is expanded and recast as **Figure 5.17.**

Figure 5.17 Strain Exposure – 52 Operational Cycles

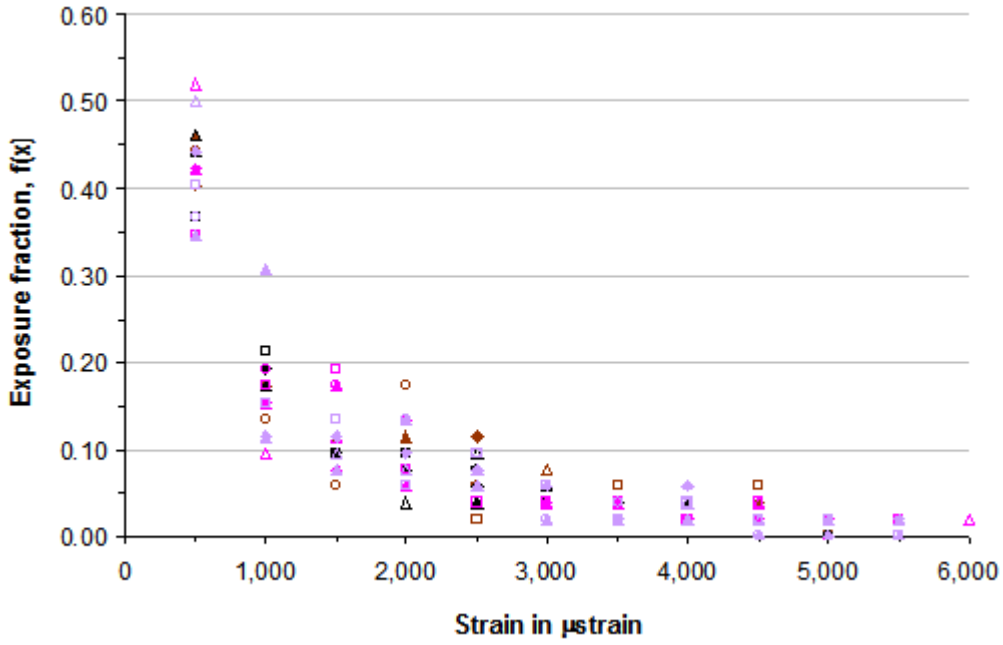

This data can be re-arranged to establish bounding curves in order to establish the 1% and 99% confidence limits for the exposure profile shown in **Figure 5.18.**

Figure 5.18 Strain Range Exposures – 52 Cycles

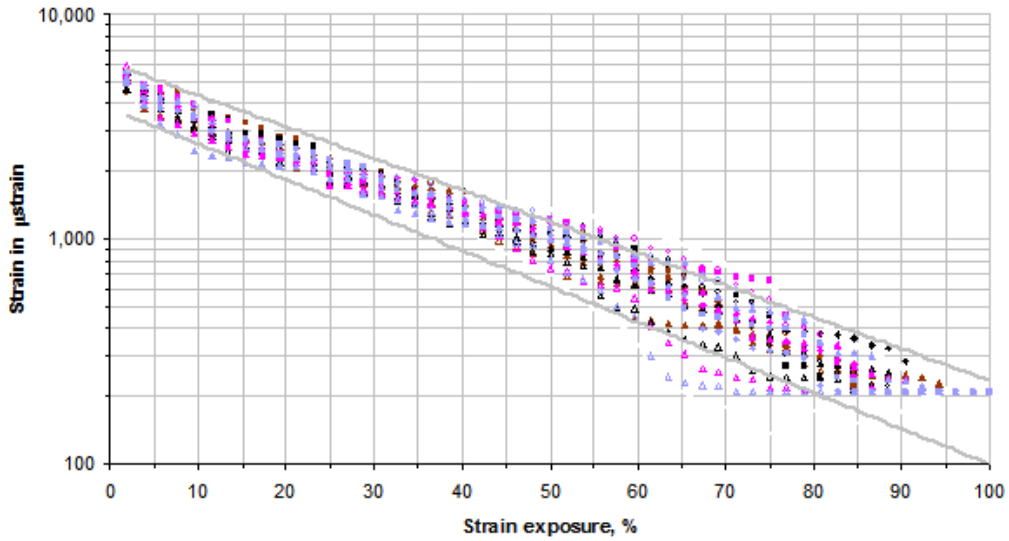

The data from **Figure 5.18** is use to enter **Figure 5.19** which presents the combined strain – cyclic service life curve for the commonly used materials of construction for coke drums compiled from the data presented in § 2.

Figure 5.19 99% Confidence Level – Cyclic Service Life

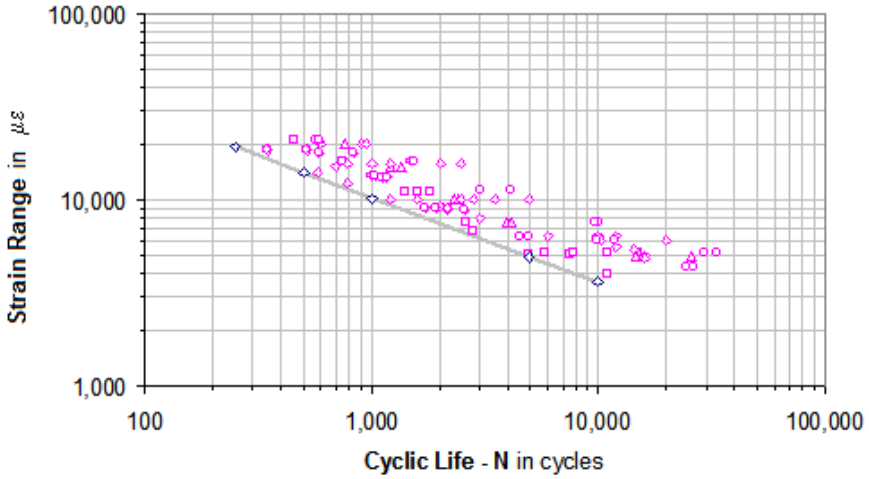

To enter **Figure 5.19**, the upper bound curve of **Figure 5.18** is used to enter the the bounding curve of **Figure 5.19**; the anticipated, unconditioned fatigue life would be 23,255 operational cycles [96 years at the 99% confidence limit]. In addition, the lower bound curve of **Figure 5.18** is used to enter the same bounding curve **Figure 5.19** for which the anticipated upper bound, unconditioned service fatigue life is calculated as 111,690 operational cycles [460 years at the 1% confidence limit]. These yearly values assume a nominal operational duty cycle of 24 hours. The Palmgren – Miner damage accumulation model is used in conformance to industry practice and is detailed in the next chapter. The fatigue service life is reported as an "unconditioned" life estimate since it does not account for localized effects from weldments (which contain Code acceptable internal defects, residual stresses) and shell distortions.

The literature suggests coke drum life is from twenty to fifty years. **Figure 5.20** is taken from reference [13] and indicates more than 100 cracks for a drum with less than 3,000 operational cycles [8 years] and several drums experiencing apparent accelerated cracking after reaching 6,000 operational cycles [16 years].

Figure 5.20 Total Number of Cracks vs Total Number of Cycles

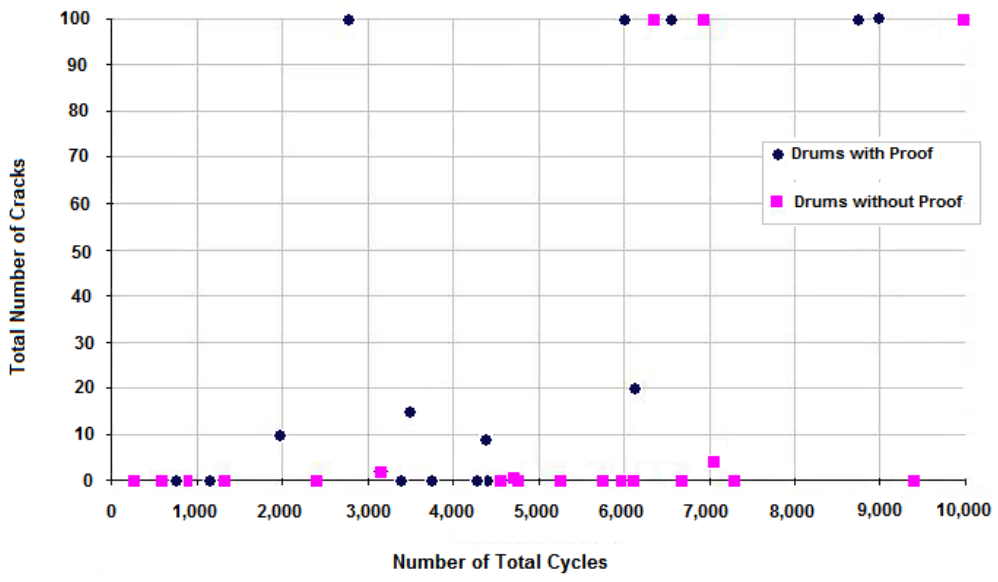

In Figure 5.21, a single drum is shown with approximately 20,000 cycles / 54 years with a gap in data showing that the bulk of drums, in the survey consisting of 145 drums, have exposures of less than 10,000 cycles / 27 years. Chevron Corporation indicates a coke drum was replaced at the El Segundo, California refinery which had a service life of forty six years [59]. Actual life is indicative of the complication of shell distortions, otherwise described as shell bulging.

Figure 5.21 Number of Bulges vs Total Cycles

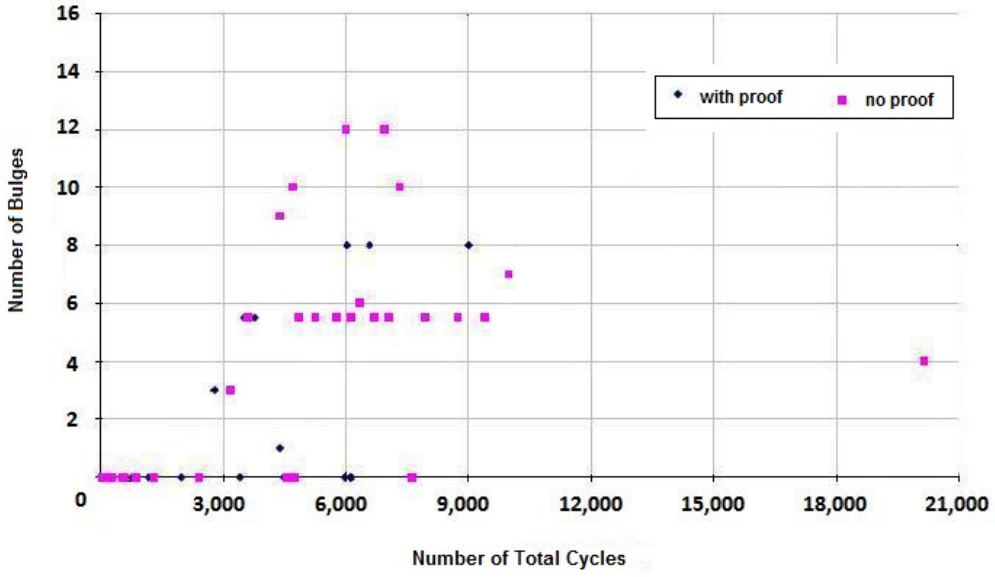

It is evident that the 1st pass model provides a viable presentation of the thermomechanical strains that are induced in the coke drum during water quench based on comparsion to collected strain data; accordingly, the use of partial material temperature dependency and linear behavior are efficacious.

For interest, a temperature dependent, non-linear model is provided in a later chapter for comparison.

CHAPTER 6 CYCLIC LIFE DETERMINATION FOR A COKE DRUM

When a new coke drum is exposed to thermo-mechanical loading, damage is eventually incurred in the form of shell bluging and cracking. Cracking may occur at shell welds, in unwelded portions of the shell plate or at shell bulges. The mechanism of shell bulging is not definitively explicated in the literature with only some competing notions stated. These include

- coke crushing
- weld strength mismatch
- hot & cold region formation

This thesis examines cracking at both undistorted and distorted shell areas; this work does not address the specific causes of bulge formation but, rather, the consequences of these general shell distortions. Although all three possible causes can contribute to shell distortion damage, the most plausible leading cause is hot and cold shell region formation.

Shell bulging is classified as a general shell distortion in several industry trade publications. Two authors have attempted to address shell bulging by indirect assessment methodologies which will also be described.

6.1 Industry Practice Code and Standards

ASME / API Documents

Standard industry documents ASME VIII Division 1 and Division 2 and dual marked API 579 –1 / ASME FFS –1 deal with shell dimensional tolerances.

Since ASME VIII Division 1 and Division 2 are intended for new construction, discussion of deviations in shell dimension are limited to shell out – of – roundness. The acceptable tolerance on shell out – of – roundness, $D_{max} – D_{min}$ is limited to 1% of D per paragraph UG – 80(a) of Division 1 and Division 2 paragraph AF – 130.1. Both of these pressure vessel construction Codes do not address peaking of welds. Peaking is an industry idiom referring to angular misalignment of longitudinal and circumferential weld joints.

However, ASME VIII Division 2 does require that the dimensions characterizing the peaking distortion are to be measured and included in the fatigue analysis of the vessel, if a general fatigue analysis has been deemed necessary.

An industry document not usually referenced for pressure vessel work is API Standard 650 applying to welded steel oil storage tanks [60]. Oil storage tanks can be very large, exceeding 250 feet [76 m] in diameter and fabricated from 1inch to 2 inch [25.4 mm to 50.8mm] thick steel plate. Due to their large diameter to thickness ratio, D / t, the standard provides for an explicit rules – based limit on shell peaking. Peaking is not to exceed ½ inch [13 mm] in a 36 inch [900 mm] sweep board in both longitudinal and circumferential directions. This rule sets a lower limit for assessment of a coke drum.

ASME VIII Division 2 provides for a fatigue analysis on the basis of a simplified elastic – plastic analysis which uses a penalty factor technique. Analysis using elastic – plastic analysis is recognized but not mandatory.

API 579 – 1 / ASME FFS –1 Level 2 Evaluation

To quantify the impact of peaking in longitudinal and circumferential welded joints or plate, API 579 – 1 / ASME FFS –1 provides a closed form approach, presented as a Level 2 analysis approach. A finite element study would be considered as a Level 3 evaluation.

The Level 2 assessment methods are completed by closed form solutions.

The method of API 579 – 1 / ASME FFS –1 determines a secondary stress load due to axial and angular misalignments. Since modern coke drum construction methods use single thickness shell plates, axial misalignment is not a primary consideration. However, the effect of bulges and general shell distortion is to impose angular and bulge misalignments.

The API / ASME practice standard calculates a ratio of induced bending stress to the applied membrane stress in a component that results from pressure. A second ratio of induced bending stress to the applied membrane stress from supplemental loads is under development.

Bulge Intensity Factor (BIF™) [27]
Samman describes an intuitive technique for assessing the severity of shell misalignments using the notion of bulge intensity factor [BIF™].

The authors indicate that the motivation for the technique arose from the apparent lack of correlation between stress profiles generated from finite element analyses and shell cracking histories. They attribute the lack of correlation to inability to assess stresses from thermal transients during the fill cycle and by shell-coke interaction during the quench cycle. The authors cite the work of Farraro & Boswell – 1996 [21] and, Boswell – 1997, Boswell & Farraro – 1998 [61].

Significantly, the thermo-mechanical loading during the quench cycle is referenced as a further complication together with shell bulging rendering analysis far too complex. Therefore, a simplified methodology is needed. The BIF™ parameter is based on pattern recognition techniques and, for coke drums is utilized to discern geometric features associated with cracking failure. Thus, the technique is heuristic and dependent on a sufficient database of geometries and associated shell cracking failures.

Accordingly, there are no publicly available calculation protocols and reliance is based on a ranking scheme dependent on a proprietary algorithm.

Plastic Strain Index [PSI™] [27]

Samman et al. state the shortcomings of the API 579 –1 / ASME FFS –1 practice standard in assessing coke drum shell bulges using the Level 3 approach, i.e., numerical analysis, and the inaccuracy of the Level 2 assessment techniques therein.

The reasons for these shortcomings are attributed to the complex and random nature of thermo-mechanical loads [26].

The authors suggest that a numerical analysis using elastic – plastic methods and using the strain criteria of API 579 –1 / ASME FFS –1 would provide a determination of equipment suitability for continued operation. The numerical analysis is based on pressure loading only. To facilitate communication of these results, the authors ranked the results of the strain analysis against the limit strain criteria defined in the practice document.

The practice standard defines the limit strain as a function of several factors;

- applied stress
- material yield strength
- material tensile strength
- material reduction of area
- a multi-axial material strain limit value, α_{sl} = 2.2 for ferritic steels

The basis of the strain limit according to the practice standard is monotonic loading.

The index rankings are linear; ranking of severity grade, crack likelihood and monitoring frequency being qualitative and apparently arbitrary. **Table 6.1** is provided for illustration of the method.

Table 6.1 Plastic Strain Index Severity Grades per Samman [27]

% strain limit	Severity Grade	Likelihood of Bulged-Induced Crack	Monitoring Frequency
80 to 100	Failure	Likely	½ – 1 year
60 to 80	Danger	Probable	1 year
40 to 60	Concern	Possible	1 – 2 years
0 to 40	Design	Unlikely	2 – 3 years

Bulge Severity Factor

Araque et al. [37] define the Bulge Severity Factor [*BSF*] using the ratio of longitudinal stress for the damaged geometry to the longitudinal stress for the undamaged geometry of a coke drum considering only the primary pressure and weight loads according to

$$BSF = \frac{\sigma_{damaged}}{\sigma_{undamaged}} \tag{6.1}$$

The *BSF*, therefore, is a stress concentration factor. The investigators also use a temperature interpolation scheme to develop a temperature distribution for intermediate data points. The heuristic scheme uses convective heat transfer analysis to force calculated temperatures to match temperatures at known data points. The investigators state that a linear interpolation scheme was required to reduce the time step for achieving convergence in stress analysis. The investigators reported significant stress oscillations in the analytical model which forced use of a 0.25 second time step. Mesh sizing was reduced to 18 mm x 18 mm [0.7 inch x 0.7 inch] to achieve convergence.

Analysis was made using the pseudo-elastic stress basis. BSF stress concentrations approaching 8 were determined. This was combined with use of a fatigue strength reduction factor of 2 to enter the traditional stress – fatigue life curve of ASME VIII Division 3 [62]. This Code is intended to be used for high pressure vessels where pressure exceeds 10,000 psi [70 MPa] although lower pressure applications in the order of 1,000 to 3000 psi [6.9 to 20.7 MPa] are treated using the Division 3 methods. The authors do not indicate why this Code was used in preference to the expected industry practice documents.

6.2 Deterministic Approaches to Coke Drum Life Evaluation

Coke drum fatigue cracking failure has been problematic for the industry since the earliest installations made in the 1930's.

Focused efforts in defining the problem and identifying solutions began in the 1950's with publication of the survey performed by Weil and Rapasky who worked for an industry engineering contractor, M W Kellogg [3]. Later work was undertaken by industry trade groups such as the API and the MPC.

The difficulties for the investigators was a lack of numerical data and technology, specifically

- finite element analysis software
- coke drum shell temperature data
- coke drum strain data
- materials of construction data
- calculation methodology

Recent industry practice documents provide materials of construction data. The industry practice documents have also evolved from being focused on new construction to assessing damaged equipment for continued service. However, in detail, the newer documents have some difficulties, including

- retaining overly conservative approaches
- generalized treatment of materials properties
- overly complicated and complex calculation approaches

ASME Simplified Elastic – Plastic Analysis

In chapter three, a discussion of a number of applications of industry practices that were incorrectly applied was discussed. This section explores two difficulties in the accurate determination of coke drum life evaluation, namely the penalty factor [Ke] and fatigue strength reduction factor [FSRF].

In the 1969 release of the ASME Section B31.7 Code for nuclear piping and subsequently, the release of the ASME Section III Code for nuclear construction, a simplified method for elastic – plastic analysis was contributed by Langer [63] . ASME Section VIII Division 2 parallels the design-by-analysis motivation of Section III for industry and contains a number of its provisions.

ASME VIII Division 2 FSRF and Penalty Factor Ke

The Code provides for a simplified elastic – plastic analysis using a penalty factor approach whenever the local stress exceeds two times the specified minimum yield strength of the material.

$$Ke = 1.0 \qquad \text{for } S_n \le S_{PS} \tag{6.2}$$

$$= 1.0 + \frac{(1-n)}{n(m-1)} \cdot (S_n / SPS - 1) \qquad \text{for } S_{PS} < S_n < m \cdot S_{PS} \tag{6.3}$$

$$= 1/n \qquad \text{for } S_n \ge m \cdot S_{PS} \tag{6.4}$$

S_n = range of primary plus secondary stress intensity

S_{PS} = allowable limit on the primary plus secondary stress range;

S_{PS} is the larger of 3 times the average of S at lowest and highest temperature during the operational cycle or 2 times the average of SMYS at the lowest and highest during the operational cycle

S = allowable stress based for the material of construction

n, m define material constants, with

n = 0.2 for low alloy steels such as C – ½ Mo, Cr – Mo and C – Mn – Mo steels

m = 2.0 for low alloy steels

Figure 6.1 illustrates the scheme used by ASME for the simplified approach. The intent of the procedure is to use the elastic numerical analysis and condition it for stress and strain concentration without the necessity of conducting an explicit elastic-plastic analysis prior to entering the fatigue life curves [7].

Figure 6.1 Ke Factor for Simplified Elastic – Plastic Analysis

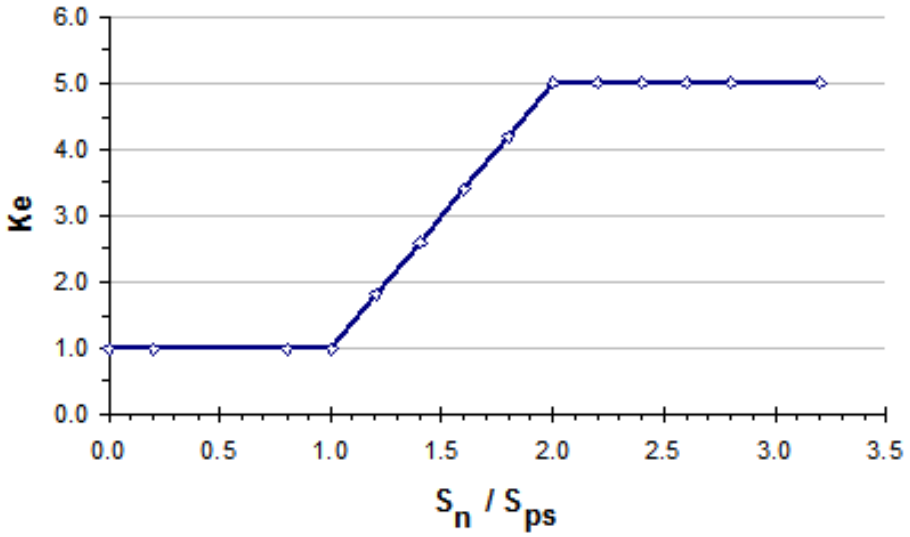

Hickerson provides data showing experimentally derived values of fatigue strain reduction factor [FSRF'] per **Figure 6.2**, to differentiate from the concept of fatigue strength reduction factor [FSRF] for the low cycle fatigue life range of A 302B plate [63]. This suggests that the strain value to enter the ε – N curve is determined from

$$\Delta\varepsilon = FSRF' \cdot \Delta\varepsilon_{nom} \qquad (7.5)$$

where $\Delta\varepsilon_{nom}$ is the elastically or pseudo-elastically derived strain range [64, 65].

These experimental results are based on three types of local geometrical discontinuities with elastic stress concentrations varying for 1.9 to 3.1

- notches; k_t varying from 1.4 to 5.0
- holes; $k_t = 2.2$
- fillets; $k_t = 2.1$

Coke drums are manufactured to a relatively high degree of weld joint quality compared to other industry applications. This includes fatigue compatible weld design and 100% radiography [100% RT]. Fatigue compatible weld design includes zero weld reinforcement so as to eliminate any geometric stress concentrations. The industry practice is to assign a FSRF of 1.2 in this instance and to modify the calculated stress level as

$$\Delta\varepsilon = FSRF \cdot Ke \cdot \Delta\varepsilon_{nom} = 1.2 \cdot Ke \cdot \Delta\varepsilon_{nom} \qquad (7.6)$$

Strains were measured by means of strain gauges on unnotched and notched specimens. The FSRF' varies over cyclic life N from 1.2 at N = 2,000 cycles to 1.7 at N = 20,000 cycles.

Figure 6.2 Fatigue Strain Reduction Factor for A 302B [66]

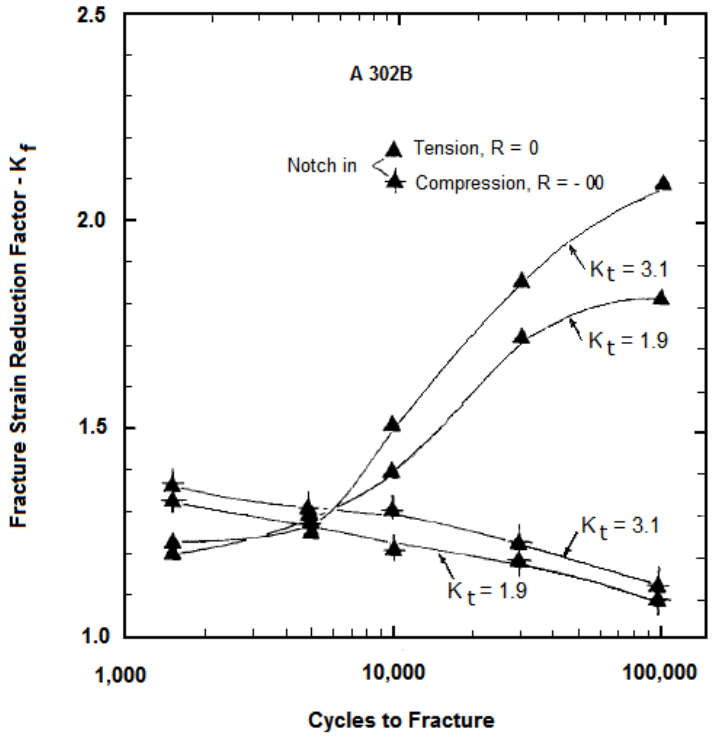

The same trend is displayed in **Figure 6.3**, also provided by Hickerson**.** The data of **Figures 6.2** and **6.3** is in contradiction to the direction of current industry practices provided in the Code [7]. Whereas the fatigue strength reduction factor is given as a constant depending on weld fabrication quality and independent of stress concentration, experimental data suggests that the fatigue strength reduction factor is

- a function of geometric stress concentration
- a function of stress / strain level
- a function of stress / strain direction (compressive / tensile)
- accounts for non-linearity implicitly

Figure 6.3 Fatigue Strain Reduction Factor [66]

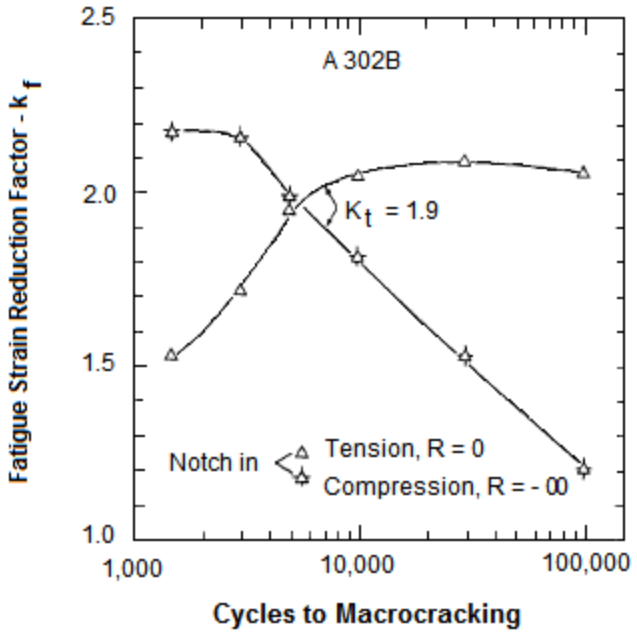

Chen's data is in agreement with the work of Hickerson for R = 0 and shows a positive relationship of FSRF to cyclic count, i.e., FSRF increases as strain decreases [66].

Chen studied two types of notches in fully reversed loading (R= -1), one associated with the weld material and the second associated with the weld heat affected zone. The FSRF, studied by Chen, associated with the weld material corresponds with the Hickerson studies. The FSRF, studied by Chen, associated with the HAZ shows increasing strength reduction with cyclic life (reduced strain).

Figure 6.4 Fatigue Strength Reduction Factor [35]

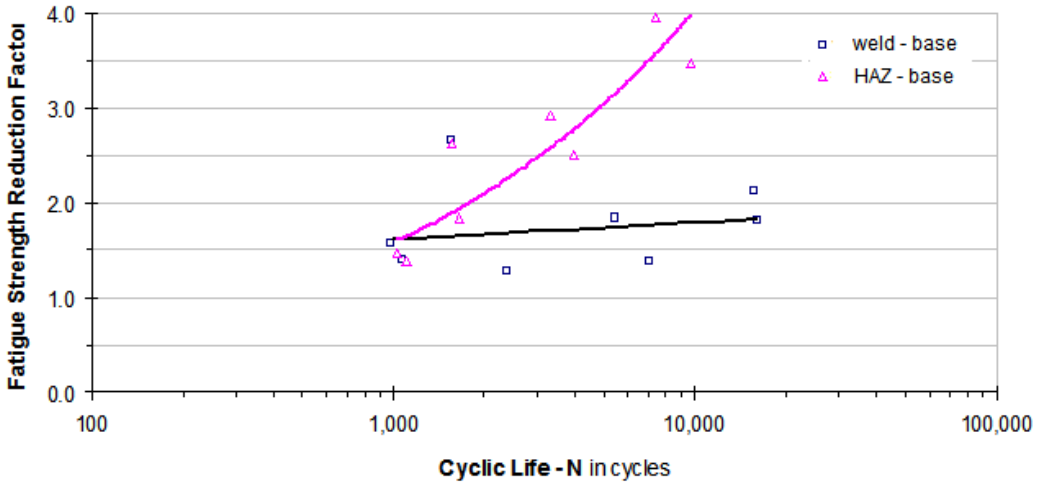

The source data for Chen's results is derived from the experimental data presented in **Figure 6.5.** It can be seen that the fatigue life diverges for the three material types as cyclic strain exposure level decreases, i.e. cyclic life, N increases, consistent with the tensile testing regime of **Figures 6.2 and 6.3.**

Figure 6.5 Strain – Life Data Establish FSRF in [35]

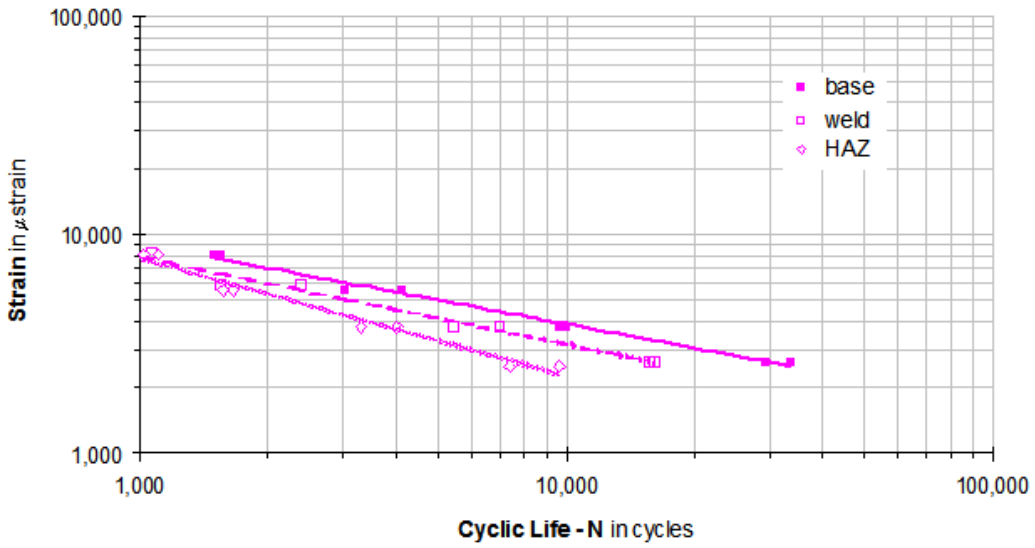

In contrast, testing by Ramos showed, **using Figure 6.6**, a converging fatigue life for the two material areas as cyclic strain exposure level decreases, i.e. cyclic life N increases, consistent with the compressive testing regime (R = – ∞) of **Figures 6.2 and 6.3.**

Figure 6.6 Strain – Life Data from Ramos to Establish FSRF [19]

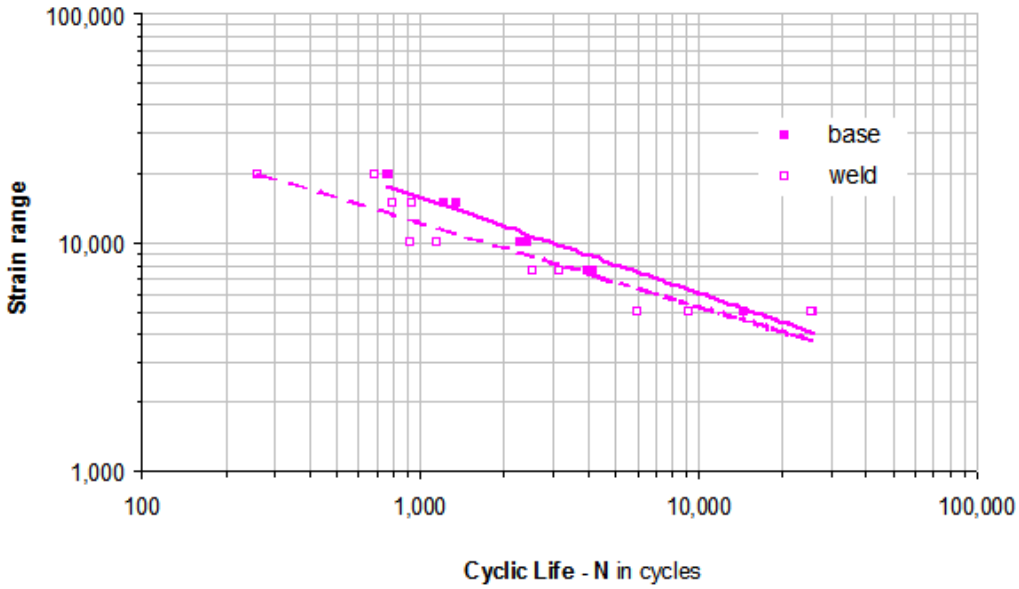

The apparent FSRF suggested in **Figure 6.6,** presented in **Figure 6.7**, is seen increasing to a limit value (strain increasing) of 4.0 and is consistent with the practice of some industry practitioners to use an FSRF of 2.0 for complete joint penetration (buttwelds) in fatigue calculations.

Figure 6.7 Fatigue Strength Reduction Factor [19]

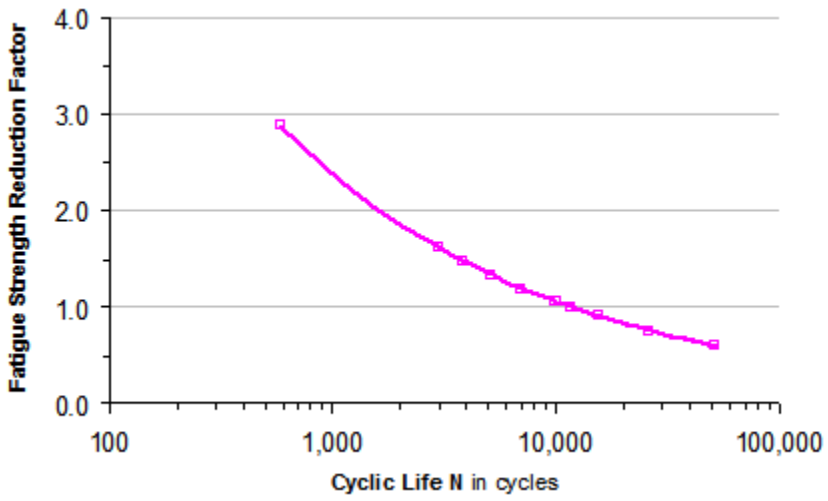

Papers

Slagis reviews that the first appearance of "simplified elastic-plastic discontinuity analysis" occurred with publication of rules for nuclear piping in 1969 [67]. These were then incorporated into the ASME III rules for construction of nuclear vessels in 1971 and piping rules were incorporated into the Section III rules. The Code allowed certain primary-plus-secondary stresses to exceed the stress limit of $3 \cdot S_m$ if a penalty was taken on the fatigue analysis. This penalty was designated as the penalty factor, Ke and was designed to vary with the stress level and was a function of material property. For low alloy steel, Ke could be as much as 5.0. Slagis advises that additional testing showed that the penalty factor was too large and other codes have proposed lower values [63].

The meaning of Ke was given by Langer [68]

Strain concentration can occur in any structural member with stress gradients as soon as the loading exceeds the point at which the highest-stressed region becomes plastic. If the plastic zone is highly localized, the surrounding elastic material controls the strain in the plastic material and no strain concentration occurs. When the plastic zone is large enough to become a significant factor in the stress distribution, however, the strains in the plastic zone become larger than those which would be calculated by the theory of elasticity and strain concentration must be considered.

Langer calculated plastic strain concentration factors on a tapered flat bar in tension and a cantilevered beam in bending to establish that the limiting value of Ke = 1 / n. For low alloy steels, n = 0.2.

Testing by Gerber using cylindrical specimens with two types of local discontinuities, groove and shoulder with an elastic stress concentration of 2.0 against a smooth specimen established that Ke was about 2.2 for Sn / 2•SMYS = 2 for carbon steel [63, 69].

Krempl defined the fatigue strength reduction factor as [64]

$$k_f = \frac{\Delta \bar{S}_n}{\Delta S} \equiv \frac{\text{nominal stress of notched bar}}{\text{nominal stress of unnotched bar}} \text{ and,} \qquad (7.7)$$

found for 2¼ Cr – 1Mo material that k_f approached ~ 1.0 in the plastic region.

Slagis provides data from Japanese research by Iida indicating that a Ke value approaching 2.0 should be used for k_t values of 1.85 to 2.26 over a temperature range from room temperature to 575 °F [300 °C] over a ratio of $\Delta\varepsilon$ / 2*ε_Y from 0.5 to 3.25 as shown in **Figure 6.8** [70]. The experimentally derived value was found to be slightly higher than the calculation methodology of Neuber.

Figure 6.8 Ke Data – Slagis [70]

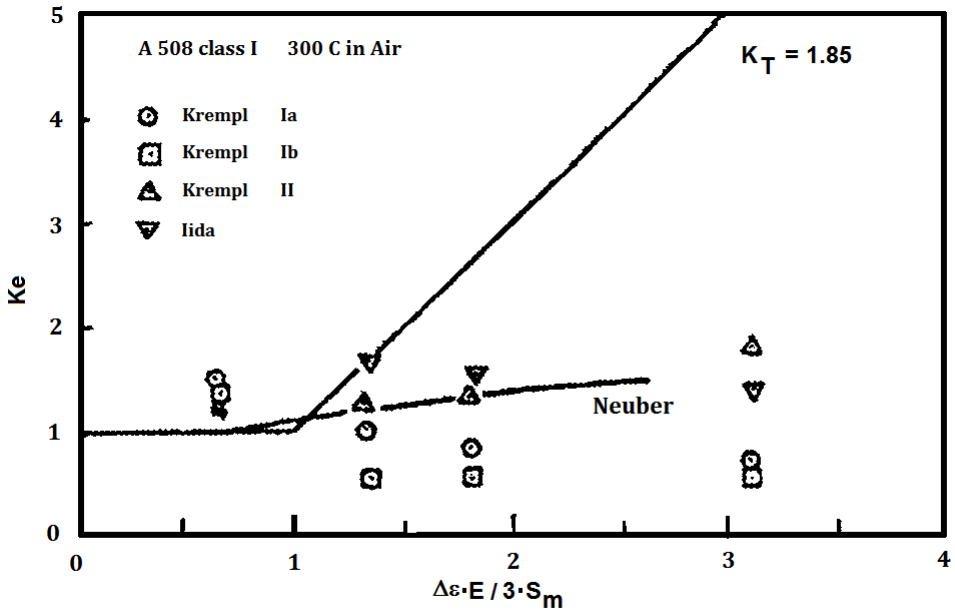

Discussion

The data and indications suggest the ASME Ke values are overly simplistic, very conservative and not appropriate for determining service fatigue life. This approach needs, however, to be retained for determination of the design fatigue life in order to comply with current Code design requirements.

The FSRF approach suggested by Slagis, Iida, Krempl and Hickerson is a more vigorous method and should be used for the determination of service fatigue life. A complicating attribute, as shown by the testing of Hickerson and Chen is that the FSRF is dependent on strain loading direction, i.e. tensile or compressive; fully reversed loading appears to track tensile strain cycling.

FSRF values varying from 1.2 to 2.2, as a function of strain level is appropriate for the range of strain exposure experienced by a coke drum. The work of Chen indicates that some caution is required in that the FSRF values associated with failure of the HAZ can approach 4.0.

To progress a more robust approach, in view of the difficulty in assigning an appropriate FSRF, is to consider using a lower bound material fatigue life curve, ε - N that accounts for the scatter in welded materials. Both Ramos and Chen have studied this in detail and their findings are provided in **Figure 6.9.**

Figure 6.9 Lower Bound Fatigue Life Curve – Welds, HAZ

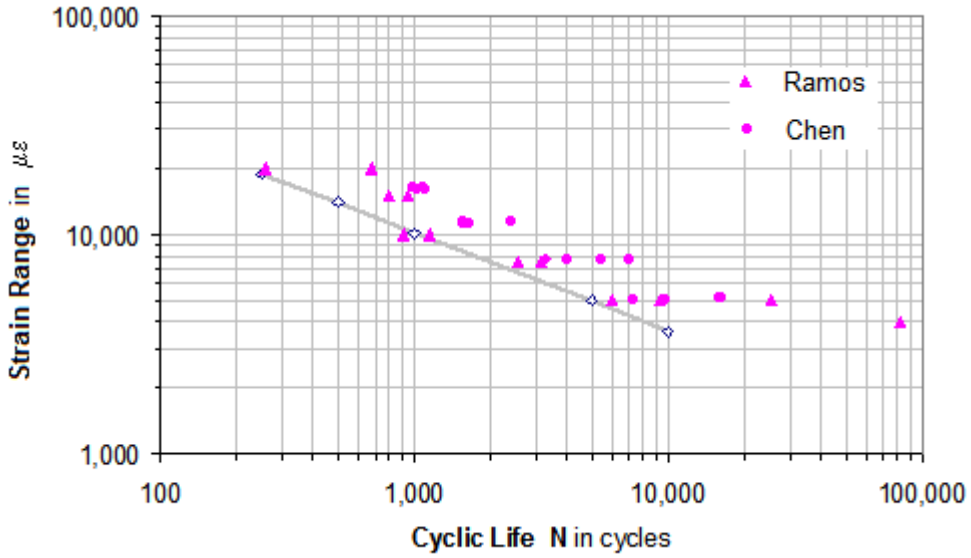

In **Figure 6.9**, the lower bound curve (gray line) from **Figure 5.19** is included to show that the fatigue life of weld and HAZ zones is captured by the variability in testing such that the lower bound curve established by the testing of base materials may be used to establish coke drum service fatigue life without recourse to the Code penalty approach.

While strain concentrations occur for a given material, they may be pragmatically addressed by use of the proposed bounding curve. Where warranted, specific service fatigue life data may be established.

6.3 Calculation of Strain Based Service Fatigue Life for a Coke Drum

The calculation of strain-based fatigue service life for a coke drum is determinable using a phenomenological approach since;

- ε – N, strain to low cycle fatigue life mechanical properties have been established for the main coke drum materials of construction, **Figure 5.19**
- thermo-mechanical loading of the shell is probabilistic, see **Figure 5.18**
- a simplified elastic – plastic analysis is practical and accurate without using the fatigue strength reduction factor, FSRF
- the fatigue penalty factor, Ke as prescribed in the Code is overly conservative, and though more accurately established by Krempl and Hickerson, is not required for service life assessment
- the damage to coke drum shells may be bound between two types of damage; angular misalignment and bulge misalignment

Service Fatigue Life of a Newly Constructed Coke Drum

The preceding sections have demonstrated that using a lower bound fatigue life curve will provide the requisite accuracy in determination of a service fatigue life.

The life value is based on use of the damage accumulation expression wherein

$$D = \sum_{k=1}^{m} \frac{n_k}{N_k} \leq 1.0 \qquad \text{applies over the fatigue life.} \qquad (6.8)$$

The efficacy of this expression is based on its inclusion in several pressure vessel construction Codes and is not addressed in this work. The expression is known as the Palmgren – Miner rule. Research data indicates the damage criteria, D varies between 0.4 and 1.4 but that for reversed loading, a value of 1.0 is considered adequate [15, 33].

Strain exposures are defined in **Figure 5.18** by taking the intersection of the upper bound line for each of the 52 exposures as the 99% confidence level for strain range loading, $\Delta\varepsilon$.

For each n_k thus established, the corresponding N_k value is established from **Figure 5.19** by intercepting the strain exposure value with the lower bound curve representing the 99% confidence level for cyclic life, N.

To exemplify the preceding;

- enter **Figure 5.18** at n_1 = 1/52 (0.0192), intercept $\Delta\varepsilon$ = 5,711 $\mu\varepsilon$
- enter **Figure 5.19** at $\Delta\varepsilon$ = 5,711 $\mu\varepsilon$, intercept N_1 = 2,675 cycles
- calculate n_1 / N_1 = 19.2 / 2,675 per 1,000 cycles
- for $\Delta\varepsilon$ < 3,500 $\mu\varepsilon$, sum the remaining n_k , set N_k = 100,000 cycles
- complete n_k / N_k = for all 52 exposures
- sum the n_k / N_k , this is the damage fraction for 1,000 cycles
- calculate 1,000 / $\Sigma\, n_k$ / N_k to obtain the number of cycles corresponding to D = 1.0; designate as N_{total}
- calculate service life, N_{years} at the 99% confidence level as N_{total} / 365 assuming 1 operational cycle for each 24 hour period.

The calculated life, N_{years} thus is 72 years at the 99% confidence level.

The 50% confidence interval is similarly calculated as 151 years for comparison.

Using the methodology established above, the service fatigue life of a newly constructed coke drum can be determined to be between 72 and 151 years, assuming one operational cycle every twenty four hours. This service life is limited by the quality of the undeformed shell welds.

Service Fatigue Life of a Damaged Coke Drum

Coke drums deteriorate in service from development of shell distortions. These distortions were exhibited in **Figure 5.1**. All drums experience damage soon after entering service; hence, a more informative and valued service life estimate is given based on the actual physical condition of the drum.

There were no detailed damage profiles available in the literature; but some large scale data was retrieved. **Figure 6.10** shows a shell contour plot for a coke drum; the maximum shell radial deviation is ± 2 inches [50.8 mm].

Figure 6.10 Drum Bulge Profile – Radial ∆=2" [50.8 mm]

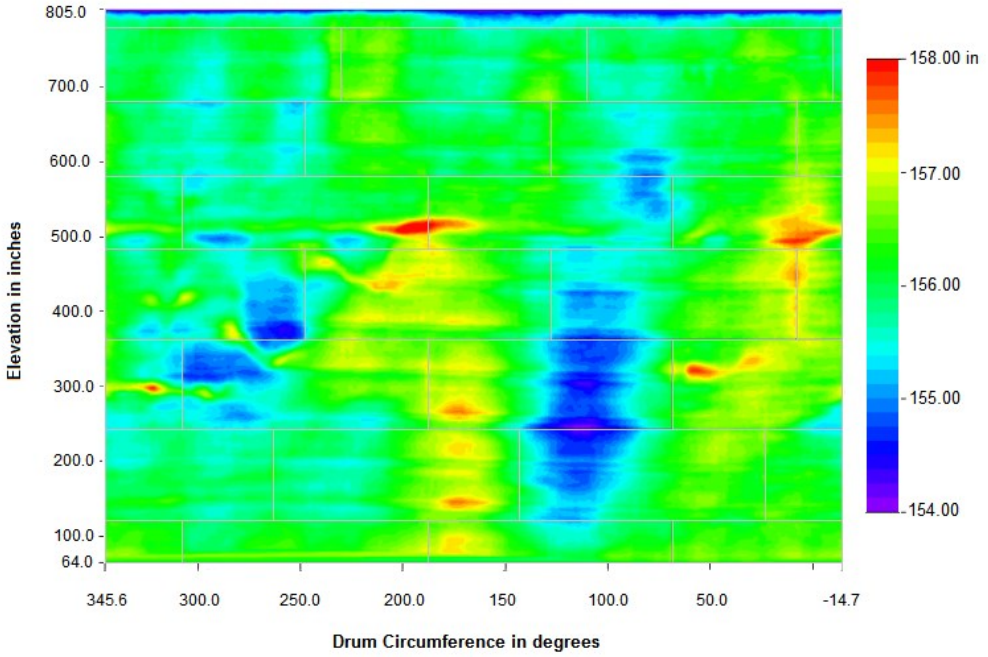

In **Figure 6.11**, the shell radial deviation is ± 4 inches [101.6 mm]. In both drums, an accurate local profile is not available and is not provided in practice.

However, in order to bound the damage, two types of local damage profiles can be considered;

- an angular axial misalignment
- a rounded axial misalignment

Figure 6.11 Drum Bulge Profile – Radial Δ = ± 4" [101.6 mm]

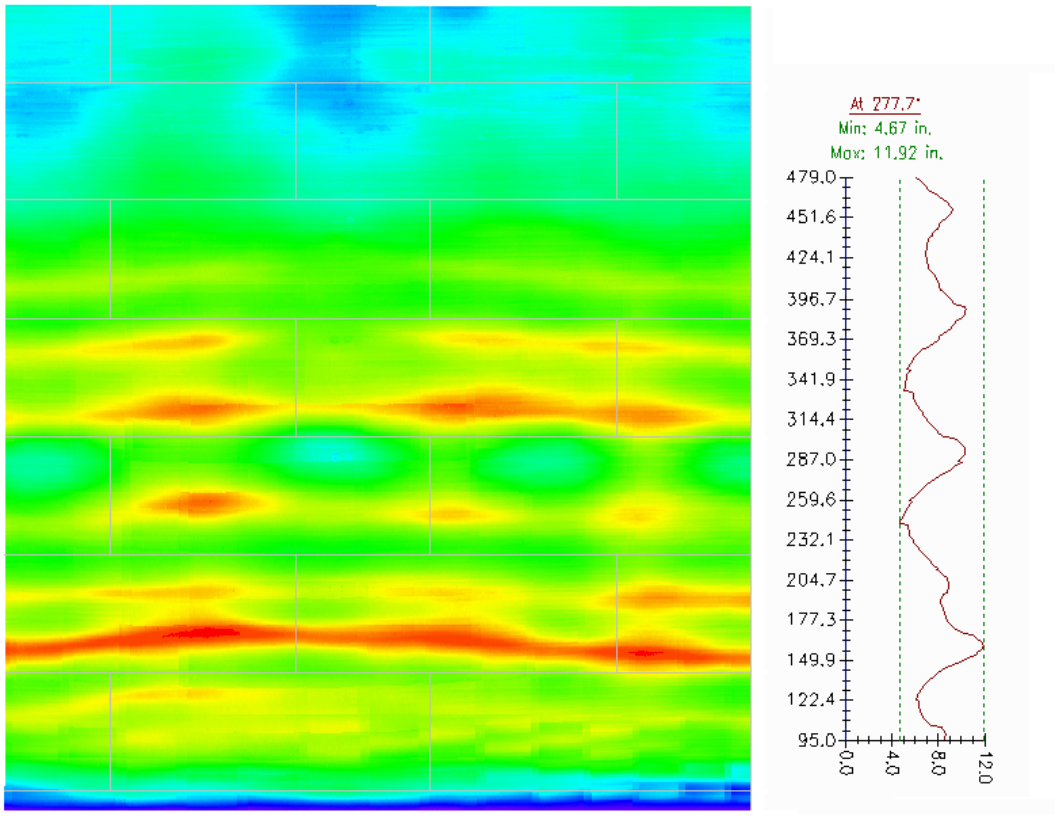

The two bounding misalignment profiles are illustrated in **Figure 6.12**; angular misalignment entails that the shell edges intersect at the weld course without a transition radius. The bulge misalignment presents as shell edges intersecting at the weld course with a smooth transition.

Figure 6.12 Bounding Drum Bulge Profiles in Axial Misalignment

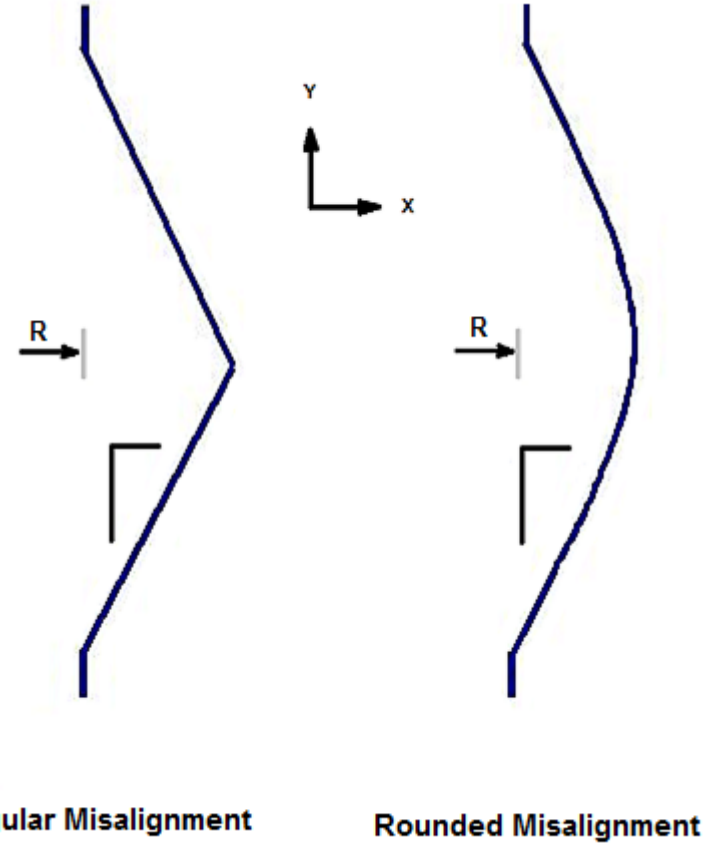

Notes

1. The profiles represent bounding limits for various tapers that are presented in Table 6.2.
2. R ≡ mean radius and R = 150 inches [3,810 mm]

Figure 6.13 illustrates an actual bulge misalignment distortion in a coke drum which demonstrates that this misalignment profile actually occurs and is regular.

Figure 6.13 Photograph of a Drum Bulge

To calculate the impact of shell distortion on service life, the previous procedural scheme is modified to account for two considerations

- the stress / strain concentration, k_t caused by the alignment profile
- the increased strain value $\Delta\varepsilon$ with which the ε – N service life curve is entered

The stress / strain concentration factor is calculated using numerical methods (i.e., FEA) for the several geometries presented by **Figure 6.10, Figure 6.11** and within the constraints of **Figure 6.14.**

Figure 6.14 Bulge Growth in Damaged Drums [13]

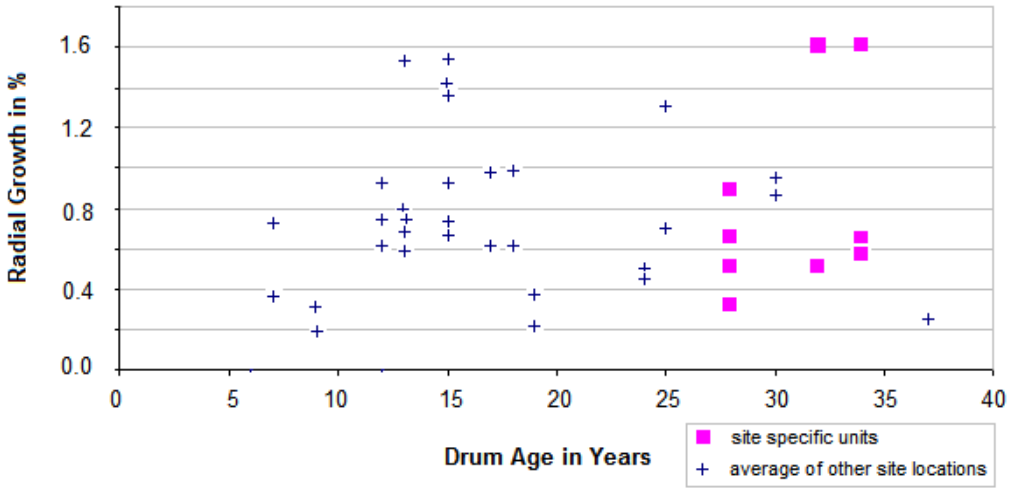

Determination of k_t Factors for Damaged Drums

The stress / strain concentration factors for a damaged drum can be determined for the bounding profiles given in **Figure 6.12.** A complication is to recognize that the stress / strain fields for pressure and thermal loading are different. Whereas, pressure loading in a cyclinder creates a bi-axial, 2:1 hoop to axial stress field, thermal loading presents a 1:1 stress field.

For specific industry application to a damaged drum, the dimensional data from a laser scan will be used in construction of the shell numerical model. Hence, strain results will inherently reflect stress / strain concentration effects caused by dimensional distortions. Where detailed laser scans are not available, estimates of drum shell distortions may be made from visual approximation.

To illustrate the impact on stress / strain results, the differences can be reviewed for a sample defect under pressure and temperature loading.

In **Figure 6.15**, a quarter symmetry flat plate with hole is modeled; pressure and temperature loading are applied under boundary conditions appropriate for the loading.

Figure 6.15 ¼ Symmetry FEA Model for SCF Determination

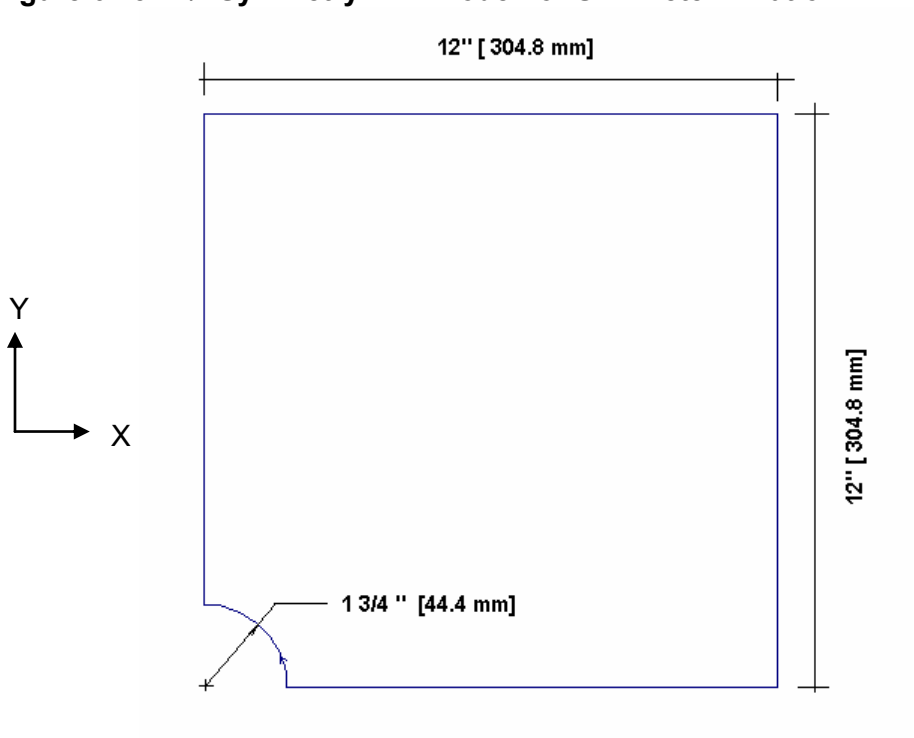

Notes to Figure 6.1x

1. Flat panel, 1" [25.4 mm] thickness; SHELL4 element with 6 degrees of freedom
2. No out of plane displacement;
   UZ = 0 under all conditions
   AR = at all edges
3. UX = 0 at left edge, for 1D pressure loading in X direction
   UX, UY = 0 at left, bottom edge for pressure loading in X, Y directions
4. UX = 0 at left, right edges, for 1D temperature loading
   UX, UY = 0 at all four straight edges 2D temperature loading
5. Pressure loading at free edges varied to suit loading ration regime; base pressure load of 5,250 psi applied, corresponding to hoop stress in coke drum

The results are presented in **Table 6.2** for pressure and temperature loading cases. The data demonstrates that for temperature loading, under 2D restraint, the SCF developed at the discontinuity is identical to a pressure loading using a 1:1 biaxial stress field. The 2D restraint field induces a 1:1 biaxial stress field in the plate.

The SCF for a 2:1 pressure loading is 2.6 for the model (2.5 theoretical) and is greater than the 2D restraint temperature loading case. Hence, the pressure load is more conservative and can be used to estimate the effect of discontinuities encountered under temperature loading of the damage models.

The primary purpose of this effort is to illustrate that thermomechanical loading results in a smaller SCF value compared to pressure loading for the hole-in-plate model and similar results are expected for the SCF for a bulged shell.

Table 6.2 Results for Pressure / Temperature Loading Cases

	Theoretical		Numerical		
	Value [psi]	SCF	Value [psi]	SCF	Δ %
Pressure					
1:0	15,750	3.0	16,602	3.2	6.7
1:1	10,500	2.0	10,945	2.1	5.0
2:1	13,125	2.5	13,638	2.6	4.0
Temperature (-100 F°)					
1D restraint	66,045	3.0	64,203	2.90	-3.3
2D restraint	44,030	2.0	61,270	1.98	-1.0

The SCF values for various damage conditions can be estimated from finite element method models from the damage profiles presented in Figure 6.12. A particularized model is presented as a rounded bulge in Figure 6.16.

Figure 6.16 Rounded Bulge in Axial Misalignment, FEA Model

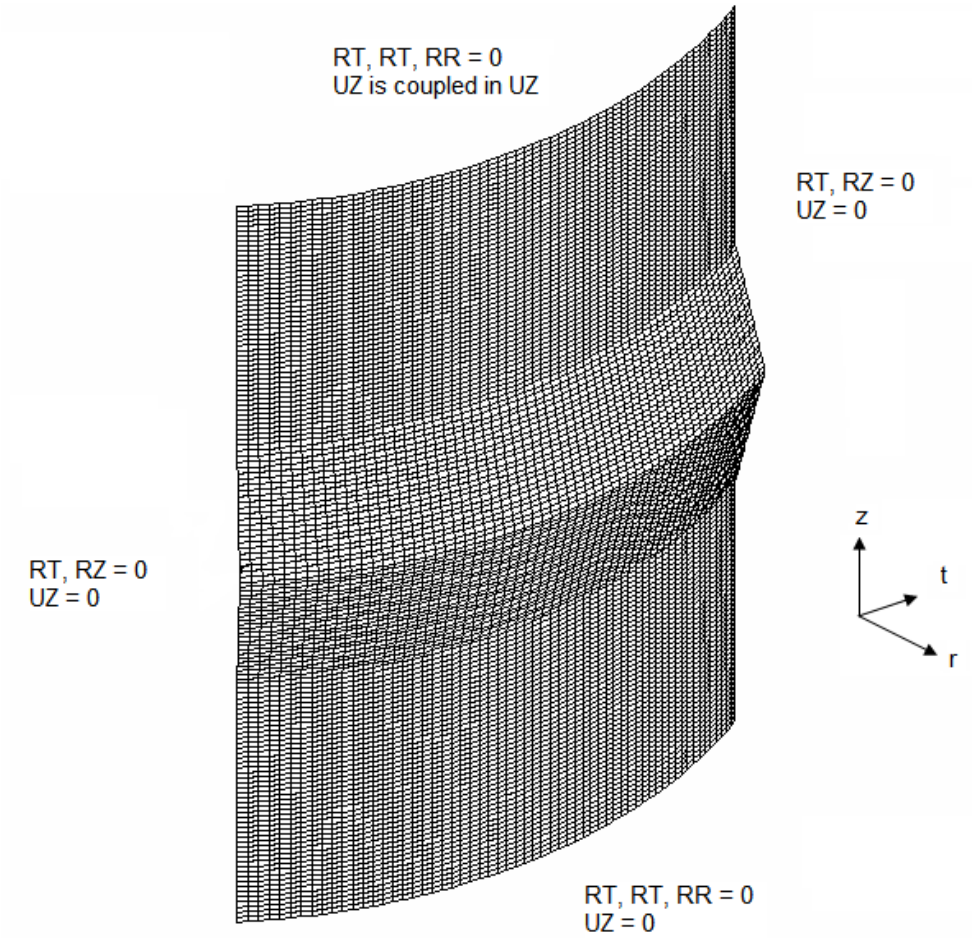

Notes to Figure 6.16

1. The element used for the model is the SHELL4L 4-node multi-layer quadrilateral shell element, 8,640 elements used; elements have
   - membrane and bending capabilities for the analysis of three-dimensional structural and thermal models
   - up to 50 layers can be used; 2 layers are used for this analysis
   - six degrees of freedom (3 translations and 3 rotations) are considered per node
   - each layer can be associated with different isotropic or orthotropic material properties; isotropic material behaviour is used for the model
2. UZ, UR, UT ≡ translational displacement; in the cylindrical coordinate system RZ, RR, RT ≡ rotational displacement; in the cylindrical coordinate system
3. The top edge of the model is coupled / constrained to preserve plane-remains-plane boundary condition; this ensures no local part of the model can displace relative to other elements on the boundary
4. Radial displacement is unconstrained
5. Internal pressure loading of 35 psi [241 kPa] and corresponding longitudinal pressure stress loading is applied to the upper edge.

Table 6.3 summarizes SCF factors derived by particularizing the models for various profile geometries; the values fall within the range of values studied in the referenced literature and pose no new difficulties or suggest an altered treatment. The SCF factors are perfuntorally calculated as

$$SCF \equiv \frac{longitudinal\ stress\ with\ discontinuity}{longitudinal\ stress\ without\ discontinuity} \tag{6.9}$$

Service life is simply calculated according to summation expression (6.8) and expressed in years on the basis of 1 operational cycle per 24 hours during the life of the equipment. The service life determinations are summarized in Table 6.3.

In this case, the stress is the nominal longitudinal stress and is used to streamline computational resources given the lack of benchmarking data available to us.

Table 6.3 Life Potential for Undamaged and Damaged Coke Drum – years

	Undamaged		Misalignment Damage					
	99%	50%		99%	50%		99%	50%
Taper	$k_t = 1$		k_t	Sharp-edged		k_t	Rounded	
1:1	72	151		-	-		-	-
1:36	-	-	1.3	34	61	1.08	55	114
2:36	-	-	1.5	23	41	1.16	45	90
3:36	-	-	1.8	15	25	1.23	38	73
4:36	-	-	2.0	11	19	1.30	34	61

Figure 6.17 presents the data of Table 6.3 for the 99% confidence interval.

Figure 6.17 Coke Drum Service Life Estimate – 99% Confidence Level

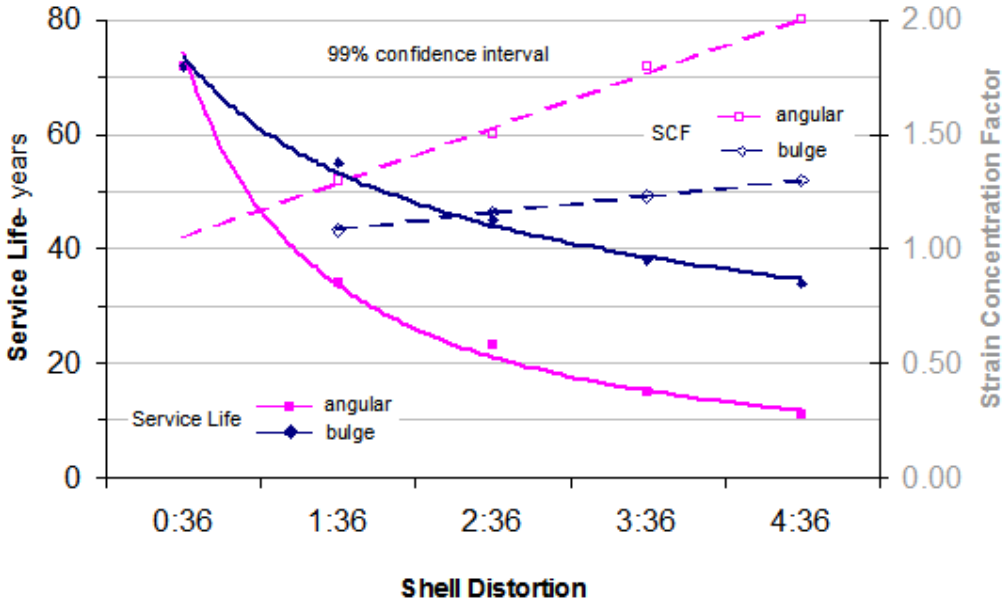

Figure 6.18 presents the data in Table 6.2 for the 50% confidence interval.

Figure 6.18 Coke Drum Service Life Estimate – 50% Confidence Level

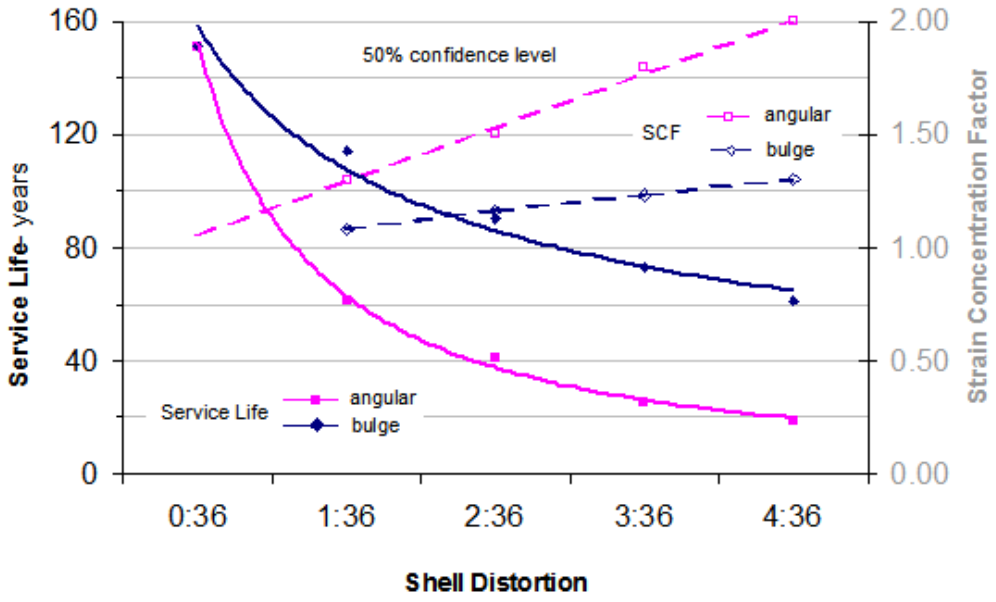

CHAPTER 7 TEMPERATURE DEPENDENCY AND NON-LINEAR ANALYSIS

As outlined in the foregoing work, implementation of the engineering analysis has been consistent with industry methodology so as to remain within a level of sophistication commensurate with industry established and widely accepted practices.

As seen, however, Code and industry methods include important simplifications which are not sufficiently substantiated. These include

- penalty factor for elastic – plastic analysis
- constant valued fatigue strength reduction factor
- design fatigue life approach
- categorical material properties

These simplifications, if implemented by rote, preclude sufficient accuracy in establishing a service life estimate. This thesis has addressed these four items in detail.

The Code defers to the experience and skill of the practitioner, in a numerical analysis, as regards the use of

- temperature dependent / partially dependent material properties
- linear – elastic structural analysis
- non-linear – plastic structural analysis

Linear – elastic analysis is preferred for pragmatic reasons, including

- simplicity in implementation
- robustness, stability
- efficacy
- reduced run time
- minimized debugging effort
- suitability

In this chapter, the impact of a linear – elastic to non-linear – plastic analysis are evaluated by using a comparative study.

7.1 Evaluation of Temperature Dependent Material Properties

The properties of interest using fully temperature dependent properties are

- the coefficient of thermal expansion CTE, also symbolized by "α"
- the elastic modulus E, otherwise referenced as Young's modulus
- cyclic yield strength

The values of the CTE, i.e., α and the elastic modulus directly impact the magnitude of strain in determination of the thermo-mechanical strain, ε^{mech} arising from both the differential expansion of clad and base layers and, the thermo-mechanical strain from self – constraint imposed between "cold spots" and "hot spots".

Equations (2.6) and (2.7) are repeated here for convenience:

$$\sigma_c = \frac{(\alpha_b - \alpha_c)\cdot(T_h - T_0)\cdot E_c}{1+\frac{t_c \cdot E_c}{t_b \cdot E_b}} \cdot \frac{1}{1-\mu} \tag{7.1}$$

$$\sigma_b = \frac{(\alpha_c - \alpha_b)\cdot(T_h - T_0)\cdot E_b}{1+\frac{t_b \cdot E_b}{t_c \cdot E_c}} \cdot \frac{1}{1-\mu} \tag{7.2}$$

For a partially temperature dependent material treatment, material properties are treated as uniform values for the operating temperature range of interest, 100 °F to 900 °F [38 to 482 °C]. For the work described in this thesis, a temperature of 650 °F [343 °C] was selected as a reasonable compromise.

Temperature dependent behaviour of CTE

The CTE values for C – ½ Mo, 1 ¼ Cr and 2 ¼ Cr alloy steels are equal, being in the same material group according to the Code, and rise continuously. For TP 410S, the increase is less and even stationary in the vicinity of approximately 500 °F to 650 °F [260 °C to 343 °C] before increasing at a reduced rate. This results in an increased difference in expansion between the two material groups; as a result, as temperature increases TP 410S will experience tensile loads while the C – ½ Mo and Cr – Mo steels will experience compressive loads, all consistent with the expressions provided in equations (7.1) and (7.2).

Figure 7.1 CTE Values versus Temperature

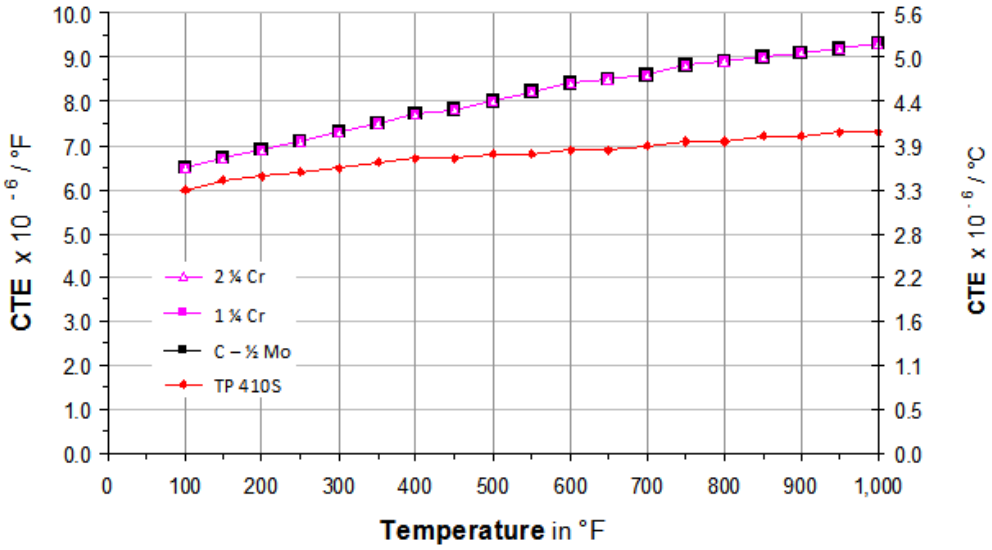

Temperature dependent behaviour of the Elastic Modulus

At 650 °F [343 °C], a rapid reduction occurs in the elastic modulus, as evidenced in **Figure 7.2.** For C – ½ Mo steels and TP 410S, the reduction is more rapid than the Cr – Mo steels. At higher temperatures, material creep, a time dependent material property becomes a consideration and has been previously discussed in this work.

Figure 7.2 Young's Modulus Values versus Temperature

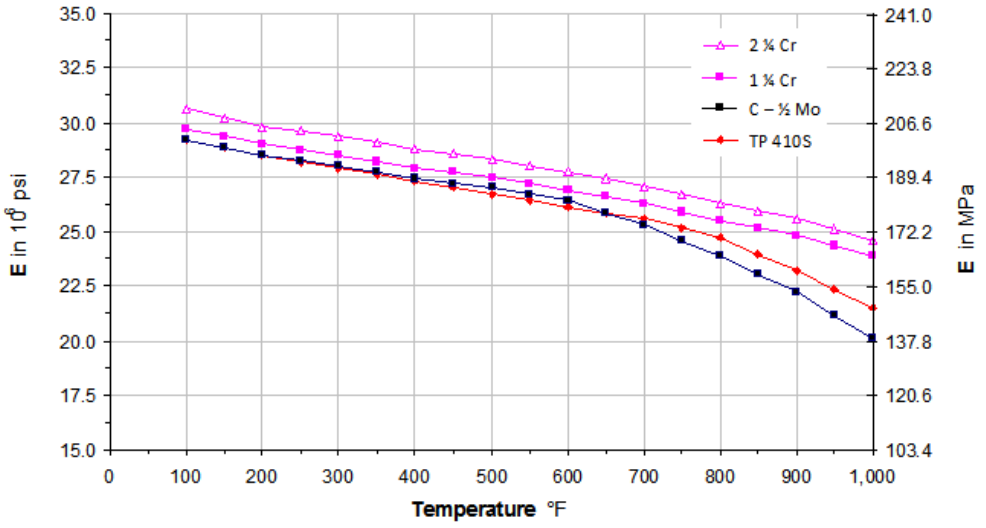

Temperature dependent behaviour of Yield Strength

A material property directly affecting material selection for the construction of coke drums is yield strength. The common construction materials are temperature dependent as seen in **Figure 7.3** where the specified minimum yield strength [SMYS] values are plotted. The SMYS values are stipulated by Code and provide an implicit design margin by specifying an allowable stress which accounts for the temperature dependency of the SMYS; refer to **section 1.3.4** and **Table 1.3.** It is commonly known in industry that these values are surpassed by the actual yield strength [YS] of supplied materials.

Figure 7.3 SMYS Values versus Temperature

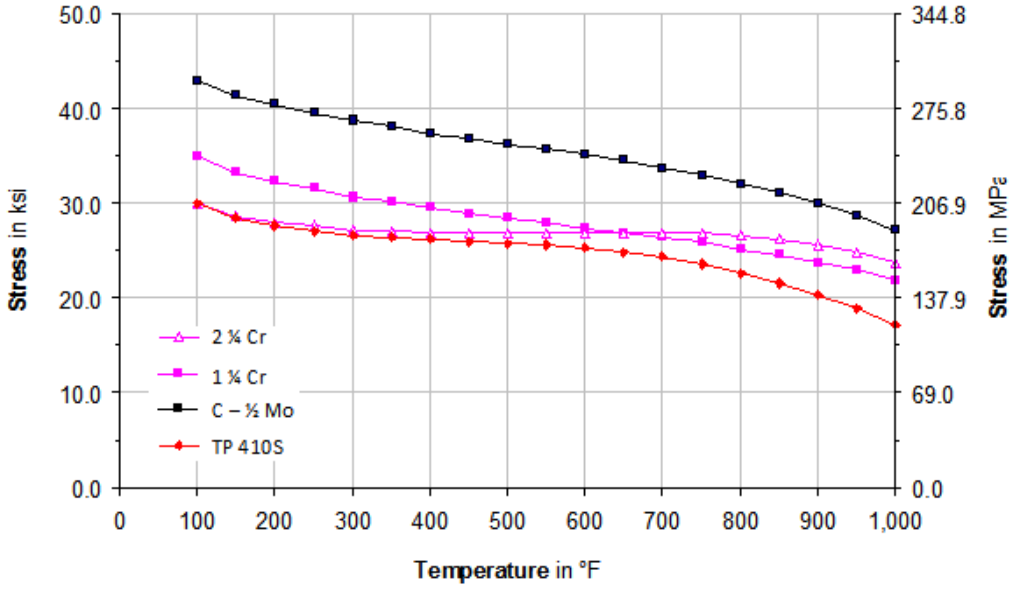

In addition, the SMYS values used by Code for pressure design determination are the monotonic properties; for cyclic loading, the cyclic yield strength is the more appropriate material property to consider. **Figure 7.3 is** replotted as **Figure 7.4** with the addition of the cyclic yield strength for SA 204C material included.

Figure 7.4 Cyclic Yield Strength Compared to Monotonic SMYS

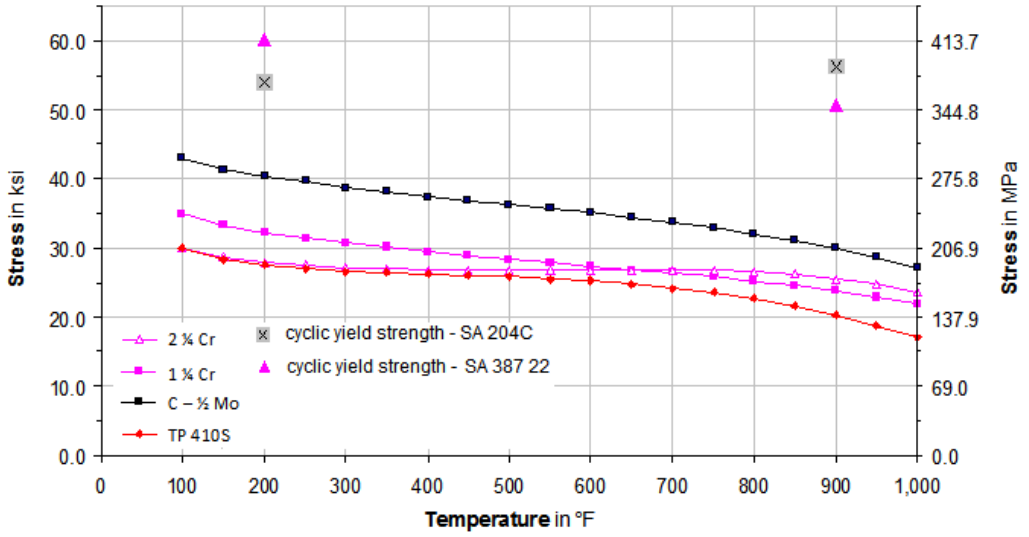

Noting that the cyclic yield strength of C – ½ Mo (specifically, SA 204 C) is greater than the cyclic yield strength of Cr – Mo (specifically, 2 ¼ Cr – 1 Mo, i.e., SA 387 22 Class 2) at elevated temperatures and that the elastic modulus for the former is much reduced in comparison to the latter (**Figure 7.2**), the observation is made that SA 204 steels are mechanically "tougher" [30]. Hence, the apparent better reliability observed of SA 204 steels in coke drum service.

In Figure 7.5, the cyclic strength curve for C – ½ Mo, SA 204C is provided to illustrate its retention in cyclic strength over the temperature range of interest for coker drum operation.

Figure 7.5 Cyclic Yield Strength for SA 204C at Temperature [34]

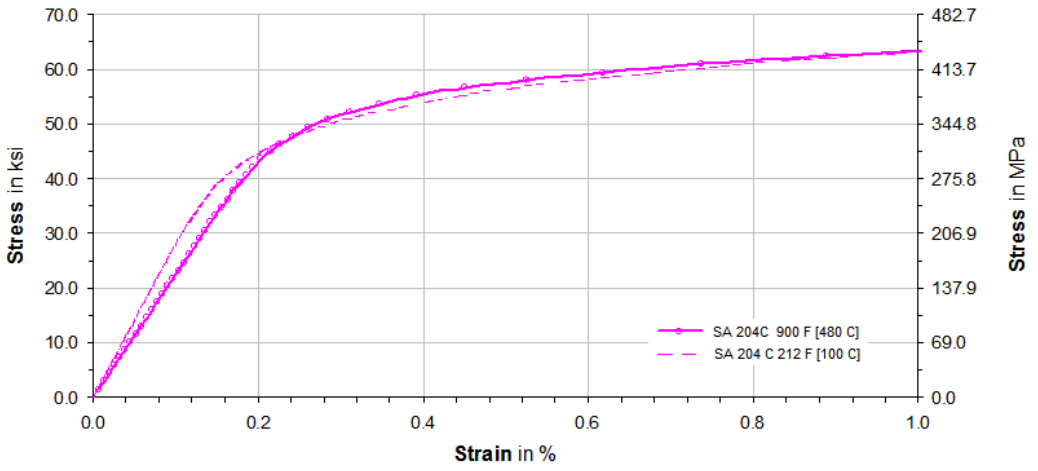

7.2 Application of Temperature Dependent Material Properties to Analysis

In order to assess any impact from temperature dependent material properties and the linear – elastic structural analysis, a plane stress FEA model was studied. The model is provided in **Figure 7.6**. Several model permutations were evaluated incrementally; however, the two bounding analyses consisted of the two approaches;

- linear elastic with partial temperature dependent material properties
- non-linear plastic with temperature dependent material properties

Figure 7.6 Plane Stress Model for FEA Modeling Validation

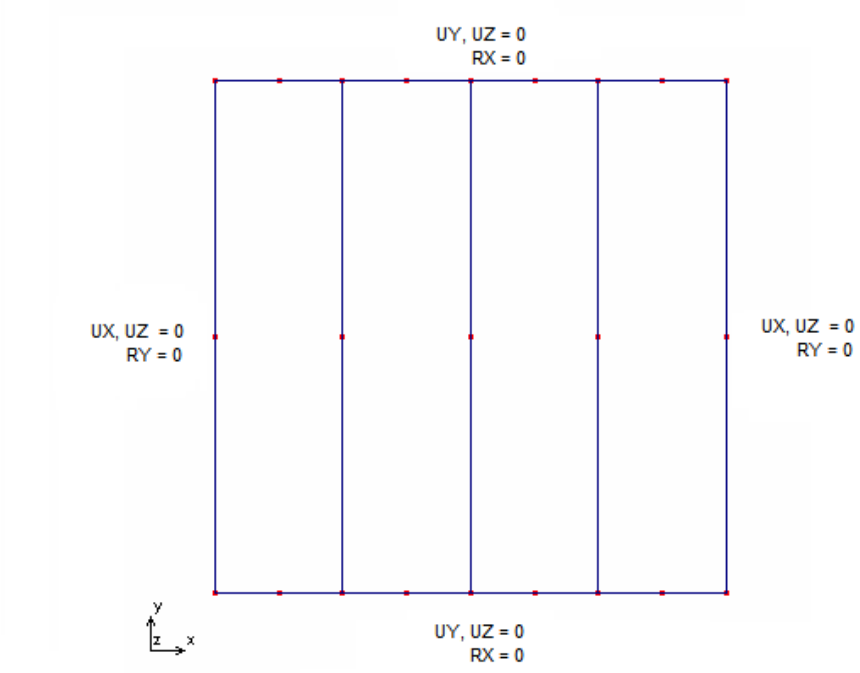

Notes to Figure 7.6

1. The element used for the model is the PLANE2D 8 - node isoparametric two-dimensional plane stress for linear and non-linear analysis with
   - linear elastic, non – linear elasticity, plasticity, thermo-plasticity capability
   - two degrees of freedom (2 translations) are considered per node
   - one degree of freedom per node representing the temperature is used for the thermal module
2. UX, UY, UZ ≡ translational displacement; Cartesian coordinate system
   RX, RY, RZ ≡ rotational displacement; Cartesian coordinate system
3. Fixed support plate model, no rotation at edges
4. Parametric temperature variation from 100 °F to 900 °F [38 °C to 482 °C]
5. Temperature independent and temperature dependent material behavior used

In **Figure 7.7**, the results of the linear – elastic, temperature independent and non – linear thermo-plastic responses are presented for the calculated stresses and strains.

The pseudo – elastic line, $\sigma^{\text{pseudo – elastic}}$, represents the calculated linearized stresses from the linear – elastic, temperature independent structural analysis. The corresponding strain line is shown as $\varepsilon^{\text{linear}}$. The true stress response is shown by σ^{true} and the non – linear, plastic strain by $\varepsilon^{\text{plastic}}$. The combined linear and plastic strain response is shown by $\varepsilon^{\text{total}}$.

Figure 7.7 Linear and Non – Linear Benchmarking Comparison

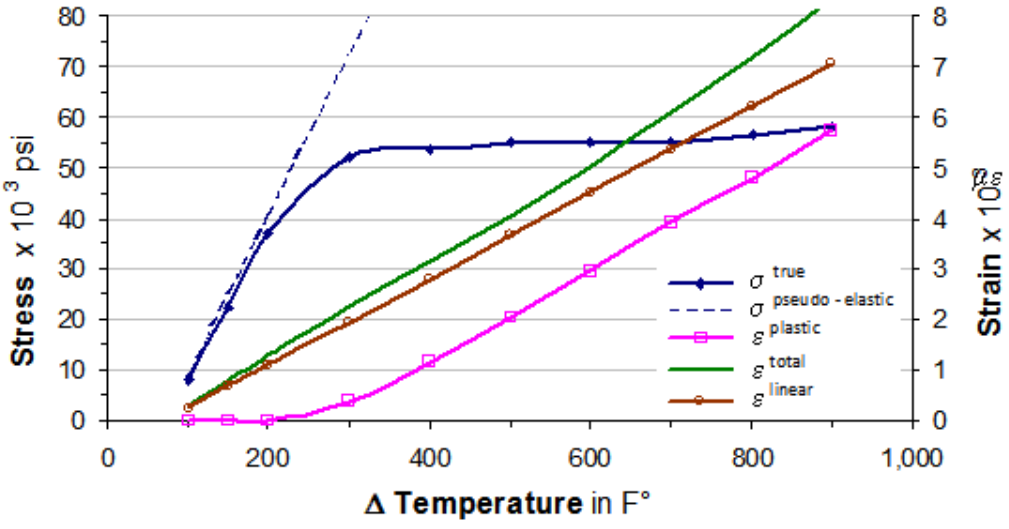

This response is slightly larger than the linearized strain response. Since neither "hot" spots or "cold" spots involve the high – end temperature differences posed in **Figure 7.7**, the use of a linearized, temperature independent structural analysis is reasonable.

This is demonstrated by examining the strain evolution of a temperature snapshot for the shell panel studied in section five (§ 5). **Figure 7.8** plots the temperature snapshot for the linearized strain plot presented previously in **Figure 5.9**.

Figure 7.8 **Temperature Snapshot for a Cold Spot** in [°F]

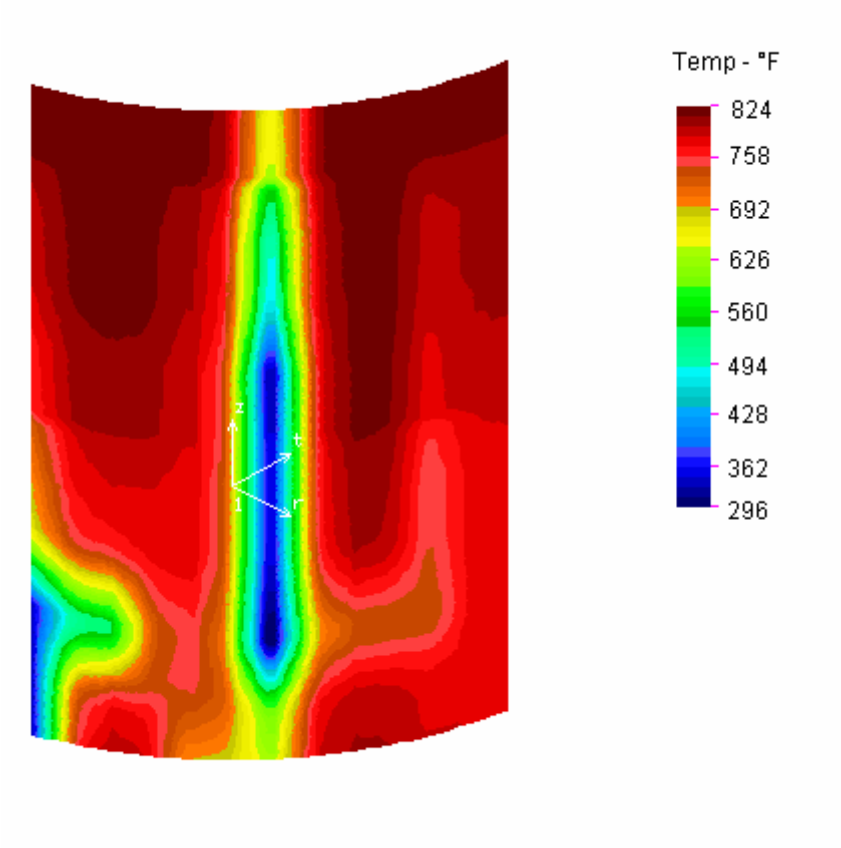

Figure 7.9 plots the linearized strains from the linear – elastic, temperature independent, composite element FEA study for the temperature snapshot depicted in **Figure 7.8**.

Figure 7.9 Strain Report from Linear – Elastic Analysis in με

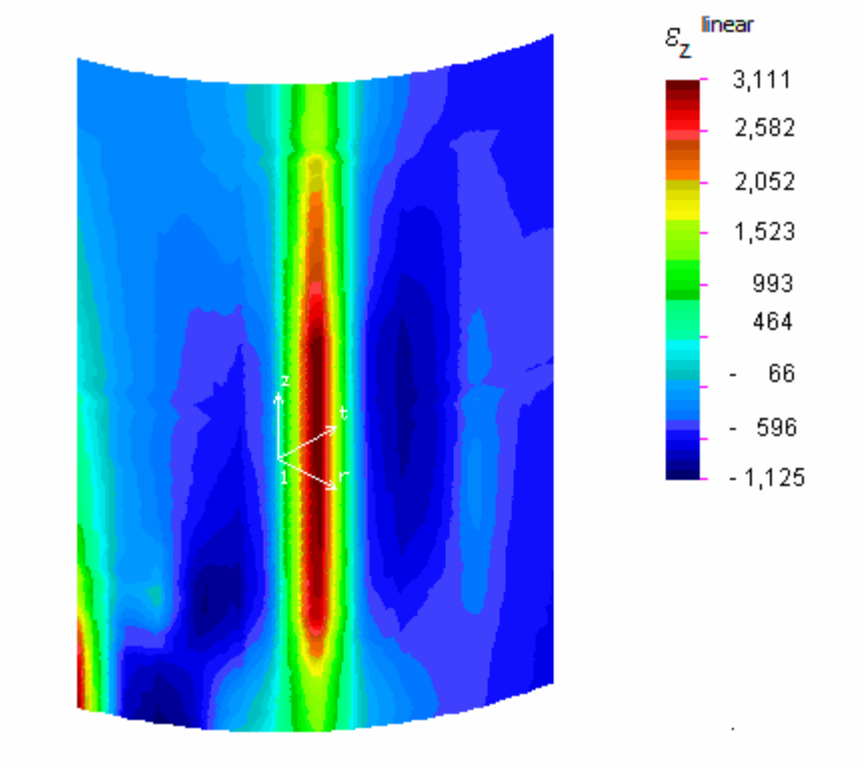

Figure 7.10 plots the linearized strains from a linear – elastic FEA study for a comparable single – layer flat plane defined by the coke drum curved shell model. The flat plane model is required to address the limitations of the layered element model. The figure shows the flat plane model produces near – identical results and is slightly conservative.

Figure 7.10 Mechanical Strains for Linear Flat Plane Model

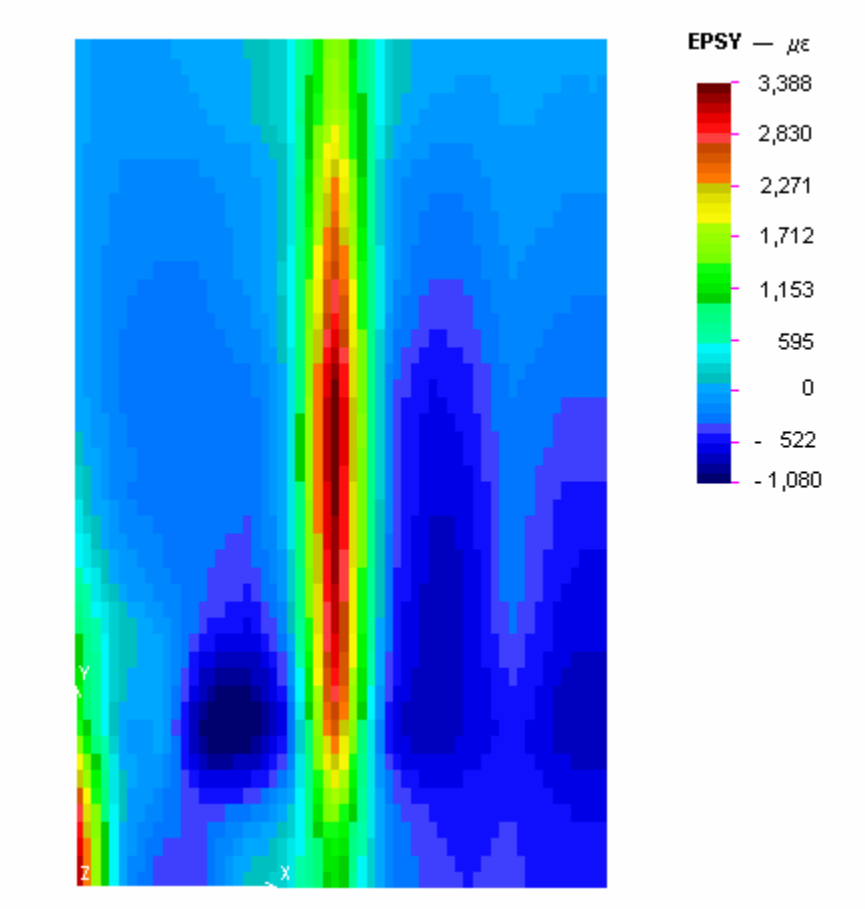

In **Figure 7.11**, temperature dependent material properties are employed to gauge the impact of the more rigorous non-linear thermo-plastic analysis.

Figure 7.11 Mechanical Strains for Non – Linear Flat Plane Model

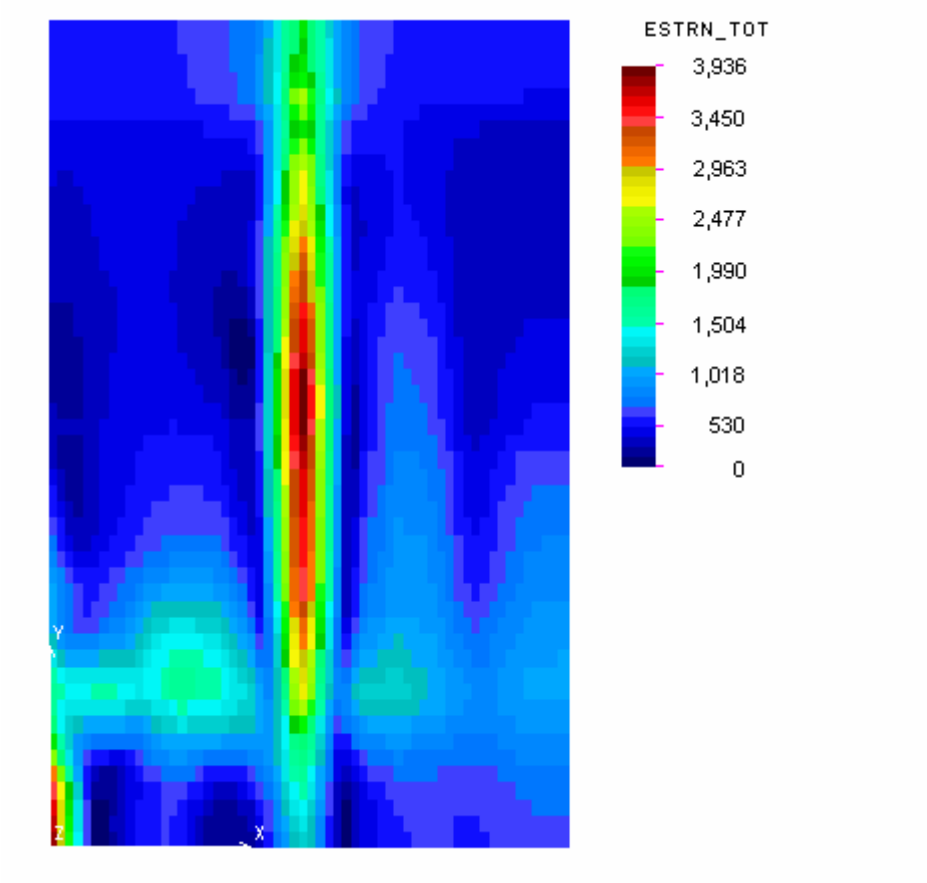

The strain results are reported in **Table 7.1** for an element located in the "cold spot" of the linear and non-linear models exhibited in **Figures 7.10** and **Figure 7.11** respectively. The data shows good agreement between the reported and calculated strain results from the linear model compared to the reported results from the non – linear model.

It can be concluded that the strain results obtained from a linear analysis can be used to determine strains from cyclic thermal loading with sufficient accuracy for an industry service life estimate for a coke drum shell. The practice in the industry of using averaged mechanical properties is reasonable.

Table 7.1 Strain Results from Linear versus Non – Linear Models

			Strain results				
Model	Temp	stress	$\mu\varepsilon^{pl}$	$\mu\varepsilon^{el}$	$\mu\varepsilon^{mech}$	$\mu\varepsilon^{th}$	$\mu\varepsilon^{total}$
	F	psi	με	με	με	με	με
Non - linear	300	61,284	998	1,884	2,882	2,157	5,039
Linear	300	73,125					
calculated			–	2,823	2,823	–	–
reported			–	2,547	2,547	–	–

CHAPTER 8 CONCLUSIONS

The primary objective of this work was to determine the service fatigue life for both a new coke drum and a damaged coke drum using industry practice codes and standards. Coke drums are subject to various loadings such as internal pressure loading, live weight loading and dead weight loading. These were shown in previous work to be unlikely causes of shell cracking. In this work, thermo-mechanical, low cycle fatigue cracking of the shell was shown to be the primary damage mechanism and quantifiable in sufficient detail to allow consequent calculation of a service life estimate for both new and damaged drums.

There is only very limited temperature and strain data available in the few open industry literature sources; more detailed information was provided by a confidential source. This latter data allowed quantification of the thermo-mechanical strains and development of a probabilistic thermo-mechanical loading profile.

Material fatigue properties were retrieved from open literature sources and original work conducted at the University of Alberta. These data are in excellent agreement. Industry practices are directed to pressure vessel design; for vessels in fatigue service, the practices establish a fatigue design life which provides an alert for more rigorous inspections; this is especially directed to the nuclear industry. Consequently for the problem at hand, the practices are overly conservative and not suited for determination of practical service life estimates.

Conversely, industry practice documents contain effective and practical methodologies which can be used, where specifically modified, to render accurate assessments in timely and practical effort for industry use. The Code penalty factor derived from disregarded industry research provides an accurate method of performing simplified elastic – plastic analysis.

Accurate strain exposure profiles can be determined for a coke drum by

- judicious and effective use of industry practice calculation methods
- specific modification for use in fatigue service life determination
- use of accurate fatigue strength reduction estimates
- use of measured material properties
- use of numerical analysis tools as outlined in this work.

Not all loading mechanisms have been discussed in this work because of the complexity of the topic and the paucity of specific details in the open literature. The lack of data is most likely due to the confidentiality of industry business practices. The most damaging loading mechanism, thermo-mechanical loading caused by significant temperature differences in adjacent portions of the coke drum shell has been quantitatively shown to be the leading damage mechanism contributing to shell bulging and cracking.

The following has been established in this work;

1. The service fatigue life of both a new drum and service damaged drum can be practically determined.

2. Thermo-mechanical loading of the shell is sufficient to cause low cycle fatigue failure in the time intervals suggested in the literature.

3. Service life is demonstrably affected by the severity of shell distortions which unavoidably develop in service.

4. The service life and remaining life of a coke drum can be evaluated directly by well established engineering principles and industry practices, as modified and implemented by this research work

5. The prevalent use of TP 410S cladding may be a competing source of crack initiation especially where operational temperature exceed 850 °F [454 °C] due to creep cracking in combination with the applied thermo-mechanical loading during water quench.

8.1 Contributions to the Field

This work has demonstrated the practicality of making service life estimates for coke drums by industry practitioners using accurate material properties, industry consistent calculation methodologies and recognition of those aspects of the calculation methodologies which are overly conservative or not adequately suited.

This work has shown that coke drums, even though in a very severe operational environment, have a reasonable service life when installed. As service damage accumulates, the service life is reduced. By making an accurate assessment of damage progression, equipment owners may better devise operational changes and maintenance practices to preserve the integrity and manage reliability of coke drum equipment.

Specifically, the contributions of this thesis can be listed;

1. that basic industry solution methodologies, as modified by this work, can be used to determine service fatigue life estimates

2. that service fatigue life estimates can be derived for new and damaged coke drums

3. that insight into the thermo-mechanical damage mechanism offers opportunity to modify operational and maintenance practices to optimize the service life of coke drums

4. recognition that coke drum construction materials need to be fatigue tough

5. recognition that specific thermal loading exposure profiles for coke drums are needed to determine installation specific service life

6. demonstration that simplified linear – elastic numerical analysis is sufficiently accurate, time effective and robust to calculate thermo-mechanical loading profiles

7. that specific areas of research may be identified to further understand the design, fabrication, operation and maintenance of coke drums for more economic and safe operation of this equipment

8. that basic industry solution methodologies have been misapplied by industry practitioners, to date

9. that proxy damage criteria by industry practitioners have been and are inadequate to determine service life

8.2 Recommendations for Further Study

The recommendations of prior work have been completed for this effort; however there are a number of possible research opportunities to improve the predictive accuracy of coke drum life determination:

1. identification of alternate materials of construction for both base and clad construction which would be better suited to high strain, low cycle fatigue failure

2. compilation of detailed data on drum operating and inspection history, vessel condition and life retirement practices to benchmark calculation procedures

3. to investigate the impact on FSRF of weld and HAZ from alternate welded joint fabrication technology

4. to investigate the effect Code construction allowable weld defects on shell cracking and fatigue life

5. to develop operational practices to limit shell bulging and set optimal bulge limit criteria

6. to develop maintenance practices to remediate coke drum shell bulging damage

7. to design improved industry surveys to elicit more appropriate information and data for better engineering analysis of the coke drum bulging and cracking failure mechanisms

REFERENCES

1. Ellis, P.J., Paul, C.A., “Tutorial: Delayed Coking Fundamentals”, Session Paper 29a, AIChE Spring National Meeting, March 1998, New Orleans, LA

2. Diwoky, R.J., “Continuous residuum coking by delayed coking process” , original article present at API meeting in Chicago, 18 Nov 1938, reprinted in 2002 by Oil & Gas Journal, Houston, TX

3. Weil, N.A., Rapasky, F.S. “Experience with Vessels of Delayed Coking Units” Proceedings, v. 38 [III] 214-232 1958 Division of Refining, American Petroleum Institute, Washington, DC

4. Thomas, J.W. “API Survey of Coke Drum Experience” 1980 American Petroleum Institute, Washington, DC

5. API, “Technical Report 934-G, Design, Fabrication, Operational Effects, Inspection, Assessment and Repair of Coke Drums and Peripheral Components in Delayed Coking Units”, 1st edition, April 2016 American Petroleum Institute, Washington, DC

6. ASME, “Section VIII Division 1 Rules for Construction of Pressure Vessels”, 2010 ASME, New York, NY

7. ASME, “Section VIII Division 2 Alternative Rules for Construction of Pressure Vessels”, 2007 ASME, New York, NY

8. API / ASME , “579 –1 / FFS –1 Fitness for Service”, 2nd Edition, 2007 American Petroleum Institute, Washington, DC and ASME, New York, NY

9. CRD Partner Information Packages; confidential information packages provided by industry partner(s), 2003, 2007

10. “Hazards of Delayed Coker Unit (DCU) Operations”, EPA 550-F-03-001 Aug 2003 Chemical Emergency Preparedness and Prevention Office, United States Environmental Protection Agency, Washington, DC

11. ASME, “Section II Materials Part A Ferrous Material Specifications”, 2010 ASME, New York, NY

12. ASME, “Section II Part D Properties”, ASME Boiler and Pressure Vessel Code for 2010, ASME , New York, NY

13. API Proceedings “1996 API Coke Drum Survey – Final Report”, 1996 American Petroleum Institute, Washington, DC

14. MPC, “Coke Drum Evaluation Manual and Final Report” 1999, The Materials Properties Council, New York NY

15. Collins, J.A., “Failure of Materials in Mechanical Design – Analysis, Prediction and Prevention”, 2nd Ed., 1993 John Wiley & Sons, New York, NY

16. British Standard, “BS 5500:1997 Specification for Unfired fusion welded pressure vessels”, 1997 The British Standards Institution, London, UK

17. Stress Engineering Services, ”2008 Coke Drum Seminar”, September 2008 Stress Engineering Services Inc., Houston TX

18. Ramos, A., Rios, C.C., Vargas, J., Tahara, T., Hasegawa, T., “Mechanical Integrity Evaluation of Delayed Coke Drums”, PVP volume 359 1997: 291-298 ASME, New York, NY

19. Ramos, A., Rios, C.C., Vargas, J., Johnsen, E., Gonzalez, M., “Delayed Coking Assessment Using Field Measurements & FEA”, PVP volume 368 1998: 231-237 ASME, New York, NY

20. Penso, J.A., Lattarulo, Y.M., Seijas, A.J., Torres, J., Howden, D., Tsai, C.L., “Understanding Failure Mechanisms to Improve Reliability of Coke Drums”, PVP volume 395 1999: 243-253, ASME, New York, NY

21. Boswell, R.S., Farraro, T., Sober, M.J., “Remaining Life Evaluation of Coke Drums”, 1997 Energy Week Conference and Plant Engineering, Operations, Design & Reliability Symposium, ASME / API, Houston, TX

22. Church, J.M., Lim, L.B., Brear, J.M., Jarvis, P., Lant, R.P.D., Middleton, C.J., “Crack growth modeling and probabilistic life assessment of coke drums operating under fatigue conditions”, International Journal of Pressure Vessels and Piping, v 78 2001:1011-1020, Elsevier Science Ltd., Amsterdam, Netherlands

23. Boswell, R.S., Wright, B., “State-of-the-Art Improvements in Coke Drum Design and Life Extension Practices”, CREEP 2007 – 26254, Proceedings of CREEP8, 8th International Conference on Creep and Fatigue at Elevated Temperatures, July 2007, ASME, San Antonio, TX

24. Ohata, M., Kawai, N., et al., “Investigation of Bulging Behavior of Coke Drum – Feasible Study on Causes of Bulging”, PVP2011 – 57276, Proceedings of the ASME 2011 Pressure Vessels & Piping Division Conference, Baltimore, MD

25. Yamamoto, T., Arii, K., et al., “Investigation of Bulging Behavior of Coke Drum – A Practical Analysis of Bulging Under Complex Quench Conditions”, PVP2011 – 57428, Proceedings of the ASME 2011 Pressure Vessels & Piping Division Conference, Baltimore, MD

26. Samman, M., Samman, M., “Stress Analysis of Bulges in Cylindrical and Oval Pressure Vessels”, PVP2014 – 28138, Proceedings of the ASME 2014 Pressure Vessels & Piping Division Conference, Anaheim, CA

27. Samman, M., Tinoco, E.B., Marangone, F.C., “Comparison of Stress and Strain Analysis Techniques for Assessment of Bulges in Coke Drums”, PVP2014 – 28139, Proceedings of the ASME 2014 Pressure Vessels & Piping Division Conference, Anaheim, CA

28. Samman, M., DuPlessis, P., “The Bulging Intensity Factor (BIF™), A technique for assessing the bulging severity of coke drums”, RMC-07-100 2007 NPRA Reliability & Maintenance Conference, NPRA Houston, TX

29. Barsom, J.M., Vecchio, R.S., “WRC Bulletin 432 Fatigue of Welded Structures” June 1997 Welding Research Council, New York, NY

30. Harvey, J.F., “Theory and Design of Pressure Vessels”, 1985 Van Nostrand Reinhold Company, New York, NY

31. Aumuller, J., “Aspects of the Thermo Elasto-Plastic Response for a Coke Drum under Cyclic Loading” M. Sc. Thesis 2009, University of Alberta, Edmonton, Alberta

32. J.H. Gross, “WRC Bulletin 101 PVRC Interpretive Report on Pressure Vessel Research, Section 2 – Materials Considerations“ Nov 1964 Welding Research Council, New York, NY

33. Dowling, N.E., ”Mechanical Behaviour of Materials – Engineering Methods for Deformation, Fracture, and Fatigue”, 4th Ed., 2013 Pearson Education Prentice Hall, Upper Saddle River, NJ

34. Chopra, O.K., Shack, W.J., “Low-cycle fatigue of piping and pressure vessel steels in LWR environments” volume 184 (1998) pp. 49 – 76 Nuclear Engineering and Design, Elsevier Science S.A., Amsterdam, Netherlands

35. Chen, J., “Fatigue Behavior of Coke Drum Materials and Its Application to Extend the Service Lives of Coke Drums”, Ph. D. Thesis 2014, University of Alberta, Edmonton, Alberta

36. Jaske, C.E., Hechmer, J.L., “WRC Bulletin 422 Fatigue Strength Reduction Factors for Welds in Pressure Vessels and Piping” June 1998 Welding Research Council, New York, NY

37. Araque, E.D., Vivas, G.A., Moret, A.J., Bello, R.E., “Fitness for Service Evaluation of a Bulging Coke Drum”, PVP2015– 45190, Proceedings of the ASME 2015 Pressure Vessels & Piping Division Conference, Boston, MA (not included in official publication of conference proceedings)

38. Zhang, Y., Xia, Z., “Simplified Thermo-elasto-plastic Analysis Models for Determination of Global and Local Stresses in Coke Drums”, PVP2013 – 97296, Proceedings of the ASME 2013 Pressure Vessels and Piping Conference, Paris, France

39. Beckwith,T.G., Buck, N.L., “Mechanical Measurements”, 2nd Edition 1973 Addison Wesley, Reading, MA

40. TML, “Strain Gauges Catalog Pam E – 1007A” pg 14 Tokyo Sokki Kenkyujo Co., Ltd., Tokyo, Japan

41. ASTM, “E 8 – 04 Standard Test Methods for Tension Testing of Metallic Materials”, 2004 ASTM, West Conshohocken, PA

42. Gray, T.G.F., Spence, J., North, T.H., “Rational Welding Design”, 1975 Newnes – Butterworths, London, UK

43. Manson, S.S., “Thermal Stress and Low-Cycle Fatigue”, 1966 McGraw-Hill Inc., New York, NY

44. Langer, B.F., “Design of Pressure Vessels for Low-Cycle Fatigue”, vol 84 iss 3 pp. 389 – 399 1962 ASME Journal of Basic Engineering, New York, NY

45. Coffin, L.F., “A Study of the Effects of Cyclic Thermal Stresses on a Ductile Metal”, Trans. ASME vol. 76, p 931 1954 ASME, New York, NY

46. Tavernelli, J.F., Coffin, L.F.,”A Compilation and Interpretation of Cyclic Fatigue Tests on Metals”, vol. 51 p 438 1959 Trans. ASM, American Society for Metals, Materials Park, OH

47. Manson, S.S., Hirschberg, M.H., “The Role of Ductility, Tensile Strength and Fracture Toughness in Fatigue”, vol 290 pp 539 – 548 no. 6 1970 The Journal of the Franklin Institute, Philadelphia, PA

48. ASME, “Criteria of the ASME Boiler and Pressure Vessel Code for Design by Analysis in Sections III and VIII Division 2” 1969 ASME, New York, NY

49. Jaske, C.E., “Materials-Data Needs for Fatigue of Pressure Vessel Systems”, pp.600 - 611 Low Cycle Fatigue and Life Prediction, 1982 ASTM STP 770, Amzallag, C., Leis, B.N., Rabbe, eds., Philadelphia, PA

50. Jaske, C.E., in “Thermal-Mechanical, Low Cycle Fatigue of AISI 1010 Steel”, Thermal Fatigue of Materials and Components, 1976 ASTM STP 612, pp 170 – 198, Spera, D.A., Mowbray, D.F., eds, ASTM, Philadelphia, PA

51. Manson, S.S., “A Simple Procedure for Estimation High-temperature Low-cycle Fatigue” 5 (7) pp. 349 – 355 1968 Experimental Mechanics, Springer, Society for Experimental Mechanics, Bethel, CT

52. Manson, S.S., “ Some Perspectives on Future Directions in Low Cycle Fatigue”, Low Cycle Fatigue, 1988 ASTM 942, pp 5 - 14, H. D. Solomon, G. R. Halford, L. R. Kaisand, and B. N. Leis, eds., American Society for Testing and Materials, Philadelphia, PA

53. Kalnins, A., Dowling, N.E., “Design Criterion of Fatigue Analysis on Plastic Basis by ASME Boiler and Pressure Vessel Code”, 126 pp. 461 – 465 2004 Journal of Pressure Vessel Technology, ASME, New York, NY

54. O’Donnell, W.J., “§ 39, Code Design and Evaluation for Cyclic Loading – Sections III and VIII”, Companion Guide to the ASME Boiler & Pressure Vessel Code,2nd Edition, 2006, ASME, New York, NY

55. Stephens, R.I., Fatemi, A., Stephens, R.R., Fuchs, O.H., “Metallic Fatigue in Engineering”, 2nd Edition, 2001 John Wiley & Sons, New York, NY

56. Kreith, F., “Principles of Heat Transfer”, 3rd Ed., Intext Press Inc., 1973 New York, NY

57. Kelkar, V.S., Sewell, R.T., “Fundamentals of the Analysis & Design of Shell Structures”, 1987 Prentice Hall Inc., Englewood Cliffs, NJ

58. ASTM, “E 1049 – 85(2011) Standard Practices for Cycle Counting in Fatigue Fatigue Analsysi”, 2011 ASTM International, West Conshohocken PA

59. “World Class Coke Drum Replacement”, http://nooterconstruction.com/world-class-coke-drum-replacement-el-secundo-chevron-nooter/ accessed 24 Oct 2016

60. API, “API Standard 650 Welded Tanks for Oil Storage”, 12th Edition, March 2013 American Petroleum Institute, Washington, DC

61. Boswell, R. S., Farraro, T.D., “Method of Designing and manufacturing a delayed coke drum”, US Patent 5,827,403 granted 27 October 1998, Alexandria, VA

62. ASME, “Section VIII Division 3 Alternative Rules for High Pressure Vessels”, 2007 ASME, New York, NY

63. Slagis, G.C., “Meaning of Ke in Design-by-Analysis Fatigue Evaluation”, [128] Feb 2006, Transactions of the ASME, ASME, New York, NY

64. Krempl, E., “Notched High-Strain Fatigue Behavior of Three Low-Strength Structural Steels” General Electric Report GEAP-5714 1969, Atomic Power Equipment Department, General Electric, San Jose, CA

65. Lang, H., Rundolph, J., Ziegler, R., “Performance study of Ke factors in simplified elastic plastic fatigue analysis with emphasis on thermal cyclic loading”, 88 2011 pp 330 – 347 International Journal of Pressure Vessels and Piping, Elsevier B.V., Amsterdam, Netherlands

66. Wundt, B.M., ed. “Fatigue Strength Reduction Factors in Bending”, ASTM STP 490 Effect of Notches on Low-Cycle Fatigue, A Literature Survey, 1972 pp 29 – 44, ASTM, Philadelphia, PA

67. ASME, “B31.7 - 1969 Nuclear Power Piping”, 1969 ASME, New York, NY

68. Langer, B. F., “Design-Stress Basis for Pressure Vessels,” Pressure Vessel and Piping: Design and Analysis, A Decade of Progress, Volume 1, pp. 84 – 94, 1972 ASME, New York, NY

69. Gerber, T. L., “Effect of Constraint and Loading Mode on Low-Cycle Fatigue Crack Initiation—Comparison with Code Design Rules,” General Electric Report GEAP-20662 1974, Atomic Power Equipment Department, General Electric, San Jose, CA

70. Iida, K., Kitagawa, M., Tamura, K., Matsushita, A., Fukagawa, M., and Saiga, Y., “Safety Margin of the Simplified Elasto Plastic Fatigue Analysis Method of ASME B and PV Code Section III,” 1980, Institution of Mechanical Engineers, London, UK